



UNIVERSITAT DE
BARCELONA

Mitochondria and stem cell function: from somatic cells to iPSC-based disease modeling

Damià Romero Moya



Aquesta tesi doctoral està subjecta a la llicència **Reconeixement- NoComercial – Compartir Igual 4.0. Espanya de Creative Commons.**

Esta tesis doctoral está sujeta a la licencia **Reconocimiento - NoComercial – Compartir Igual 4.0. España de Creative Commons.**

This doctoral thesis is licensed under the **Creative Commons Attribution-NonCommercial-ShareAlike 4.0. Spain License.**

Programa de doctorat en Biomedicina

DEPARTAMENT DE BIOMEDICINA - FACULTAT DE
MEDICINA - UNIVERSITAT DE BARCELONA



Mitochondria and stem cell function: from somatic cells to iPSC- based disease modeling

Memòria presentada per:

Damià Romero Moya

Damià Romero Moya

El doctorand

Pablo Menéndez Buján

El director

Neus Agell Jané

La tutora



Barcelona, 2017

El Dr. Pablo Menéndez Buján, Investigador Principal del grup “*stem cells, mesenchymal cancer and development*” de l’Institut Josep Carreras, Professor d’Investigació ICREA y Professor Associat de la Universitat de Barcelona,

CERTIFICA:

- Que la tesis doctoral titulada “*Mitochondria and stem cell function: from somatic cells to iPSC-based disease modeling*” presentada per en Damià Romero Moya ha sigut realitzada sota la meua direcció i compleix amb els requisits formals i científics para ser defensada enfront del tribunal corresponent.

- Que els articles directament derivats d’aquesta tesis doctoral s’han publicat com articles originals en las següents revistes científiques internacionals indexades:
 - Haematologica. Romero-Moya *et al.* 2013; 98(7): 1022-9. Factor d’impacte: 6.8
 - Stem Cells. Velasco *et al.* 2014; 32(11):2811-7 Factor d’impacte: 5.9
 - Stem Cell Research. Romero-Moya *et al.* 2016 Acceptat. Factor d’impacte: 3.8
 - Stem Cells. Romero-Moya *et al.* 2016. En revisió. Factor d’impacte: 5.9

- Que el doctorand ha liderat en la seva plenitud aquests treballs. Ha dissenyat i discutit amb el seu mentor els experiments a realitzar per donar resposta als objectius. Sobre aquesta base ha realitzat els experiments i ha analitzat i interpretat les dades. Finalment, només ell ha organitzat els resultats en les figures finals dels treballs.

- La resta de co-autors han col·laborat experimentalment o han ajudat en la formació del candidat en aspectes logístics de mostres primàries o noves tècniques.

Per a que així consti, firmo a Barcelona, a 11 d'Octubre del 2016.

A handwritten signature in black ink, consisting of a long horizontal stroke with a vertical stroke crossing it near the left end, and a small loop at the top of the vertical stroke.

Pablo Menéndez Buján

DNI: 10.892.394-P

$$B > \frac{1}{n} \sum_{i=1}^n X_i$$

be greater than average

ACKNOWLEDGMENTS

Alguna vez me han comentado que los agradecimientos es lo más fácil, ya que no hay que buscar en ningún lado, ni referenciar, ni estar seguro de si lo que pones es verdad. Ya que cada uno escribe lo que le parece correcto. Estas cosas necesitan inspiración y no sé si hoy es el mejor día ni tampoco sé si eso es lo mío. Pero tengo que agradecer a mucha gente la paciencia que ha tenido conmigo, el esfuerzo que ha dedicado, el conocimiento que me ha transmitido y sobre todo el tiempo que ha “perdido”.

Primero de todo, quiero agradecer a mi director de tesis Pablo, por confiar en mí y darme la oportunidad de empezar la tesis en Granada. Gracias a eso he conocido una de las mejores ciudades donde he vivido, y no sólo por la ciudad, sino también por la gente que allí vive.

Me gustaría agradecer también a TODA la gente que conocí en GENyO (Seguridad, servicios comunes, pasillos, salas de cultivos ajenas, comedor, etc.) y Granada, especialmente a mi grupo de investigación allí: Clara, Pedro, René, Iván, Vero R y Vero A de los cuales aprendí lo que es la base de lo que sé ahora, también aprendí que hace falta una Vero A en cualquier laboratorio para mantener el orden y la disciplina, ya que una regañina a tiempo evita el caos posterior. A los predocs de aquel momento; Ruth, esa chica sevillana que se apuntaba a todo; a Rosi y nuestros paseos al animalario donde teníamos nuestras inquietantes charlas; a Óscar/Navarrete/Adonis según quien lo llamara, un gran amigo que quiero mantener durante mucho tiempo que me ha hecho pasar grandes momentos; a Cris que hemos tenido nuestros más y nuestros menos, quizá más menos que más pero ha sido una gran compañera y amiga durante todo este tiempo. También tengo que agradecer al equipo pHímetro en los momentos de dificultad de calcular y calibrar el pH, donde siempre varias cabezas piensan más que una. A la Suyi, esa chica guapa, sonriente y alegre que te ríes de ella y con ella cuando se inventa enfermedades para llamar la atención...Y finalmente al resto de la gente que he conocido allí y han dejado huella y recuerdo en este tiempo: Javi, Rubén, Tamara, Santi, Eva, Angélica, Angelina...

Del grupo de Barcelona quiero agradecer a los técnicos ya que sin ellos y el trabajo que hacen en la sombra no habría sido lo mismo, Angélica, Lorena, Cris, José Antonio, Heleia y Anna. A Julio, Alessandra y Alejandra de los que he aprendido mucho de sus

respectivas áreas. A Clara y a Cris otra vez, por estar en los dos lados, que ya por fin me despegaré de vosotras. A Rafa y Belén esa extraña pareja, el día y la noche, en cada una de sus aficiones/gustos/carácter... A los que han estado menos tiempo, pero igual de importante Erica, Pamela y “Alvarito”. A los que han llegado los últimos al grupo de los CARTs, formado por María, Matteo y Adrián y también Virginia. Hay que agradecer también a esas meriendas/vermuths que me han regalado discusiones científicas, cotilleos, opiniones, celebraciones... dignas de un perfil.

Agradecer a los colaboradores del proyecto, a la gente de Sevilla ya sean del IBiS o de la UPO, a los colaboradores de Barcelona, en Sant Joan de Déu, Cellex y PRBB. I also would like to thank the people from Newcastle, especially Majlinda Lako, who allowed me to do a short-stay in her Lab, where I learnt the first steps of the reprogramming. The rest of the people from that Lab, who helped me when I needed.

Finalmente a mi familia, especialmente a mi padre y a mi madre, que aunque no sepan mucho lo que hago, el apoyo que me han dado es muy grande y aún tiene más valor. Siempre me han apoyado y animado a seguir adelante en las decisiones que he tomado.

Gracias a todos por aguantarme!

INDEX

I.	ABSTRACT	15
II.	ABBREVIATIONS.....	19
III.	INTRODUCTION.....	23
III.1.	Stem cells: Definition, classification and localization	25
III.1.1.	Induced pluripotent stem cells	28
III.1.2.	Hematopoietic stem cells and hematopoiesis	31
III.1.3.	Nervous tissue.....	35
III.1.4.	Skeletal muscle tissue	37
III.2.	Metabolism.....	39
III.2.2.	Glycolysis.....	40
III.2.3.	Oxidative phosphorylation.....	40
III.2.4.	Reactive oxygen species	43
III.2.5.	Mitochondrial metabolism.....	44
III.2.6.	Coenzyme Q ₁₀	45
III.2.6.1.	Coenzyme Q ₁₀ deficiency.....	47
III.2.6.2.	<i>COQ4</i> mutations	48
III.3.	Disease modeling	49
III.4.	CRISPR/Cas9: a unique an unprecedented tool for gene editing..	51
III.5.	Article I:.....	53

IV.	HYPOTHESIS AND OBJECTIVES	63
V.	METHODS AND RESULTS	67
V.1.	Summary of the results.....	69
V.2.	Article II:	75
V.3.	Article III:.....	87
V.4.	Article IV:	95
VI.	DISCUSSION	141
VII.	CONCLUSIONS	159
VIII.	REFERENCES.....	163
IX.	ANNEX.....	187
X.	NOTES.....	209

I.ABSTRACT

Homeostasis of the hematopoietic stem/progenitor cell pool relies on a finely tuned balance between self-renewal, differentiation and proliferation. Recent work has revealed the importance of mitochondria during stem cell differentiation; however, it remains unclear whether mitochondrial content/function affects human hematopoietic stem *versus* progenitor function. We sorted cord blood-derived CD34⁺ cells on the basis of mitochondrial mass and examined their homeostasis and clonogenic potential *in vitro* and hematopoietic repopulation potential *in vivo*. CD34⁺ cells with high mitochondrial mass contained and expressed 2-fold high ATP levels and mitochondrial-specific genes than cells with low mitochondrial mass, however, *HIF-1α* and *MEIS1* were high in the CD34⁺ cells with low mitochondria. We found that CD34⁺ cells with low mitochondrial content were enriched for hematopoietic stem cell function as demonstrated by significantly higher hematopoietic reconstitution potential in immunodeficient mice. By contrast, CD34⁺ cells with high mitochondrial content were enriched for hematopoietic progenitor function with high *in vitro* clonogenic capacity.

Coenzyme Q₁₀ (CoQ₁₀) plays a critical role in mitochondria as an electron carrier within the electron transport chain (ETC) and is an essential antioxidant. Mutations in genes responsible for CoQ₁₀ biosynthesis (*COQ* genes) cause primary CoQ₁₀ deficiency, a rare and heterogeneous mitochondrial disorder with no clear genotype-phenotype association, mainly affecting tissues with high energy demand including brain and skeletal muscle (SkM). A four-year-old girl was identified with a heterozygous mutation (c.483G>C; E161D) in *COQ4*, associated with a reduction in [CoQ₁₀], CoQ₁₀ biosynthesis and ETC activity affecting complexes I/II+III. *Bona fide* induced pluripotent stem cell (iPSC) lines carrying the *COQ4* mutation

(CQ4-iPSCs) were generated, characterized and genetically corrected using CRISPR/Cas9 genome-editing (CQ4^{ed}-iPSCs). Comprehensive differentiation and metabolic analysis of control-iPSCs, CQ4-iPSCs and CQ4^{ed}-iPSCs faithfully reproduced the disease phenotype. Accordingly, the *COQ4* mutation in iPSCs was associated with CoQ₁₀ deficiency, metabolic dysfunction and impaired differentiation into SkM. Remarkably, differentiation of CQ4-iPSCs into dopaminergic or motor neurons was unaffected. This study offers an unprecedented iPSC model recapitulating CoQ₁₀ deficiency-associated functional and metabolic phenotypes caused by *COQ4* mutation.

II.ABBREVIATIONS

ADP	Adenosine diphosphate
AGM	Aorta-gonad-mesonephros
ALS	Amyotrophic lateral sclerosis
ATP	Adenosine triphosphate
BM	Bone marrow
CB	Cord blood
CI	Complex I or NADH-coenzyme Q oxidoreductase
CII	Complex II or Succinate-Q oxidoreductase
CIII	Complex III or coenzyme Q-cytochrome c oxidoreductase
CIV	Complex IV or Cytochrome c oxidase
CNS	Central nervous system
CRISPR	Clustered regularly interspaced short palindromic repeats
DAn	Dopaminergic neurons
DNA	Deoxyribonucleic acid
DSB	Double-strand break
ECAR	Extracellular acidification rate
ESC	Embryonic stem cell
ETC/ MRC	Electron transport chain/ Mitochondrial respiratory chain
FAD	Flavin adenine dinucleotide
HDR	Homology direct repair
HPC	Hematopoietic progenitor cell
HSC	Hematopoietic stem cell
HSPC	Hematopoietic stem/progenitor cell
IDH1	Isocitrate dehydrogenase 1
IDH2	Isocitrate dehydrogenase 2
iPSC	Induced pluripotent stem cell
KDH	α -ketoglutarate dehydrogenase
LT-HSC	Long-term hematopoietic stem cell

MMP	Mitochondrial membrane potential
MN	Motor neurons
mtDNA	Mitochondrial DNA
NAD	Nicotinamide adenine dinucleotide
NGPS	Néstor-Guillermo progeria syndrome
NHEJ	Non-homologous end joining
NSC	Neural stem cell
OCR	Oxygen consumption rate
OXPHOS	Oxidative phosphorylation
PDH	Pyruvate dehydrogenase
RNA	Ribonucleic acid
ROS	Reactive oxygen species
SC	Stem cell
sgRNA	Small guide RNA
SkM	Skeletal muscle
ST-HSC	Short-term hematopoietic stem cell

III.INTRODUCTION

III.1. STEM CELLS: DEFINITION, CLASSIFICATION AND LOCALIZATION

Stem cells (SCs) are immature and undifferentiated cells with both self-renewal and multilineage potential. Self-renewal, which is the ability to undergo symmetrical division while preserving multilineage potential [1, 2] is maintained by a balance between symmetric and asymmetric cell division, whereby daughter cells produce one cell identical to the progenitor and another cell which undergoes differentiation (asymmetric division) or produce two cells identical to the progenitor (symmetric division) (**Figure 1**). Multilineage potential or potency, a hallmark of SCs, is the ability to differentiate into other cell types. Accordingly, the more cell types the cell can give rise to the greater is the potency [2].

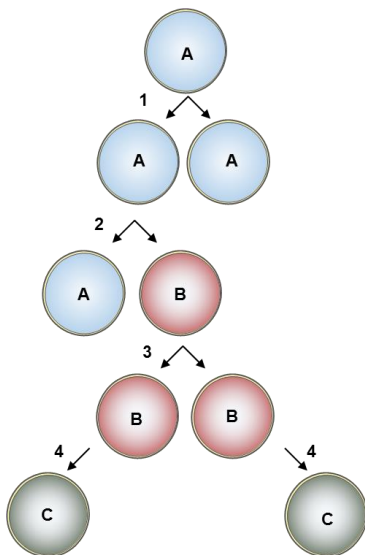


FIGURE 1: Schematic representation of the balance between symmetric and asymmetric division. Symmetric division expands the stem cell pool and allows a cell to self-renew and maintain its status, while asymmetric division maintains the stem cell pool and also creates a committed cell. **A:** Stem cell; **B:** Progenitor cell; **C:** Differentiated cell; **1:** Symmetric stem cell division; **2:** Asymmetric stem cell division; **3:** Progenitor division; **4:** Terminal differentiation.

This differentiation potency forms the core of a classification system whereby SCs can be ordered based on their multilineage potency as follows: (see **Figure 2**)

- **Totipotent SCs:** are cells with the potential to differentiate into any embryonic and extraembryonic tissue. Totipotent SCs have the greatest differentiation potential and can generate a complete organism. In mammals this cell type is the zygote [2].
- **Pluripotent SCs:** are the next cells to appear during embryonic development. Pluripotent SCs can differentiate into almost all cell types and generate any tissue of the three embryonic germ layers (endoderm, mesoderm and ectoderm). However, they have lost the capacity to differentiate into extraembryonic tissue. An example of a pluripotent cell would be the discovery of human embryonic stem cells (ESCs) derived from the inner cell mass of a blastocyst, reported for the first time by Thomson *et al.* in 1998 [3]. ESCs can proliferate indefinitely while maintaining pluripotency. In 2007, Takahashi *et al.* induced the pluripotent state from human somatic cells using a cocktail of specific transcription factors, thus establishing induced pluripotent stem cells (iPSCs), which display similar capacity to proliferate and differentiate to ESCs [2, 4, 5].
- **Multipotent SCs:** are cells with the ability to differentiate into most cell types of a specific tissue. In humans, several types of tissue-specific multipotent SCs have been described e.g., neural stem cells (NSCs) [6], hematopoietic stem cells (HSCs) [7], and mesenchymal stem cells (MSCs) [8].
- **Oligopotent SCs:** are cells that can differentiate into only a few cell types of a given tissue. In the hematopoietic system, common lymphoid progenitors

(CLPs) and common myeloid progenitors (CMPs) are representative of oligopotent SCs [7].

- Unipotent SCs: can only produce their own cell type. They are located in adult tissues and play a key role in tissue homeostasis. Muscle and epidermal SCs are examples of unipotent cells.

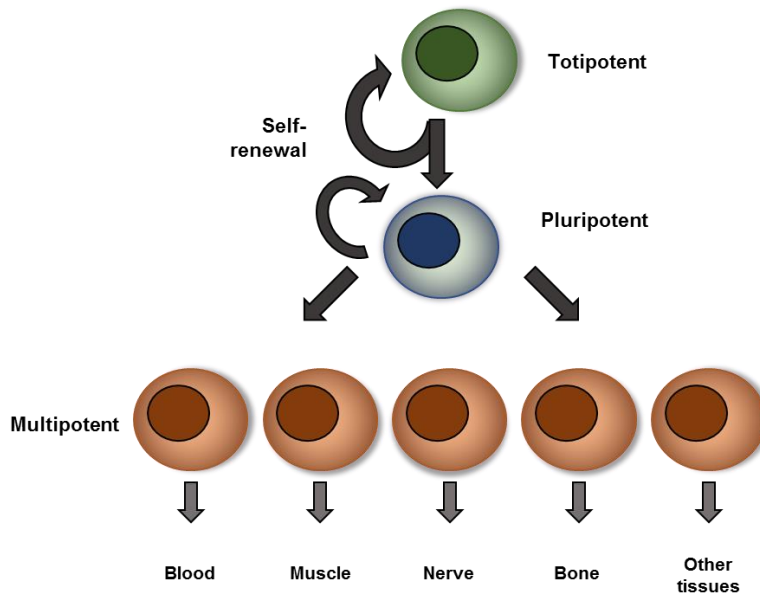


FIGURE 2: Schematic representation of different types of SCs based on their potency. A totipotent SC is represented by the zygote. Pluripotent SCs include ESCs and iPSCs. Multipotent SCs are tissue-specific SCs such as HSCs, MSCs, NSCs, etc.

SCs are acknowledged as a potentially powerful tool for cell therapy and regenerative medicine applications. Furthermore, the differentiation of SCs into tissue-specific lineages has aided in the elucidation of key biological process during development and is a promising platform for disease modeling [9]. Below, we describe the SC populations utilized in the present work.

III.1.1. INDUCED PLURIPOTENT STEM CELLS

iPSCs were generated for the first time in 2006 in a pioneering study using retroviruses to ectopically express defined pluripotency-associated transcription factors in embryonic and adult mouse cells [10]. One year later, the same group generated human iPSCs in a similar approach using the transcription factors *OCT3/4*, *SOX2*, *KLF4* and *C-MYC* (OSKM), colloquially known as “Yamanaka factors” [5] (**Figure 3**). iPSCs are generated by direct transcriptomic, epigenetic and metabolic reprogramming of somatic cells and behave like ESCs with regards to pluripotency and self-renewal. Since the first descriptions of iPSCs, many reports have reviewed the similarities and differences between iPSCs and ESCs with contentious results. Several groups reported that despite sharing similar pluripotency capacity, iPSCs differ from ESCs by their epigenetic memory of somatic origin [2, 11-13]. However, other groups have demonstrated that no such differences exist [2, 14]. In the 10 years since its first description, a broad variety of somatic cells have been successfully reprogrammed using different combinations of genes and/or small molecule inducers [15-21]. The relative ease with which iPSCs are generated has led to their wide use in developmental biology, disease modeling, drug testing and also cell therapy (**Figure 4**) [9].

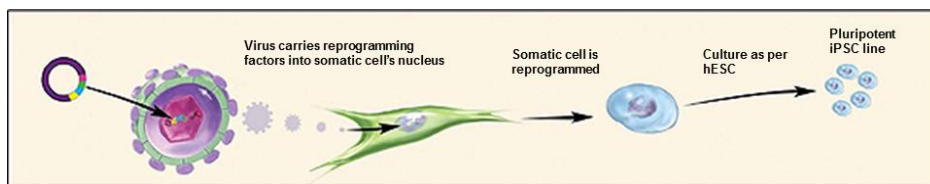


FIGURE 3: Representative scheme of somatic cell reprogramming (iPSC generation) after transgene (OSKM) transduction. Modified from the National Institutes of Health.

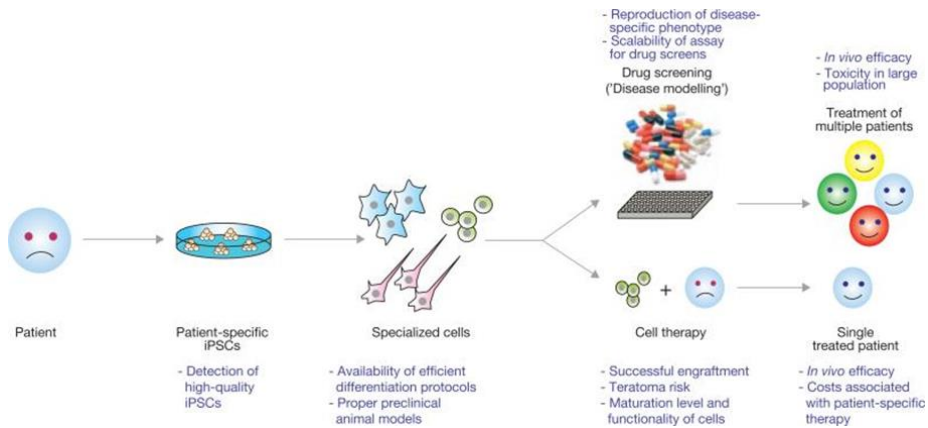


FIGURE 4: Schematic representation of the potential utility of iPSCs in regenerative medicine and drug screening. Introduction of reprogramming factors into a patient’s somatic cells give rise to iPSCs. These iPSCs can then be differentiated into a variety of specialized cell types for potential use in disease modeling or cell therapy. Modified from [9].

Bona fide characterization of pluripotency is crucial after iPSC generation to confirm their identity [22]. Transgene expression has to be silenced shortly after iPSC generation; the inability to silence the ectopic expression of the Yamanaka factors makes iPSCs transgene-dependent, thus preventing subsequent differentiation [23]. Because chromosomal alterations can occur during the reprogramming process, a key test to ensure that iPSCs have a diploid karyotype is to assess genome stability by G-banding (as a minimum). Moreover, pluripotency-specific cell surface markers, such as SSEA-3, SSEA-4, TRA-1-60, TRA-1-81, and transcription factors including OCT-3/4, NANOG, SOX2, REX1, CRIPTO, among others, have to be expressed in iPSCs. Teratoma formation in immunodeficient mice is the most stringent functional assay and the gold standard to define *bona fide* iPSCs [22]. While the first gene delivery methods used to reprogram somatic cells were traditional integrative vectors, such as lentivirus or retrovirus [24], more recently non-integrative methods such as Sendai virus [15] or

episomal vectors, as well as epigenetic modifiers/compounds [21], have been used successfully to deliver reprogramming factors [24].

ESCs and iPSCs hold great promise in cell therapy and regenerative medicine. The successful prospective differentiation of iPSCs into tissue/lineage-specific cells will render cell populations of potential clinical value. The utility of iPSC-derivatives relies on the ability to generate functional and homogeneous cell subsets for transplantation. In hematopoietic tissue, functional HSCs with long-term hemato-immune engraftment potential have not yet been reported [9, 25, 26]. This may be due to the fact that additional, yet unknown, intrinsic factors and/or extrinsic signals are required for the generation of *in vivo* long-term hematopoietic reconstitution [25]. By contrast, several studies have demonstrated the capacity of iPSC-derived neurons to engraft in experimental animal models [27-29]. Several clinical trials using iPSC- and ESC-derivatives are ongoing. No side effects thus far have been reported in these preliminary trials, and some degree of success has been found with retinal pigment epithelium [30], cardiac progenitors [31] and pancreatic endoderm cells [32], among other lineages. The current status of pluripotent SC applications in the clinic has been recently reviewed by Kimbrel *et al.* [33].

Recent publications have demonstrated that human iPSCs can be grown under standard conditions in the primed state or grown in the naïve state [34, 35]. Primed iPSCs retain the gene expression and methylation profile of the tissue from which they were derived, whereas naïve iPSCs, regardless of their cellular origin, share a similar transcriptional and epigenetic profile. However, when naïve iPSCs revert to the primed state, surprisingly they re-establish their original transcriptomic and epigenetic profile,

suggesting epigenetic memory [13]. Importantly, the differentiation capacity of iPSC lines is influenced by genetic and epigenetic variability [13, 36, 37], presumably reflecting their cellular origin, the genetic background and the different reprogramming strategies. To rule out the variability among different iPSCs, isogenic iPSCs should be used for disease modeling studies. Accordingly, pairs of iPSC lines can be engineered with only one specific modification by genome editing strategies against an otherwise isogenic background. Among the different techniques available, Zinc Finger Nuclease (ZFN), Transcription Activator-Like Effector Nucleases (TALENs), Clustered Regularly Interspaced Short Palindromic Repeat/Cas9 (CRISPR/Cas9) and Helper-Dependent Adenoviral Vectors (HDAdVs) are those most commonly used to correct and/or edit the monogenic mutations to generate isogenic iPSC pairs for disease modeling [38, 39].

III.1.2. HEMATOPOIETIC STEM CELLS AND HEMATOPOIESIS

HSCs are multipotent SCs that emerge early during development and maintain hematopoiesis throughout the entire lifespan of the organism [40]. Human hematopoiesis is a complex process involving several organs during development. The definitive HSC emerges first in the aorta-gonad-mesonephros (AGM) region [41, 42], and then migrates to liver and placenta. The fetal liver is the principal hematopoietic organ during development. Later, the spleen, thymus and lymphatic nodes are colonized by HSCs, which further migrate to the bone marrow (BM) where they reside throughout the lifetime of the organism (**Figure 5**) [40, 42, 43].

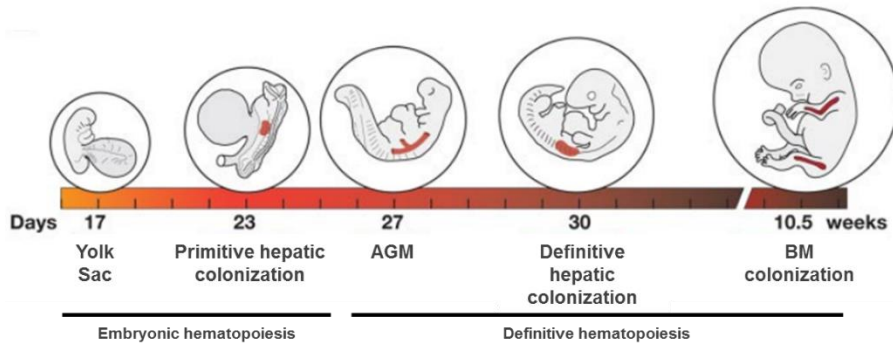


FIGURE 5: Human embryonic blood development: primitive hematopoiesis starts in the yolk sac by day 17. Definitive hematopoiesis starts in the AGM region, and by day 30 migrates to the fetal liver. The BM is the last and definitive niche for HSCs. Modified from [43].

III

Hematopoiesis is a hierarchical process where the most immature cells (HSCs) reside at the apex and undergo several stages of differentiation to generate a variety of mature blood cells. HSCs, hematopoietic progenitor cells (HPCs), lineage committed cells (myeloid or lymphoid) and mature cells can be phenotypically and functionally distinguished (**Figure 6**). Hematopoietic stem/progenitor cells (HSPCs) are almost exclusively enriched in the CD34⁺ fraction, which represents a small population (<1%) in cord blood (CB) and BM [44, 45]. Phenotypically, human HSCs are enriched in the Lin⁻CD34⁺CD38⁻ fraction and HPCs are enriched in the Lin⁻CD34⁺CD38⁺ fraction. Functionally, HSCs are the only cells able to complete hematopoietic engraftment after HSPC transplantation. Within the HSC fraction are Long-Term HSCs (LT-HSCs), which are responsible for durable hematopoietic engraftment, and Short-Term HSCs (ST-HSCs), which ensure short-term reconstitution. Consequently, HPCs have a lower reconstitution capacity due to lineage commitment [7, 44]. Hematologic malignancies

and severe immunodeficiencies are target diseases for HSPC transplantation. Umbilical CB has been extensively used as a source of HSPCs since the 1980s as it represents a unique source of HSPCs due to its high percentage of CD34⁺ cells and low immunogenicity [46, 47]. In the setting of clinical transplantation, the dose of total CD34⁺ cells infused per kg of the patient's bodyweight is used as a predictor of short-term hematopoietic recovery and establishment of long-term engraftment [44, 48].

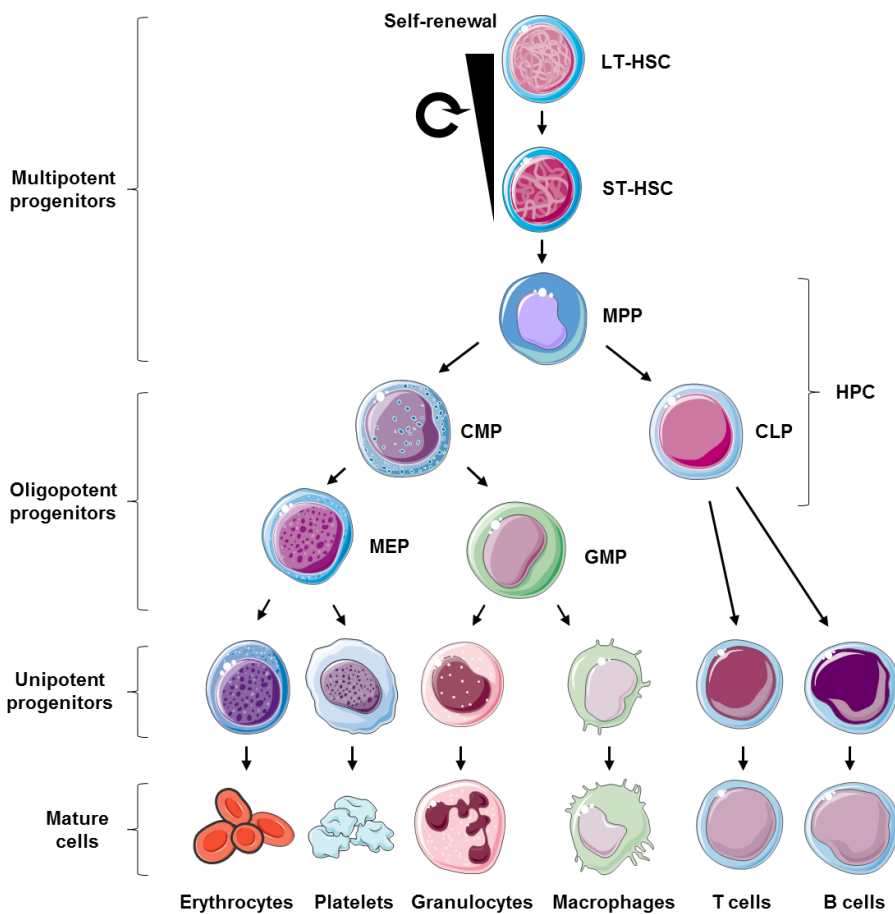


FIGURE 6: Developmental hierarchy of hematopoiesis: LT-HSC and ST-HSC are Lin⁻CD34⁺CD38⁻. HPC comprise multipotent progenitors (MPP), common myeloid progenitors (CMP) and common lymphoid progenitors (CLP) and are Lin⁻CD34⁺CD38⁺.

Initially, CB transplantation was restricted to children or low-weight adults due to the limited number of HSPCs. Over the last years, however, different strategies have been implemented to improve CB transplantation efficacy, including CB-derived CD34⁺ cell expansion, *ex vivo* and *in vivo* homing techniques, or double CB administration [49].

BM stem cell niche is functionally defined as a specialized cellular structure which is essential for long-term maintenance of adult HSCs. The balance between quiescence and self-renewal is most probably regulated by dynamic reciprocal interaction between single HSCs and their niches [50]. Stem cells are regularly distributed either in quiescent or cycling states. The majority of LT-HSCs are in a quiescence, which is accompanied by low metabolic activity, as a mechanism for avoiding accumulation of DNA damage, and necessary to preserve the self-renewal capacity of HSCs and to prevent stem cell exhaustion. Despite their quiescence, HSCs exhibit the highest self-renewal potential of all blood cells [51, 52]. HSCs and HPCs are identified *in vivo* and *in vitro* based on the expression of cell surface markers [53] or by their unique metabolic profiles [51, 54-56]. Simsek *et al.* defined the metabolic phenotype of mouse HSCs, demonstrating that HSC are enriched in a distinct population of cells characterized by low mitochondrial potential (i.e., mitochondrial membrane potential or MMP, ATP and oxidative phosphorylation or OXPHOS). The metabolic phenotype of LT-HSC confers them a survival advantage in both physiological hypoxic or anoxic BM niche [57, 58]. Under hypoxic conditions, glycolytic metabolism predominates, providing sufficient amounts of ATP to sustain HSCs. Glycolysis allows ATP generation with limited reactive oxygen species (ROS) production, being a less efficient but safer cellular process. The transcription factor hypoxia-inducible factor-1 (HIF-1) plays an essential role in the maintenance of oxygen homeostasis. HIF-1 is a

heterodimeric protein that comprises two subunits: HIF-1 α , which is stabilized by hypoxia, and HIF-1 β , which is constitutively expressed [59]. HIF-1 is a master regulator of the transcriptional response to hypoxia and induce the expression of glycolytic enzymes, allowing the production of energy when mitochondria are starved of oxygen. HIF-1 is thus considered the key protein responsible for the metabolic adaptation to hypoxia [60-63].

III.1.3. NERVOUS TISSUE

Mammalian nervous tissue is composed by the central nervous system (CNS) and the peripheral nervous system, which regulates body functions and activity. The CNS is largely made up by two types of cells: neurons and glial cells. Neurons are excitable cells that transmit information, whereas glial cells have a basically supportive function. The adult nervous system has classically been considered incapable of generating new neurons because they are post-mitotic and do not divide. However, this view was changed by the discovery of brain neurogenesis and the existence of NSCs in the adult mammalian brain [6, 64]. NSCs are self-renewing multipotent progenitors that give rise to neurons, astrocytes and oligodendrocytes in the CNS (**Figure 7**). Neurogenic niches within the adult CNS are well characterized and are localized to the subventricular zone, the subgranular zone and the carotid body [6, 65]. NSCs isolated at different developmental stages share expression of NESTIN, MUSASHI, NCAM and SOX2. The expression of the majority of these markers is regulated during the initial phases of neural induction and is then maintained in NSCs throughout ontogeny [66].

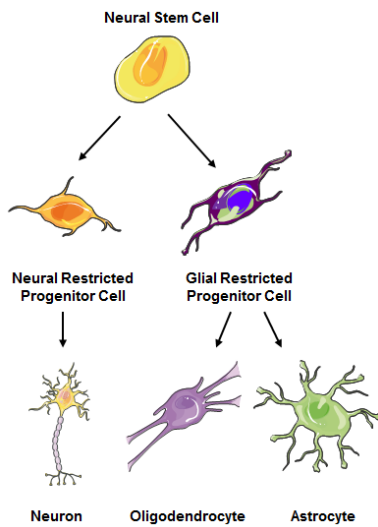


FIGURE 7: Representative human neural hierarchy: Neural stem cells have self-renewal capacity and can differentiate into two different progenitors: neuronal restricted progenitors and glial restricted progenitors.

Every region in the brain possesses its own type of neurons, which differ in their morphology, connectivity and electrophysiological properties. Although the function of some of these neurons has yet to be determined, recent work has enabled their classification based on RNA expression [67]. Two of the most well characterized types of neurons are dopaminergic neurons (DANs) and motor neurons (MNs) due to their dysfunction in Parkinson disease and amyotrophic lateral sclerosis (ALS), respectively, which are common neurodegenerative diseases. Midbrain DANs are located in three major nuclei (A8, A9 and A10) [68, 69] that originate from the ventricular zone in the ventral midbrain and produce the neurotransmitter dopamine. OTX2, FOXA2 and LMX1 α cooperate to enhance dopaminergic commitment [70-72] by inducing the expression of several specific transcription factors such as PITX3, NURR1, EN1/2 and TH, among others [68, 69, 73]. MNs can originate in the cerebral cortex (upper MNs) or in the brainstem and spinal cord (lower MNs), and control directly or indirectly the effector organs e.g., muscle [74]. Early in development, retinoic acid (RA) is crucial

for the initial distinction of neurons of the hindbrain and spinal cord. Next, a sonic hedgehog (SHH) gradient regulates rostral-caudal differentiation. Definitive MN-specific transcription factors include, among others, HB9, ISL1 and LHX3 [74, 75].

In vitro neurogenesis has been reported by direct conversion of somatic cells or from ESCs/iPSCs [17, 38, 76]. Neural commitment can be achieved after neuroectoderm induction by RA or dual SMAD inhibition from iPSCs [27, 29, 77-82], and several neuronal subtypes have been successfully generated *in vitro* [83]. Patient-specific iPSCs can be prospectively differentiated into different neural cell types, which are expected to become a unique tool/strategy for disease modeling and future *in vivo* cell replacement therapies [38].

III.1.4.SKELETAL MUSCLE TISSUE

Muscle is a soft tissue formed during embryogenesis through a process known as myogenesis [84]. Three types of muscle are found in mammals, which vary with respect to function and anatomical location: skeletal muscle (SkM), smooth muscle and cardiac muscle. SkM refers to multiple bounded cells called muscle fibers or muscle cells. During myogenesis, SkM cells are formed through the fusion of developing myoblasts. Embryonic muscle progenitor cells express two master genes responsible for the survival and specification of the myogenic lineage, PAX3 and PAX7, and are maintained as a self-renewing proliferative population [85]. These muscle progenitors are quiescent and are held in reserve as resident satellite cells until needed for postnatal growth or repair. During embryogenesis or after muscle damage, satellite cells are activated to proliferate and differentiate to form new muscle cells [86]. The PAX7 transcription factor is a *bona fide* marker for quiescent satellite cells, and upon

stimulation/activation, satellite cells express the myogenic determination factor MYF5, a PAX7 target, which is required for proliferation and further commitment into myoblasts [85, 87]. Along with MYF5, the myogenic regulatory factors MYOD and MYOGENIN, which are essential for SkM differentiation from myoblasts, are upregulated. Concomitantly, PAX7 is downregulated and myotubes (the mature SkM cell) present PAX7 inactivation and an upregulation of myotube-specific markers such α -actin, MHC and muscle creatine kinase (**Figure 8**) [88]. This terminal differentiation is accompanied by the absence of proliferation [87].

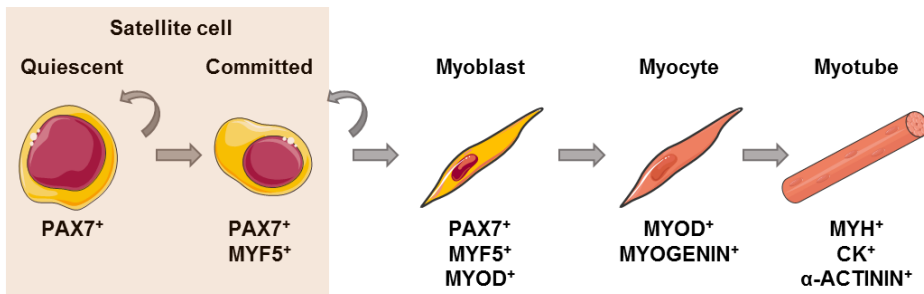


FIGURE 8: Representation of SkM differentiation and maturation.

Several studies have demonstrated the capacity of ESC/iPSCs to differentiate into SkM [89-93]. The most efficient methodology described thus far is the introduction of an inducible transgene, such as PAX7 or MYOD, which drives cells towards the myogenic lineage, acquiring engraftment and regenerative potential *in vivo*. Nevertheless, a major challenge for cell therapy or drug screening is to scale up the differentiation process such that it renders a large enough supply of homogeneous SkM cells for downstream application [93, 94].

III.2.METABOLISM

Metabolism can be considered a homeostatic process by which living organisms produce a well-synchronized network of chemical/enzymatic reactions aimed at modifying cellular structures and basic/elemental metabolites to meet physiological demands.

Metabolism can be divided into two phases:

1. Anabolism: set of metabolic pathways through which complex functional molecules are built from simple precursors. These reactions require chemical energy, which is supplied as ATP. Anabolic processes usually promote cell growth and differentiation.
2. Catabolism: set of metabolic pathways that break down large molecules (e.g., polysaccharides, lipids, nucleic acids and proteins) into smaller units (e.g., monosaccharides, fatty acids, nucleotides and amino acids), which are either oxidized to release energy (ATP) or used in other anabolic reactions. Catabolism therefore provides the chemical energy required for anabolic cell growth and maintenance. Glucose is the main carbon source to produce ATP and its catabolism is tightly regulated by a balance between glycolysis, which occurs in the absence of oxygen, and OXPHOS, which is supplied with reducing power generated by the Krebs cycle in the mitochondrial matrix, leading to the consumption of oxygen.

III.2.2. GLYCOLYSIS

Glycolysis is a catabolic pathway that converts glucose into pyruvate required for synthesis of ATP and NADH. Pyruvate can either be catabolized by the Krebs cycle to produce more ATP by OXPHOS, or converted to lactic acid by fermentation in the absence of ATP synthesis. Glycolysis is less efficient in terms of energy production (2 ATPs are produced compared with 36 from OXPHOS); however, it produces energy at a faster rate and with a lower generation of ROS, which reduces oxidative damage, and also allows for ATP generation in the absence of oxygen. Cancer cells use glycolysis preferentially even in the presence of sufficient oxygen, a process termed the Warburg effect, to generate energy while preventing ROS generation and genome instability [95, 96].

During embryogenesis, the blastocyst switches metabolism from OXPHOS to glycolysis to prevent oxidative damage [97, 98]. Thus, ESCs derived from the inner cell mass as well as iPSCs maintain this glycolytic metabolism as a primary source of ATP [99]. In addition, early stage somatic cell reprogramming to iPSCs is accompanied by a switch from mainly OXPHOS to mainly glycolytic metabolism [99-103]. The predominantly glycolytic state allows the cell to produce energy linked to low levels of ROS and is maintained by the expression of HIF-1 and UCP2 [103, 104].

III.2.3. OXIDATIVE PHOSPHORYLATION

OXPHOS is a mitochondrial process that uses oxidation of nutrients to generate a proton gradient between the mitochondrial matrix and the intermembrane space that is then used for multiple purposes including the import of proteins and calcium into the

mitochondrion, and for generating heat and ATP [105]. It is the main aerobic route to generate ATP from glucose and is more efficient than glycolysis. Electron donors (NADH + H⁺ and FADH₂) produced by the Krebs cycle or by β-oxidation in the mitochondrion matrix are passed to electron acceptors such as oxygen in redox reactions to form water. These redox reactions are executed by four protein complexes embedded in the mitochondrial inner membrane that constitute the electron transport chain (ETC). The efficiency by which the electron transport is converted to ATP by OXPHOS is known as the coupling efficiency. This is determined by the efficiency through which protons are pumped out of the matrix by complexes I, III and IV and the efficiency by which proton flux through complex V is converted to ATP [105].

Mitochondrial OXPHOS consist of two subsystems, the ETC (from complex I to complex IV) and the ATP synthase (Complex V) (**Figure 9**):

- Complex I (CI) or NADH-coenzyme Q oxidoreductase: is the largest and most robust electron acceptor and oxidizes NADH to NAD, transferring electrons to coenzyme Q₁₀ (CoQ₁₀), which is reduced. It is a proton pump formed by 46 subunits and is the major ROS producer in the cell, which can damage the mitochondrial DNA (mtDNA) and cause aging-like degenerative changes and sporadic Parkinson disease [106-109].
- Complex II (CII) or succinate-Q oxidoreductase: is the second entry point to the ETC. CoQ₁₀ is reduced by the electrons transferred from succinate or FADH₂. This complex is unable to transfer protons into the intermembrane space. Succinate accumulation can be generated by mutations in CII, which

can increase ROS generation and related genomic instability provoking metabolic disease [110-112].

- Complex III (CIII) or coenzyme Q-cytochrome c oxidoreductase: is a dimer, with each monomer containing 11 protein subunits. The reaction catalyzed is the oxidation of CoQ₁₀ and the reduction of the electron carrier cytochrome c, which shuttles electrons to complex IV and protons are pumped into the intermembrane space. Encephalomyopathy or Leber hereditary optic neuropathy provoked by superoxide overproduction can be caused by mutations in CIII [113-115].
- Complex IV (CIV) or cytochrome c oxidase: is the final complex in the ETC. It contains 13 subunits and mediates electron transfer from cytochrome c to oxygen to form water, at the same time removing protons from the matrix and contributing to the proton gradient. CIV deficiencies are heterogenic disorders and range from myopathy to multisystemic disorders [116].
- Complex V (CV) or ATP synthase: is the final enzyme of OXPHOS. This enzyme uses the energy stored in the proton gradient across the mitochondrial membrane to synthesize ATP from ADP and Pi. This phosphorylation reaction is in equilibrium, which can be shifted by altering the protonmotive force. In the absence of protonmotive force, ATP synthase hydrolyzes ATP.

The function or textbook description of the ETC in the mitochondria cannot be fully explained by the classical fluid model [117] or the solid model, which proposes that the respirasome (CI, CIII and CIV) is the only functional mitochondrial ETC [118]. It is thought that both models coexist in a dynamic way. Complexes are organized into

independent supercomplexes [119], likely due to their dependence on physical interaction for functionality and to optimize the use of available substrates [120].

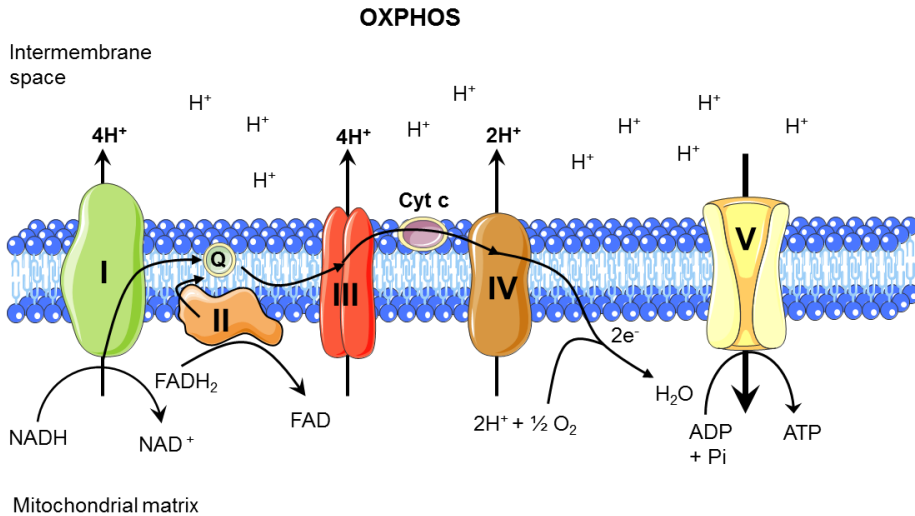


FIGURE 9: Classical view of OXPHOS: Representation of the electron transport chain in the mitochondrial inner membrane. Complexes I and II transfer electrons from NADH and FADH₂, respectively, to complex III via CoQ₁₀ (Q). Complex III transfers electrons to complex IV via cytochrome c (Cyt c). Complex IV uses the electrons to reduce oxygen to water. Complex V uses the proton gradient force created by electron transfer across the inner mitochondrial membrane to synthesize ATP.

III.2.4. REACTIVE OXYGEN SPECIES

ROS are chemical species formed after the incomplete reduction of oxygen, and include peroxides, superoxides, hydroxyl radicals and singlet oxygen [121]. In a biological context, ROS are formed as natural byproducts of oxygen metabolism and play key roles as second messengers in cell signaling and homeostasis [108, 122-124]. ROS levels can increase after environmental stress, and can damage cellular structures by oxidation. ROS can be produced by exogenous insults (drugs, radiation) or endogenously from normal cellular metabolic processes. Mitochondria generate the

majority of endogenous ROS during OXPHOS [109, 125], which under physiological conditions is tightly regulated [126]. Dysfunction in the ETC can lead to a leakage of superoxide anion, which can subsequently be converted to other types of ROS including hydrogen peroxide. ROS can damage cellular proteins, lipids and nucleic acids [105], a phenomenon known as oxidative damage. If too much oxidative damage is present in mitochondria, the cell launches the apoptosis mechanism *via* the pro-apoptotic BCL-2 family and/or cytochrome c pathways. Excessive production of ROS can cause deleterious effects in the organism, which is evident in the human degenerative diseases such as Parkinson or Alzheimer [127, 128]. Mitochondrial dysfunction is a source of ROS that can provoke oxidative damage and induce cellular senescence [129-131].

III.2.5.MITOCHONDRIAL METABOLISM

The mitochondrion is a double membrane organelle found in all eukaryotic organisms, although some cells such as erythrocytes lack mitochondria and use glycolysis to synthesize ATP. The mitochondrial genome is a double-stranded circular molecule of 16659 base pairs and encodes 13 polypeptides involved in OXPHOS [132, 133]. Mitochondria vary considerably in terms of size and structure due to continuous cycles of fission and fusion, termed mitochondrial dynamics, which regulates mitochondrial morphology and function [134]. Mitochondrial fusion and fission not only merges the mitochondrial inner and outer membranes, but also mixes mitochondrial matrices and redistributes mtDNA. Loss of mitochondrial fusion causes a normally connected network to fragment into multiple small mitochondria due to fission [134, 135]. Besides their traditional role as the cellular powerhouse, mitochondria are involved in cellular

signaling and differentiation as well as cell death, cell growth and proliferation [105, 136, 137].

Mutations in either mtDNA genes or in nuclear genes that encode mitochondrial polypeptides required for aerobic ATP production cause a broad and often devastating spectrum of human mitochondrial diseases, which can affect any organ in the body. Tissues with high energetic demand like the CNS or SkM are those mainly affected in mitochondrial diseases [138]. In addition, there is a wide degree of clinical heterogeneity in mitochondrial disease. Some of this heterogeneity can be explained by the fact that cells can contain a variable percentage of mutated mtDNA, the presence of more than one type of mtDNA in the cell is named heteroplasmy and is an important factor of disease severity. Mitochondrial diseases are not only related to the ETC and metabolic disorders, but they can also contribute to cancer and neurodegenerative diseases, such as Parkinson, Alzheimer or Huntington disease [138-142].

III.2.6. COENZYME Q₁₀

CoQ₁₀ was discovered by Festenstein and Crane in the mid-1950s [143, 144] as a redox-active lipophilic molecule present in all eukaryotic species. It is composed of a quinone ring, which provides redox function, connected to a polyisoprenoid side chain of variable length, which anchors it to cellular membranes (**Figure 10A**) (10 in humans, 9 in mice and 6 in yeast) [145, 146]. CoQ₁₀ is found in the plasma membrane and several endomembrane systems. CoQ₁₀ has an essential role in the inner mitochondrial membrane because of its function in the ETC, which is to shuttle electrons from CI and CII to CIII (**Figure 9**). CoQ₁₀ also cooperates in the oxidation of fatty acids, pyrimidine

biosynthesis [147], and opening of the permeability transition pore [148]. It is also one of the main cellular antioxidants [149] and an essential cofactor of uncoupling proteins [146, 150, 151].

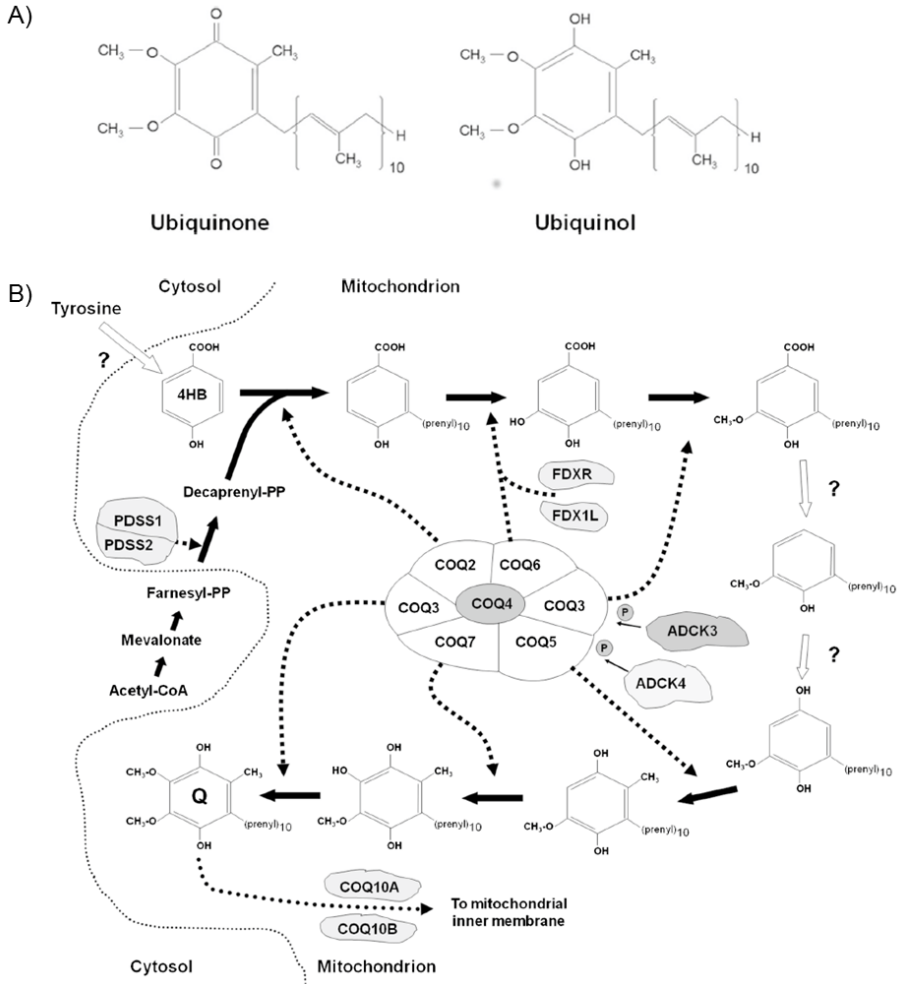


FIGURE 10: CoQ₁₀ structure and biosynthesis. **A)** Structure of the oxidized (ubiquinone) and reduced (ubiquinol) form of CoQ₁₀. **B)** Schematic representation of CoQ₁₀ biosynthesis in mammalian cells. 4-hydroxybenzoate (4HB) is derived from tyrosine. COQ4 has a central structural role in the multienzymatic complex. Several enzymatic steps are still unclear and are represented by question marks. Modified from [145].

CoQ₁₀ biosynthesis is a complex pathway that remains incompletely understood. Proteins encoded by different *COQ* genes are involved in CoQ₁₀ biosynthesis between the cell cytoplasm and mitochondria by multienzymatic complex assembly, the exact composition and organization of which is not completely clear (**Figure 10B**) [145, 152]. The precursor of the quinone ring is 4-hydroxybenzoate, which is derived from tyrosine through a still uncharacterized set of reactions, while the isoprenoid tail is synthesized through the mevalonate pathway by PDSS1/PDSS2 to be condensed to the quinone ring by COQ2. COQ3, COQ5, COQ6 and COQ7 proteins are involved in methylation and decarboxylation, hydroxylation (COQ6 and COQ7), respectively. FDX1L and FDXR provide electrons for COQ6 activity. ADCK3 and ADCK4 are kinases essential for phosphorylation of COQ3, COQ5 and COQ7. COQ9 is a lipid-binding protein necessary to stabilize COQ7. COQ10A/B is most probably a chaperone required for correct localization of CoQ₁₀ within the mitochondrial membrane. The function of COQ4 is still unknown; there is evidence however that is required for the assembly and stability of the multienzymatic complex [145, 153, 154].

III.2.6.1. COENZYME Q₁₀ DEFICIENCY

CoQ₁₀ has been implicated in many common disorders that present with increased oxidative stress, such as neurodegenerative diseases, cancer, diabetes, aging and Alzheimer, among others. However, a specific group of rare conditions has been characterized by a deficiency in CoQ₁₀ [155]. CoQ₁₀ deficiency was described in patients for the first time in 1989 [156], and was associated with a diverse range of clinical phenotypes. The hallmark of this disease is a decrease in the concentration of CoQ₁₀ in muscle and/or fibroblasts below 50% of standard values. CoQ₁₀ deficiency is

considered a rare and heterogeneous group of metabolic/mitochondrial disorders (OMIM #607426) that are frequently diagnosed during childhood [157].

Mutations in COQ genes cause primary CoQ₁₀ deficiency, whereas secondary CoQ₁₀ deficiency is caused by mutations in genes not related to the CoQ₁₀ biosynthetic pathway [154, 157], such as *APTX*, *ETFDH*, *BRAF1*, as well as many mtDNA defects. However, not all mutations in *APTX* or *ETFDH* lead to CoQ₁₀ deficiency, and thus it is unclear why some patients develop the deficiency and other not. Moreover, in all these scenarios CoQ₁₀ deficiency is always a secondary insult and it is not the critical event of the disease [154, 157]. Since the first described case of primary CoQ₁₀ deficiency [156], several mutations in genes involved in CoQ₁₀ biosynthesis have been reported, such as *COQ2* [158-162], *COQ6* [163], *ADCK3* [160, 164, 165], *ADCK4* [166], *COQ9* [160, 167], *PDSSI* [168], *PDSS2* [169] and *COQ7* [170], and all result in a reduction in CoQ₁₀ levels. These conditions are very rare, and the clinical manifestations have been clustered into five main phenotypes: encephalomyopathy, cerebellar ataxia, severe infantile multisystem disorder, nephropathy and isolated myopathy [145, 153, 156-158, 171-183].

III.2.6.2. *COQ4* MUTATIONS

The *COQ4* gene, which contains seven exons spanning approximately 12 kb [184], encodes a component of the CoQ₁₀ biosynthesis pathway. It has been previously suggested that COQ4 has an essential structural role in the biosynthesis of CoQ₁₀ [152, 154, 184]. In addition, several biallelic missense mutations in *COQ4* as well as *COQ4* haploinsufficiency cause a broad spectrum of mitochondrial disorders affecting mainly the CNS and SkM, such as encephalomyopathy, cerebellar atrophy, hypotonia,

respiratory distress and neurological deterioration, among others, which are associated with CoQ₁₀ deficiency with early fatal outcome [175, 176, 178]. The pathogenic role of some identified mutations has been experimentally validated in a recombinant yeast model: null-*COQ4* yeast can be effectively complemented by human *COQ4*. Moreover, yeast have been transformed with mutated variants of human COQ4 to functionally test the effect of some mutations for CoQ₁₀ biosynthesis [175, 184].

III.3.DISEASE MODELING

Human diseases are generally studied once the full genetic, epigenetic and metabolic events are already in place and, therefore, the mechanisms of disease pathophysiology are not amenable to analysis with primary patient samples [9]. In this sense, the advent of iPSC technology has revolutionized biomedical research, opening up unprecedented avenues in developmental biology and also drug screening and disease modeling, which are some of the most promising applications for regenerative medicine. While iPSCs are widely being used in disease modeling, they are envisioned to become a unique tool for disease-specific drug screening, and possibly, patient-specific cell replacement approaches [24]. The full potential of iPSC technology relies on the ability to modify/correct specific genome sequences, with the ultimate goal of personalized therapy. Importantly, genome editing techniques such as CRISPR/Cas9 system offer a new perspective on genome editing, which together with iPSCs may provide a unique *in vitro* model to explore the developmental impact of specific mutations [1, 9, 20, 24].

Fibroblasts are the main source of iPSCs, although other sources of iPSCs have been reported, including CB cells and mature B cells, etc [2, 15, 20, 23, 24]. iPSCs may be differentiated *in vitro* into a variety of cell lineages. Over the last years, many attempts

have been made to optimize various differentiation protocols to achieve a homogeneous and functional cell population [25-29, 89, 93, 185]. The unlimited source of differentiated cells from patient-derived iPSCs would allow the investigation of the initiation and development of diseases *in vitro*. For example, patient-derived iPSCs differentiated *in vitro* and in experimental models *in vivo* can reproduce the patient's phenotype in some neural diseases, such as retinitis pigmentosa [186], frontotemporal dementia [187] or Rett syndrome [188, 189]. Additionally, iPSC-derived neurons from Parkinson patients manifested autophagy dysfunction [190] or oxidative damage [127]. A comprehensive study using monozygotic twins demonstrated that iPSC-derived neurons are more affected in the diseased twin than in the healthy twin, revealing the significance of this model [191]. Moreover, non-neural diseases are also recapitulated with *in vitro* iPSC differentiation, such as Fanconi anemia, progeria and familial cancers, among others [24, 192-195].

As stated earlier, CoQ₁₀ deficiency is a heterogeneous disease that leads to encephalomyopathies because the disruption in energy metabolism affects tissues with high-energy demands such as the CNS and SkM. Since many *COQ* genes have been implicated in primary CoQ₁₀ deficiency, the molecular diagnosis and clinical heterogeneity remains challenging. To date, there is no clear genotype-phenotype association [145, 153], and the only current treatment is CoQ₁₀ supplementation, which is usually variable in the patients and is a demanding treatment [145, 177]. It is therefore an ideal candidate disease to be reproduced with iPSCs to gain insight into the developmental impact of *COQ4* mutations in mitochondrial dynamics, CoQ₁₀ biosynthesis and also in the observed neuronal and SkM phenotypes.

III.4. CRISPR/CAS9: A UNIQUE AND UNPRECEDENTED TOOL FOR GENE EDITING

CRISPR/Cas9 systems are genetic hallmarks of adaptive immunity in bacteria and archaea that have evolved to target and eliminate invading genetic elements such as viruses and plasmids [196]. During last few years, the CRISPR/Cas9 system has become a powerful tool for basic and applied science. Among the increasing numbers of papers published in the field, one of the latest studies has utilized this system as a tool to track RNAs in living cells, exploiting the inactivated-nuclease activity of Cas9 to bind in the cell to RNA [197], thus expanding the utility of such a methodology.

CRISPR/Cas9 specification is based on RNA-DNA recognition. Several delivery systems, such as lentiviral transduction, electroporation and transfection, have been employed to introduce the small guide RNAs (sgRNA) and the Cas9 protein into cells. Cas9 is a nuclease that is guided by ~20 nucleotides sgRNAs towards a specific DNA cleavage site, which is three nucleotides upstream of the protospacer-adjacent motif (PAM) (5'-NGG-3'), introducing a double-strand break (DSB) [198, 199]. The DSBs generated by CRISPR are preferentially repaired by non-homologous end joining (NHEJ), which is an error-prone process and thus useful to introduce insertions and deletions into mammalian cells. In addition, DSBs are resolved at a lower frequency by homology direct repair (HDR) and therefore can be used to modify endogenous loci, such as generating point mutations, inserting genes or DNA editing. HDR can be influenced by the presence of an exogenous template, which can either be in a double-stranded DNA with homology arms flanking the insertion sequence, or single-stranded DNA (**Figure 11**). Generation of DSBs in off-target locations can occur because

gRNAs bind to a nonspecific DNA sequences similar to the target site. To increase the specificity of Cas9-mediated genome editing, a Cas9 has been developed with nickase activity to enhance HDR over NHEJ [200, 201]. The CRISPR/Cas9 system has been used recently to repair a wide range of monogenic diseases both in human and mouse models [202-206].

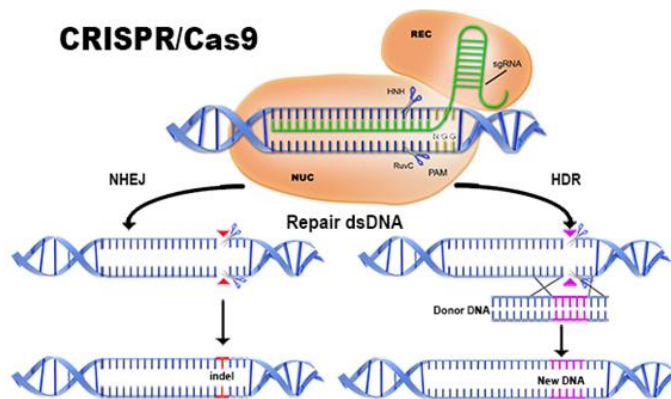


FIGURE 11: Representative cartoon of CRISPR/Cas9 system and dsDNA repair after the formation of a double-strand break (DSB). NUC: DNA nuclease Cas9. NHEJ: non-homologous end joining. HDR: homology direct repair. PAM: protospacer-adjacent motif Modified from Advanced analytical (<http://www.aati-us.com>).

III.5.ARTICLE I:

Concise review: Generation of neurons from somatic cells of healthy individuals and neurological patients through induced pluripotency or direct conversion.

Velasco I, Salazar P, Giorgetti A, Ramos-Mejía V, Castaño J, **Romero-Moya D**, Menendez P.

Stem Cells. 2014; 32(11):2811-7.

Concise Review: Generation of Neurons From Somatic Cells of Healthy Individuals and Neurological Patients Through Induced Pluripotency or Direct Conversion

IVAN VELASCO,^{a,b} PATRICIA SALAZAR,^{a,b} ALESSANDRA GIORGETTI,^c VERÓNICA RAMOS-MEJÍA,^b JULIO CASTANO,^c DAMIA ROMERO-MOYA,^c PABLO MENENDEZ^{c,d}

Key Words. Induced pluripotent stem cells • Neural differentiation • Induced neurons • Direct conversion • Neurodegenerative diseases • Genome editing

^aInstituto de Fisiología Celular-Neurociencias, Universidad Nacional Autónoma de México, México, D.F., México; ^bCentro GENYO, Granada, Spain; ^cJosep Carreras Leukemia Research Institute, Cell Therapy Program, University of Barcelona, Barcelona, Spain; ^dInstitució Catalana de Recerca i Estudis Avançats (ICREA), Barcelona, Spain

Correspondence: Pablo Menéndez, Ph.D., MBA, ICREA Research Professor, Josep Carreras Leukemia Research Institute, Facultat de Medicina, University of Barcelona, Carrer Casanova 143, 08036 Barcelona, Spain. Telephone: +34 93 557 2809; Fax: +34 93 323 1751; e-mail: pmenendez@carreerasresearch.org; or Iván Velasco, Ph.D., Instituto de Fisiología Celular-Neurociencias, Universidad Nacional Autónoma de México, Circuito Exterior S/ N, Ciudad Universitaria, México, D.F. 04510, México. Telephone: +52 55 5622 5649; Fax: +52 55 5622 5607; e-mail: ivelasco@ifc.unam.mx

Received April 7, 2014; accepted for publication June 4, 2014; first published online in STEM CELLS EXPRESS July 3, 2014.

© 2014 The Authors. STEM CELLS Published by Wiley Periodicals, Inc. on behalf of AlphaMed Press 1066-5099/2014/\$30.00/0

<http://dx.doi.org/10.1002/stem.1782>

This is an open access article under the terms of the Creative Commons Attribution License, which permits use, distribution and reproduction in any medium, provided the original work is properly cited.

ABSTRACT

Access to healthy or diseased human neural tissue is a daunting task and represents a barrier for advancing our understanding about the cellular, genetic, and molecular mechanisms underlying neurogenesis and neurodegeneration. Reprogramming of somatic cells to pluripotency by transient expression of transcription factors was achieved a few years ago. Induced pluripotent stem cells (iPSC) from both healthy individuals and patients suffering from debilitating, life-threatening neurological diseases have been differentiated into several specific neuronal subtypes. An alternative emerging approach is the direct conversion of somatic cells (i.e., fibroblasts, blood cells, or glial cells) into neuron-like cells. However, to what extent neuronal direct conversion of diseased somatic cells can be achieved remains an open question. Optimization of current expansion and differentiation approaches is highly demanded to increase the differentiation efficiency of specific phenotypes of functional neurons from iPSCs or through somatic cell direct conversion. The realization of the full potential of iPSCs relies on the ability to precisely modify specific genome sequences. Genome editing technologies including zinc finger nucleases, transcription activator-like effector nucleases, and clustered regularly interspaced short palindromic repeat/CAS9 RNA-guided nucleases have progressed very fast over the last years. The combination of genome-editing strategies and patient-specific iPSC biology will offer a unique platform for in vitro generation of diseased and corrected neural derivatives for personalized therapies, disease modeling and drug screening. STEM CELLS 2014;32:2811–2817

INDUCED PLURIPOTENCY

Pluripotency is defined by the ability to produce from a single undifferentiated cell type, cell derivatives representing the three germ layers: meso-, endo-, and ectoderm. Pluripotent stem cells (PSCs) of human origin were first isolated from teratocarcinomas, giving rise to embryonal carcinoma cell lines [1]. This property is expected to be present in cells giving rise to gametes during human development and thus, pluripotent embryonic germ cells were described in 1998 [2]. The most widely used PSCs of mammalian origin are mouse embryonic stem cells (ESCs), derived from the inner cell mass of preimplantation embryos at the blastocyst stage [3, 4]. Using a similar approach, human ESCs (hESCs) were isolated from embryos almost 2 decades later [5]. During human development, germline cells undergo meiosis to produce gametes. The remaining cellular types are known as somatic

cells, and they do not contribute to reproductive tissues. Early work has shown that misexpression of MyoD can convert cell fate between germ layers [6, 7]. Similarly, ectopic expression of master lineage-specific transcriptional regulators allows cells to change from one blood lineage to another [8]. However, it was not recognized until recently how relatively easy is for a terminally differentiated somatic cell to re-acquire pluripotency properties or change cell fate across germ layers.

Successful reprogramming of somatic cells to a pluripotent state by transient expression of four transcription factors (OCT4, SOX2, KLF4, and c-MYC) was achieved for the first time with mouse cells in 2006 [9] and with human fibroblasts in 2007 [10, 11] using retroviral vectors. Many researchers have produced induced pluripotent stem cells (iPSCs) by expressing the Yamanaka factors through integrative or nonintegrative methods. Among the former, retroviral and lentiviral vectors are the

©2014 The Authors. STEM CELLS Published by Wiley Periodicals, Inc. on behalf of AlphaMed Press

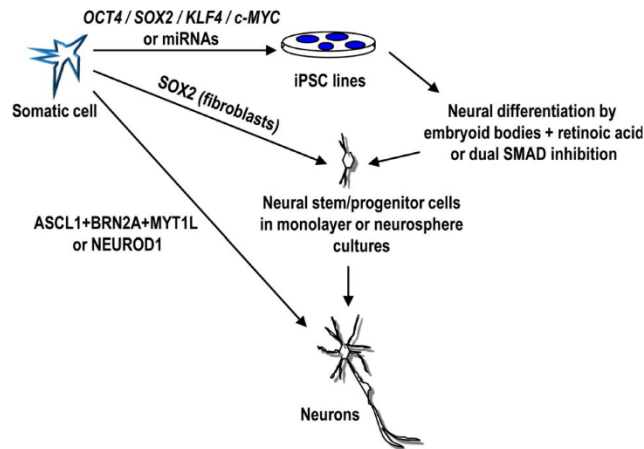


Figure 1. Scheme showing the different methods to produce neurons from a somatic non-neuronal cell. Neural differentiation from human iPSCs requires neural inducers, such as formation of embryoid bodies combined with stimulation with retinoic acid or inhibition of transforming growth factor- β and bone morphogenic proteins (dual SMAD inhibition), followed by expansion of neural stem/progenitor cells in monolayer or neurosphere cultures. Alternatively, fibroblasts, cord blood cells, or astrocytes can be directly converted to neurons, either in vitro or in vivo. Abbreviations: miRNAs, microRNAs; iPSC, induced pluripotent stem cell.

most widely used [12]. Induced pluripotency requires endogenous activation of a pluripotency-associated gene expression signature and a concomitant silencing of ectopic reprogramming factors. Genomic integration of these transgenes is random and becomes epigenetically regulated so that their residual expression after long-term culture due to a lack of complete silencing may prevent subsequent differentiation [13] and make iPSCs prone to genomic alterations [14]. The most common nonintegrative methodologies include Sendai virus (SeV) [15], mRNA [16], plasmid DNA [17], or introduction of the recombinant proteins into somatic cells [16]. Also, small molecules [18] can substitute some reprogramming genes. Interestingly, microRNAs (miR) [19, 20] can produce iPSCs on their own, without the pluripotency reprogramming genes. It is especially relevant the ability of miR-302 to contribute to iPSCs generation, which is in line with the well-established role of miR-302 as a key regulator of pluripotency in hESCs [21–25].

However, the generation of iPSCs is still inefficient, yielding a low proportion of reprogrammed cells [18]. Many small molecules and epigenetic remodeling drugs have been reported to increase iPSC efficiency [26]. However, how these ectopic factors can make a somatic cell to travel back in development and become pluripotent through epigenetic reprogramming remains elusive. Cellular reprogramming is assumed to be a stressful cellular process. In fact, during the reprogramming process several genomic insults including coding mutations, insertions/deletions (indels), and chromosomal rearrangements occur. This genomic instability may activate the DNA damage response (DDR) which may in turn contribute to a selection of specific clones during reprogramming to pluripotency [27–29]. Also, whether or not induced pluripo-

tency is a purely stochastic process remains controversial [30]. There are important regulators of this process, such as p53 [31–33] and Mbd3. Indeed, inhibition of Mbd3 allowed a reprogramming efficiency of almost 100% [34]. Recently, differences in cell cycle length allowed the identification of rapid-cycling cells as responsible for the bulk of reprogrammed cells [35]. Together, although many technical and biological questions about the cellular, molecular, and epigenetic mechanisms underlying reprogramming remain elusive, making induced reprogramming an obscure and low efficient process, human iPSCs (hiPSCs) have revolutionized biomedical research opening up unprecedented avenues in developmental biology, drug screening, and disease modeling. Because access to healthy or diseased human neural tissue is a challenge and limits our understanding on neurogenesis and neurodegeneration, diseases affecting the central nervous system might particularly benefit from iPSC biology.

NEURAL DIFFERENTIATION OF PSCs

Several protocols for neuronal differentiation of human PSCs, including iPSCs, have been reported. Neural commitment of PSCs can be achieved through formation of embryoid bodies and treatment with retinoic acid, a neuroectoderm inducer, or by pharmacological inhibition of transforming growth factor- β and bone morphogenic protein pathways (dual SMAD inhibition). The resulting neural stem/progenitor cells can be expanded either attached to a substrate or as floating neurospheres to be further exposed to growth factors inducing specific neuronal subtypes (i.e., spinal motor, cerebellar, dopaminergic, or cortical interneurons) [36–40] (Fig. 1). For

instance, motor neuron differentiation of hESCs and hiPSCs has been refined to a point that spinal lateral column phenotypes can be obtained [36, 41]. Similarly, for dopaminergic neurons, midbrain phenotypes can be successfully produced in high yields from hESCs and hiPSCs [38, 39]. These human PSC (hPSC)-derived neurons were transplanted in animal models of neurological disease where survived and contributed to the partial recovery of several neurological parameters, including behavior. These results should encourage us to further explore hPSC-derived neurons in preclinical settings [42]. Beyond potential cell therapy applications, hPSC-derived neurons open up new avenues in drug screening and disease modeling applications.

Induced PSCs have been generated from biopsies of patients harboring mutations associated to amyotrophic lateral sclerosis [41], spinal muscular atrophy [43, 44], Parkinson disease [45, 46], Alzheimer disease [47], and Rett syndrome [48]. Some of these patient/disease-specific iPSCs give rise, under proper inductive conditions, to the affected neuronal subtype, opening up new avenues to explore: (a) the potential of these neurons to graft the patient in an autologous setting, provided the procedure is safe and effective, (b) the *in vitro* neuronal differentiation of mutated iPSC as a disease model to unravel the developmental, cellular, and molecular mechanisms underlying the disease onset and progression, and (c) large-scale drug screening aimed at restoring impaired functions or preventing neuronal degeneration. In fact, long-term culture of dopamine neurons differentiated from mutant Parkinson hiPSCs showed increased apoptosis and decreased number and shorter neurites [45]. In another study, Parkinson patient-specific iPSC were generated and differentiated into neural derivatives that were challenged with mitochondrial stressors, revealing an increased susceptibility as compared to neural cells from control iPSCs. Furthermore, supplementation of the culture medium with the antioxidant coenzyme Q10 or rapamycin caused partial protection against neural degeneration [49]. These studies underscore the potential of iPSCs and iPSC-neural derivatives to gain insights into the underlying mechanisms of neurodegeneration and to explore them as a biological platform to screen potential therapeutic molecules, eventually contributing to the development of novel pharmacological approaches.

Collections of patient/disease-specific hiPSCs, including neurological conditions [50], will be of utmost value to advance our understanding of the disease. Furthermore, an initiative for public banking of diseased fibroblasts from patients with mutations related to neurodegenerative diseases is already ongoing [51]. It will be important to consider both sporadic and familial forms of neurological diseases to allow comparisons among patients and mutations in order to identify common and distinct mechanisms underlying the disease pathogenesis as well as wide-acting drugs. However, the generation of functional neurons from hPSCs, namely cells that express markers of neuronal differentiation (β -III tubulin, microtubule associated protein-2, or NeuN), fire action potentials, synthesize and release neurotransmitters and form synapses with neighboring neurons, often requires extended periods of culture and the available protocols are complex and suffer from high variability. Recently, lineage priming to neurons from hESCs and iPSCs was induced by forced expression of a single transcription factor (either NEUROGENIN-2 or

NEUROD1) which resulted in the emergence of mature neurons within 2 weeks, speeding up significantly the time required to obtain mature human neurons *in vitro* [52]. Besides differentiation efficiency, a homogeneous population of lineage-specific cells (i.e., neuronal populations) from hPSCs must be eventually obtained to prevent the presence in the culture of residual undifferentiated cells which may exert undesired/misleading effects both *in vitro* and *in vivo*.

DIRECT CONVERSION OF SOMATIC CELLS INTO NEURONS

After the seminal reprogramming work of Yamanaka and coworkers, other investigators started testing the hypothesis that expression of transcriptional regulators might act as neural cell determinants to non-neural differentiated somatic cells. Indeed, ectopic expression of *ASCL1*, *BRN2A*, and *MYT1L* turned fibroblasts directly (no pluripotent stage involved) into induced neurons (iNs) [53, 54] (Fig. 1). Expression of additional neural lineage-specific transcriptional regulators further promoted the conversion of human fibroblasts into dopamine [55, 56] and motor neurons [57]. Interestingly, although this direct conversion into iNs rarely requires the neural progenitor state, human fibroblasts can also be induced by the sole expression of *SOX2* to become multipotent neural stem cells, able to differentiate into neurons, astrocytes, and oligodendroglia [58]. Direct conversion of fibroblasts into iNs usually requires a skin biopsy that is expanded in culture to generate enough starting material. Therefore, the use of a more accessible source in medical diagnostic procedures, such as blood, would be highly advantageous. In fact, cord blood stem cells have been recently reprogrammed into iNs by forced expression of *SOX2* and *c-MYC* [59]. This work showed for the first time that cells from mesodermal origin can be switched to an ectodermal fate with only two transcription factors. The procedure for generating iNs relies on the use of integrative vectors, and similar to the production of hiPSCs, is rather complex and inefficient. Recently, some progress has been made in direct reprogramming of non-human primate fibroblasts into region-specific neural progenitors through transient expression of the four Yamanaka factors using nonintegrative SeV in combination with specific neural culture conditions [60]. These results represent an important technical progress for the generation of iNs, although the presence of a pluripotent intermediate cellular stage cannot be ruled out in these experiments, and the process continues to be quite inefficient. Because SeV vectors seem to be one of the most efficient nonintegrative strategies for reprogramming blood cells into iPSCs [61, 62] it will be of interest to determine if delivery of *SOX2* and *c-MYC* by means of SeV transduction might enhance the direct reprogramming efficiency of blood cells into iNs. Blood-derived iNs could provide a unique tool for drug screening and will facilitate the development of a cellular platform for the generation of patient-specific neuronal cells for future biomedical applications.

Direct conversion of non-neuronal cells into neurons is also possible *in vivo*. Human fibroblasts or astrocytes engineered to express doxycycline-inducible *ASCL1*, *BRN2A*, and *MYT1L* are converted into neurons within the rodent brain after doxycycline addition. Interestingly, endogenous brain astrocytes were also converted into iNs highlighting a spec-

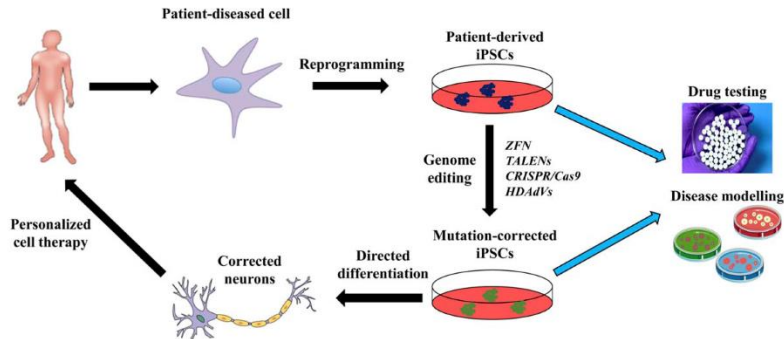


Figure 2. Cartoon depicting the strategy for combining genome editing and patient-specific human iPSCs (hiPSCs) for in vitro generation of diseased and corrected lineage-specific derivatives for disease modeling and drug screening. Studies on disease modeling and drug screening should be undertaken in parallel on both diseased and genetically corrected cell lines. Due to the high variability existing among hiPSC lines derived from distinct starting cells, using different methods, and from different genetic backgrounds, the use of an isogenic mutation-corrected iPSC line is essential as a control. Abbreviations: CRISPR/CAS9, clustered regularly interspaced short palindromic repeat/CAS9 RNA-guided nucleases; HDAdV, helper-dependent adenoviral vectors; iPSCs, induced pluripotent stem cells; TALENs, transcription activator-like effector nucleases; ZFN, zinc finger nucleases.

independent direct conversion [63]. In a similar approach, NeuroD1 transduction of reactive astrocytes and oligodendrocytes present after acute brain damage or as a consequence of a chronic damage in a transgenic Alzheimer disease mouse model also rendered iNs in vivo. Notably, astrocyte-derived iNS mainly produced glutamatergic neurons whereas oligodendrocyte-derived iNs generated both glutamatergic and gabaergic neurons [64]. To what extent neuronal direct conversion is possible in other diseased somatic non-neural cells remains an open question. While these results are promising, the field has yet to clearly address how much these iNs resemble to neurons/neural progenitors and whether iNs retain epigenetic memory; that is, they retain gene expression and epigenetic profiles similar to the donor cell type (fibroblasts, hematopoietic cells and astrocytes) that was originally reprogrammed. This epigenetic memory is crucial since it may influence subsequent differentiation potential. Taken together, integration of technical and biological expertise gained from hiPSCs and hiNs will boost our ability to move the field forward facilitating the implementation of disease modeling and drug screening applications. Eventually, the realization of the full potential of iPSCs/iNs relies on the ability to improve the reprogramming/direct conversion and combine efficient differentiation protocols with the precise modification of specific genome sequences.

TARGETED GENOME EDITING IN HUMAN iPSCS

hiPSCs are widely being used in developmental biology and disease modeling. However, they are envisioned to become a unique tool for disease-specific drug screening, and possibly, a patient-specific cell replacement approach [65] (Fig. 2). However, the realization of the full potential of hiPSCs relies on the ability to precisely modify/correct specific genome sequences, with a prospect of personalized cell therapy.

Importantly, genome editing in hPSCs has evolved from being a daunting task to a widely spread procedure in worldwide laboratories. The reasons for this are twofold: (a) human PSCs are especially amenable for genome editing since they can undergo extensive culture manipulations, such as drug selection and clonal expansion, while still maintaining their pluripotency and genome stability [66], and (b) genome editing technology has progressed extremely rapid over the last few years including zinc finger nucleases (ZFNs), transcription activator-like effector nucleases (TALENs), clustered regularly interspaced short palindromic repeat/CAS9 RNA-guided nucleases (CRISPR/CAS9) (Table 1), and helper-dependent adenoviral vectors (HDAdVs). An important aspect is that cells that have undergone genome editing should contain only the intended change in an otherwise isogenic background, thus providing the most stringent test of gene function. However, this may not be the case due to off-target effects of ZFNs, TALENs, and CRISPR/CAS9. However, these genome-editing tools are under continuous improvement [67, 68]. The biological mechanisms underlying these genome-editing tools in human PSCs cannot be covered in this review due to space constraints, but they have been extensively and elegantly reviewed elsewhere [66]. Table 1 summarizes the differential biological and technical features of cutting-edge main genome-editing approaches. Although only a minority of the neurodegenerative diseases is caused by a specific identified mutation, there are examples showing the potential of genome editing in iPSC for neurological diseases.

Huntington disease is caused by expansion of a polyglutamine motif in HUNTINGTIN. Through homologous recombination in iPSCs, the number of glutamines in this protein was reduced, resulting in decreased apoptosis and improvement in oxygen consumption rate in corrected neural progenitors [69]. Spinal muscular atrophy is a genetic autosomal recessive disease caused by mutations of the *SMN2* gene which results in a nonfunctional protein causing motor neuron

Table 1. Main biological-technical features of genome-editing technologies

Feature	ZFNs	TALENs	CRISPR/CAS
Type of recognition	Protein-DNA	Protein-DNA	RNA-DNA
Mechanism of action	Induces DSB	Induces DSB	Induces DSB and SSB (nickase)
Design/construction	Intermediate/easy	Simple/easy	Very simple/very easy
Success rate	Low	Moderate	High
Methylation sensitive	Not sensitive	Sensitive	Not sensitive
Multiplexing/high-throughput	No	Feasible (but technically challenging)	Yes
Off-target effects	Common	Few	Common (few with nickase)
Toxicity	Variable	Low	Low
Cost	High	Moderate	Very low

Abbreviations: CRISPR/CAS, clustered regularly interspaced short palindromic repeat/CAS9 RNA-guided nucleases; DSB, double strand breaks; SSB, single strand breaks; TALENs, transcription activator-like effector nucleases; ZFNs, zinc finger nucleases.

degeneration. As a compensatory mechanism, these patients rely on the expression of *SMN2*, which is highly homologous to *SMN1* but has a change in a nucleotide that alters its splicing, with a consequent reduction in the amount of SMN produced. Using single-stranded DNA sequences, editing of the *SMN2* was performed, resulting in a *SMN1*-like protein that includes the exon 7. This change was shown to be stable and correlated with increased motor neuron survival in repaired cells [43]. Recently, ZFN-mediated genome editing and iPSC technology were combined to generate sets of isogenic diseased and control hiPSCs that differ exclusively at either of two susceptibility variants for Parkinson's disease by modifying the underlying point mutations in the α -synuclein gene [46]. In addition, a point mutation related to familial Parkinson has been corrected using HDAdVs. Notably, these diseased hiPSCs produced neural stem cells that showed alterations in the nuclear architecture, a finding that was not previously reported as related to this pathology. Genetic correction of hiPSCs resulted in normalization of the nuclear alterations, decreased susceptibility to apoptosis, as well as increased neuronal production [70]. The robust capability to genetically correct Parkinson disease-causing point mutations in patient-derived hiPSCs represents a noteworthy progress in basic neurosciences, and a significant advance toward hiPSC-based cell replacement therapies and drug testing. Whether or not the corrected neurons will survive after transplantation in the altered central nervous system (environment) represents a next level of complexity that still needs to be addressed.

CONCLUSION

Over the last decade we have witnessed significant progress in both our understanding of cell fate determinants and also in the possibilities to use reprogramming in the preclinical setting. The generation of human neurons by these methodol-

ogies will definitely allow the analysis of the mechanisms causing familial and sporadic cases of neurological conditions. Patients therefore can benefit from in vitro differentiated neurons and specific drugs identified by high-throughput screening. If genome editing turns out to be safe and effective, we envision a future prospective production of clinically relevant neuronal types within the brain of affected people. Whether or not the synaptic communication will be re-established properly in the diseased brain is a different question, but repopulation of the affected neuronal phenotype, either by transplantation of differentiated neurons or by direct conversion of resident glial cells is a very encouraging step forward.

ACKNOWLEDGMENTS

This work was supported by the E-Rare-ERA-NET/ISCIII (PI12/03112) and the MINECO (SAF2013-43065) to P.M. I.V. was supported by Conacyt (sabbatical fellowship in P.M. lab and CB-131281) and Dirección General de Asuntos de Personal Académico (PASPA and PAPIIT IN208713), Universidad Nacional Autónoma de México. D.R.-M. was supported by PFIS scholarship (F111/0511). P.M. also acknowledges the financial support of the Obra Social La Caixa-Fundació Josep Carreras, Spanish Association against Cancer and Fundación Sandra Ibarra.

AUTHOR CONTRIBUTIONS

All the authors contributed to conception and design, data collection and assembly, and manuscript writing. All authors approved submission.

DISCLOSURE OF POTENTIAL CONFLICT OF INTEREST

The authors indicate no potential conflict of interest.

REFERENCES

- Martin GR. Teratocarcinomas and mammalian embryogenesis. *Science* 1980;209:768-776.
- Shamblott IJ, Axelman J, Wang S et al. Derivation of pluripotent stem cells from cultured human primordial germ cells. *Proc Natl Acad Sci USA* 1998;95:13726-13731.
- Evans MJ, Kaufman MH. Establishment in culture of pluripotential cells from mouse embryos. *Nature* 1981;292:154-156.

- Martin GR. Isolation of a pluripotent cell line from early mouse embryos cultured in medium conditioned by teratocarcinoma stem cells. *Proc Natl Acad Sci USA* 1981;78:7634-7638.
- Thomson JA, Itskovitz-Eldor J, Shapiro SS et al. Embryonic stem cell lines derived from human blastocysts. *Science* 1998;282:1145-1147.
- Ludolph DC, Neff AW, Mescher AL et al. Overexpression of XMyoD or XMyf5 in Xenopus embryos induces the formation of

- enlarged myotomes through recruitment of cells of nonsomitic lineage. *Dev Biol* 1994;166:18-33.
- Yutzey KE, Rhodes SJ, Konieczny SF. Differential trans activation associated with the muscle regulatory factors MyoD1, myogenin, and MRF4. *Mol Cell Biol* 1990;10:3934-3944.
- Graf T, Enver T. Forcing cells to change lineages. *Nature* 2009;462:587-594.
- Takahashi K, Yamanaka S. Induction of pluripotent stem cells from mouse embryonic



- and adult fibroblast cultures by defined factors. *Cell* 2006;126:663–676.
- 10 Takahashi K, Tanabe K, Ohnuki M et al. Induction of pluripotent stem cells from adult human fibroblasts by defined factors. *Cell* 2007;131:861–872.
- 11 Yu J, Vodyanik MA, Smuga-Otto K et al. Induced pluripotent stem cell lines derived from human somatic cells. *Science* 2007;318:1917–1920.
- 12 Malik N, Rao MS. A review of the methods for human iPSC derivation. *Methods Mol Biol* 2013;997:23–33.
- 13 Ramos-Mejia V, Montes R, Bueno C et al. Residual expression of the reprogramming factors prevents differentiation of iPSC generated from human fibroblasts and cord blood CD34+ progenitors. *PLoS One* 2012;7:e35824.
- 14 Ramos-Mejia V, Munoz-Lopez M, Garcia-Perez JL et al. iPSC lines that do not silence the expression of the ectopic reprogramming factors may display enhanced propensity to genomic instability. *Cell Res* 2010;20:1092–1095.
- 15 Nakanishi M, Otsu M. Development of Sendai virus vectors and their potential applications in gene therapy and regenerative medicine. *Curr Gene Ther* 2012;12:410–416.
- 16 Schott JW, Galla M, Godinho T et al. Viral and non-viral approaches for transient delivery of mRNA and proteins. *Curr Gene Ther* 2011;11:382–398.
- 17 Okita K, Nakagawa M, Hyenjong H et al. Generation of mouse induced pluripotent stem cells without viral vectors. *Science* 2008;322:949–953.
- 18 Lorenzo IM, Fleischer A, Bachiller D. Generation of mouse and human induced pluripotent stem cells (iPSC) from primary somatic cells. *Stem Cell Rev* 2013;9:435–450.
- 19 Anokye-Danso F, Trivedi CM, Juhr D et al. Highly efficient miRNA-mediated reprogramming of mouse and human somatic cells to pluripotency. *Cell Stem Cell* 2011;8:376–388.
- 20 Miyoshi N, Ishii H, Nagano H et al. Reprogramming of mouse and human cells to pluripotency using mature microRNAs. *Cell Stem Cell* 2011;8:633–638.
- 21 Barroso-del Jesus A, Lucena-Aguilar G, Menendez P. The miR-302–367 cluster as a potential stemness regulator in ESCs. *Cell Cycle* 2009;8:394–398.
- 22 Barroso-delJesus A, Lucena-Aguilar G, Sanchez L et al. The Nodal inhibitor Lefty is negatively modulated by the microRNA miR-302 in human embryonic stem cells. *FASEB J* 2011;25:1497–1508.
- 23 Barroso-delJesus A, Romero-Lopez C, Lucena-Aguilar G et al. Embryonic stem cell-specific miR302–367 cluster: Human gene structure and functional characterization of its core promoter. *Mol Cell Biol* 2008;28:6609–6619.
- 24 Card DA, Hebbard PB, Li L et al. Oct4/Sox2-regulated miR-302 targets cyclin D1 in human embryonic stem cells. *Mol Cell Biol* 2008;28:6426–6438.
- 25 Rosa A, Brivanlou AH. A regulatory circuitry comprised of miR-302 and the transcription factors OCT4 and NR2F2 regulates human embryonic stem cell differentiation. *EMBO J* 2011;30:237–248.
- 26 Onder TT, Kara N, Cherry A et al. Chromatin-modifying enzymes as modulators of reprogramming. *Nature* 2012;483:598–602.
- 27 Gore A, Li Z, Fung HL et al. Somatic coding mutations in human induced pluripotent stem cells. *Nature* 2011;471:63–67.
- 28 Hussein SM, Batada NN, Vuoristo S et al. Copy number variation and selection during reprogramming to pluripotency. *Nature* 2011;471:58–62.
- 29 Pasi CE, Derelli-Oz A, Negrini S et al. Genomic instability in induced stem cells. *Cell Death Differ* 2011;18:745–753.
- 30 Hanna JH, Saha K, Jaenisch R. Pluripotency and cellular reprogramming: Facts, hypotheses, unresolved issues. *Cell* 2010;143:508–525.
- 31 Hong H, Takahashi K, Ichisaka T et al. Suppression of induced pluripotent stem cell generation by the p53-p21 pathway. *Nature* 2009;460:1132–1135.
- 32 Kawamura T, Suzuki J, Wang YV et al. Linking the p53 tumour suppressor pathway to somatic cell reprogramming. *Nature* 2009;460:1140–1144.
- 33 Marion RM, Strati K, Li H et al. A p53-mediated DNA damage response limits reprogramming to ensure iPSC cell genomic integrity. *Nature* 2009;460:1149–1153.
- 34 Rais Y, Zviran A, Geula S et al. Deterministic direct reprogramming of somatic cells to pluripotency. *Nature* 2013;502:65–70.
- 35 Guo S, Zi X, Schulz VP et al. Nonstochastic reprogramming from a privileged somatic cell state. *Cell* 2014;156:649–662.
- 36 Amoroso MW, Croft GF, Williams DJ et al. Accelerated high-yield generation of limb-innervating motor neurons from human stem cells. *J Neurosci* 2013;33:574–586.
- 37 Erceg S, Ronaghi M, Zipancic I et al. Efficient differentiation of human embryonic stem cells into functional cerebellar-like cells. *Stem Cells Dev* 2010;19:1745–1756.
- 38 Jaeger I, Arber C, Risner-Janiczek JR et al. Temporally controlled modulation of FGF/ERK signaling directs midbrain dopaminergic neural progenitor fate in mouse and human pluripotent stem cells. *Development* 2011;138:4363–4374.
- 39 Kriks S, Shim JW, Piao J et al. Dopamine neurons derived from human ES cells efficiently engraft in animal models of Parkinson's disease. *Nature* 2011;480:547–551.
- 40 Maroof AM, Keros S, Tyson JA et al. Directed differentiation and functional maturation of cortical interneurons from human embryonic stem cells. *Cell Stem Cell* 2013;12:559–572.
- 41 Dimos JT, Rodolfa KT, Niakan KK et al. Induced pluripotent stem cells generated from patients with ALS can be differentiated into motor neurons. *Science* 2008;321:1218–1221.
- 42 Lopez-Gonzalez R, Velasco I. Therapeutic potential of motor neurons differentiated from embryonic stem cells and induced pluripotent stem cells. *Arch Med Res* 2012;43:1–10.
- 43 Corti S, Nizzardo M, Simone C et al. Genetic correction of human induced pluripotent stem cells from patients with spinal muscular atrophy. *Sci Transl Med* 2012;4:165ra162.
- 44 Ebert AD, Yu J, Rose FF, Jr. et al. Induced pluripotent stem cells from a spinal muscular atrophy patient. *Nature* 2009;457:277–280.
- 45 Sanchez-Danes A, Richaud-Patin Y, Carballo-Carbajal I et al. Disease-specific phenotypes in dopamine neurons from human iPSC-based models of genetic and sporadic Parkinson's disease. *EMBO Mol Med* 2012;4:380–395.
- 46 Soldner F, Laganier J, Cheng AW et al. Generation of isogenic pluripotent stem cells differing exclusively at two early onset Parkinson point mutations. *Cell* 2011;146:318–331.
- 47 Israel MA, Yuan SH, Bardy C et al. Probing sporadic and familial Alzheimer's disease using induced pluripotent stem cells. *Nature* 2012;482:216–220.
- 48 Marchetto MC, Carromeu C, Acab A et al. A model for neural development and treatment of Rett syndrome using human induced pluripotent stem cells. *Cell* 2010;143:527–539.
- 49 Cooper O, Seo H, Andrabi S et al. Pharmacological rescue of mitochondrial deficits in iPSC-derived neural cells from patients with familial Parkinson's disease. *Sci Transl Med* 2012;4:141ra190.
- 50 Park IH, Arora N, Huo H et al. Disease-specific induced pluripotent stem cells. *Cell* 2008;134:877–886.
- 51 Wray S, Self M, Consortium NPsDi et al. Creation of an open-access, mutation-defined fibroblast resource for neurological disease research. *PLoS One* 2012;7:e43099.
- 52 Zhang Y, Pak C, Han Y et al. Rapid single-step induction of functional neurons from human pluripotent stem cells. *Neuron* 2013;78:785–798.
- 53 Pang ZP, Yang N, Vierbuchen T et al. Induction of human neuronal cells by defined transcription factors. *Nature* 2011;476:220–223.
- 54 Vierbuchen T, Ostermeier A, Pang ZP et al. Direct conversion of fibroblasts to functional neurons by defined factors. *Nature* 2010;463:1035–1041.
- 55 Caiazzo M, Dell'Anno MT, Dvoretzskova E et al. Direct generation of functional dopaminergic neurons from mouse and human fibroblasts. *Nature* 2011;476:224–227.
- 56 Pfisterer U, Kirkeby A, Torper O et al. Direct conversion of human fibroblasts to dopaminergic neurons. *Proc Natl Acad Sci USA* 2011;108:10343–10348.
- 57 Son EY, Ichida JK, Wainger BJ et al. Conversion of mouse and human fibroblasts into functional spinal motor neurons. *Cell Stem Cell* 2011;9:205–218.
- 58 Ring KL, Tong LM, Balestra ME et al. Direct reprogramming of mouse and human fibroblasts into multipotent neural stem cells with a single factor. *Cell Stem Cell* 2012;11:100–109.
- 59 Giorgetti A, Marchetto MC, Li M et al. Cord blood-derived neuronal cells by ectopic expression of Sox2 and c-Myc. *Proc Natl Acad Sci USA* 2012;109:12556–12561.
- 60 Lu J, Liu H, Huang CT et al. Generation of integration-free and region-specific neural progenitors from primate fibroblasts. *Cell Rep* 2013;3:1580–1591.
- 61 Ban H, Nishishita N, Fusaki N et al. Efficient generation of transgene-free human induced pluripotent stem cells (iPSCs) by temperature-sensitive Sendai virus vectors.

- Proc Natl Acad Sci USA 2011;108:14234–14239.
- 62** Merling RK, Sweeney CL, Choi U et al. Transgene-free iPSCs generated from small volume peripheral blood nonmobilized CD34+ cells. *Blood* 2013;121:e98–107.
- 63** Torper O, Pfisterer U, Wolf DA et al. Generation of induced neurons via direct conversion in vivo. *Proc Natl Acad Sci USA* 2013;110:7038–7043.
- 64** Guo Z, Zhang L, Wu Z et al. In Vivo direct reprogramming of reactive glial cells into functional neurons after brain injury and in an Alzheimer's disease model. *Cell Stem Cell* 2014;14:188–202.
- 65** Simara P, Motl JA, Kaufman DS. Pluripotent stem cells and gene therapy. *Transl Res* 2013;161:284–292.
- 66** Li M, Suzuki K, Kim NY et al. A cut above the rest: Targeted genome editing technologies in human pluripotent stem cells. *J Biol Chem* 2014;289:4594–4599.
- 67** Shen B, Zhang W, Zhang J et al. Efficient genome modification by CRISPR-Cas9 nickase with minimal off-target effects. *Nat Methods* 2014;11:399–402.
- 68** Wu Y, Gao T, Wang X et al. TALE nickase mediates high efficient targeted transgene integration at the human multi-copy ribosomal DNA locus. *Biochem Biophys Res Commun* 2014;446:261–266.
- 69** An MC, Zhang N, Scott G et al. Genetic correction of Huntington's disease phenotypes in induced pluripotent stem cells. *Cell Stem Cell* 2012;11:253–263.
- 70** Liu GH, Qu J, Suzuki K et al. Progressive degeneration of human neural stem cells caused by pathogenic LRRK2. *Nature* 2012;491:603–607.

IV.HYPOTHESIS AND OBJECTIVES

1. Part I:

- Hypothesis: Mitochondrial activity and/or mitochondrial mass segregate stem *versus* progenitor function in CB-derived CD34⁺ (CB-CD34⁺) cells.
- Objectives:
 - a. To examine the correlation between mitochondrial activity and mitochondrial mass in CB-CD34⁺ cells.
 - b. To assess *in vitro* the mitochondrial energetic balance in CB-CD34⁺ cells.
 - c. To assess *in vivo* hematopoietic stem/progenitor cell function in CB-CD34⁺ cells contingent on their mitochondrial contribution.

2. Part II:

- Hypothesis: Patient-specific iPSCs carrying a mutation in *COQ4* could be useful to determine its developmental impact on CoQ₁₀ metabolism and also on the phenotypes observed in the patient.
- Objectives:
 - a. To generate and characterize human iPSCs from CoQ₁₀-deficient fibroblasts.
 - b. To edit the *COQ4* mutation using CRISPR/Cas9 technology in CoQ₁₀-deficient iPSCs.
 - c. To characterize the metabolic profile of patient-derived iPSCs and iPSC-derived SkM cells.
 - d. To assess the developmental impact of the *COQ4* mutant in iPSCs differentiated into neural and SkM cells.

V.METHODS AND RESULTS

V.1.SUMMARY OF THE RESULTS

A brief summary of the main results achieved during the development of this work is described below. All figures and extended results are available in the published papers included in this thesis.

CB-CD34⁺ hematopoietic cells with low mitochondrial mass are enriched in hematopoietic repopulating stem cells (Article II).

1. FACS sorting of CD34⁺ cells based on mitochondrial mass.

A strong correlation was found between mitochondrial mass and MMP in CB-CD34⁺ cells i.e., the greater the mitochondrial content, the higher the MMP. CD34⁺ cells were sorted according to their mitochondrial mass into CD34⁺ Mito^{High} and CD34⁺ Mito^{Low} populations. Both ATP levels and the expression of the mitochondrial-specific *NDI* and *COX2* genes were higher in sorted CD34⁺ Mito^{High} cells than in equivalent CD34⁺ Mito^{Low} cells.

2. Stem versus progenitor cell function of sorted CD34⁺ cells.

We used clonogenic colony-forming units (CFU) assays as an *in vitro* read-out of HPC function, and BM xenotransplantation assays into NSG (NOD.Cg-Prkdc^{scid} Il2rg^{tm1Wjl/SzJ}) mice as an *in vivo* read-out of HSC function. CD34⁺ Mito^{High} cells displayed higher clonogenic activity both in primary and secondary CFU assays than CD34⁺ Mito^{Low} cells. However, the level of engraftment was higher in mice transplanted with CD34⁺ Mito^{Low} cells than in those transplanted with CD34⁺ Mito^{High} cells irrespective of the tissue analyzed, and was more significant in the injected BM. We also analyzed the proportion of CD34⁺CD38⁻ (HSC) cells within the CD34⁺ Mito^{High} and Mito^{Low}

fraction and found that the CD34⁺ Mito^{Low} fraction contained a 6-fold higher number of HSC than the CD34⁺ Mito^{High} fraction. Together, these data suggest that the CD34⁺ Mito^{High} fraction is enriched in HPC whereas the CD34⁺ Mito^{Low} fraction is enriched in HSC.

3. *In vitro* homeostasis of Mito^{High} and Mito^{Low} CD34⁺ cells.

Expansion of CD34⁺ cells *in vitro* while retaining their stem/progenitor properties remains challenging [46, 49]. We analyzed the *in vitro* differentiation kinetics of CD34⁺ Mito^{High} and Mito^{Low} cells by tracing the loss of the CD34 antigen. CD34 expression declined progressively during differentiation in both populations; however, the decline was less pronounced in CD34⁺ Mito^{Low} cells. Moreover, whereas the expansion of CD34⁺ Mito^{High} and Mito^{Low} cells was similar during the first few days of differentiation, the number of CD34⁺ Mito^{Low} cells was significantly higher after 10–15 days of culture. Finally, the complete differentiation of CD34⁺ Mito^{Low} cultures and their expansion from day 15 was accompanied by mitochondrial adaptation, as demonstrated by an increase in ATP production and expression of the mitochondrial genes *ND1* and *COX2*. These data suggest that the mitochondrial response underlies the high proliferative capacity of the CD34⁺ Mito^{Low}-differentiated derivatives.

Genetic rescue of mitochondrial and SkM impairment in an iPSC model of CoQ₁₀ deficiency (Article III & IV).

1. **A *COQ4* mutation causes a mitochondrial disorder associated with CoQ₁₀ deficiency.**

A 4-year-old girl was diagnosed in our Institution with minor mental retardation and lethal rhabdomyolysis. Genetic analysis identified a heterozygous point mutation in the *COQ4* gene (c.483G>C; E161D). A comparative analysis of the patient's fibroblasts (CQ4-F) and control fibroblasts (Ctrl-F) revealed that the concentration and biosynthesis of CoQ₁₀ was 75% and 87% lower, respectively, in CQ4-F than in Ctrl-F. In line with its role in the ETC, the reduction in CoQ₁₀ in CQ4-F was reflected in the functional reduction in the activity of CI+III and CII+III of 41% and 64%, respectively. Moreover, cellular proliferation was considerably lower in CQ4-F than in Ctrl-F and the proportion of cycling cells was decreased in CQ4-F, which was accompanied by a 17-fold increase in senescence. Finally, histological analysis of SkM from the patient revealed extensive damage associated with rhabdomyolysis.

2. Generation and characterization of patient-specific CQ4-iPSCs.

CQ4-F were reprogrammed into iPSCs in an attempt to model CoQ₁₀ deficiency by exploring the functional impact of the *COQ4* mutation on neuronal and muscle cell fate. iPSC colonies emerged 16–18 days after OSKM transduction and were picked and expanded for further characterization. After 8–10 passages, iPSC lines were OSKM transgene independent, expressed the pluripotency-associated markers (OCT4, SOX2, REX1, NANOG, TRA-1-60, SSEA4), and were genetically stable. As a final test of pluripotency, iPSCs were able to form teratomas in immunodeficient mice.

3. iPSC gene editing by CRISPR/Cas9.

Because the differentiation capacity among iPSCs lines is influenced by epi/genetic variability [36, 37], the best method to identify genotype-phenotype associations is to use isogenic pairs of iPSCs. We therefore used the CRISPR/Cas9 system to edit (and correct) the *COQ4* mutation in iPSCs (CQ4^{ed}-iPSCs). CQ4-iPSCs were co-transfected with Cas9-GFP vector and ssDNA. Two days later, GFP⁺ cells were FACS-sorted as single cells. Individual established clones were analyzed and a homozygous edited clone was observed and confirmed by sequencing. Importantly, CQ4^{ed}-iPSCs remained pluripotent.

4. *COQ4* genome editing reverses metabolic/mitochondrial dysfunction.

CoQ₁₀ is involved in the ETC and low levels of CoQ₁₀ in fibroblasts or muscle are linked to CoQ₁₀ deficiency [146, 150, 157]. We found that CoQ₁₀ concentration and biosynthesis was significantly lower (36% and 61%, respectively) in CQ4-iPSCs than in Ctrl-iPSCs. Interestingly, full restoration both of CoQ₁₀ concentration and biosynthesis was found in CQ4^{ed}-iPSCs. Next, we evaluated OXPHOS and glycolysis by ATP production, basal live-oxygen consumption rate (OCR) and extracellular acidification rate (ECAR). To produce the same amount of ATP, ECAR and OCR rates were 2-fold higher in CQ4-iPSCs than in CQ4^{ed}-iPSCs, suggesting a respiration dysfunction as confirmed by a 2-fold increase in proton leak. Together, these results suggest that CQ4-iPSCs maintain the CoQ₁₀ deficiency and metabolic dysfunction, however the correction in CQ4^{ed}-iPSCs ameliorates these deficiencies.

5. The *COQ4* mutation does not impair iPSC differentiation into dopaminergic or motor neurons.

The majority of CoQ₁₀-deficient patients present neurological symptoms [172, 174]; however, the patient described here presented only minor mental retardation. To study the potential developmental impact of the *COQ4* mutation in human neurogenesis Ctrl-, CQ4- and CQ4^{ed}-iPSCs were differentiated into DANs [27] and MNs [29]. No differences were found between Ctrl- and CQ4-iPSCs irrespective of the differentiation protocol. We evaluated the differentiation capacity to neural progenitors (SOX2⁺NESTIN⁺) and immature neurons (TUJ1⁺) at early time points. Furthermore, we assessed the differentiation potential of the neural progenitors and neural maturation by TH⁺ (DAN) or HB9⁺/ISL1⁺ (MN) at later time points. CQ4^{ed}-iPSCs obtained similar percentages of differentiation to those of CQ4-iPSCs. We then carried out functional analysis to confirm these results. HPLC determination of dopamine release revealed similar levels of dopamine in Ctrl- and CQ4-iPSCs-derived neurons. Whole-cell patch clamp recording of MNs indicated that CQ4-iPSC-derived MNs were electrophysiologically active. Together, these data reveal that the c.483 G>C mutation in *COQ4* does not impact dopaminergic or motor neurogenesis from iPSCs, faithfully recapitulating the patient's phenotype.

6. A *COQ4* mutation recapitulates CoQ₁₀-deficiency-associated SkM functional and metabolic defects.

Muscle impairment is common in CoQ₁₀-deficient patients [154]. To study the developmental and metabolic impact of the *COQ4* mutation in skeletal

myogenesis, Ctrl-, CQ4- and CQ4^{ed}-iPSCs were differentiated into SkM [89]. Transgenic iPSCs lines carrying a PAX7-GFP-inducible lentivirus vector were generated. Although the cell cycle profile and levels of apoptosis were very similar between Ctrl- and CQ4-PAX7⁺ myogenic progenitors, the number of senescent CQ4-PAX⁺ cells was 2-fold higher, a phenotype that was corrected in CQ4^{ed}-PAX7⁺ myogenic progenitors. The senescence observed in CQ4-PAX7⁺ cells might be explained by their increased ROS production, leading to a 1-log reduction in cell expansion. Again, this functional deficiency was corrected in CQ4^{ed}-PAX7⁺ cells. PAX7⁺ myogenic progenitors were further differentiated into muscle cells. A significant reduction in the generation of fully differentiated MYH⁺ cells was noted for CQ4-PAX7⁺ myogenic progenitors, and this was paralleled by a decrease in creatine kinase activity. Moreover, gene expression analysis of specific myogenic markers (*MYF5*, *MGN* and *MYH3*) showed that their kinetics were deregulated in CQ4-PAX7⁺ when compared with Ctrl-PAX7⁺ differentiating muscle cells. Moreover, mitochondrial dynamics (circularity, form factor and aspect ratio) and ETC activity (CI+III) were also reduced in complexity and activity, respectively, in CQ4-PAX7 differentiated cells relative to Ctrl- and CQ4^{ed}-PAX7⁺ differentiated cells. Collectively, these results establish the utility of an iPSC-based disease model that partially reproduces the disease phenotype.

V.2.ARTICLE II:

Cord Blood-derived CD34⁺ hematopoietic cells with low mitochondrial mass are enriched in hematopoietic repopulation stem cell function.

Romero-Moya D, Bueno C, Montes R, Navarro-Montero O, Iborra FJ, López LC, Martin M, Menendez P.

Haematologica. 2013; 98(7): 1022-9

Cord blood-derived CD34⁺ hematopoietic cells with low mitochondrial mass are enriched in hematopoietic repopulating stem cell function

Damia Romero-Moya,¹ Clara Bueno,¹ Rosa Montes,¹ Oscar Navarro-Montero,¹ Francisco J. Iborra,² Luis Carlos López,³ Miguel Martín,³ and Pablo Menendez^{1,4,5}

¹GENyO (Centre for Genomics and Oncological Research: Pfizer / University of Granada / Andalusian Government), Granada;

²Department of Molecular and Cellular Biology, Centro Nacional de Biotecnología, Consejo Superior de Investigaciones Científicas, Madrid; ³Centro de Investigación Biomédica, Instituto de Biotecnología, Universidad de Granada; ⁴Josep Carreras Leukemia Research Institute, Barcelona; and ⁵Institució Catalana de Recerca i Estudis Avançats, (ICREA), Barcelona, Spain

ABSTRACT

The homeostasis of the hematopoietic stem/progenitor cell pool relies on a fine-tuned balance between self-renewal, differentiation and proliferation. Recent studies have proposed that mitochondria regulate these processes. Although recent work has contributed to understanding the role of mitochondria during stem cell differentiation, it remains unclear whether the mitochondrial content/function affects human hematopoietic stem *versus* progenitor function. We found that mitochondrial mass correlates strongly with mitochondrial membrane potential in CD34⁺ hematopoietic stem/progenitor cells. We, therefore, sorted cord blood CD34⁺ cells on the basis of their mitochondrial mass and analyzed the *in vitro* homeostasis and clonogenic potential as well as the *in vivo* repopulating potential of CD34⁺ cells with high (CD34⁺ Mito^{high}) *versus* low (CD34⁺ Mito^{low}) mitochondrial mass. The CD34⁺ Mito^{low} fraction contained 6-fold more CD34⁺CD38⁻ primitive cells and was enriched in hematopoietic stem cell function, as demonstrated by its significantly greater hematopoietic reconstitution potential in immunodeficient mice. In contrast, the CD34⁺ Mito^{high} fraction was more enriched in hematopoietic progenitor function with higher *in vitro* clonogenic capacity. *In vitro* differentiation of CD34⁺ Mito^{low} cells was significantly delayed as compared to that of CD34⁺ Mito^{high} cells. The eventual complete differentiation of CD34⁺ Mito^{low} cells, which coincided with a robust expansion of the CD34⁺ differentiated progeny, was accompanied by mitochondrial adaptation, as shown by significant increases in ATP production and expression of the mitochondrial genes ND1 and COX2. In conclusion, cord blood CD34⁺ cells with low levels of mitochondrial mass are enriched in hematopoietic repopulating stem cell function whereas high levels of mitochondrial mass identify hematopoietic progenitors. A mitochondrial response underlies hematopoietic stem/progenitor cell differentiation and proliferation of lineage-committed CD34⁺ cells.

Introduction

Human hematopoietic stem cells (HSC) and hematopoietic progenitor cells (HPC) are almost exclusively enriched in the CD34⁺ fraction, which represents a rare cell subset (<1%) in cord blood, bone marrow and mobilized peripheral blood.^{1,2} In the setting of clinical transplantation, the dose of total CD34⁺ cells infused per kilogram of patient's bodyweight is used as a predictor of short-term hematopoietic recovery and establishment of long-term engraftment.^{3,4} Although distinct surface markers (CD38, CD90, CD45RA, CD133, etc.)⁵ have been experimentally used to distinguish between HSC or HPC, *bona fide* segregation of HSC and HPC relies on *in vitro* and *in vivo* functional assays.

It has been extensively demonstrated that the CD34⁺ fraction is phenotypically and functionally heterogeneous. Experimentally, only 1:10 to 1:4 of CD34⁺ or CD34⁺CD38 cells display clonogenic potential. Clinically, different outcomes/hematopoietic recovery are reported in patients with identical underlying disease who undergo hematopoietic stem/progenitor cell (HSPC) transplantation with equal doses

of CD34⁺ cells after receiving identical chemotherapy treatment. It can, therefore, be speculated that genetically identical CD34⁺ cells within the graft may exhibit cell-to-cell variations not only in the amount of individual gene products but also in metabolic homeostasis/mitochondrial status, resulting in phenotypic and functional diversity.⁶ The metabolic status of HSC and HPC becomes crucial during clinical HSPC transplantation since the efficiency of donor-derived HSC/HPC to engraft, survive, home, proliferate and differentiate into multiple lineages in a chemotherapy-induced aplastic patient is markedly influenced by their hypoxic niche, demanding a significant metabolic adaptation to survive and promote rapid and stable hematopoietic reconstitution in chemotherapy-induced aplastic microenvironments.^{7,8}

As in other tissues, mitochondria play key roles in HSC/HPC and have recently come under increased scrutiny because compelling evidence has revealed their role in numerous cellular processes, beyond ATP production and apoptosis regulation, and they have recently even been suggested to act as cell-fate or lineage determinants.⁹⁻¹¹ In fact, deregulation of mitochondrial function plays a pathophysio-

©2013 Ferrata Storti Foundation. This is an open-access paper. doi:10.3324/haematol.2012.079244

The online version of this article has a Supplementary Appendix.

*These authors contributed equally to this work

Manuscript received on October 11, 2012. Manuscript accepted on January 9, 2013.

Correspondence: pablo.menendez@genyo.es

logical role in a range of hematologic diseases, such as inherited dyserythropoiesis, sideroblastic anemias and low-grade myelodysplastic syndromes.^{8,12} In addition, transcriptome, epigenetic and proteomic studies in stem cell systems have indicated that specific metabolic/mitochondrial properties are essential for regulating the balance between self-renewal and differentiation.^{13,14}

Although recent work has begun to shed light on the mitochondrial response during murine stem cell differentiation,^{7,10,15,16} how and to what extent the mitochondrial mass/function contributes to human hematopoietic stem and progenitor function remains poorly understood. Here, we found that mitochondrial mass correlates strongly with mitochondrial membrane potential ($\Delta\Psi_m$). This led us to separate cord blood-derived CD34⁺ cells based on their mitochondrial mass and to analyze the *in vitro* homeostasis and clonogenic potential as well as the *in vivo* repopulating potential of CD34⁺ cells with high (CD34⁺ Mito^{high}) versus low (CD34⁺ Mito^{low}) mitochondrial mass.

Design and Methods

Cord blood collection and CD34⁺ cell isolation and culture

Fresh umbilical cord blood units from healthy neonates were obtained from local hospitals following approval from our local Ethics and Biohazard Board Committee. The cord blood samples were pooled to reduce variability among individual units. Mononuclear cells were isolated using Ficoll-Hypaque and after lysing the red cells (Cytognos, Salamanca, Spain), CD34⁺ cells were purified by magnetic bead separation using the human CD34 MicroBead kit and the AutoMACS Pro separator (Miltenyi Biotec) as instructed by the manufacturer.^{15,17} The purity of the CD34⁺ fraction was assessed by flow cytometry using an anti-CD34-PE antibody (Miltenyi Biotec), and only CD34⁺ fractions showing purity higher than 90% were used.^{15,17} The CD34⁺ fraction was irradiated (15 Gy) and used as accessory cells for co-transplantation with CD34⁺ cells.

MitoTracker staining and cell sorting

CD34⁺ cells were stained with MitoTracker Red (CMXRos) and MitoTracker Green FM dye (Molecular Probes) for 10 min and 20 min, respectively, according to the manufacturer's guidelines and analyzed by wide confocal cytometry.⁶ For functional assays, CD34⁺ cells were FACS-sorted (FACSARIA-II, BD Biosciences) based on MitoTracker Green levels into CD34⁺ Mito^{high} and CD34⁺ Mito^{low} (n=10).

Measurements of ATP and reactive oxygen species

ATP levels were measured using a Cell-Titer-Glo[®] Luminescent Cell Viability Assay (Promega) according to the manufacturer's guidelines. Briefly, equal numbers of cells (5x10⁴/100 μ L) were seeded in a 96-well plate and 100 μ L of the reaction reagent were added to each well. After 10 min of shaking, the luminescence signal was detected using the GloMax[®]-Multi Detection System (Promega) and compared against the ATP Standard Curve using ATP disodium salt (Promega).⁵

Reactive oxygen species were measured using the mitochondrial superoxide indicator MitoSOX Red, as previously described.²⁰ Briefly, CD34⁺ Mito^{low} and CD34⁺ Mito^{high} cells were treated with 3 μ M MitoSOX for 20 min and were then washed twice in Hanks balanced salt solution and analyzed by flow cytometry (Online Supplementary Figure S1A).

Gene expression by quantitative reverse transcriptase polymerase chain reaction analysis

RNA was extracted using the All Prep DNA/RNA kit (Qiagen) and cDNA was synthesized by using SuperScript[™] First-Strand Synthesis System for reverse transcriptase polymerase chain reaction (Invitrogen). The expression of the mitochondrial genes ND1 and COX2 as well as HIF-1 α and Meis1 was compared between CD34⁺ Mito^{high} and CD34⁺ Mito^{low} cellular fractions by quantitative polymerase chain reaction analysis. Values were normalized to β -actin. The primers used were: ND1-Fw-5'-TGC-GAGCAGIAGCCCAACAATCT-3', ND1-Rw-5'-TTATGGC-CAAGGTCATGATGGCA-3', COX2-Fw-5'-ACAGATG-CAATCCCGGACGTCTA-3', COX2-Rw-5'-GAC-GATGGGCATGAACTGTGGTT-3', HIF-1 α -Fw-5'-CTGCAA-CATGGAAGTATTGCA-3', HIF-1 α -Rw-5'-TACCCACACTI-GAGTTGGTACTG-3', Meis1-Fw-5'-AAAAGCGTCA-CAAAAAGCGT-3', Meis1-Rw-5'-GATGTGTGAGTCCCGT-GTCTT-3', β -actin-Fw-5'-GATGCCACGGCTGCTT-3' and β -actin-Rw-5'-AGGACTCCATGCCAGGAA-3'. The polymerase chain reaction conditions were 50°C for 2 min followed by 90°C for 10 min and 40 cycles of 95°C for 15 s and 60°C for 60 s.¹⁵ The expression of each gene was analyzed in three independent experiments performed in triplicate.

In vitro liquid culture, cell cycle, and apoptosis analyses of Mito^{high} and Mito^{low} CD34⁺ cells

FACS-sorted CD34⁺ Mito^{high} and CD34⁺ Mito^{low} cells were cultured for 40 days on StemSpan media (Stem Cell Technologies) supplemented with early hematopoietic cytokines [stem cell factor (100 ng/mL), FLT3L (100 ng/mL) and interleukin-3 (10 ng/mL); PeproTech].²¹ To determine the growth kinetics of Mito^{high} and Mito^{low} CD34⁺ cultures, cells were counted twice a week and replated at a density of 1x10⁵ cells/cm². Similarly, the maintenance of the CD34⁺ phenotype was analyzed twice a week as an approach to trace the "default" differentiation of both Mito^{high} and Mito^{low} CD34⁺ cells. For cell cycle analysis, Mito^{high} and Mito^{low} CD34⁺ cells were fixed in 70% ice-cold ethanol and stored at -20°C. Subsequently, cells were washed with ice-cold phosphate-buffered saline and suspended in propidium iodide buffer containing 5 μ g of propidium iodide and 100 μ g/mL of RNAase. Cell cycle distribution discriminating between quiescent cells (G0/G1) and cycling cells (S/G2/M phase) was analyzed on a FACSCanto-II cytometer using FACSDiva and ModFit software (BD Bioscience).²¹ The apoptotic status of Mito^{high} and Mito^{low} CD34⁺ cells was assessed using the annexin-V apoptosis detection kit (BD Biosciences) according to the manufacturer's instructions.²¹ Briefly, cells were harvested and washed twice with phosphate-buffered saline before staining with annexin V-phycoerythrin and 7-amino actinomycin D. Apoptotic cells were detected by gating the annexin V-positive fraction.²¹

Colony-forming unit assay

Primary human clonogenic progenitor assays (n=6) were performed by plating 1000 sorted CD34⁺ cells into methylcellulose H4434 (Stem Cell Technologies) containing the human growth factors stem cell factor (50 ng/mL), granulocyte-macrophage colony-stimulating factor (10 ng/mL), interleukin-3 (10 ng/mL) and erythropoietin (3 U/mL). Colonies were counted and scored on day 14 of the colony-forming unit (CFU) assay using standard morphological criteria.²¹ For secondary replating, all the CFU colonies from the primary methylcellulose culture were harvested, and a single-cell suspension was achieved, washed in Iscove's modified Dulbecco's medium and replated in the secondary CFU assay.

Mice transplantation and analysis of engraftment

NOD/LtSz-scid IL2R $\gamma^{-/-}$ mice (NSG) were housed under sterile conditions. The Animal Care Committee of the University of Granada approved all animal protocols (Ref. UGR-CEEA 2011-361). Mice (n=22) at 8 to 12 weeks of age were sublethally irradiated (2.5 Gy) for 6 to 12 h before transplantation. Mice were anesthetized by isoflurane inhalation, and intrabone marrow transplantation was performed as described in detail elsewhere.^{21,25} A total of 2×10^6 Mito^{high} or Mito^{low} CD34⁺ cells together with 5×10^4 irradiated accessory cells were transplanted in a volume of 50 μ L. For pain relief, 0.1 mg/kg buprenorphine and 5 mg/kg carprofen were administered immediately after transplantation and 24 h after.^{21,25} Mice were killed 7 weeks after transplantation. Cells from the bone marrow (injected tibia and from the contralateral tibia and femur), spleen, liver and peripheral blood were stained with anti-hHLA-ABC-FITC and anti-hCD45-APC-Cy7 (BD Biosciences) to analyze human chimerism by flow cytometry. All engrafted mice were assessed for multilineage analysis using anti-hCD33-PE for myeloid cells, anti-hCD19-APC for B cells, and anti-hCD34-PE-Cy7 for immature hematopoietic cells (BD Biosciences).^{21,22,24}

Statistical analysis

Data are expressed as mean \pm SD. Statistical comparisons were performed using a paired Student's *t* test. Differences were considered statistically significant when the *P* value was <0.05.

Results

FACS sorting of CD34⁺ cells based on mitochondrial mass

We first analyzed by confocal cytometry the mitochondrial membrane potential ($\Delta\Psi_m$) and the mitochondrial mass using MitoTracker Red (CMXRos) and MitoTracker Green, respectively. A strong correlation was observed between mitochondrial mass and function ($\Delta\Psi_m$) in cord blood-derived CD34⁺ cells; the greater the mitochondrial content, the higher the $\Delta\Psi_m$ (Figure 1A). Accordingly, CD34⁺ cells were FACS-sorted based on mitochondrial mass (MitoTracker Green) into CD34⁺ Mito^{high} and CD34⁺ Mito^{low} (Figure 1B). Sorted CD34⁺ Mito^{high} contain 2-fold higher ATP levels (Figure 1C) and also express the mitochondrial-specific genes NDI and COX2 at a level 2-fold higher than that of CD34⁺ Mito^{low} (Figure 1D), confirming that CD34⁺ Mito^{high} cells have more expression of the mitochondrial-specific genes NDI and COX2, and produce more ATP.

Hematopoietic stem versus progenitor cell characteristics of metabolically sorted cells

We next tested whether isolation of cord blood-derived CD34⁺ cells based solely on their mitochondrial mass enriches for stem and/or progenitor cell function. We utilized *in vitro* clonogenic CFU assays as a read-out for HPC function, and bone marrow xenotransplantation assays into NSG mice as an *in vivo* read-out for SCID-repopulating HSC function. Equal numbers of CD34⁺ Mito^{high} and CD34⁺ Mito^{low} were plated in CFU assays and hematopoietic colonies were counted after 14 days. CD34⁺ Mito^{high} cells displayed higher clonogenic capacity in both primary and secondary CFU compared to CD34⁺ Mito^{low} (Figure 2A). Scoring of the CFU revealed no differences in the CFU types (granulocyte-, macrophage-, granulocyte-macrophage-, erythroid- and mix-) obtained from CD34⁺

Mito^{high} versus CD34⁺ Mito^{low}. These data suggest that the CD34⁺ Mito^{high} fraction is enriched in HPC.

In vivo hematopoietic reconstitution studies were undertaken to determine the long-term repopulating capacity of CD34⁺ Mito^{high} and CD34⁺ Mito^{low}. Equal numbers of cells were transplanted into tibiae and mice were sacrificed 7 weeks later for chimerism analysis in multiple hematopoietic organs. Human chimerism was determined by flow cytometry using anti-CD45 and anti-HLA-ABC (Figure 2B). All engrafted mice were assessed for multilineage reconstitution using anti-CD19 (B cells), anti-CD33 (myeloid cells) and anti-CD34 (immature cells) (Figure 2B). The level of engraftment was higher in the mice transplanted with CD34⁺ Mito^{low} than in those transplanted with CD34⁺ Mito^{high} regardless of the tissue analyzed, being more significant in the injected bone marrow (79 \pm 18% versus 59 \pm 17%; *P*<0.05; Figure 2C, left panel). We next characterized the engraftment composition, and found very similar multilineage composition in all tissues reconstituted with CD34⁺ Mito^{high} or CD34⁺ Mito^{low} (Figure 2C, right panel) except for the more immature (CD45⁺CD34⁺) hematopoietic fraction which was significantly higher (15 \pm 3% versus 10 \pm 4%; *P*<0.05) in the bone marrow of mice engrafted with CD34⁺ Mito^{low} cells.

The vast majority of CD34⁺ cells co-express the activation surface marker CD38 which is routinely associated with HPC whereas a very small proportion of CD34⁺ cells lack CD38 expression and are considered to be enriched in HSC.^{5,23,25} We, therefore, analyzed the proportion of CD34⁺CD38⁻ cells within the CD34⁺ Mito^{high} and CD34⁺ Mito^{low} fractions (Figure 2D). The CD34⁺ Mito^{low} fraction contained 6-fold higher numbers of CD34⁺CD38⁻ primitive cells, thus supporting the concept that the CD34⁺ Mito^{low} fraction is enriched in repopulating HSC and also explaining, at least in part, the lower progenitor function of CD34⁺ Mito^{low} cells (Figure 2A,C). Together, these data indicate that the CD34⁺ Mito^{low} fraction is enriched in HSC function.

It has been reported¹⁶ recently that murine long-term HSC are highly enriched in HIF-1 α and Meis1. We, therefore, analyzed the expression of these factors on our CD34⁺ Mito^{high} and Mito^{low} cells. As shown in *Online Supplementary Figure S1B*, both HIF-1 α and Meis1 were up-regulated, by 5- and 4-fold, respectively, in CD34⁺ Mito^{low} cells as compared to in CD34⁺ Mito^{high} cells, confirming that these factors are robustly expressed in the CD34⁺ cell fraction enriched in repopulating stem cell function.

In vitro homeostasis of CD34⁺ Mito^{high} and CD34⁺ Mito^{low} cells

It remains a challenge to expand CD34⁺ cells *in vitro* while retaining their stem/progenitor properties.²⁶ The homeostasis of sorted CD34⁺ Mito^{high} and CD34⁺ Mito^{low} cells was analyzed *in vitro*. We first analyzed the *in vitro* differentiation kinetics of CD34⁺ Mito^{high} and CD34⁺ Mito^{low} cultures by tracing the loss of the CD34 antigen. Interestingly, although the number of CD34⁺ cells diminished progressively over time, the differentiation of CD34⁺ Mito^{low} cultures was significantly delayed as compared to that of CD34⁺ Mito^{high} (Figure 3A). After 15 days of liquid culture, CD34⁺ cells were no longer present in either CD34⁺ Mito^{high} or CD34⁺ Mito^{low} cultures (Figure 3A,B). Expansion of CD34⁺ Mito^{high} and CD34⁺ Mito^{low} cultures was moderate during the first 11-15 days of liquid culture (Figure 3B). However, coinciding with the complete differ-

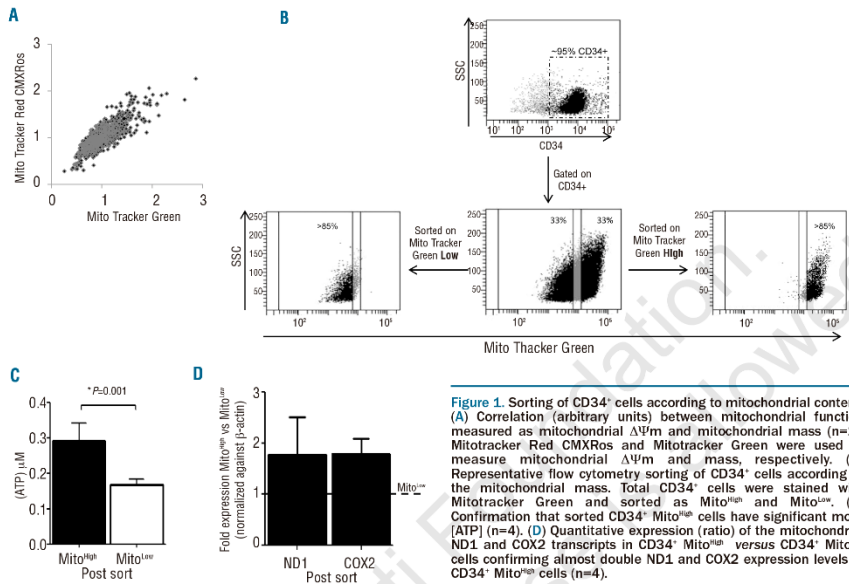


Figure 1. Sorting of CD34⁺ cells according to mitochondrial content. (A) Correlation (arbitrary units) between mitochondrial function measured as mitochondrial $\Delta\Psi_m$ and mitochondrial mass (n=2). Mitotracker Red CMXRos and Mitotracker Green were used to measure mitochondrial $\Delta\Psi_m$ and mass, respectively. (B) Representative flow cytometry sorting of CD34⁺ cells according to the mitochondrial mass. Total CD34⁺ cells were stained with Mitotracker Green and sorted as Mito^{High} and Mito^{Low}. (C) Confirmation that sorted CD34⁺ Mito^{High} cells have significant more [ATP] (n=4). (D) Quantitative expression (ratio) of the mitochondrial ND1 and COX2 transcripts in CD34⁺ Mito^{High} versus CD34⁺ Mito^{Low} cells confirming almost double ND1 and COX2 expression levels in CD34⁺ Mito^{High} cells (n=4).

entiation (loss of CD34⁺ cells) of the CD34⁺ cultures after 11-15 days, the cell expansion of differentiated (CD34⁺) Mito^{High} and Mito^{Low} cultures was significantly boosted, especially in the cultures seeded with CD34⁺ Mito^{Low} cells (Figure 3B). After sorting, >99% of the CD34⁺ Mito^{Low} cells were quiescent (G0/G1 cell cycle phases) while ~20% of the CD34⁺ Mito^{High} cells were cycling (Figure 3C), but as CD34⁺ cells differentiated into CD34⁺ cells, Mito^{Low} cultures displayed a higher proportion of cycling cells (31±5% versus 22±6%, P<0.05) and lower apoptotic rate (21±3% versus 29±4%, P<0.05) than Mito^{High} cultures (Figure 3C,D), explaining the robust increased cell expansion of differentiated CD34⁺ Mito^{Low} cultures as compared to differentiated CD34⁺ Mito^{High} cultures (Figure 3B). Finally, the complete differentiation of CD34⁺ Mito^{Low} cultures by day 15 of liquid culture coupled with their robust expansion from day 15 onwards (Figure 3A,B) was accompanied by a mitochondrial adaptation, as demonstrated by a significant increase in energy (ATP) production (Figure 3E) and expression of the mitochondrial genes ND1 and COX2 (Figure 3F). This suggests that a mitochondrial response underlies the high proliferative activity of the CD34⁺ Mito^{Low}-differentiated derivatives.

Discussion

Mitochondria are multi-functional organelles that play a vital role in the cell, providing most of the cellular energy and regulating Ca²⁺ homeostasis, cell death, and differentiation; furthermore, they have recently been suggested to act as cell-fate or lineage determinants.^{9,11} Hematopoietic

tissue homeostasis relies on a finely tuned balance between very dynamic intrinsically and extrinsically regulated processes of self-renewal, differentiation and proliferation. Based on recent transcriptomic, epigenomic and proteomic studies, it has been proposed that the cellular metabolism regulates these processes in different stem cell systems.¹⁴ The metabolic status of human HSC/HPC becomes crucial during clinical HSPC transplantation since the efficiency of donor-derived HSC/HPC to engraft, survive, home, proliferate and differentiate in chemotherapy-induced aplastic patients demands a significant metabolic adaptation to survive and promote rapid and stable hematopoietic reconstitution in chemotherapy-induced aplastic microenvironments.^{7,8} Furthermore, deregulation of mitochondrial functions plays a pathophysiological role in several hematologic diseases.^{8,12} Although recent work has begun to shed light on the mitochondrial response during stem cell differentiation,^{7,10,15,16} how, and to what extent the mitochondrial content affects human hematopoietic stem versus progenitor function remains elusive.

Here, we report that mitochondrial content correlates strongly with $\Delta\Psi_m$ in CD34⁺ cells. Thus, cord blood-derived CD34⁺ cells were sorted based solely on their mitochondrial mass, and the *in vitro* repopulating potential of CD34⁺ cells with high (CD34⁺ Mito^{High}) versus low (CD34⁺ Mito^{Low}) mitochondrial content were analyzed. As expected, the ATP levels and expression of mitochondrial-specific genes were higher in CD34⁺ Mito^{High} than in CD34⁺ Mito^{Low} cells. We show for the first time in human CD34⁺ cells that hematopoietic stem and progeni-

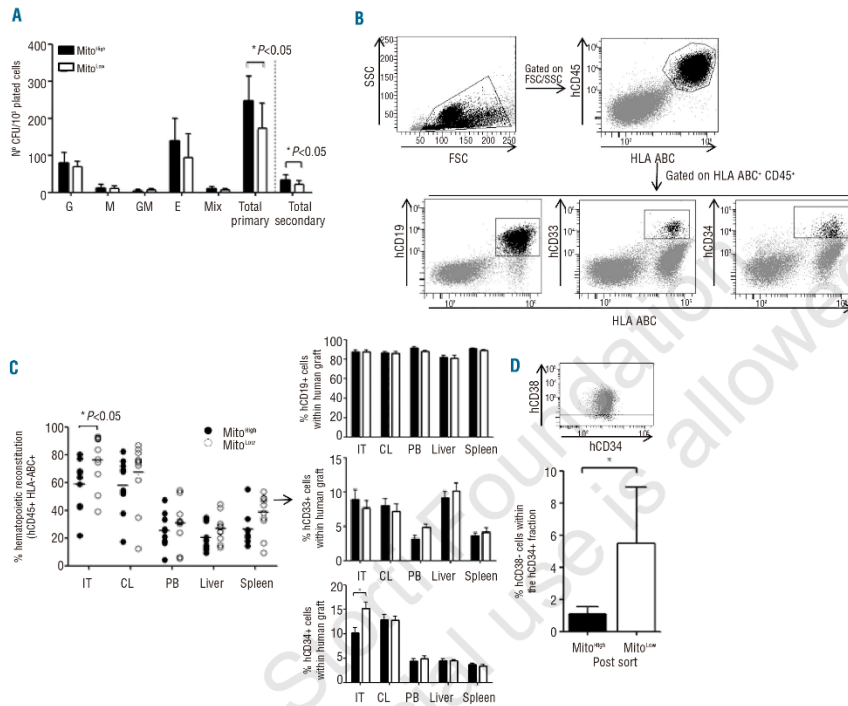


Figure 2. Mito^{high} and Mito^{low} CD34⁺ cells display *in vitro* and *in vivo* functional differences. (A) Clonogenic (CFU) potential of Mito^{high} versus Mito^{low} CD34⁺ progenitor cells (n=6). Primary CFU cultures were harvested and re-plated in secondary CFU assays. (B) Representative flow cytometric analysis of human multi-lineage engraftment in NSG mice. Human cells were identified as HLA-ABC⁺ CD45⁺. Within the human graft, myeloid (CD33⁺), B-lymphoid (CD19⁺) and immature (CD34⁺) lineages were analyzed. (C) Levels of human multi-lineage chimerism in injected tibia (IT), contra-lateral tibia (CL), peripheral blood (PB), spleen and liver indicating successful migration of the human CD34⁺ cells from the injected tibia. Each dot/square represents an individual mouse and the horizontal line indicates the mean of each experimental condition. (D) Proportion of CD38⁺ primitive/stem cells within CD34⁺ Mito^{high} and CD34⁺ Mito^{low} fractions (bottom panel). The upper panel depicts a representative flow cytometry analysis of CD38 and CD34 staining.

tor cell functions segregate partially between metabolically sorted cells. The CD34⁺ Mito^{low} fraction displayed significantly higher *in vivo* reconstitution potential upon inoculation in NSG mice whereas the CD34⁺ Mito^{high} fraction was more enriched in progenitor function with higher *in vitro* clonogenic capacity. This is in line with the “dogma” that stem cells are usually quiescent and contain low numbers of mitochondria whereas progenitors are more proliferative and contain higher numbers of mitochondria.^{9,10} The vast majority of CD34⁺ cells co-express the activation surface marker CD38 which is associated with HPC whereas a very small proportion of CD34⁺ cells lack CD38 expression and are considered to be enriched in HSC.^{5,23,25} Accordingly, the proportion of CD34⁺CD38⁻ primitive cells was 6-fold higher in the CD34⁺ Mito^{low} than in the CD34⁺ Mito^{high} fraction, supporting the concept that the CD34⁺ Mito^{low} fraction is enriched in repopulating HSC function, and also explaining, at least in part, the lower

progenitor function of CD34⁺ Mito^{low} cells. Our data confirm previous findings in mice showing that the Mito^{low} cellular fraction of murine bone marrow is highly enriched in repopulating HSC, partially due to the enrichment of long-term HSC in this Mito^{low} fraction.¹⁶ Furthermore, Simsek *et al.*¹⁸ recently reported that murine long-term HSC are highly enriched in Meis1, a HSC-associated transcriptional factor required for definitive hematopoiesis, and in HIF-1 α , a master regulator of glycolysis and mitochondrial respiration, including a metabolic shift toward anaerobic glycolysis. In line with this study, the expression of both HIF-1 α and Meis1 was found to be robustly up-regulated in CD34⁺ Mito^{low} cells as compared to in CD34⁺ Mito^{high} cells, confirming that these factors are robustly expressed in the CD34⁺ cell fraction enriched in repopulating stem cell function. Interestingly, mitochondrial content enriches for either HSC or HPC but it does not seem to act as a determinant in progenitor/lineage com-

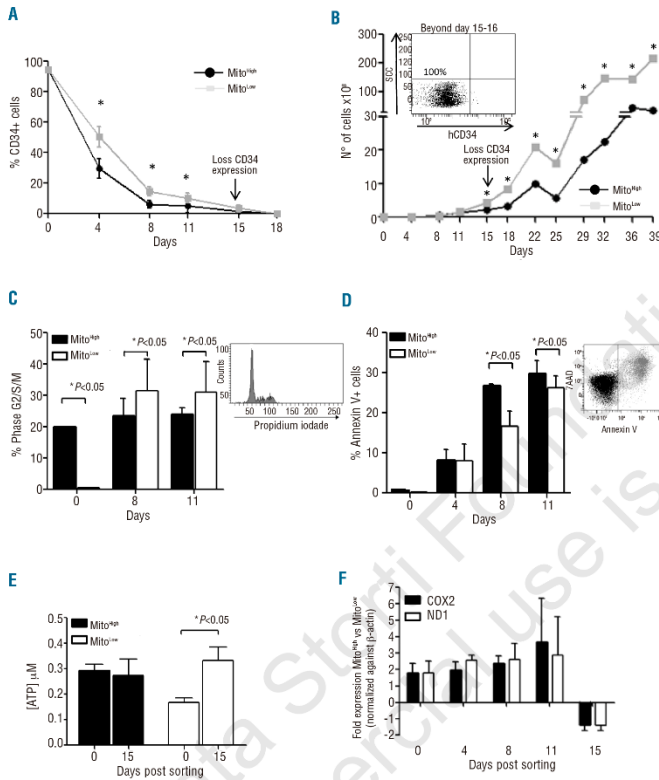


Figure 3. *In vitro* homeostasis of CD34⁺ Mito^{Hsb} and CD34⁺ Mito^{Low} cells. (A) Loss of CD34 antigen over time in liquid cultures seeded with Mito^{Hsb} versus Mito^{Low} CD34⁺ cells (n=6). (B) *In vitro* expansion of liquid cultures initially seeded with Mito^{Hsb} versus Mito^{Low} CD34⁺ cells (n=6). Note that after day 15 there are no residual CD34⁺ cells in the culture. From day 15 onwards the entire culture is comprised of differentiated CD34 cells (flow cytometry panel as inset). (n=6). (C) Proportion of cycling cells (S/G2/M cell cycle phase) measured at the indicated time points in Mito^{Hsb} versus Mito^{Low} CD34⁺ cultures (n=2). (D) Proportion of apoptotic cells (annexin V) measured at the indicated time points in Mito^{Hsb} versus Mito^{Low} CD34⁺ cultures (n=2). (E-F) *In vitro* differentiation of CD34⁺ Mito^{Low} cultures (loss of CD34 antigen) is associated with increased ATP production (E) and higher levels of ND1 and COX2 expression (F).

mitment since the multilineage composition in both CFU and repopulating assays was very similar between CD34⁺ Mito^{Hsb} and CD34⁺ Mito^{Low} cells. These data suggest that mitochondrial mass/activity determines global *in vitro* clonogenic potential and *in vivo* repopulating function but does not impair/skew normal developmental stem cell fate/hematopoietic lineage commitment.

Homeostasis of CD34⁺ Mito^{Hsb} and CD34⁺ Mito^{Low} cultures was further analyzed *in vitro*. The differentiation of CD34⁺ Mito^{Low} cultures was significantly delayed as compared to that of CD34⁺ Mito^{Hsb}, but CD34⁺ cells were no longer present in either CD34⁺ Mito^{Hsb} or CD34⁺ Mito^{Low} cultures after 15 days. Expansion of CD34⁺ Mito^{Hsb} and CD34⁺ Mito^{Low} cultures was limited during the first 15 days; however, coinciding with the complete differentiation of the CD34⁺ cultures after 15 days, the expansion of differentiated (CD34⁺) Mito^{Hsb} and Mito^{Low} cells was significantly boosted, especially in the cultures seeded with CD34⁺ Mito^{Low} cells. The fact that the CD34⁺ Mito^{Low} cells display a delayed differentiation coupled to a much higher expan-

sion rate of their CD34⁺ differentiated cells supports the better hematopoietic engraftment of NSG mice transplanted with the CD34⁺ Mito^{Low} fraction because efficient *in vivo* hematopoietic reconstitution relies on a finely tuned balance between low proliferative/self-renewing CD34⁺ HSC and rapidly amplifying progenitors, many of which are far lineage-committed and lack CD34 expression.

Mitochondrial biogenesis during the differentiation of embryonic stem cells has recently been studied.^{11,27} Undifferentiated embryonic stem cells have a low mitochondrial content and low levels of ATP. Upon differentiation the mitochondrial content increases and mitochondrial biogenesis is activated to promote the synthesis of increased levels of ATP which seem to be required for the homeostasis of the differentiated cells.²⁸⁻³⁰ Similarly, we found that the complete differentiation of CD34⁺ Mito^{Low} cells, which coincided with a robust expansion of the differentiated progeny, was accompanied by mitochondrial adaptation as demonstrated by a significant increase in ATP production and expression of the mitochondrial

genes ND1 and COX2. This suggests that HSPC differentiation and proliferation of rapidly amplifying lineage-committed CD34⁺ cells are processes demanding up-regulation of mitochondrial content and biogenesis, and these properties seem to be conserved among embryonic stem cells and HSC/HPC.

Increased bioenergetics and mitochondrial activity come at an increased risk of oxidative damage, primarily in the form of reactive oxygen species (ROS) which are mainly generated by the mitochondria.^{10,31} Various recent studies in mice have provided evidence for a link between intracellular ROS levels and preservation of stem cell function, with increased levels of ROS being associated with reduced repopulating stem cell activity.^{23,28} Stem cells have strategies to lessen the negative impact of ROS such as lowering the numbers of mitochondria and ATP generation by promoting glycolysis over oxidative phosphorylation.^{25,4} In this study, human CD34⁺ Mito^{low} cells which were shown to be more enriched in HSC function displayed significantly lower levels of ROS than CD34⁺ Mito^{high} cells (Online Supplementary Figure S1A) which are more enriched in HPC function, suggesting that HSC function may be enriched in the CD34⁺ Mito^{low} fraction as a strategy to lessen the negative impact of ROS, which can induce cell damage/death. Finally, during mitosis mitochondria may be segregated to daughter cells either symmetrically or asymmetrically. Asymmetric cellular distri-

bution of mitochondria is a dynamic process which has been observed in some species and may play a role in cell-fate determination, differentiation and self-renewal.^{11,27,35,37} Whether symmetric or asymmetric mitochondrial segregation occurs in human CD34⁺ cells is unknown. It would be worth studying in future work whether asymmetric mitochondrial segregation could be an underlying mechanism explaining why phenotypically identical CD34⁺ cells may exhibit cell-to-cell variations in mitochondrial content resulting in functional diversity.

Funding

This work was funded by the CICE/FEDER (P08-CTS-3678) de la Junta de Andalucía with a grant to PM, the FIS/FEDER (PI10/00449 to PM and PI11/00119 to CB), the MICINN (Fondo Especial del Estado para Dinamización de la Economía y Empleo/PLE-2009-0111) with a grant to PM, and the Foundation "Spanish Association Against Cancer/Junta Provincial de Albacete (C1110023 to PM). DRM (PFI scholarship FI11/0511), RM and CB (CP07/0059) are supported by the ISCIII. ON-M was supported by the Health of Department of the Junta de Andalucía.

Authorship and Disclosures

Information on authorship, contributions, and financial & other disclosures was provided by the authors and is available with the online version of this article at www.haematologica.org.

References

- Menendez P, Perez-Simon JA, Mateos MV, Caballero MD, Gonzalez M, San-Miguel JF *et al.* Influence of the different CD34⁺ and CD34⁺ cell subsets infused on clinical outcome after non-myeloablative allogeneic peripheral blood transplantation from human leucocyte antigen-identical sibling donors. *Br J Haematol.* 2002;119(1):135-43.
- Sutherland DR, Keating A. The CD34 antigen: structure, biology, and potential clinical applications. *J Hematother.* 1992;1(2):115-29.
- Menendez P, Caballero MD, Prosper F, Del Canizo MC, Perez-Simon JA, Mateos MV, *et al.* The composition of leukapheresis products impacts on the hematopoietic recovery after autologous transplantation independently of the mobilization regimen. *Transfusion.* 2002;42(9):1159-72.
- Menendez P, Prosper F, Bueno C, Arbona C, San Miguel JF, Garcia-Conde J, *et al.* Sequential analysis of CD34⁺ and CD34⁺ cell subsets in peripheral blood and leukapheresis products from breast cancer patients mobilized with SCF plus G-CSF and cyclophosphamide. *Leukemia.* 2001;15(3):430-9.
- Menendez P, del Canizo MC, Orfao A. Immunophenotypic characteristics of PB-mobilized CD34⁺ hematopoietic progenitor cells. *J Biol Regul Homeost Agents.* 2001;15(1):53-61.
- das Neves RE, Jones NS, Andreu L, Gupta R, Enver T, Iborra FJ. Connecting variability in global transcription rate to mitochondrial variability. *PLoS Biol.* 2010;8(12):e1000560.
- Danet GH, Pan Y, Luongo JL, Bonnet DA, Simon MC. Expansion of human SCID-repopulating cells under hypoxic conditions. *J Clin Invest.* 2003;112(1):126-35.
- Fontenay M, Cathelin S, Amiot M, Cyan E, Solary E. Mitochondria in hematopoiesis and hematological diseases. *Oncogene.* 2006;25(34):4757-67.
- Inoue S, Noda S, Kashima K, Nakada K, Hayashi J, Miyoshi H. Mitochondrial respiration defects modulate differentiation but not proliferation of hematopoietic stem and progenitor cells. *FEBS Lett.* 2010;584(15):3402-9.
- Mantel C, Messina-Graham S, Broxmeyer HE. Upregulation of nascent mitochondrial biogenesis in mouse hematopoietic stem cells parallels upregulation of CD34 and loss of pluripotency: a potential strategy for reducing oxidative risk in stem cells. *Cell Cycle.* 2010;9(10):2008-17.
- Parker GC, Acsadi G, Brenner CA. Mitochondria: determinants of stem cell fate? *Stem Cells Dev.* 2009;18(6):803-6.
- Lyu BN, Ismailov SB, Ismailov B, Lyu MB. Mitochondrial concept of leukemogenesis: key role of oxygen-peroxide effects. *Theor Biol Med Model.* 2008;5:23.
- Macarthur BD, Ma'ayan A, Lemischka IR. Systems biology of stem cell fate and cellular reprogramming. *Nat Rev Mol Cell Biol.* 2009;10(10):672-81.
- Suda T, Takubo K, Semenza GL. Metabolic regulation of hematopoietic stem cells in the hypoxic niche. *Cell Stem Cell.* 2011;9(4):298-310.
- Ramos-Mejia V, Bueno C, Roldan M, Sanchez L, Ligerio G, Menendez P, *et al.* The adaptation of human embryonic stem cells to different feeder-free culture conditions is accompanied by a mitochondrial response. *Stem Cells Dev.* 2012;21(9):1549-58.
- Simsek T, Kocabas F, Zheng J, Deberardinis RJ, Mahmoud AI, Olson EN, *et al.* The distinct metabolic profile of hematopoietic stem cells reflects their location in a hypoxic niche. *Cell Stem Cell.* 2010;7(3):390-90.
- Bueno C, Catalina F, Melen GJ, Montes R, Sanchez L, Ligerio G, *et al.* Etoposide induces MLL rearrangements and other chromosomal abnormalities in human embryonic stem cells. *Carcinogenesis.* 2009;30(9):1628-37.
- Bueno C, Montes R, Martin L, Prat I, Hernandez MC, Orfao A, *et al.* NG2 antigen is expressed in CD34⁺ HPCs and plasmacytoid dendritic cell precursors: is NG2 expression in leukemia dependent on the target cell where leukemogenesis is triggered? *Leukemia.* 2006;22(3):1475-8.
- Bueno C, Montes R, Menendez P. The ROCK inhibitor Y27632 negatively affects the expansion/survival of both fresh and cryopreserved cord blood-derived CD34⁺ hematopoietic progenitor cells. *Stem Cell Rev.* 2010;6(2):215-23.
- Bergamini C, Moruzzi N, Sblendido A, Lenaz G, Fato R. A water soluble CoQ10 formulation improves intracellular distribution and promotes mitochondrial respiration in cultured cells. *PLoS One.* 2012;7(3):e33712.
- Montes R, Ayllon V, Gutierrez-Aranda I, Prat I, Hernandez-Lamas MC, Ponce L, *et al.* Enforced expression of MLL-AF4 fusion in cord blood CD34⁺ cells enhances the hematopoietic repopulating cell function and clonogenic potential but is not sufficient to initiate leukemia. *Blood.* 2011;117(18):4746-58.
- Bueno C, Montes R, de la Cueva T, Gutierrez-Aranda I, Menendez P. Intra-bone marrow transplantation of human CD34⁺ cells into NOD/LSZ-scid IL-2gamma(null)

- mice permits multilineage engraftment without previous irradiation. *Cytherapy*. 2010;12(1):45-9.
23. Levac K, Menendez P, Bhatia M. Intra-bone marrow transplantation facilitates pauciclonal human hematopoietic repopulation of NOD/SCID/beta2m(-/-) mice. *Exp Hematol*. 2005;33(11):1417-26.
24. Navarro-Montero O, Romero-Moya D, Montes R, Ramos-Mejia V, Bueno C, Real FJ, et al. Intrahepatic transplantation of cord blood CD34⁺ cells into newborn NOD/SCID-IL2Rgamma(null) mice allows efficient multi-organ and multi-lineage hematopoietic engraftment without accessory cells. *Clin Immunol*. 2012;145(2):89-91.
25. Terstappen LW, Huang S, Safford M, Lansdorf PM, Loken MR. Sequential generations of hematopoietic colonies derived from single nonlineage-committed CD34-CD38- progenitor cells. *Blood*. 1991; 77(6):1218-27.
26. Lindemann A, Dorken B, Henschler R, Mertelsmann R, Herrmann F. Screening for expression of cytokines with hematopoietic growth factor activity by permanent human B-cell lines. *Leukemia* 1991;5(8):715-8.
27. Facucho-Oliveira JM, St John JC. The relationship between pluripotency and mitochondrial DNA proliferation during early embryo development and embryonic stem cell differentiation. *Stem Cell Rev*. 2009; 5(2):140-53.
28. Cho YM, Kwon S, Pak YK, Seol HW, Choi YM, Park do J, et al. Dynamic changes in mitochondrial biogenesis and antioxidant enzymes during the spontaneous differentiation of human embryonic stem cells. *Biochemical and biophysical research communications*. 2006;348(4):1472-8.
29. Facucho-Oliveira JM, Alderson J, Spikings EC, Egginton S, St John JC. Mitochondrial DNA replication during differentiation of murine embryonic stem cells. *J Cell Sci*. 2007;120(22):4025-34.
30. St John JC, Ramalho-Santos J, Gray HL, Petrosko P, Rawe VY, Navara CS, et al. The expression of mitochondrial DNA transcription factors during early cardiomyocyte in vitro differentiation from human embryonic stem cells. *Cloning Stem Cells*. 2005;7(3): 141-53.
31. Morgan MJ, Kim YS, Liu ZG. TNFalpha and reactive oxygen species in necrotic cell death. *Cell Res*. 2008;18(3):343-9.
32. Ito K, Hirao A, Arai F, Takubo K, Matsuoka S, Miyamoto K, et al. Reactive oxygen species act through p38 MAPK to limit the lifespan of hematopoietic stem cells. *Nat Med*. 2006;12(4):446-51.
33. Ito K, Hirao A, Arai F, Matsuoka S, Takubo K, Hamaguchi I, et al. Regulation of oxidative stress by ATM is required for self-renewal of haematopoietic stem cells. *Nature*. 2004;431(7011):997-1002.
34. Jang YY, Sharkis SJ. A low level of reactive oxygen species selects for primitive hematopoietic stem cells that may reside in the low-oxygenic niche. *Blood*. 2007;110(8): 3056-63.
35. Dinkelmann MV, Zhang H, Skop AR, White JG. SPD-3 is required for spindle alignment in *Caenorhabditis elegans* embryos and localizes to mitochondria. *Genetics*. 2007; 177(5):1609-20.
36. Kruger N, Tolic-Norrelykke IM. Association of mitochondria with spindle poles facilitates spindle alignment. *Curr Biol*. 2008;18 (15):R646-R7.
37. Stauber W. Asymmetric distribution of mitochondria and of spindle microtubules in opposite directions in differential mitosis of germ line cells in *Aricotopus*. *Cell Tiss Res*. 2007;329(1):197-203.

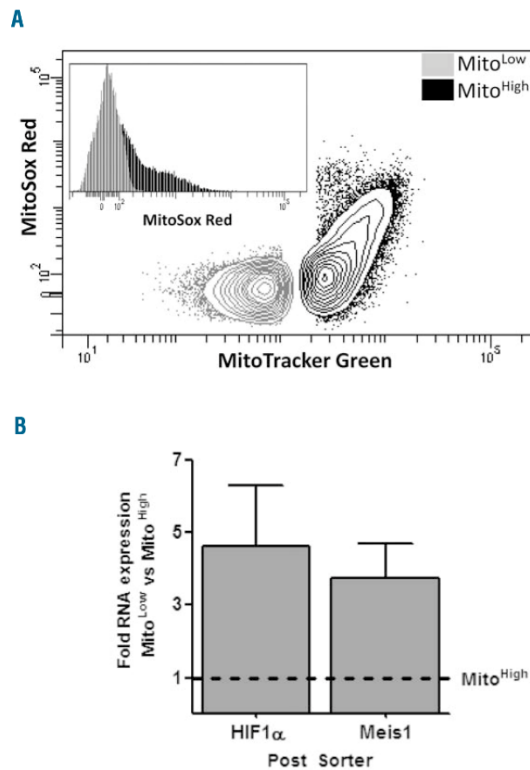
SUPPLEMENTARY APPENDIX

Cord blood-derived CD34⁺ hematopoietic cells with low mitochondrial mass are enriched in hematopoietic repopulating stem cell function

Damia Romero-Moya,¹ Clara Bueno,¹ Rosa Montes,¹ Oscar Navarro-Montero,¹ Francisco J. Iborra,² Luis Carlos López,³ Miguel Martín,¹ and Pablo Menendez^{1,4,5}

¹GENyo (Centre for Genomics and Oncological Research: Pfizer / University of Granada / Andalusian Government), Granada; ²Department of Molecular and Cellular Biology, Centro Nacional de Biotecnología, Consejo Superior de Investigaciones Científicas, Madrid; ³Centro de Investigación Biomédica, Instituto de Biotecnología, Universidad de Granada; ⁴Josep Carreras Leukemia Research Institute, Barcelona; and ⁵Institució Catalana de Recerca i Estudis Avançats, (ICREA), Barcelona, Spain

©2013 Ferrata Storti Foundation. This is an open-access paper. doi:10.3324/haematol.2012.079244



Online Supplementary Figure S1. (A) Levels of reactive oxidative species (ROS) measured by MitoSox staining in CD34⁺ Mito^{Low} cells and Mito^{High} cells. (B) Quantitative reverse transcriptase polymerase chain reaction analysis of HIF1 α and Meis1 in CD34⁺ Mito^{Low} cells relative to CD34⁺ Mito^{High} cells. The dotted horizontal line represents the gene expression level in CD34⁺ Mito^{High} cells. β -actin was used as a housekeeping gene.

V.3.ARTICLE III:

Generation, genome edition and characterization of iPSC lines from a patient with coenzyme Q10 deficiency harboring a heterozygous mutation in COQ4 gene.

Romero-Moya D*, Castaño J, Santos-Ocaña C, Navas P, Menendez P*.

Stem Cell Research. 2016 (In Press)

***Co-corresponding.**

Accepted Manuscript

Generation, genome edition and characterization of iPSC lines from a patient with coenzyme Q₁₀ deficiency harboring a heterozygous mutation in *COQ4* gene

Damià Romero-Moya, Julio Castaño, Carlos Santos-Ocaña, Plácido Navas, Pablo Menendez

PII: S1873-5061(16)30122-2
DOI: doi:[10.1016/j.scr.2016.09.007](https://doi.org/10.1016/j.scr.2016.09.007)
Reference: SCR 826

To appear in: *Stem Cell Research*

Received date: 4 September 2016
Accepted date: 14 September 2016



Please cite this article as: Romero-Moya, Damià, Castaño, Julio, Santos-Ocaña, Carlos, Navas, Plácido, Menendez, Pablo, Generation, genome edition and characterization of iPSC lines from a patient with coenzyme Q₁₀ deficiency harboring a heterozygous mutation in *COQ4* gene, *Stem Cell Research* (2016), doi:[10.1016/j.scr.2016.09.007](https://doi.org/10.1016/j.scr.2016.09.007)

This is a PDF file of an unedited manuscript that has been accepted for publication. As a service to our customers we are providing this early version of the manuscript. The manuscript will undergo copyediting, typesetting, and review of the resulting proof before it is published in its final form. Please note that during the production process errors may be discovered which could affect the content, and all legal disclaimers that apply to the journal pertain.



Lab Resource: Stem Cell Line

Generation, genome edition and characterization of iPSC lines from a patient with coenzyme Q₁₀ deficiency harboring a heterozygous mutation in *COQ4* gene

Damià Romero-Moya^{a,*}, Julio Castaño^a, Carlos Santos-Ocaña^b, Plácido Navas^b, Pablo Menéndez^{a,c}

^a Josep Carreras Leukemia Research Institute, Department of Biomedicine, School of Medicine, University of Barcelona, Barcelona, Spain

^b Centro Andaluz de Biología del Desarrollo, Universidad Pablo Olavide, Sevilla, Spain

^c Institut Catalana de recerca i Estudis Avançats (ICREA), Barcelona, Spain

ARTICLE INFO

Article history:
Received 4 September 2016
Accepted 14 September 2016
Available online xxx

ABSTRACT

We report the generation, CRISPR/Cas9-edition and characterization of induced pluripotent stem cell (iPSC) lines from a patient with coenzyme Q₁₀ deficiency harboring the heterozygous mutation c.483G > C in the *COQ4* gene. iPSCs were generated using non-integrative Sendai Viruses containing the reprogramming factors *OCT4*, *SOX2*, *KLF4* and *C-MYC*. The iPSC lines carried the c.483G > C *COQ4* mutation, silenced the OSKM expression and were mycoplasma-free. They were *bona fide* pluripotent cells as characterized by morphology, immunophenotype gene expression for pluripotent-associated markers/genes, *NANOG* and *OCT4* promoter demethylation, karyotype and teratoma formation. The *COQ4* mutation was CRISPR/Cas9 edited resulting in isogenic, diploid and off-target free *COQ4*-corrected iPSCs.

© 2016 Published by Elsevier Ltd.

1. Resource table

Name of stem cell line	CQ4-iPSC
Institution	Josep Carreras Leukemia Research Institute (LJC)
Person who created resource	Damià Romero-Moya, Julio Castaño, Pablo Menéndez
Contact person and email	Pablo Menéndez, pmenendez@carrerasresearch.org
Date archived/stock date	May 2015
Origin	Human dermal fibroblasts
Type of resource	Biological Reagent: human COQ4-mutated iPSC line and its CRISPR/Cas9-genome corrected isogenic iPSC line.
Sub-type	Cell line
Key transcription factors	<i>OCT4</i> , <i>SOX2</i> , <i>KLF4</i> , <i>C-MYC</i>
Authentication	Identity of the iPSC line confirmed by fingerprinting and PCR
Link to related literature	http://www.ncbi.nlm.nih.gov/pubmed/22368301 http://www.ncbi.nlm.nih.gov/pubmed/26183144 http://www.ncbi.nlm.nih.gov/pubmed/25658047 http://www.ncbi.nlm.nih.gov/pubmed/26850912 http://www.ncbi.nlm.nih.gov/pubmed/26500142
Information in public databases	http://www.isctii.es/ISCTII/es/contenidos/fd-cl-instituto/fd-organizacion/fd-estructura-directiva/fd-subdireccion-general-investigacion-terapia-celular-medicina-regenerativa/fd-centros-unidades/fd-banco-nacional-lineas-celulares/fd-lineas-celulares-disponibles/lineas-de-celulas-ips.shtml
Ethics	Ethics Review Board-competent authority approval obtained

* Corresponding author.

Email address: dromero@carrerasresearch.org (D. Romero-Moya)

2. Resource details

A 4-year-old girl was diagnosed in our Institution with minor mental retardation and lethal rhabdomyolysis associated with Coenzyme Q₁₀ deficiency (Trevisson et al., 2011). Genetic analysis identified a heterozygous c.483G > C mutation in the *COQ4*, leading to the amino acid change E161D. COQ4-mutated dermal fibroblasts were reprogrammed into iPSCs. Patient and control fibroblasts were transduced with OSKM-expressing Sendai virus (SeV, CytoTune™-iPS Reprogramming System, Life Technologies) as previously described (Buono et al., 2016; Munoz-Lopez et al., 2016). iPSC colonies emerged 16–18 days after OSKM transduction and were picked for further characterization. iPSCs revealed an embryonic stem cell (ESC)-like morphology and alkaline phosphatase activity (Fig. 1A). Short tandem repeat analysis confirmed iPSC identity (Fig. 2). PCR analysis and Sanger sequencing confirmed the c.483G > C mutation in all CQ4-iPSC clones (Fig. 1B). After 8–10 passages, iPSC lines were OSKM transgene independent as revealed by immunostaining and qRT-PCR analysis for SeV (Fig. 1C). Endogenous expression of *NANOG* and *OCT4* was accompanied by the extensive loss of CpG methylation in their promoters (Fig. 1D). CQ4-iPSCs were CRISPR/Cas9 edited in c.483 and introduced a TaqI restriction site with a synonymous change of nucleotides (Fig. 1E). The top off-target predicted beforehand, *GRID2*, was sequenced in CQ4-edited iPSC (CQ4^{ed}-iPSC) lines with no alteration (Fig. 1F). Importantly, mutated and edited iPSCs remained diploid after cell reprogramming and further CRISPR/Cas9 edition (Fig. 1G). In addition, the endogenous pluripotency-associated genes *OCT4*, *SOX2*, *REX1*, *NANOG* and *CRIP1* were expressed at comparable levels to human ESCs in both, CQ4- and CQ4^{ed}-iPSCs by qRT-PCR (Fig. 1H). Similarly, im-

<http://dx.doi.org/10.1016/j.scr.2016.09.007>

1873-5061/© 2016 Published by Elsevier Ltd.

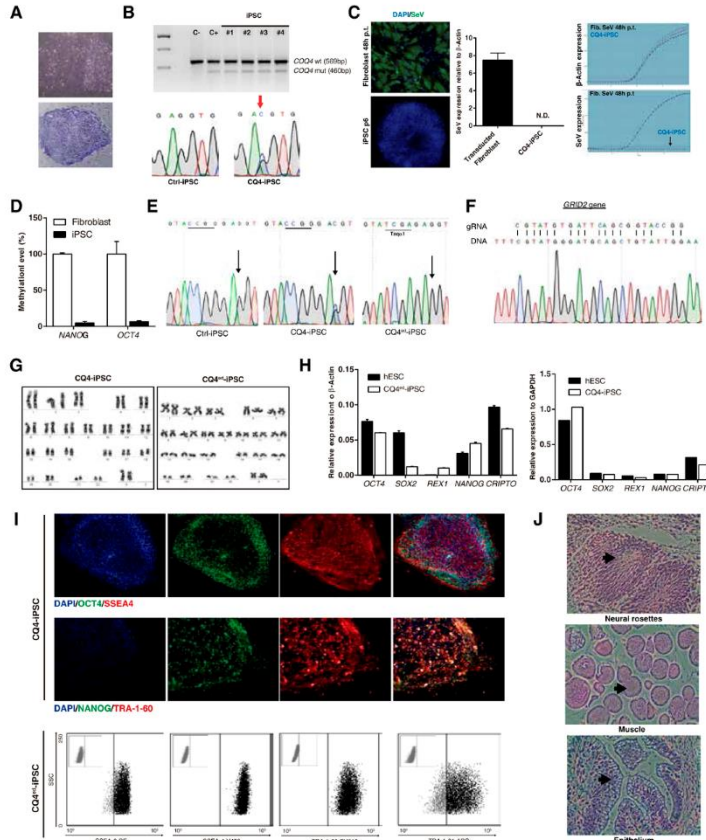


Fig. 1. iPSC generation, genome editing and characterization: (A) Representative morphology and alkaline phosphatase staining of CQ4-iPSC. (B) PCR and Sanger sequencing confirming the presence of *COQ4*-mutated allele in several representative CQ4-iPSC clones. (C) Immunostaining confirming high-level infection with SeV 48 h post-transduction and SeV elimination on all iPSC clones at p8-10 (left panel), qPCR reflecting complete absence of SeV at p8-10 (right panel). (D) Pyrosequencing revealing demethylation of *NANOG* and *OCT4* promoters in *COQ4*-mutated iPSCs as compared to original fibroblasts. (E) Sanger DNA sequencing confirming the gene edition. (F) Sanger DNA sequencing of the major predicted off-target *GRID2* gene. (G) Diploid karyotype of CQ4-iPSC and CQ4^{del}-iPSC. (H) qRT-PCR for the pluripotency genes *OCT4*, *SOX2*, *REX1*, *NANOG*, and *CRIP1* in hESC and CQ4-mutated and CQ4-edited iPSCs. (I) Representative immunostaining (top panels) for the pluripotency markers OCT4, SSEA-4, NANOG, TRA-1-60 and representative flow cytometry plots (bottom panel) for the pluripotency markers SSEA-3, SSEA-4, TRA-1-60, TRA-1-81. (J) Representative teratoma analysis revealing three germ layer differentiation of iPSC: CQ4-iPSC; CQ4^{del}-iPSC; Ctrl-iPSC; Control iPSC; CQ4^{del}-iPSC; CQ4-edited iPSC.

monostaining and flow cytometry revealed *bona fide* expression of OCT4, NANOG, TRA-1-60, TRA-1-81, SSEA3 and SSEA4 in both CQ4- and CQ4^{del}-iPSCs (Fig. 1I). *In vivo* differentiation capacity was demonstrated by teratoma formation in immunodeficient mice comprising tissue representing all three germ layers (Fig. 1J).

3. Materials and methods

3.1. iPSC generation and maintenance

Fibroblasts were maintained in low glucose DMEM supplemented with 20% FBS and 1% penicillin/streptomycin (P/S). The iPSCs were

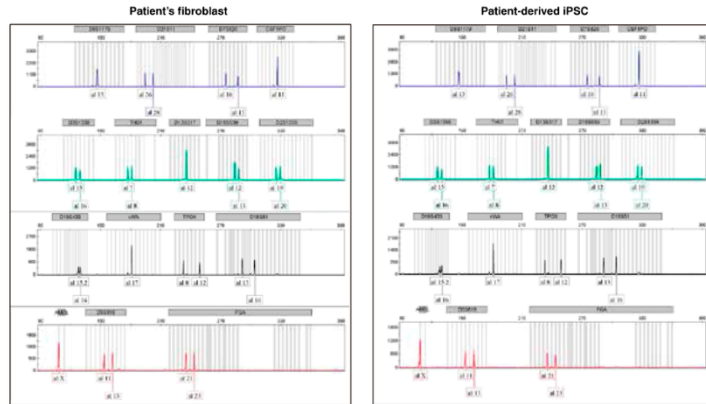


Fig. 2. Cell identity confirmed by fingerprinting analysis of patient fibroblasts and iPSCs.

generated using the CytoTune®-iPS Sendai Reprogramming Kit (Life Technologies). iPSC clones were fully characterized and maintained undifferentiated on irradiated mouse embryonic fibroblasts (iMEF) in hESC media (KO-DMEM supplemented with 20% KO Serum Replacement, 1% GlutaMAX, 1% P/S, 1% NEAA and 0.1 mM β -mercaptoethanol (all from Life Technologies) and 10 ng/ml basic fibroblast growth factor (bFGF; Miltenyi), or on Matrigel (BD) with MEF-conditioned media (MEF-CM) (Montes et al., 2009; Ramos-Mejía et al., 2012). iPSCs were passaged when confluent with 0.1% collagenase IV/dispase or 0.05% trypsin.

3.2. iPSC characterization

Established iPSC was fully characterized as previously described (Bueno et al., 2016). SeV elimination was determined by qRT-PCR. Expression of pluripotency markers was performed by immunostaining (alkaline phosphatase, OCT4, NANOG, SSEA3, SSEA4, TRA-1-60, TRA-1-81) and qRT-PCR (*OCT-4*, *NANOG*, *SOX2*, *REX1*, *CRIP1*) using the primers and antibodies described in Table 1 and Table 2. G-banding karyotype was performed as previously described (Catalina et al., 2008). For teratoma assays, the different iPSC clones were collected through enzymatic dissociation using collagenase IV, and 2 million cells were re-suspended and injected with 250 μ l DMEM and 50 μ l Matrigel subcutaneously in the back of the NSG mice (Gutierrez-Aranda et al., 2010). Animal experimentation was approved by the Animal Care Committee of the University of Barcelona. Tumors generally developed within 6–8 weeks. Animals were sacrificed for teratoma dissection. After sectioning, the presence of cells from the three germ layers was assessed following Hematoxylin & Eosin staining (Gutierrez-Aranda et al., 2010).

3.3. DNA and RNA extraction and (qRT)-PCR

DNA was obtained using the Maxwell 16 Blood DNA Purification kit (Promega). Isolation of total RNA was performed using RNAqueous-Micro kit (Ambion). The cDNA synthesized by using SuperScript III Reverse Transcriptase kit (Invitrogen). qRT-PCR was

Table 1
Primers used in this study.

<i>β-ACTIN-FW</i>	GATGGCCACGGCTGCTT
<i>β-ACTIN-RV</i>	AGGACTCATGCCAGGAA
<i>GAPDH-FW</i>	ACCACAGHCCATGCAATCAC
<i>GAPDH-RV</i>	TCCACCACCCCTGTTCTGT
SeV-Fw	GGACTACTAGGTGATATCGAGC
SeV-RV	ACCAGACAAGAGTTAAGAGATATGTATC
<i>OCT4-FW</i>	GGGTTTTGGGATTAAGTTCTTCA
<i>OCT4-RV</i>	GCCTCCACCTTTGTGTT
<i>REX1-FW</i>	CCTGAGGGCGAAATAGAAC
<i>REX1-RV</i>	GCACACATAGGCATCACATAAAG
<i>NANOG-FW</i>	ACAACCTGGCCGAAGAATAGCA
<i>NANOG-RV</i>	GTTCCAGTCGGGTTCCAC
<i>SOX2-FW</i>	CAAAATGGCCATGCAGTT
<i>SOX2-RV</i>	AGTTGGGATCGAACAAAAGTATT
<i>COQ4-FW</i>	CTGGGAACCATCAGGAAGG
<i>COQ4-RV</i>	CCAAGAGTGAACAGGAAGGAG
<i>COQ4-Mut-FW</i>	ATTCAGCGGTACCGGACCC
<i>SEQ-COQ4-FW</i>	CCAGACACCCGAGCACC
<i>SEQ-COQ4-RV</i>	AGAAGGGATAGGGATGGA
<i>GRID2-FW</i>	GTGCAGATTCAACCAGCCAT
<i>GRID2-RV</i>	CTCGTAAGGACTGCATGT

Table 2
Antibodies used in this study.

Antibody	Supplier	Reference	Dilution
OCT-4	ABCAM	AB19857	1:500
SSEA-4	ABCAM	AB16287	1:50
NANOG	ABCAM	AB21624	1:50
TRA-1-60	ABCAM	AB16288	1:50
Alexa Fluor® 488 α -Rabbit	Jackson ImmunoResearch	711-545-152	1:500
Alexa Fluor® 555 α -Mouse	Life Technologies	A31570	1:500
SSEA-3-PE	BD Bioscience	560,237	1:100
SSEA-4-V450	BD Bioscience	561,156	1:100
TRA-1-60-BV510	BD Bioscience	563,188	1:100
TRA-1-81-AlexaFlour647®	BD Bioscience	560,793	1:100

done using SyberGreen (Applied) and values were normalized to *β -ACTIN* or *GAPDH*. PCR conditions were 95 °C for 10 min, followed by 40 cycles of 95 °C for 15 s and 60 °C for 60 s.

3.4. Immunophenotyping

Cells were fixed with 2–4% PFA in PBS for 20 min at RT and washed 3 times with PBS. Antigen blocking was done with 6% donkey FBS with 0.5% Triton X-100. Cells were then washed and incubated at 4 °C overnight with the primary antibody diluted in blocking solution with 0.1% Triton X-100. After washing, cells were incubated with the secondary antibody for 2 h at RT. To check by flow cytometry the pluripotency-associated markers the iPSCs were dissociated by incubation with trypsin 0.05% for 40 s. Then, were resuspended in FACS Buffer (5% FBS, 2 mM EDTA in PBS) and incubated with the specific antibody in 200 µl for 15 min in the darkness. Next, the cells were washed twice and stained with 7-aminoactinomycin D (7-AAD) (BD Bioscience) for 5 min. Stained cells were analyzed using FACS Canto II (BD).

3.5. COQ4 mutation detection

For genomic detection of the COQ4 mutation, a touchdown PCR was performed with 100 ng of gDNA. PCR conditions were 1 cycle of 5 min at 95 °C; 24 cycles of 30 s at 95 °C, 30 s at 62 °C (– 0.5 °C per cycle), 1 min at 72 °C; 6 cycles of 30 s at 95 °C, 30 s at 50 °C, 1 min at 72 °C; 1 cycle of 10 min at 72 °C. PCRs were resolved in 1% agarose gels. Primers used to confirm the mutation on patient's fibroblast and iPSC as well as primers used for Sanger sequencing are described in Table 1.

3.6. Promoter demethylation

Bisulfite pyrosequencing of *OCT4* and *NANOG* promoters was done as described (Bueno et al., 2016). Briefly, bisulfite modification

of genomic DNA was performed with the EZ DNA Methylation-Gold kit (Zymo Research) following the manufacturer's instructions. The set of primers for PCR amplification and sequencing of NANOG and OCT4 were designed using the software PyroMark Assay Design and are detailed elsewhere (Bueno et al., 2016).

References

- Bueno, C., Sardiná, J.L., Di Stefano, B., Romero-Moya, D., Muñoz-Lopez, A., Ariza, L., Chillón, M.C., Balanzategui, A., Castano, J., Herreros, A., Fraga, M.F., Fernández, A., Granada, I., Quintana-Bustamante, O., Segovia, J.C., Nishimura, K., Ohtaka, M., Nakanishi, M., Graf, T., Menendez, P., 2016. Reprogramming human B cells into induced pluripotent stem cells and its enhancement by C/EBPalpha. *Leukemia* 30 (3), 674–682.
- Catalina, P., Montes, R., Ligeró, G., Sanchez, L., de la Cueva, T., Bueno, C., Leone, P.E., Menendez, P., 2008. Human ESCs predisposition to karyotypic instability: is a matter of culture adaptation or differential vulnerability among hESC lines due to inherent properties?. *Mol. Cancer* 7, 76.
- Gutierrez-Aranda, I., Ramos-Mejía, V., Bueno, C., Muñoz-Lopez, M., Real, P.J., Marcia, A., Sanchez, L., Ligeró, G., García-Pareja, J.L., Menendez, P., 2010. Human induced pluripotent stem cells develop teratoma more efficiently and faster than human embryonic stem cells regardless the site of injection. *Stem Cells* 28 (9), 1568–1570.
- Montes, R., Ligeró, G., Sanchez, L., Catalina, P., de la Cueva, T., Nieto, A., Melen, G.J., Rubio, R., Garcia-Castro, J., Bueno, C., Menendez, P., 2009. Feeder-free maintenance of hESCs in mesenchymal stem cell-conditioned media: distinct requirements for TGF-beta and IGF-II. *Cell Res.* 19 (6), 698–709.
- Munoz-Lopez, A., van Roon, E.H., Romero-Moya, D., Lopez-Millan, B., Stam, R.W., Colomer, D., Nakanishi, M., Bueno, C., Menendez, P., 2016. Cellular ontogeny and hierarchy influence the reprogramming efficiency of human B cells into induced pluripotent stem cells. *Stem Cells* 34 (3), 581–587.
- Ramos-Mejía, V., Bueno, C., Roldán, M., Sanchez, L., Ligeró, G., Menendez, P., Martín, M., 2012. The adaptation of human embryonic stem cells to different feeder-free culture conditions is accompanied by a mitochondrial response. *Stem Cells Dev.* 21 (7), 1145–1155.
- Trevisson, E., DiMauro, S., Navas, P., Salvati, L., 2011. Coenzyme Q deficiency in muscle. *Curr. Opin. Neurol.* 24 (5), 449–456.

V.4.ARTICLE IV:

Genetic rescue of mitochondrial and skeletal muscle impairment in an iPSC model of coenzyme Q10 deficiency

Romero-Moya D, Santos Ocaña C, Castaño J, Garrabou G, Rodríguez-Gómez JA, Ruiz-Bonilla V, Perdiguero E, Bueno C, Moren-Nuñez C, González-Rodríguez P, Giorgetti A, Prieto C, Muñoz-López A, Fernández-Ayala DJ, Cascajo MV, Velasco I, Montero R, Yubero D, Jou C, López-Barneo J, Cardellach F, Artuch R, Muñoz-Cánoves P, Navas P, Menendez P.

Stem Cells. 2016 (Under revision)

Genetic rescue of mitochondrial and skeletal muscle impairment in an iPSCs model of coenzyme Q₁₀ deficiency

An iPSC model for coenzyme Q10 deficiency

Damià Romero-Moya¹, Carlos Santos-Ocaña^{2,3§}, Julio Castaño^{1,§}, Gloria Garrabou^{3,4}, José A Rodríguez-Gómez⁵, Vanesa Ruiz-Bonilla^{6,7}, Clara Bueno¹, Patricia González-Rodríguez^{5,6}, Alessandra Giorgetti¹, Eusebio Perdiguero^{6,7}, Cristina Prieto¹, Álvaro Muñoz-López¹, Constanza Moren-Nuñez^{3,4}, Daniel J Fernández-Ayala^{2,3}, Maria Victoria Cascajo^{2,3}, Iván Velasco⁸, Raquel Montero^{3,9}, Delia Yubero⁹, Cristina Jou^{3,9}, José López-Barneo^{5,6}, Francesc Cardellach^{3,4}, Pura Muñoz-Cánoves^{6,7}, Rafael Artuch^{3,9}, Plácido Navas^{2,3}, Pablo Menéndez^{1,10*}

¹Josep Carreras Leukemia Research Institute. Department of Biomedicine, School of Medicine. University of Barcelona. Barcelona. Spain. ²Centro Andaluz de Biología del Desarrollo. Universidad Pablo Olavide-CSIC. ³CIBER de Enfermedades Raras (CIBERER). Sevilla. Spain. ⁴Muscle Research and Mitochondrial Function Laboratory, Cellex-IDIBAPS-School of Medicine, University of Barcelona, Barcelona. Spain. ⁵Institute of Biomedicine of Seville, Hospital Universitario Virgen del Rocío-Consejo Superior de Investigaciones Científicas (CSIC)-University of Seville, Seville, Spain. ⁶CIBER on Neurodegenerative Diseases (CIBERNED). ⁷Department of Experimental and Health Sciences. Pompeu Fabra University (UPF). Barcelona. Spain. ⁸Instituto de Fisiología Celular-Neurociencias, Universidad Nacional Autónoma de México, México. ⁹Institut de Recerca-Sant Joan de Déu. Barcelona. Spain. ¹⁰Institució Catalana Recerca Estudis Avançats (ICREA). Lluís Companys 23, Barcelona. Spain.

§These authors equally contributed to this work

*Correspondence should be addressed to:

Pablo Menendez PhD. ICREA Research Professor

Josep Carreras Leukemia Research Institute. School of Medicine. University of Barcelona.

Casanova 143, 08036. Barcelona. Spain. pmenendez@carrerasresearch.org

AUTHOR CONTRIBUTION

D.R-M: conceived the study, designed and performed experiments, analyzed data and wrote the manuscript. C.S-O, J.C, G.G, J.A.R, V.R-B, E.P, C.B, C.M-M, P.G-R, A.G, C.P, A.M-L, D.J.F-A, M.V.C, I.V: performed experiments and analyzed data. R.A, F.C, P.M-C, J.L-B, P.N: provided biological samples, clinical data and advice. P.M: conceived the study, designed experiments, analyzed data and wrote the manuscript

Key words: Coenzyme Q10, COQ4, iPSC, CRISPR-Cas9, dopaminergic & motor neurons, skeletal muscle.

ABSTRACT

Coenzyme Q₁₀ (CoQ₁₀) plays a crucial role in mitochondria as an electron carrier within the mitochondrial respiratory chain (MRC), and is an essential antioxidant. Mutations in genes responsible for CoQ₁₀ biosynthesis (COQ genes) cause primary CoQ₁₀ deficiency, a rare and heterogeneous mitochondrial disorder with no clear genotype-phenotype association, mainly affecting tissues with high-energy demand including brain and skeletal muscle (SkM). Here, we report a 4-year old girl diagnosed with minor mental retardation and lethal rhabdomyolysis harboring a heterozygous mutation (c.483G>C (E161D)) in COQ4. The patient's fibroblasts showed a decrease in [CoQ₁₀], CoQ₁₀ biosynthesis and MRC activity affecting complexes I/II+III. *Bona fide* induced pluripotent stem cell (iPSCs) lines carrying the COQ4 mutation (CQ4-iPSCs) were generated, characterized and genetically edited using CRISPR-Cas9 (CQ4^{ed}-iPSCs). Extensive differentiation and metabolic assays of control-iPSCs, CQ4-iPSCs and CQ4^{ed}-iPSCs demonstrated a genotype association, reproducing the disease phenotype. The COQ4 mutation in iPSC was associated with CoQ₁₀ deficiency, metabolic dysfunction and impaired differentiation into SkM; remarkably, iPSC differentiation in dopaminergic or motor neurons was unaffected. This study offers an unprecedented iPSC model recapitulating CoQ₁₀ deficiency-associated functional and metabolic phenotypes caused by COQ4 mutation.



INTRODUCTION

Coenzyme Q₁₀ (CoQ₁₀) is a lipid-soluble molecule ubiquitous to cellular membranes that has essential functions in many cellular processes including energy/ATP production, where it shuttles electrons from complex I and II to complex III in the mitochondrial respiratory chain (MRC). CoQ₁₀ also participates in beta-oxidation of fatty acids, pyrimidine biosynthesis, and it is one of the main cellular antioxidants[1, 2]. Proteins encoded by different *COQ* genes are involved in the pathway of CoQ₁₀ biosynthesis between the cytoplasm and mitochondria by functioning as a multienzymatic complex[3]. Several mutations in genes involved in CoQ₁₀ biosynthesis, such as *COQ2*[4-7], *COQ6*[8], *ADCK3*[7, 9, 10], *ADCK4*[11], *COQ9*[7, 12], *PDSS1*[13], *PDSS2*[7, 14] and *COQ7*[15], have been described, and all result in a reduction in CoQ₁₀ levels. CoQ₁₀ levels below 50% of standard values are indicative of CoQ₁₀ deficiency, which is a rare and heterogeneous group of metabolic/mitochondrial disorders (OMIM#607426)[16], frequently diagnosed during childhood. CoQ₁₀ deficiency associates with multiple clinical phenotypes including kidney failure[13] and neurological and neuromuscular diseases, such as mental retardation, seizures, and ataxias, affecting tissues with high energetic demand such as muscle and neurons[16-18].

It has been suggested that *COQ4* has an essential structural and functional role for the biosynthesis of CoQ₁₀[19-21]. Indeed, *COQ4* mutations as well as *COQ4* haploinsufficiency cause a broad spectrum of mitochondrial disorders associated with CoQ₁₀ deficiency[22-24]. We identified CoQ₁₀ deficiency in a 4-year-old girl with a heterozygous missense mutation (c.483 G>C) in *COQ4*. This patient did not display (or very mild) symptoms of impaired neurodevelopment or neurodegeneration, but presented severe metabolic/mitochondrial defects accompanied with lethal rhabdomyolysis. CoQ₁₀ deficiency is a heterogeneous disease, and a major obstacle to study this disorder is the lack of association between the genotype and phenotype[3, 25], which partly explains the highly variable patient response to CoQ₁₀ supplementation[3, 26, 27]. Interestingly, the *COQ4* E161D variant found in this patient has also been reported to have a minor allele frequency (<0.5%) in the population, so that whether it represents a driver pathogenic mutation or a cooperating hit in the underlying pathogenesis of more diseases is unknown.

Human disease is generally studied once all (epi)genetic/metabolic insults have already occurred and, therefore, the mechanisms by which disease-specific mutations impair normal homeostasis are not amenable to analysis with patient samples. In this regard, induced pluripotent stem cells (iPSC) together with genome editing strategies for correction of disease-causing mutations are powerful tools for modeling different aspects of human disease that cannot otherwise be addressed by patient sample analyses or animal models[28, 29]. iPSC are routinely generated from different cell types derived from both healthy donors and patients[30-33], thus providing a unique *in vitro* platform to explore the developmental impact of disease-specific genetic aberrations on human stem cell fate, especially in early-onset or developmental diseases[28].

Here, we have generated and CRISPR/Cas9-edited iPSC lines from a patient carrying a *COQ4* missense mutation to analyze its developmental and metabolic/mitochondrial impact. Developmental and metabolic assays reproduce the disease phenotype. In line with the patient's symptoms, the *COQ4* mutation was associated with CoQ₁₀ deficiency, metabolic dysfunction and impaired differentiation into skeletal muscle (SkM). Notably, the *COQ4* c.483 G>C (E161D) did not impair iPSC differentiation into neural tissues. This study offers a unique human iPSC model recapitulating CoQ₁₀ deficiency-associated functional and metabolic phenotypes caused by *COQ4* mutation.



MATERIAL AND METHODS

iPSC generation, maintenance and characterization

Fibroblasts were maintained in low glucose DMEM supplemented with 20% FBS and 1% penicillin/streptomycin (P/S). Control iPSCs (Ctrl-iPSC) and *COQ4*-mutated iPSC (CQ4-iPSC) were generated using the CytoTune®-iPS Sendai Reprogramming Kit (Life Technologies) (**Fig 2A**). iPSC clones were fully characterized and maintained undifferentiated on irradiated mouse embryonic fibroblasts (iMEF) in hESC media (KO-DMEM supplemented with 20% KO Serum Replacement, 1% GlutaMAX, 1% P/S, 1% NEAA and 0.1 mM β -mercaptoethanol (all from Life Technologies)) and 10 ng/ml basic fibroblast growth factor (bFGF; Miltenyi), or on Matrigel (BD) with MEF-conditioned media (MEF-CM). iPSCs were passaged when confluent with 0.1% collagenase IV/dispase or 0.05% trypsin.

The *COQ4* mutation was characterized in both patient fibroblasts and iPSC using PCR and Sanger sequencing. Primary dermal fibroblasts (CQ4-F) were obtained from the patient in accordance with procedures approved by the Clinic Hospital of Barcelona. Informed consent was obtained in accordance with the Declaration of Helsinki. Age-matched control human dermal fibroblasts (Ctrl-F) were obtained from Tebu-Bio.

Established iPSC were fully characterized as previously described [31, 34]. SeV elimination was determined by qRT-PCR. Expression of pluripotency markers was performed by immunostaining (alkaline phosphatase, OCT4, NANOG, SSEA4, TRA-1-60) and qRT-PCR (*OCT-4*, *NANOG*, *SOX2*, *REX1*, *CRIP1* and *DNMT3 β*) using the primers and antibodies previously described (**Table S1** and **S2**). G-banding karyotype was performed as previously described [35]. For teratoma assays, the different iPSC clones were collected through enzymatic dissociation using collagenase IV, and 2 million cells were re-suspended and injected with 250 μ l DMEM and 50ul Matrigel subcutaneously in the back of the NSG mice [36]. Animal experimentation was approved by the Animal Care Committee of the University of Barcelona. Tumors generally developed within 6-8 weeks. Animals were sacrificed for teratoma dissection. After sectioning, the presence of cells from the three germ layer was assessed following Hematoxylin & Eosin staining [36]. Bisulfite pyrosequencing of *OCT4* and *NANOG* promoters was done as described [31]. Briefly, bisulfite modification of genomic DNA was performed with the EZ DNA Methylation-Gold kit

(Zymo Research) following the manufacturer's instructions. The set of primers for PCR amplification and sequencing of NANOG and OCT4 were designed using the software PyroMark Assay Design (**Table S1**). Primer sequences were designed to hybridize with CpG-free sites to ensure methylation-independent amplification. PCR was performed with primers biotinylated to convert the PCR product to single-stranded DNA templates, using the Vacuum Prep Tool. After PCR amplification, pyrosequencing reactions and methylation quantification were performed using PyroMark Q24 reagents, equipment and software (Qiagen), according to manufacturer's instructions.

CRISPR/Cas9 gene editing

For CRISPR-Cas9 gene editing, undifferentiated CQ4-iPSC were treated with 10 μ M ROCK inhibitor (Y27632) for 24 hours and then 2×10^5 cells were plated on Matrigel-coated 12-well plates. Cells were transfected with Lipofectamine 3000 (Life Technologies) and 5 μ g of pSpCas9(BB)-2A-GFP (PX458) (Addgene plasmid # 48138), allowing the expression of both the guide RNA and the Cas9-GFP, together with 10 nM of antisense ssDNA donor. At 3 days post-transfection, cells were GFP-sorted and plated as single cells on Matrigel-coated 48-well plates. The CRISPR Design Tool (<http://tools.genome-engineering.org>) was used for guide RNA design. The site-specific cleavage efficiency of up to 4 guide RNAs was tested in 293T cells using the T7 surveyor assay [37]. The most efficient guide RNA (~25%) was used. Predicted off-targets were identified using CRISPR Design Tool and analyzed in COQ4-edited iPSC (CQ4^{ed}-iPSC) by Sanger sequencing.

Dopaminergic differentiation

Six different clones of iPSC were differentiated into dopaminergic (DA) neurons using the protocol for midbrain DA neuron induction described by Kriks *et al.*[38]. Briefly, iPSC were maintained in hESC media to day 5 and were then gradually adapted (25%, 50%, 75%, every 2 days) to NIM medium (DMEM/F12, 1% N2 supplement, 2 μ g/ml heparin, 1% NEAA, 1% GlutaMax and 1% P/S). From day 11, iPSC were grown in Neurobasal media (Neurobasal, 1% B27, 1% GlutaMax and 1% P/S). Media were supplemented with SB-431542 (10 μ M; d0-d5; Sigma), LDN193189 (100 nM; d0-d11; Miltenyi), CHIR99021 (3 μ M; d3-d13; Miltenyi), FGF8 (100 ng/ml; d1-d7; Miltenyi), purnormorphamine (2 μ M; d1-d7; Stemgent), SAG (1 μ M; d1-d7;

Tocris), BDNF (20 ng/ml; from d11; Miltenyi), GDNF (20 ng/ml; from d11; Miltenyi), DAPT (10 μ M; from d11; Tocris), db-cAMP (500 μ M; from d11; Sigma), TGF β 3 (1 ng/ml; from d11; Miltenyi) and ascorbic acid (AA, 200 μ M; from d11; Sigma) (**Fig 4A**). On day 20, cells were dissociated using Accutase (Merck) and replated at 3×10^5 cells/cm² on dishes pre-coated with polyornithine (15 μ g/ml), laminin (1 μ g/ml) and fibronectin (5 μ g/ml) until analysis. Quantification of neural precursors and neurons was assessed by confocal microscopy/flow cytometry using anti-NESTIN, anti-SOX2, anti-TUJ1, anti-TH and anti-NCAM antibodies, and qRT-PCR. Antibodies and primers used are detailed in **Table S1** and **S2**.

Motor neuron differentiation

Six different clones of iPSC were differentiated into motor neurons (MN) using the protocol described by Amoroso *et al.*[39]. Briefly, iPSC were grown on iMEF, and embryoid bodies (EB) were generated by first treating cells with 0.1% collagenase IV/0.1% dispase during 60 minutes, followed by washing with KO-DMEM and replating into low-attachment plates in hESC media. Three days later, the medium was changed to NIM media until day 17, and then to Neurobasal media. Media were supplemented with Y27632 (10 μ M; d0-d3; Sigma), SB-431542 (10 μ M; d0-d7; Sigma), LDN193189 (200 nM; d0-d7; Miltenyi), all-*trans* retinoic acid (RA, 1 μ M; from d5; Sigma), AA (2 μ M; from d5; Sigma), BDNF (10 ng/ml; from d5; Miltenyi), purlmorphamine (1 μ M; from d7; Stemgent), SAG (1 μ M; from d7; Tocris), GDNF (10 ng/ml; from d17; Miltenyi), CNTF (10 ng/ml; from d17; Miltenyi), and IGF-1 (10 ng/ml; from d17; Miltenyi) (**Fig 5A**). To analyze MN differentiation, EBs were dissociated into single cells using collagenase B for 2 hours and Dissociation Buffer for 10 minutes, and replated at 2.5×10^5 cells/cm² into dishes pre-coated with polyornithine (15 μ g/ml), laminin (1 μ g/ml) and fibronectin (5 μ g/ml) for 2 days. Quantification of neural precursors and MN was assessed by confocal microscopy/flow cytometry using anti-NESTIN, anti-SOX2, anti-TUJ1, anti-ISL1, anti-HB9 and anti-NCAM antibodies, and qRT-PCR. Antibodies and primers used are detailed in **Table S1** and **S2**.

Skeletal muscle differentiation

iPSC were differentiated into skeletal muscle (SkM) using the protocol described by Darabi *et al.*[33]. Briefly, iPSC were transduced with rtTA and iPAX7-GFP lentiviruses overnight and the medium was then changed to fresh MEF-CM. EBs were generated as described and plated on

low-attachment plates in MEF-CM medium with Y27632 (10 μ M; d0-d7). After 2 days, the medium was replaced with myogenic induction medium (MIM) (IMDM, GlutaMax, 15% FBS, 10% horse serum and 1% P/S) supplemented with 1% Chicken Embryo Extract (US Biological), AA (25 μ g/ml) and 1-monothioglycerol (0.45 mM; Sigma). At day 7, EBs were plated into 0.1% gelatin-coated flasks with MIM plus bFGF (10 ng/ml). Doxycycline (1 μ g/ml; Sigma) was added from day 10 of differentiation onwards. Cells were treated with 10 μ M Y27632 24 hours before GFP sorting on a FACSAria Fusion cell sorter (BD), and sorted cells were replated at 2.5×10^5 cells in a T-25 gelatin-coated flask (**Fig 6A**). PAX7 expression and GFP was confirmed immediately after sorting. PAX7⁺ muscle progenitors were grown in complete MIM with bFGF and doxycycline until passage 3. For further maturation, PAX7⁺ muscle progenitors were first plated at 1.5×10^4 cells/cm². One day before confluency, cells were washed to remove doxycycline and were grown in MIM. At confluency, cells were grown in Differentiation Medium (KO DMEM, 20% KO Serum Replacement, 1% NEAA, 1% GlutaMax, and 1% P/S) for 12–14 days. SkM differentiation was assessed by immunofluorescence using anti-PAX7 and anti-MYH1 antibodies, and qRT-PCR. Primers and antibodies used are detailed in **Table S1** and **S2**. Levels of creatine kinase in iPSC-derived SkM cells were measured using clinical standards in the biochemical diagnostic laboratory at the Clinic Hospital of Barcelona.

CoQ₁₀ biosynthesis, concentration, mitochondrial respiratory chain activity and metabolic measurements

To measure CoQ₁₀ biosynthesis, ¹³C₆-p-hydroxybenzoic acid (PHB) was added to fibroblast and iPSC cultures for 48 hours. Cell pellets were then suspended in 300 μ l of a solution containing 0.25 mM sucrose, 2 mM EDTA, 10 mM Tris and 100 U/ml heparin (pH 7.4), and sonicated twice for 5 sec. Homogenates were then used to determine CoQ₁₀ biosynthesis as previously described [40]. The physiological content of CoQ₁₀ in cultures was determined by HPLC with electrochemical detection as described [40, 41]. Activities of NADH:coenzyme Q1 oxidoreductase (complex I), succinate dehydrogenase (complex II), ubiquinol:cytochrome c oxidoreductase (complex III), cytochrome c oxidase (complex IV), NADH:cytochrome c reductase (complex I+III), succinate:cytochrome c reductase (complex II+III) and citrate synthase (CS) were determined using described spectrophotometric methods[42].

Live cell oxygen consumption (OCR) and extracellular acidification rate (ECAR)

OCR and ECAR were measured using the Seahorse Bioscience equipment (Agilent). CQ4- and CQ4-edited-iPSCs were seeded at density of 25×10^3 cells per well of a XF24 cell culture microplate and incubated for 48h. For OCR the cells were equilibrated with DMEM supplemented with 4,5g/L glucose, 1 mM sodium pyruvate and 2 mM glutamine. For ECAR, cells were maintained in DMEM supplemented with 2 mM glutamine. Mitochondrial processes were examined through sequential injections of oligomycin ($4 \mu\text{M}$; ATP synthase inhibitor), carbonyl cyanide 4-(trifluoromethoxy) phenylhydrazone (FCCP; $2 \mu\text{M}$; uncoupling agent), rotenone ($1 \mu\text{M}$; CI inhibitor) and antimycin A ($5 \mu\text{M}$; CIII inhibitor). Mitochondrial function was calculated upon subtracting the non-mitochondrial respiration background after the addition of antimycin A. The basal respiration rate (baseline OCR minus Antimycin A OCR), Proton Leak (oligomycin OCR minus Antimycin A OCR). The glycolytic processes were examined through sequential injections of glucose (25mM), oligomycin ($4 \mu\text{M}$), 2-Deoxy-D-glucose (2-DG; 50mM). The glycolysis rate was calculated upon subtracting the non-glycolytic acidification after the addition of 2-DG.

ATP and ROS measurements

ATP levels were measured using a Cell-Titer-Glo® Luminescent Cell Viability Assay (Promega) according to the manufacturer's guidelines. Briefly, equal numbers of cells ($5 \times 10^4/100 \text{ mL}$) were seeded in a 96-well plate and 100 mL of the reaction reagent were added to each well. After 10 min shaking, the luminescence signal was detected using the Infinite®200PRO (Tecan) and compared against the ATP Standard Curve using ATP disodium salt (Promega) [43]. ROS generation was quantified by flow cytometry (FACS Canto-II) using CM-H2DCFDA (Life Technologies). 1×10^5 cells were incubated with $2 \mu\text{M}$ CM-H2DCFDA, with or without 0.3% H_2O_2 to analyze the responsiveness to oxidative stress, and then incubated for 45min in the darkness. 7-amino-actinomycin D (7-AAD) was added 10 min before FACS analysis. Intracellular ROS was measure in the live cells (7-AAD-).

Proliferation, apoptosis, cell cycle analysis and senescence assays

Proliferation of CQ4- and Ctrl-F was measured by growing cells in low-glucose DMEM with 20% FBS and 1% P/S. In total, $16 \times 10^3 \text{ cells/cm}^2$ were initially plated and counted every 7 days. For cell cycle analysis, cells were fixed in 70% ice-cold ethanol and stored at -20°C . Subsequently, cells were washed with ice-cold PBS and suspended in propidium iodide buffer containing

RNAse (5 µg/ml) and 0.005% Triton X-100. Cell cycle distribution was analyzed on a FACS Canto-II cytometer using the FACSDiva and ModFit LT software packages (BD).

Apoptosis was analyzed with the Annexin-V apoptosis Detection kit (BD), using annexin-V-PE and 7-AAD. Apoptotic cells were identified as Annexin-V⁺ while dead cells were 7-AAD⁺. The senescence-associated-galactosidase (SA-β-Gal) assay was performed as described[44]. Briefly, cells were fixed in 2% PFA/ 0.2% glutaraldehyde-PBS for 3 min at room temperature and then incubated with X-Gal-containing solution (ThermoFisher) for 15 hours at 37°C in the dark. Positive cells were counted manually.

Patch-clamp recordings

For electrophysiological recordings, CQ4-iPSCs were differentiated into MN. MN were transduced with the MN-specific promoter HB9:GFP lentivirus (AddGene #37080). Whole-cell recordings were obtained from GFP⁺ MNs with an EPC-10 patch-clamp amplifier (HEKA GmbH, Germany) using standard voltage and current clamp protocols designed with Patch-Master software (HEKA). In voltage-clamp configuration, depolarizing voltage steps were applied from -50 mV to +70 mV. Action potentials were evoked by applying a pulse of current of variable amplitude (20-100 pA) to neurons in current-clamp configuration. Unless otherwise specified, holding potential was -70 mV. Data were filtered at 10 kHz, digitized at a sampling interval of 20 µs and computerized. Off-line data analysis was performed using Igor6. Patch electrodes (2–3 MΩ) were pulled from capillary glass tubes (1.5–1.6 mm OD; Kimax, Kimble Products) and fire-polished on a microforge MF-830 (Narishige). All experiments were conducted at room temperature. The bath solution contained: NaCl 140mM, KCl 5mM, CaCl₂ 2mM, MgCl₂ 2mM, HEPES 10mM, Glucose 15mM (pH 7.4; osmolality 300-310 mOsm). The pipette solution contained: potassium gluconate (C₆H₁₁O₇K) 120mM, KCl 20mM, NaCl 10mM, CaCl₂ 1mM, Mg-ATP 4mM, Na-GTP 0.4mM, HEPES 10mM, EGTA 10mM and glucose 10mM (pH 7.2, osmolality 280-290 mOsm).

Determination of dopamine in differentiated neurons by HPLC.

Spontaneous neurotransmitter release was measured in cell culture medium. Neurons were incubated as regularly in 1 ml/one 24-well of medium which was harvested at the time of medium changing. Samples corresponding to different clones and differentiation experiments were

collected between day 35 and 45 of differentiation and immediately stabilized by adding to each 0.5ml sample 25 μ l of stabilization solution (88 μ l of 85% orthophosphoric acid, 4.4 mg of sodium metabisulfite and 912 μ l of H₂O). Samples were frozen in dry ice, and then stored at -80°C until measurement. Dopamine was extracted using a kit for purification of plasmatic catecholamines (Chromsystems, Germany) and 3,4-dihydroxybenzylamine (DHBA) was utilized as internal standard. Eluted samples were analyzed by a high-performance liquid chromatography (HPLC). Samples were analyzed with ALEXYS 100 (Antec Leyden, Zoeterwoude, The Netherlands) system equipped with a reverse phase C-18 column (3 μ m particle size, 150 x 2.1 mm dimension), a glassy carbon electrode and an in situ ISAAC reference electrode (all from Antec Leyden). The amount of dopamine was expressed as pg per ml of sample. The mean \pm SEM was plotted.

DNA and RNA extraction and (qRT)-PCR

DNA was obtained using the Maxwell 16 Blood DNA Purification kit (Promega). Isolation of total RNA was performed using RNAqueous-Micro kit (Ambion). The cDNA synthesized by using SuperScript III Reverse Transcriptase kit (Invitrogen). qRT-PCR was done using SyberGreen (Applied) and values were normalized to β -Actin or *GAPDH*. PCR conditions were 95°C for 10min, followed by 40 cycles of 95°C for 15s and 60°C for 60s.

COQ4 mutation detection

For genomic detection of the COQ4 mutation, a touchdown PCR was performed with 100ng of gDNA. PCR conditions were 1 cycle of 5 min at 95°C; 24 cycles of 30 sec at 95°C, 30 sec at 62°C (-0.5°C per cycle), 1 min at 72°C; 6 cycles of 30 sec at 95°C, 30 sec at 50°C, 1 min at 72°C; 1 cycle of 10 min at 72°C. PCRs were resolved in 1% agarose gels. Primers used to confirm the mutation on patient's fibroblast and iPSC as well as primers used for Sanger sequencing are described in **Table S1**.

Lentiviral transduction

Hb9::GFP lentivector (AddGene #37080) [45] was used to transduce MN. iPAX7-pSAM2 and rTtA-pSAM lentivectors used for SkM specification were kindly provided by Prof. Rita Perlingeiro (University of Minnesota). Viral particles were generated on 293T cells by Polyethylenimine or

calcium phosphate transfection (along with psPAX2 and VSV-G helper plasmids) and concentrated by ultracentrifugation, as previously described [46, 47].

Immunofluorescence and confocal microscopy

Cells were fixed with 2-4% PFA in PBS for 20 min at RT and washed 3 times with PBS. Antigen blocking was done with 6% donkey FBS with 0.5% Triton X-100. Cells were then washed and incubated at 4°C overnight with the primary antibody diluted in blocking solution with 0.1% Triton X-100. After washing, cells were incubated with the secondary antibody for 2h at RT, washed and mounted with Vectashield (Vector Labs). Antibodies, dilutions and suppliers are on **Table S2**. The percentage of antibody positive cells at different time-points was determined in at least three independent experiments for each iPSC clone. At least five images were acquired with Leica TCS SP5 Confocal microscope from each different time-point analyzed. Images for quantification were selected randomly and each image was scored first for the number of DAPI positive nuclei, followed by counting the number of cells expressing the marker of interest. Manually counting was performed with ImageJ software. All data are presented as mean±SEM.

Muscle histology and mitochondrial dynamics in muscle

Healthy and diagnostic muscle biopsies were processed for histology and immunohistochemistry following standard procedures[48]. Muscle tissue was stained with hematoxylin and eosin, and the muscle/mitochondria-specific markers SDH, COX and trichrome[48, 49]. To assess mitochondrial dynamics, differentiating myogenic cells were stained with the mitochondrial import receptor subunit TOM20 and images were taken with a Leica TCS SP5 laser scanning confocal system with a 63× oil immersion objective[50]. At least 5 cells were randomly selected and analyzed for each experimental group. Image analysis was performed with ImageJ (NIH). The following parameters were measured to analyze mitochondrial dynamics. *i*) total number of mitochondria/cellular area[51]; *ii*) mitochondrial circularity ($4\pi \cdot \text{area} / \text{perimeter}^2$). Circular mitochondria exhibit reduced interaction with each other, therefore, the higher the value, the poorer the mitochondrial dynamics/function; *iii*) Form Factor (FF) ($\text{perimeter}^2 / 4\pi \cdot \text{area}$), which is the degree of mitochondrial branching. The higher the FF value, the more dynamic/functional mitochondria are; and *iv*) Aspect Ratio (major axis/minor axis), which measures the mitochondrial



elongation/length. More elongated/elliptical mitochondria have a higher AR, indicative of more dynamic/functional mitochondria.

Statistical analysis

Results are shown as mean±SEM and the normality of data was checked using the Kolmogorov–Smirnov test. For variables with a normal distribution, Student's t-test and one-way ANOVA were used to compare the significance of differences between experimental groups. For variables with no normal distribution, Mann-Whitney U-test or Kruskal-Wallis test was applied. Statistical analysis was performed using SPSS 18.0 software. A p-value<0.05 was considered significant.

RESULTS

COQ4 mutation is linked to impaired mitochondrial function and CoQ₁₀ deficiency

A 4-year-old girl was diagnosed in our Institution with minor mental retardation and lethal rhabdomyolysis. Genetic analysis identified a heterozygous c.483 G>C mutation in the *COQ4*, leading to the amino acid change E161D (**Fig 1A**). *COQ4* mutations have been reported to be responsible for severe early-onset mitochondrial diseases with heterogeneous clinical presentations and associated CoQ₁₀ deficiency [22-24]. Analysis of fibroblasts revealed that the concentration and biosynthesis of CoQ₁₀ was 75% and 87% lower, respectively, in CQ4-F than in Ctrl-F (**Fig 1B, C**). The expression of key *COQ* genes involved in CoQ₁₀ biosynthesis was appreciably higher in CQ4-F than in Ctrl-F, suggestive of a transcriptional compensatory mechanism (**Fig. 1D**). In line with its role in electron transport, the reduction in CoQ₁₀ in CQ4-F was reflected in the reduction of 41% and 64% in the activity of complex I+III and II+III, respectively (**Fig 1E**). CoQ₁₀ is involved in pyrimidine biosynthesis, which is a requirement for cell proliferation [2, 5, 7]. Accordingly, cell proliferation was considerably lower in CQ4-F than in Ctrl-F (**Fig 1F**). Moreover, the proportion of cycling cells was lower for CQ4-F than for Ctrl-F (33% vs 24%; **Fig 1G**), and this was accompanied by a 17-fold increase in senescence as measured by SA-β-Gal staining, and a 2-fold increase in the level of the senescence-associated gene *p16* (*CDKN2A*, **Fig 1H**). Conversely, the level of apoptosis was not different between CQ4-F and Ctrl-F (**Fig 1I**). Histological analysis of the patient's SkM revealed extensive damage associated with rhabdomyolysis (**Fig 1J**), as shown by disorganized tissue structure and loss of expression of the mitochondrial markers SDH and COX (**Fig 1J**).

Generation and characterization of CQ4-iPSCs.

CQ4-F were reprogrammed into hiPSCs in an attempt to model the metabolic and functional impact of *COQ4* mutation on neural and muscle cell fate. Patient and control fibroblasts were transduced with OSKM-expressing Sendai virus (SeV) following the experimental design outlined in **Fig 2A**. iPSC colonies emerged 16–18 days after OSKM transduction and were picked for further characterization (**Fig 2A**). Reprogramming efficiency was ~5-fold higher in Ctrl-F than in CQ4-F (0.8% vs 0.17%, **Fig 2B**), likely reflecting the impaired proliferation capacity of CQ4-F. PCR analysis and Sanger sequencing confirmed the c.483 G>C mutation in all CQ4-iPSC clones

(Fig 2C). After 8–10 passages, iPSC lines were OSKM transgene independent as revealed by immunostaining and qRT-PCR analysis for SeV (Fig 2D). Characterization of iPSC lines revealed an embryonic stem cell (ESC)-like morphology and positive alkaline phosphatase staining (Fig S1A). In addition, the pluripotency-associated genes *OCT4*, *SOX2*, *REX1*, *NANOG* and *CRIPTO* were similarly expressed in Ctrl- and CQ4-iPSCs (Fig S1B). Similarly, immunocytological staining revealed *bona fide* expression of OCT4, NANOG, TRA-1-60 and SSEA4 in both CQ4- and Ctrl-iPSCs (Fig S1C). Endogenous expression of *NANOG* and *OCT4* was accompanied by the extensive loss of CpG methylation in their promoters (Fig S1D). Both Ctrl- and CQ4-iPSCs consistently displayed a diploid karyotype after >20 passages (Fig S1E), and formed teratoma in immunodeficient mice comprising tissue representing all three germ layers (Fig S1F).

iPSC gene edition by CRISPR/Cas9 system.

Because the differentiation capacity among iPSC lines is influenced by (epi)genetic variability[52, 53], the optimal scenario to unravel genotype-phenotype associations is to use isogenic iPSC lines. We therefore used the CRISPR/Cas9 system to gene edit CQ4-iPSCs (CQ4^{ed}-iPSCs). From the four sgRNAs designed surrounding the c.483 G>C mutation in exon 5 of the *COQ4* allele, one sgRNA was found to have a high cleavage activity (~25%, data not shown) in the T7 surveyor assay, cutting 8 nucleotides upstream of the mutation. Next, we designed a 90 bp-long donor ssDNA carrying a silent mutation for the generation of a Taqα1 restriction site and the mutation corrected codon (Fig 2E). CQ4-iPSCs were co-transfected with Cas9-GFP vector and ssDNA and, 2 days later, GFP⁺ clones were FACS-sorted as single cells. All individual GFP⁺ established clones were analyzed by PCR and restriction fragment length polymorphism, obtaining an allele digestion where the editing was performed (Fig 2F). Homozygous editing of the *COQ4* mutation was observed in several clones, which was further confirmed by sequencing (Fig 2G). The top off-target predicted beforehand, *GRID2*, was sequenced in CQ4^{ed}-iPSC lines and was consistently found to be in germline configuration, demonstrating the specificity of the sgRNA/gDNA used to edit the *COQ4* mutation (Fig 2H). Importantly, CQ4^{ed}-iPSCs remained pluripotent, as shown by typical ESC-like morphology, growth and by expression of pluripotency-associated transcription factors (Fig 2I) and surface markers (Fig S1G), and was cytogenetically stable (Fig S1H).

COQ4 genome edition reverses metabolic/mitochondrial dysfunction

CoQ₁₀ is a lipophilic molecule involved in the MRC [1, 2], and low levels of CoQ₁₀ in fibroblasts or muscle biopsies are linked to CoQ₁₀ deficiency [16]. To obtain a reference value for CoQ₁₀, we measured its concentration in different pluripotent stem cells (hESCs and iPSCs) (**Fig 3A left**). CoQ₁₀ concentration and biosynthesis was significantly lower (36% and 61%, respectively) in CQ4-iPSCs than in Ctrl-iPSCs and hESCs (**Fig 3A right, 3B**). Strikingly, a full restoration of both CoQ₁₀ concentration (25% increase) and biosynthesis (50% increase) was found in CQ4^{ed}-iPSCs (**Fig 3C,D**). Similarly, the activity of MRC complexes I+III and II+III was recovered in CQ4^{ed}-iPSCs (~50% increase) (**Fig 3E**). We next evaluated oxidative phosphorylation and glycolysis by ATP quantification, basal live-cell oxygen consumption rate (OCR) and extracellular acidification rate (ECAR). To produce the same ATP concentration (**Fig 3F**), CQ4-iPSCs ECAR (**Fig 3G**) and OCR (**Fig 3H**) rates were 2-fold higher than in CQ4^{ed}-iPSCs, suggesting a respiration dysfunction as confirmed by a 2-fold higher proton leak (difference between oligomycin- and actinomycin A-mediated inhibition of OCRs) in the mutated relative to edited iPSC lines (**Fig 3I**). Together, these results show that CQ4-iPSCs maintain the CoQ₁₀ deficiency and metabolic dysfunction found in CQ4-F, which is reversed upon correction of the *COQ4* mutation, thus directly linking c.483 G>C *COQ4* with the dysfunctional metabolic phenotype.

COQ4 mutation does not impair iPSC differentiation into dopaminergic or motor neurons

The impact of *COQ* mutations in neurodevelopment remains unclear. The majority of CoQ₁₀-deficient patients present neurological symptoms [17, 18] whereas patient here described did not show neurological deficits other than a minor mental retardation we therefore studied the developmental influence of the *COQ4* mutation in neurogenesis. Ctrl-, CQ4- and CQ4^{ed}-iPSCs were differentiated into midbrain dopaminergic (DA) neurons and spinal motor neurons (MN) using well-established protocols (**Fig 4A, 5A**) [38, 39]. Successful differentiation was confirmed by flow cytometry as demonstrated by a progressive increase in the proportion of Neural Cell Adhesion Molecule (NCAM⁺) cells, with >80% and >60% of NCAM⁺ cells formed by day 30 of development, in the DA and MN differentiation respectively, irrespective of the iPSC genotype (**Fig 4B, 5B**). We then evaluated the differentiation output of neural progenitors (SOX2⁺NESTIN⁺) and immature neurons (TUJ1⁺) by confocal imaging at early time points (day 15–20 of neural induction). No differences were found between Ctrl- and CQ4-iPSCs for differentiation into neural

progenitors (~50% and ~35–50% SOX2+NESTIN+ cells under DA and MN differentiation conditions, respectively) or total neurons (~15 and ~22% TUJ1+ cells under DA and MN differentiation conditions, respectively) (**Fig 4C, 5C**). Similarly, at later time points (~day 30–40 of differentiation), the proportion of TUJ1+ differentiating neurons between Ctrl- and CQ4-iPSCs was very similar (~30–40%) regardless of the differentiation protocol (**Fig 4D, 5D**). Furthermore, the yield of TUJ1+TH+ DA (~8%) and TUJ1+HB9+/TUJ1+ISL1+ MN (~4%) was also similar between Ctrl- and CQ4-iPSCs (**Fig 4D, 5D**). Accordingly, CQ4^{ed}-iPSC differentiated into DA (**Fig 4C, D**) and MN (**Fig 5C, D**) neurons as well as neural precursors to a similar extent to that achieved by CQ4-iPSCs. Immunofluorescence-based quantification was confirmed by qRT-PCR expression analysis of DA (*FOXA2* and *TH*, **Fig 4E**) and MN (*LHX3* and *FOXP1*, **Fig 5E**) master genes. We then carried out functional analyses to confirm these results. HPLC determination of dopamine release revealed very similar levels of dopamine in Ctrl- and CQ4-iPSC-derived neurons (**Fig 4F**). Whole-cell patch clamp recording of MN (identified using the HB9::GFP reporter)[39, 45] indicated that CQ4-iPSC-derived MN were electrophysiologically active, displaying inward and outward currents in voltage clamp and spontaneous action potentials suggestive of functional synapses after 40–50 days in culture. Moreover, induced action potentials and spontaneous firing were similar between Ctrl-iPSC and CQ4-iPSC-derived MN (**Fig 5F**)[45, 54]. The comparable yields of DA and MN generated from Ctrl-, CQ4- and CQ4^{ed}-iPSCs might be explained by similar neural specification from genotypically distinct iPSCs as no differences were found for cell death (**Fig 4G, 5G**) or cell cycle/proliferative status (**Fig 4H, 5H**) of the emerging NCAM+ cells. Of note, DA progenitors from CQ4-iPSCs cycled slightly less than those from Ctrl- or CQ4^{ed}-iPSCs, possibly reflecting a role for *COQ4* in the cell cycle of neural cells. Together, these data reveal that the c.483 G>C mutation in *COQ4* does not impact DA or MN neurogenesis from iPSCs, recapitulating the patient's phenotype.

COQ4 mutation recapitulates the skeletal muscle functional and metabolic defects

Muscle impairment is common in CoQ₁₀-deficient patients[19], but it was especially life-threatening in the patient reported here, who suffered from lethal rhabdomyolysis that was clinically unmanageable, resulting in her death from fatal kidney damage as a result of myoglobinuria. To study the developmental and metabolic impact of the *COQ4* mutation in skeletal myogenesis, Ctrl-, CQ4- and CQ4^{ed}-iPSCs were differentiated into SkM following a well-established protocol developed in the Perlingeiro laboratory[33]. Transgenic Ctrl-, CQ4- and CQ4^{ed}-iPSC lines

carrying a PAX7-GFP-expressing inducible lentivector were generated, and myogenic specification was induced as described in **Fig 6A**. PAX7-GFP-expressing myogenic progenitors were GFP FACS-purified on day 15 of myogenic development (**Fig 6A,B**). All FACS-sorted GFP⁺ cells co-expressed PAX7, demonstrating the reliability of the inducible reporter (**Fig 6C**). Although the cell cycle profile (**Fig 6D**) and the level of apoptosis (**Fig 6E**) were very similar between CQ4- and Ctrl-PAX7⁺ myogenic progenitors, the number of senescent CQ4-PAX7⁺ cells was 2-fold higher, a phenotype that was corrected in CQ4^{ed}-PAX7⁺ myogenic progenitors (**Fig 6F**). The enhanced senescence observed in CQ4-PAX7⁺ myogenic progenitors might be explained by their increased ROS production (**Fig 6G**) leading to a 1-log reduction in cell expansion (**Fig 6H**); both of these functional properties were corrected in CQ4^{ed}-PAX7⁺ myogenic progenitors (**Fig 6G,H**).

PAX7⁺ myogenic progenitors were allowed to further differentiate into differentiated muscle cells (i.e. myocytes) as detailed in **Fig 6A**[33]. Consistent with the muscle damage observed in the CQ4-mutated patient, CQ4-PAX7⁺ myogenic progenitors displayed a significant maturation impairment as revealed by a 30% reduction in the generation of fully differentiated myosin heavy chain-1 (MYH1)⁺ cells (**Fig 6I**) and a 3-fold reduction in the expression of creatine kinase (CK) (**Fig 6J**), a master enzyme expressed in SkM that ensures an energy reservoir for the rapid buffering and regeneration of ATP. Importantly, both the generation of MYH1⁺ cells and the levels of CK were at control levels in differentiated muscle cells derived from CQ4^{ed}-PAX7⁺ myogenic progenitors (**Fig 6I,J**). In addition, gene expression analysis of the specific myogenic markers, myogenic regulatory factor *MYF5*, myogenin (*MGN*) and myosin heavy chain 3 (*MYH3*), showed that their kinetics of expression were deregulated in CQ4-PAX7⁺ as compared with Ctrl-PAX7⁺ differentiating muscle cells (**Fig 6K**). Because *MYF5* is exclusively expressed in proliferating myogenic cells and *MGN* is an early differentiation marker[55], their enhanced expression in CQ4-PAX7⁺ versus Ctrl-PAX7⁺ cells supports the delayed entry into full differentiation of patient-derived CQ4-PAX7⁺ cells; of note, the expression kinetics of these genes returned to control values in CQ4^{ed}-PAX7⁺ differentiating cells (**Fig 6K**).

Finally, we analyzed the metabolic impact of the *COQ4* mutation in SkM derivatives generated from Ctrl-, CQ4- and CQ4^{ed}-PAX7⁺ myogenic progenitors. Consistent with the patient's phenotype, morphometric image analysis muscle cells stained with TOM20 revealed abnormalities in mitochondrial morphology caused by the *COQ4* mutation (**Fig 6L**). Accordingly,



CQ4-PAX7⁺ iPSC-derived differentiated muscle cells had smaller (n° mitochondria/cellular area, **Fig 6L-panel i**), more circular (**Fig 6L-panel ii**), less branched (FF, **Fig 6L-panel iii**), and shorter (mitochondrial length, **Fig 6L-panel iv**) mitochondria than Ctrl-PAX7⁺ iPSC-derived differentiated muscle cells[56]. Importantly, these mitochondrial dynamics-associated parameters were restored in CQ4^{ed}-PAX7⁺ iPSC-derived differentiated muscle cells. In addition, MRC complex I+III activity was 50% lower in CQ4-PAX7⁺ iPSC-derived differentiated muscle cells than in Ctrl-PAX7⁺ counterparts, and this was fully restored in CQ4^{ed}-PAX7⁺ iPSC-derived differentiated cells, (**Fig 6M**). Collectively, these results establish the utility of an iPSC-based disease model to study CoQ₁₀ deficiency, wherein the *COQ4* mutation faithfully reproduces the disease-associated SkM functional and metabolic defects.

DISCUSSION

CoQ₁₀ deficiency comprises a growing number of metabolic disorders with neurological and extraneurological manifestation. Despite being considered a rare disease, next-generation DNA sequencing techniques coupled with well-established biochemical determination of CoQ₁₀ biosynthesis has allowed the identification of a variety of primary and secondary CoQ₁₀ deficiencies[57]. Primary deficiency of CoQ₁₀ is an autosomal recessive syndrome originating from mutations in genes responsible for CoQ₁₀ biosynthesis. The pathogenesis of secondary CoQ₁₀ deficiency is less studied but may be linked to assembly defects in oxidative phosphorylation (OxPhos) complexes/metabolic pathways[19, 58]. CoQ₁₀ deficiency impairs OxPhos and global metabolic homeostasis, ultimately causing clinically heterogeneous mitochondrial diseases in primarily SkM and central nervous system, likely because the disruption of energy metabolism strongly affects tissues with high-energy demand[8, 59].

It has been recently suggested that COQ4 has an essential structural and functional role for the biosynthesis of CoQ₁₀, and COQ4 mutations as well as COQ4 haploinsufficiency cause a broad spectrum of mitochondrial disorders associated with CoQ₁₀ deficiency[19-24]. Here, we report a 4-year-old girl with a heterozygous c.483 G>C mutation in COQ4 who displayed severe metabolic/mitochondrial deficits, extensive muscle damage and lethal rhabdomyolysis. The COQ4 mutation was associated with CoQ₁₀ deficiency and MRC dysfunction, in line with the critical role of CoQ₁₀ as an electron shuttle. CQ4-mutated fibroblasts had a strongly impaired proliferative capacity linked to high senescence rates and a reduction in the proportion of cycling cells, reflecting the involvement of CoQ₁₀ in pyrimidine synthesis [2, 5, 7]. A limitation of this work is that whether or not the COQ4 E161D allele is pathogenic on its own cannot be fully inferred from our study. It could represent a nucleotide variation with functional consequences. It might for instance be a genetic modifier of another yet unknown driver pathogenic mutation, which could account for the increased susceptibility of the patient to develop CoQ₁₀ deficiency in association with COQ4 E161D. Further genetic and functional studies on a larger patient cohort should be performed to address whether COQ4 E161D allele may be a triggering factor which modifies the phenotype of different diseases.

A major obstacle to study this disorder is the lack of genotype-phenotype association. Human diseases are generally studied once the full (epi)genetic events (i.e. mutations) are already in

place and, therefore, the mechanisms of disease pathophysiology are not amenable to analysis with primary patient samples. Patient-specific iPSCs can serve to model human disease since their re-differentiation potential provides a unique strategy to explore the developmental impact of disease-specific mutations on human stem cell fate, especially in early-onset or developmental diseases[28, 60, 61]. We generated and CRISPR/Cas9 corrected iPSCs from a patient with a mutation in *COQ4* in an attempt to model its impact on MRC/mitochondrial activity and neural and skeletal muscle development. Of note, *COQ4*-mutated cells were less efficiently reprogrammed, likely reflecting the impaired proliferation of *COQ4*-F. Nevertheless, undifferentiated *COQ4*-iPSCs were functionally indistinguishable from Ctrl-iPSCs.

We show for the first time the levels of CoQ₁₀ in a panel of pluripotent stem cell lines. Interestingly, cell reprogramming failed to reestablish CoQ₁₀ levels/biosynthesis in mutated cells, but this were fully restored upon *COQ4* correction, demonstrating the causal effect of c.483G>C *COQ4* mutation in the metabolic dysfunctional phenotype associated with CoQ₁₀ deficiency. This data together with previous data in yeast[20, 62, 63] may highlight the evolutionary conserved role of CoQ₁₀ in mitochondrial function by regulating OxPhos and ultimately ATP synthesis. Indeed, MRC complexes I+III and II+III, OxPhos, and glycolysis were all severely impaired in *COQ4*-iPSC, which required a 2-fold increase in OCR and ECAR to generate the same concentration of ATP. The increased proton leak in *COQ4*-iPSC represents ATP-independent respiration and an increase in the passive leak of protons from the inner mitochondrial membrane, linking CoQ₁₀ with proton shuttling in pluripotent stem cells [60].

Neurological manifestations are very common in CoQ₁₀-deficient patients[16-18]. Interestingly, our patient failed to exhibit neurological symptoms other than modest mental retardation. Because the impact of *COQ* mutations in neurodevelopment remains unclear, we studied the developmental influence of the *COQ4* mutation in neurogenesis using well-established protocols. Our analysis revealed that the c.483 G>C mutation in *COQ4* does not impact iPSC differentiation of central nervous system neurons (midbrain DA and spinal MN), thus recapitulating the patient's normal neurological phenotype and suggesting that mutations in *COQ4* do not influence neural specification from PSCs.

Life-threatening rhabdomyolysis was severe in this patient, and eventually led to myoglobinuria and nephrotic toxicity, causing the patient's death. We used a sophisticated differentiation strategy

to generate SkM from iPSC, which proceeds through an initial myogenic induction based on the generation of PAX7⁺ myogenic progenitors, and subsequent maturation into muscle cells [33]. Our data clearly show that CQ4-iPSC-differentiated SkM recapitulates CoQ₁₀ deficiency-associated SkM functional and metabolic defects. First, CQ4-PAX7⁺ myogenic progenitors exhibited 1-log reduced cell expansion within a 15-day period, associated with increased levels of senescence, which might likely be due to the increased ROS levels produced. These dysfunctional properties were corrected in genome-edited PAX7⁺ myogenic progenitors. Second, maturation of CQ4-PAX7⁺ myogenic progenitors was lower than in Ctrl-PAX7⁺ counterparts. The generation of fully differentiated MYH1⁺ cells and the expression of CK, a master SkM enzyme for the rapid buffering and regeneration of ATP, were decreased significantly, and this was in agreement with the increased expression of myogenic cell proliferation/early differentiation markers. These parameters were recovered in muscle cells from CQ4^{ed}-PAX7⁺ cells, demonstrating the causal link of c.483G>C *COQ4* mutation in the impaired myogenic development and reproducing the main phenotypic manifestation of the disease. Third, mitochondrial morphometric imaging and analysis of MRC activity revealed abnormalities in mitochondrial morphology and a 50% decrease in the activity of MRC complex I+III, indicating that the *COQ4* mutation negatively impacts the mitochondrial/metabolic function of iPSC-derived SkM derivatives generated from PAX7⁺ myogenic progenitors. These mitochondrial dynamics-associated parameters and MRC complexes activity were restored in CQ4^{ed}-PAX7⁺ iPSC-derived differentiated muscle cells. Thus, genetic correction of *COQ4* mutation rescued the mitochondrial function of *COQ4*-mutated SkM.

In summary, we have established a patient-specific iPSC-based disease model for CoQ₁₀ deficiency associated to a heterozygous missense mutation in *COQ4*. Our findings provide evidence that the *COQ4* mutation faithfully reproduces SkM dysfunction and metabolic deficits with no neurological involvement. This may assist in the study of complex genotype-phenotype associations observed in CoQ₁₀ deficiency, opening avenues for testing new drugs to treat CoQ₁₀ deficiency.

CONFLICT OF INTEREST: The authors have no conflict of interest to disclose. All authors have read and approved the manuscript in its present form.

REFERENCES

1. Turunen M, Olsson J, Dallner G. Metabolism and function of coenzyme Q. *Biochimica et biophysica acta*. 2004;1660:171-199.
2. Lopez-Lluch G, Rodriguez-Aguilera JC, Santos-Ocana C et al. Is coenzyme Q a key factor in aging? *Mechanisms of ageing and development*. 2010;131:225-235.
3. Desbats MA, Lunardi G, Doimo M et al. Genetic bases and clinical manifestations of coenzyme Q10 (CoQ 10) deficiency. *Journal of inherited metabolic disease*. 2015;38:145-156.
4. Salviati L, Sacconi S, Murer L et al. Infantile encephalomyopathy and nephropathy with CoQ10 deficiency: a CoQ10-responsive condition. *Neurology*. 2005;65:606-608.
5. Lopez-Martin JM, Salviati L, Trevisson E et al. Missense mutation of the COQ2 gene causes defects of bioenergetics and de novo pyrimidine synthesis. *Human molecular genetics*. 2007;16:1091-1097.
6. Mollet J, Giurgea I, Schlemmer D et al. Prenyldiphosphate synthase, subunit 1 (PDSS1) and OH-benzoate polyprenyltransferase (COQ2) mutations in ubiquinone deficiency and oxidative phosphorylation disorders. *J Clin Invest*. 2007;117:765-772.
7. Quinzii CM, Lopez LC, Gilkerson RW et al. Reactive oxygen species, oxidative stress, and cell death correlate with level of CoQ10 deficiency. *FASEB journal : official publication of the Federation of American Societies for Experimental Biology*. 2010;24:3733-3743.
8. Heeringa SF, Chernin G, Chaki M et al. COQ6 mutations in human patients produce nephrotic syndrome with sensorineural deafness. *The Journal of clinical investigation*. 2011;121:2013-2024.
9. Mollet J, Delahodde A, Serre V et al. CABP1 gene mutations cause ubiquinone deficiency with cerebellar ataxia and seizures. *American journal of human genetics*. 2008;82:623-630.
10. Lagier-Tourenne C, Tazir M, Lopez LC et al. ADCK3, an ancestral kinase, is mutated in a form of recessive ataxia associated with coenzyme Q10 deficiency. *American journal of human genetics*. 2008;82:661-672.
11. Ashraf S, Gee HY, Woerner S et al. ADCK4 mutations promote steroid-resistant nephrotic syndrome through CoQ10 biosynthesis disruption. *The Journal of clinical investigation*. 2013;123:5179-5189.
12. Duncan AJ, Bitner-Glindzicz M, Meunier B et al. A nonsense mutation in COQ9 causes autosomal-recessive neonatal-onset primary coenzyme Q10 deficiency: a potentially treatable form of mitochondrial disease. *American journal of human genetics*. 2009;84:558-566.
13. Rotig A, Appelkvist EL, Geromel V et al. Quinone-responsive multiple respiratory-chain dysfunction due to widespread coenzyme Q10 deficiency. *Lancet*. 2000;356:391-395.

14. Lopez LC, Schuelke M, Quinzii CM et al. Leigh syndrome with nephropathy and CoQ10 deficiency due to decaprenyl diphosphate synthase subunit 2 (PDSS2) mutations. *American journal of human genetics*. 2006;79:1125-1129.
15. Freyer C, Stranneheim H, Naess K et al. Rescue of primary ubiquinone deficiency due to a novel COQ7 defect using 2,4-dihydroxybenzoic acid. *Journal of medical genetics*. 2015;52:779-783.
16. Quinzii CM, Hirano M. Primary and secondary CoQ(10) deficiencies in humans. *BioFactors*. 2011;37:361-365.
17. Artuch R, Brea-Calvo G, Briones P et al. Cerebellar ataxia with coenzyme Q10 deficiency: diagnosis and follow-up after coenzyme Q10 supplementation. *Journal of the neurological sciences*. 2006;246:153-158.
18. Artuch R, Salviati L, Jackson S et al. Coenzyme Q10 deficiencies in neuromuscular diseases. *Advances in experimental medicine and biology*. 2009;652:117-128.
19. Trevisson E, DiMauro S, Navas P et al. Coenzyme Q deficiency in muscle. *Current opinion in neurology*. 2011;24:449-456.
20. Marbois B, Gin P, Gulmezian M et al. The yeast Coq4 polypeptide organizes a mitochondrial protein complex essential for coenzyme Q biosynthesis. *Biochimica et biophysica acta*. 2009;1791:69-75.
21. Casarin A, Jimenez-Ortega JC, Trevisson E et al. Functional characterization of human COQ4, a gene required for Coenzyme Q10 biosynthesis. *Biochemical and biophysical research communications*. 2008;372:35-39.
22. Salviati L, Trevisson E, Rodriguez Hernandez MA et al. Haploinsufficiency of COQ4 causes coenzyme Q10 deficiency. *Journal of medical genetics*. 2012;49:187-191.
23. Brea-Calvo G, Haack TB, Karall D et al. COQ4 mutations cause a broad spectrum of mitochondrial disorders associated with CoQ10 deficiency. *American journal of human genetics*. 2015;96:309-317.
24. Chung WK, Martin K, J alas C et al. Mutations in COQ4, an essential component of coenzyme Q biosynthesis, cause lethal neonatal mitochondrial encephalomyopathy. *Journal of medical genetics*. 2015;52:627-635.
25. Acosta MJ, Vazquez Fonseca L, Desbats MA et al. Coenzyme Q biosynthesis in health and disease. *Biochimica et biophysica acta*. 2016.
26. Montero R, Pineda M, Aracil A et al. Clinical, biochemical and molecular aspects of cerebellar ataxia and Coenzyme Q10 deficiency. *Cerebellum*. 2007;6:118-122.
27. Emmanuele V, Lopez LC, Berardo A et al. Heterogeneity of coenzyme Q10 deficiency: patient study and literature review. *Archives of neurology*. 2012;69:978-983.
28. Wu SM, Hochedlinger K. Harnessing the potential of induced pluripotent stem cells for regenerative medicine. *Nature cell biology*. 2011;13:497-505.

29. Gaj T, Gersbach CA, Barbas CF, 3rd. ZFN, TALEN, and CRISPR/Cas-based methods for genome engineering. *Trends in biotechnology*. 2013;31:397-405.
30. Takahashi K, Okita K, Nakagawa M et al. Induction of pluripotent stem cells from fibroblast cultures. *Nat Protoc*. 2007;2:3081-3089.
31. Bueno C, Sardina JL, Di Stefano B et al. Reprogramming human B cells into induced pluripotent stem cells and its enhancement by C/EBPalpha. *Leukemia*. 2016;30:674-682.
32. Sun N, Panetta NJ, Gupta DM et al. Feeder-free derivation of induced pluripotent stem cells from adult human adipose stem cells. *Proc Natl Acad Sci U S A*. 2009;106:15720-15725.
33. Darabi R, Arpke RW, Irion S et al. Human ES- and iPS-derived myogenic progenitors restore DYSTROPHIN and improve contractility upon transplantation in dystrophic mice. *Cell stem cell*. 2012;10:610-619.
34. Munoz-Lopez A, van Roon EH, Romero-Moya D et al. Cellular Ontogeny and Hierarchy Influence the Reprogramming Efficiency of Human B Cells into Induced Pluripotent Stem Cells. *Stem Cells*. 2016;34:581-587.
35. Catalina P, Montes R, Ligeró G et al. Human ESCs predisposition to karyotypic instability: Is a matter of culture adaptation or differential vulnerability among hESC lines due to inherent properties? *Mol Cancer*. 2008;7:76.
36. Gutierrez-Aranda I, Ramos-Mejia V, Bueno C et al. Human induced pluripotent stem cells develop teratoma more efficiently and faster than human embryonic stem cells regardless the site of injection. *Stem Cells*. 2010;28:1568-1570.
37. Ran FA, Hsu PD, Wright J et al. Genome engineering using the CRISPR-Cas9 system. *Nat Protoc*. 2013;8:2281-2308.
38. Kriks S, Shim JW, Piao J et al. Dopamine neurons derived from human ES cells efficiently engraft in animal models of Parkinson's disease. *Nature*. 2011;480:547-551.
39. Amoroso MW, Croft GF, Williams DJ et al. Accelerated high-yield generation of limb-innervating motor neurons from human stem cells. *The Journal of neuroscience : the official journal of the Society for Neuroscience*. 2013;33:574-586.
40. Bujan N, Arias A, Montero R et al. Characterization of CoQ(1)(0) biosynthesis in fibroblasts of patients with primary and secondary CoQ(1)(0) deficiency. *Journal of inherited metabolic disease*. 2014;37:53-62.
41. Montero R, Sanchez-Alcazar JA, Briones P et al. Analysis of coenzyme Q10 in muscle and fibroblasts for the diagnosis of CoQ10 deficiency syndromes. *Clinical biochemistry*. 2008;41:697-700.
42. Spinazzi M, Casarin A, Pertegato V et al. Assessment of mitochondrial respiratory chain enzymatic activities on tissues and cultured cells. *Nat Protoc*. 2012;7:1235-1246.

43. Romero-Moya D, Bueno C, Montes R et al. Cord blood-derived CD34+ hematopoietic cells with low mitochondrial mass are enriched in hematopoietic repopulating stem cell function. *Haematologica*. 2013;98:1022-1029.
44. Debacq-Chainiaux F, Erusalimsky JD, Campisi J et al. Protocols to detect senescence-associated beta-galactosidase (SA-beta-gal) activity, a biomarker of senescent cells in culture and in vivo. *Nat Protoc*. 2009;4:1798-1806.
45. Marchetto MC, Muotri AR, Mu Y et al. Non-cell-autonomous effect of human SOD1 G37R astrocytes on motor neurons derived from human embryonic stem cells. *Cell stem cell*. 2008;3:649-657.
46. Montes R, Ayllon V, Prieto C et al. Ligand-independent FLT3 activation does not cooperate with MLL-AF4 to immortalize/transform cord blood CD34+ cells. *Leukemia*. 2014;28:666-674.
47. Prieto C, Stam RW, Agraz-Doblas A et al. Activated KRAS cooperates with MLLAF4 to promote extramedullary engraftment and migration of cord blood CD34+ HSPC but is insufficient to initiate leukemia. *Cancer Res*. 2016.
48. Brito S, Thompson K, Campistol J et al. Corrigendum: Long-term survival in a child with severe encephalopathy, multiple respiratory chain deficiency and GFM1 mutations. *Front Genet*. 2015;6:254.
49. Rubio R, Abarrategi A, Garcia-Castro J et al. Bone environment is essential for osteosarcoma development from transformed mesenchymal stem cells. *Stem Cells*. 2014;32:1136-1148.
50. Schneeberger M, Dietrich MO, Sebastian D et al. Mitofusin 2 in POMC neurons connects ER stress with leptin resistance and energy imbalance. *Cell*. 2013;155:172-187.
51. Dagda RK, Cherra SJ, 3rd, Kulich SM et al. Loss of PINK1 function promotes mitophagy through effects on oxidative stress and mitochondrial fission. *J Biol Chem*. 2009;284:13843-13855.
52. Woods NB, Parker AS, Moraghebi R et al. Brief report: efficient generation of hematopoietic precursors and progenitors from human pluripotent stem cell lines. *Stem cells*. 2011;29:1158-1164.
53. Hu BY, Weick JP, Yu J et al. Neural differentiation of human induced pluripotent stem cells follows developmental principles but with variable potency. *Proceedings of the National Academy of Sciences of the United States of America*. 2010;107:4335-4340.
54. Burkhardt MF, Martinez FJ, Wright S et al. A cellular model for sporadic ALS using patient-derived induced pluripotent stem cells. *Mol Cell Neurosci*. 2013;56:355-364.
55. Segales J, Perdiguero E, Munoz-Canoves P. Epigenetic control of adult skeletal muscle stem cell functions. *FEBS J*. 2015;282:1571-1588.
56. Koopman WJ, Verkaar S, Visch HJ et al. Inhibition of complex I of the electron transport chain causes O₂⁻-mediated mitochondrial outgrowth. *Am J Physiol Cell Physiol*. 2005;288:C1440-1450.

57. Yubero D, Montero R, Armstrong J et al. Molecular diagnosis of coenzyme Q10 deficiency. *Expert Rev Mol Diagn.* 2015;15:1049-1059.
58. Quinzii CM, Hirano M. Coenzyme Q and mitochondrial disease. *Developmental disabilities research reviews.* 2010;16:183-188.
59. DiMauro S, Schon EA. Mitochondrial disorders in the nervous system. *Annu Rev Neurosci.* 2008;31:91-123.
60. Cooper O, Seo H, Andrabi S et al. Pharmacological rescue of mitochondrial deficits in iPSC-derived neural cells from patients with familial Parkinson's disease. *Science translational medicine.* 2012;4:141ra190.
61. Ramos-Mejia V, Fraga MF, Menendez P. iPSCs from cancer cells: challenges and opportunities. *Trends Mol Med.* 2012;18:245-247.
62. Ozeir M, Muhlenhoff U, Webert H et al. Coenzyme Q biosynthesis: Coq6 is required for the C5-hydroxylation reaction and substrate analogs rescue Coq6 deficiency. *Chem Biol.* 2011;18:1134-1142.
63. Cui TZ, Kawamukai M. Coq10, a mitochondrial coenzyme Q binding protein, is required for proper respiration in *Schizosaccharomyces pombe*. *FEBS J.* 2009;276:748-759.

FIGURE LEGENDS

Figure 1: Biochemical, metabolic, proliferative and histological characterization of *COQ4*-mutated fibroblasts. (A) Sanger DNA sequencing confirming the heterozygous c.483 G>C mutation in the patient's fibroblasts. (B) Seventy-five percent reduction in [CoQ₁₀] in CQ4-F relative to Ctrl-F. (C) Eighty-seven percent reduction in CoQ₁₀ biosynthesis in CQ4-F relative to Ctrl-F. (D) qRT-PCR reflecting a higher expression of *COQ3*, *COQ4* and *COQ6* genes in CQ4-F than in Ctrl-F (n=3). (E) Defective MRC complex I+III and II+III activities relative to citrate synthase in CQ4-F. (F) Fibroblast proliferation of Ctrl-F and CQ4-F (n=3); *p-value <0.01. (G) Cell cycle analysis of Ctrl-F and CQ4-F (n=3). (H) Senescence-associated β-galactosidase quantification of Ctrl-F and CQ4-F and representative image (4×) (*left panel*), and qRT-PCR expression of *p16/CDKN2A* (*right panel*) (n=3). (I) FACS quantification of apoptotic cells (Annexin V⁺, n=3). (J) Patient's muscle histology revealing mitochondrial alterations after rhabdomyolysis. Values are expressed as mean±SEM. CQ4-F: *COQ4* mutated primary fibroblasts; Ctrl-F: Control primary fibroblasts; H&E: Hematoxylin and eosin; SDH: Succinate dehydrogenase; COX: Cytochrome c oxidase.

Figure 2: Generation of *COQ4*-mutated iPSCs and CRISPR/Cas9-mediated gene edition. (A) Schematic outline of the reprogramming process. (B) Reprogramming efficiency for Ctrl-F and CQ4-F. (C) PCR and sequencing confirming the presence of *COQ4*-mutated allele in several representative CQ4-iPSC clones. (D) Immunostaining confirming high-level infection with SeV 48 h post-transduction and SeV elimination on all iPSC clones at p8-10 (*left panel*). qPCR reflecting complete absence of SeV at p8-10 (*right panel*). (E) Schematic overview for the strategy of CRISPR/Cas9 mediated targeting to the *COQ4* locus. Sequence and synonymous modifications in the ssDNA. (F) Identification of edited iPSC clones by TaqI allele digestion in the genomic DNA after single cell cloning. (G) Sanger DNA sequencing confirming the gene edition. (H) Sanger DNA sequencing of the major predicted off-target *GRID2* gene. (I) qRT-PCR for the pluripotency genes *OCT4*, *SOX2*, *REX1*, *NANOG*, *CRIP1* and *DNMT3β* in hESC and CQ4^{ed}-iPSC (n=3). Values are expressed as mean±SEM. CQ4-F: *COQ4* mutated primary fibroblasts; Ctrl-F: Control primary fibroblasts; CQ4-iPSC: *COQ4* mutated iPSC; Ctrl-iPSC: Control iPSC; CQ4^{ed}-iPSC: *COQ4*-edited iPSC.

Figure 3: Genome editing of c.483 G>C COQ4 mutation reverses CoQ₁₀ deficiency and metabolic dysfunction retained in CQ4-iPSCs.

(A) *Left*, concentration of CoQ₁₀ in a panel of hESC (H9, AND1), fibroblast-derived iPSC and blood-derived iPSCs (●), Ctrl-iPSCs (■) and CQ4-iPSCs (▲). Solid line represents the mean; dotted lines represent the range. *Right*, summary of [CoQ₁₀] in hESCs (n=2), Ctrl-iPSCs (n=14) and CQ4-iPSCs (n=9). (B) Sixty-one percent reduction in CoQ₁₀ biosynthesis in CQ4-iPSCs (n=9) relative to Ctrl-iPSCs (n=14). (C) [CoQ₁₀] in mutated and edited CQ4-iPSCs. (D) CoQ₁₀ biosynthesis in mutated and edited CQ4-iPSCs. (E) MRC complex I+III and II+III activities relative to citrate synthase in mutated and edited CQ4-iPSCs. (F) [ATP] from mutated (n=6) and edited CQ4-iPSCs (n=6). (G) Glycolysis-associated extracellular acidification rate (ECAR) under basal conditions in mutated (n=4) and edited CQ4-iPSCs (n=4). (H) Oxygen consumption rate (OCR) under basal conditions in mutated (n=6) and edited CQ4-iPSCs (n=6). (I) OCR proton leak under basal conditions in mutated and edited CQ4-iPSCs (n=4). Values are expressed as mean±SEM. Ctrl-iPSCs: Control iPSCs; CQ4-iPSCs: COQ4 mutated iPSCs; Fib-iPSCs: fibroblast-derived iPSCs; CB-iPSCs: cord blood-derived iPSCs; Tcell-iPSCs: T cell-derived iPSCs.

Figure 4: Dopaminergic (DA) differentiation of Ctrl-iPSCs, CQ4-iPSCs and CQ4-edited iPSCs.

(A) *Top*, scheme of neuronal differentiation depicting two stages: neural induction (up to day 15–20) and neuronal maturation (up to day 33–44). *Bottom*, detailed differentiation protocol used. (B) Flow cytometry quantification of NCAM⁺ cells throughout DA differentiation (n=3). (C) Analysis of SOX2⁺NESTIN⁺ neural progenitors (*top panels*, N=42) and TUJ1⁺ neurons (*bottom panels*, N=49) from 5 iPSC clones. *Left*, differentiation efficiency in Ctrl-iPSCs (n=2) and CQ4-iPSCs (n=3) at day 15–20 of iPSC differentiation. *Middle*, DA differentiation efficiency in mutated and edited CQ4-iPSCs. *Right*, representative images of immunostaining (40×) and magnification for SOX2⁺NESTIN⁺ and TUJ1⁺ cells. White arrows point to positive cells. Scale bar, 50 μm. (D) Analysis of the TUJ1⁺ neurons (*top panels*, N=51) and TH⁺TUJ1⁺ DA (*bottom panels*, N=48). *Left*, differentiation efficiency in Ctrl-iPSCs and CQ4-iPSCs at day 33–44 of iPSC development (n=5). *Middle*, DA differentiation efficiency in mutated and edited CQ4-iPSCs. *Right*, representative image of immunostaining (40×) and magnification for TUJ1⁺ and TUJ1⁺TH⁺ cells. White arrows point to positive cells. Scale bar, 50 μm. (E) Expression of the ventral midbrain marker gene *FOXA2* after 15–20 days and the DA master gene *TH* after 33–44 days in differentiating Ctrl-, CQ4- and CQ4^{ed}-iPSC cultures (n=3). (F) Representative HPLC chromatogram (*left*) and levels (*right*) of dopamine release *in vitro* from differentiating Ctrl-, CQ4-

and CQ4^{ed}-iPSC cultures (n=2). **(G)** FACS quantification of dead cells (7-AAD⁺) within the NCAM⁺ neural population at day 15–20 of iPSC differentiation (n=3). **(H)** Cell cycle analysis (G2/S/M) within the NCAM⁺ population at day 15–20 of iPSC differentiation (n=3). Data are presented as mean±SEM. A total of six iPSC clones (three mutated and three control/edited) were used.

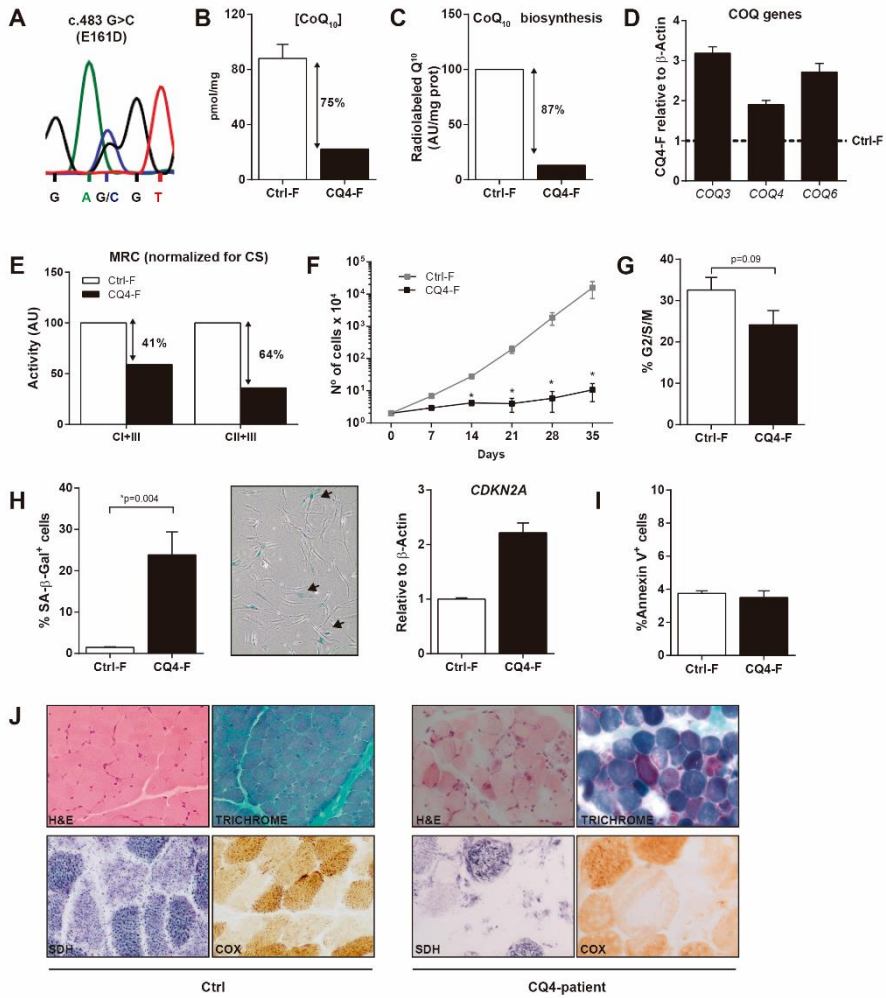
Figure 5: Motor neuron (MN) differentiation from Ctrl-iPSCs, CQ4-iPSCs and CQ4-edited iPSCs. **(A)** *Top*, scheme of neuronal differentiation depicting two stages: neural induction (up to day 15–20) and neuronal maturation (up to day 30). *Bottom*, detailed differentiation protocol used. **(B)** Flow cytometry quantification of NCAM⁺ cells throughout MN differentiation. **(C)** Analysis of the SOX2⁺NESTIN2⁺ neural progenitors (*top panels*, N=43) and TUJ1⁺ neurons (*bottom panels*, N=46). *Left*, differentiation efficiency in Ctrl-iPSCs and CQ4-iPSCs at day 15–20 of iPSC differentiation. *Middle*, MN differentiation efficiency in mutated and edited CQ4-iPSCs. *Right*, representative images of immunostaining (40×) and magnification for SOX2⁺NESTIN⁺ and TUJ1⁺ cells. White arrows point to positive cells. Scale bar, 50 μm. **(D)** Analysis of the TUJ1⁺ neurons (*top panels*, N=26) and HB9⁺ or ISL1⁺ MN (*bottom panels*, N=21). *Left*, differentiation efficiency in Ctrl-iPSC and CQ4-iPSCs at day 30 of iPSC development. *Middle*, MN differentiation efficiency in mutated and edited CQ4-iPSCs. *Right*, representative images of immunostaining (40×) and magnification for TUJ1⁺ and TUJ1⁺ISL1⁺. White arrows point to positive cells. Scale bar, 50 μm. **(E)** Expression of the MN master genes *LHX3* and *FOXP1* after 30 days in differentiating Ctrl-, CQ4- and CQ4^{ed}-iPSC cultures (n=3). **(F)** Representative electrophysiological analysis of MNs differentiated from CQ4-iPSCs (n=2). GFP⁺ MNs were recorded 4–7 days after transfection with a HB9 promoter-GFP reporter. (i) voltage-dependent K⁺ and Na⁺ currents recorded at various membrane potentials. The holding potential was -70 mV; (ii) Current-clamp recording of action potentials evoked by current injection; (iii) Spontaneous action potentials in MNs recorded in the whole-cell current-clamp configuration. **(G)** FACS quantification of dead cells (7-AAD⁺) within the NCAM⁺ neural population at day 15–20 of iPSC differentiation (n=3). **(H)** Cell cycle analysis (G2/S/M) within the NCAM⁺ population at day 15–20 of iPSC differentiation (n=3). Data are presented as mean ±SEM. A total of six iPSC clones (three mutated and three control/edited) were used.

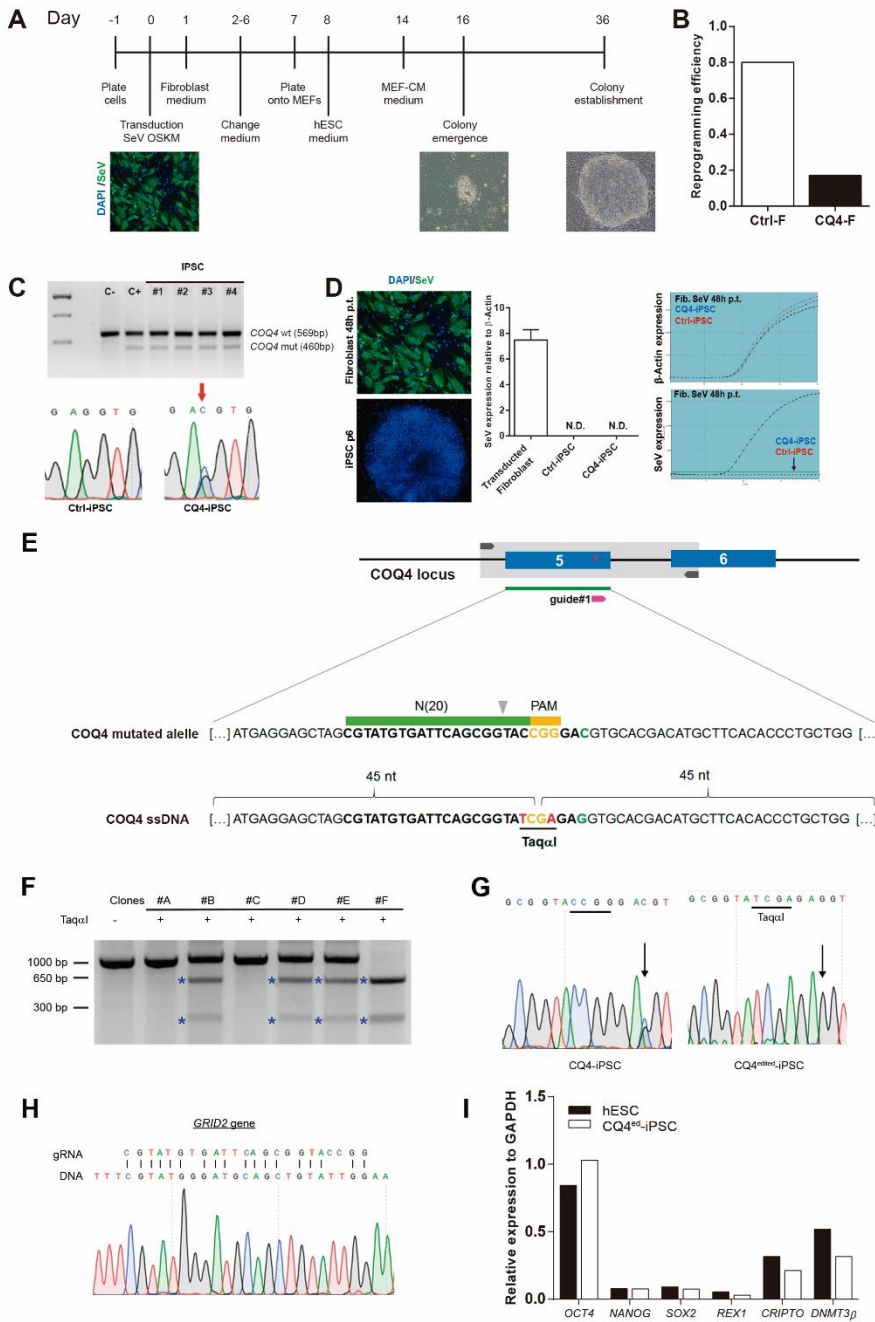
Figure 6: Impaired skeletal muscle differentiation of CQ4-iPSCs is restored upon COQ4 gene editing. **(A)** *Top*, scheme of myogenic differentiation depicting two stages: myogenic

induction (up to day 15) and differentiation into myocytes (and further fusion into myotubes) from PAX7⁺ myogenic progenitors (up to day 30). *Bottom*, detailed differentiation protocol used for myogenic induction. **(B)** Representative FACS profile showing PAX7-GFP reporter expression in dox-treated iPSCs. **(C)** Immunostaining (20×) for PAX7⁺GFP⁺ FACS-purified CQ4-mutated myogenic progenitors. Scale bar, 200 μm. **(D)** FACS quantification of cycling cells (G2/S/M) (n=3). **(E)** FACS quantification of apoptotic cells (Annexin V⁺) (n=3). **(F)** Senescence-associated β-galactosidase quantification of myogenic derivatives, and representative image (4X) (n=). Black arrowheads point to β-gal-positive cells. **(G)** Determination of ROS levels by flow cytometry (n=3). **(H)** Expansion of PAX7⁺ myogenic progenitors (n=3). **(I)** *Left*, analysis of MYH1⁺ myotubes differentiation in Ctrl-, CQ4- and CQ4^{ed}-PAX7 cultures (n=3). Representative images of MYH1⁺ immunostaining at low (*middle*) and high (*right*) magnification of CQ4-mutated muscle cells. Scale bar, 200 μm. **(J)** Creatine kinase fold-increase between day 0 and day 11 of differentiation in Ctrl-, CQ4- and CQ4^{ed}-PAX7 myogenic cells (n=6). **(K)** Expression of the SkM-specific genes *MYF5*, *MGN* and *MYH3* throughout the myogenic differentiation process (n=3). Values are expressed as mean±SEM; *p<0.05. The shadow below the graph indicates the temporal expression pattern for each gene during myogenesis. **(L)** *Top*, mitochondrial dynamics for myogenic cells: (i) number of mitochondria/cellular area; (ii) mitochondrial circularity ($4\pi\text{-area}/\text{perimeter}^2$); (iii) Form Factor (Degree of mitochondrial branching); and (iv) Aspect Ratio (mitochondrial length). *Bottom*, representative images of Ctrl-, CQ4- and CQ4^{ed}-PAX7 myogenic cells stained with TOM20. **(M)** MRC complex I+III and II+III activities relative to citrate synthase in Ctrl-, CQ4- and CQ4^{ed}-PAX7 myogenic cells (n=3). Data are presented as mean±SEM.

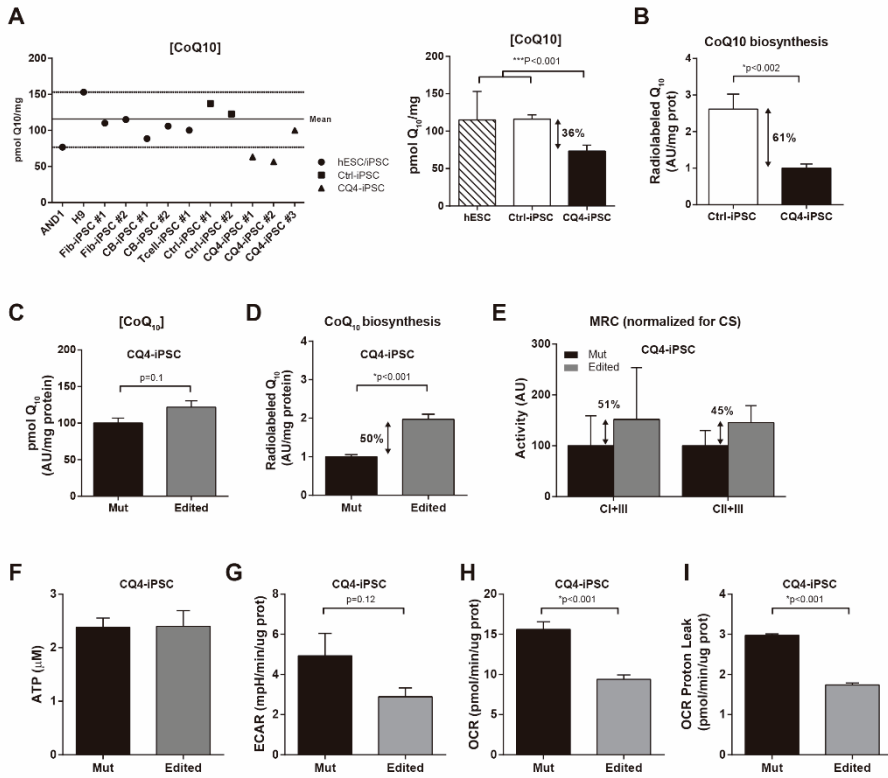


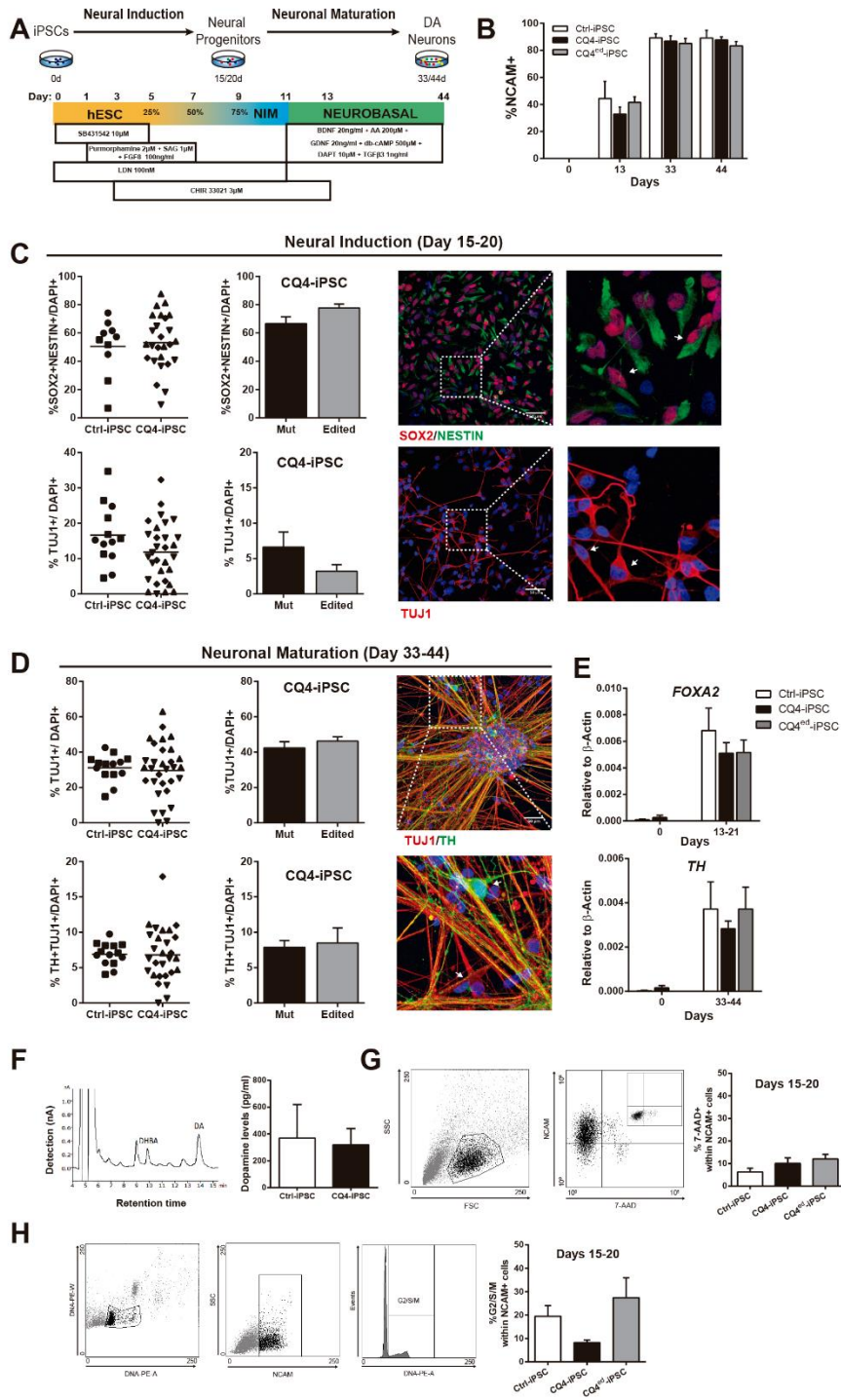
Romero-Moya et al. Fig 1





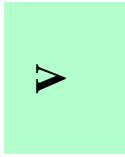
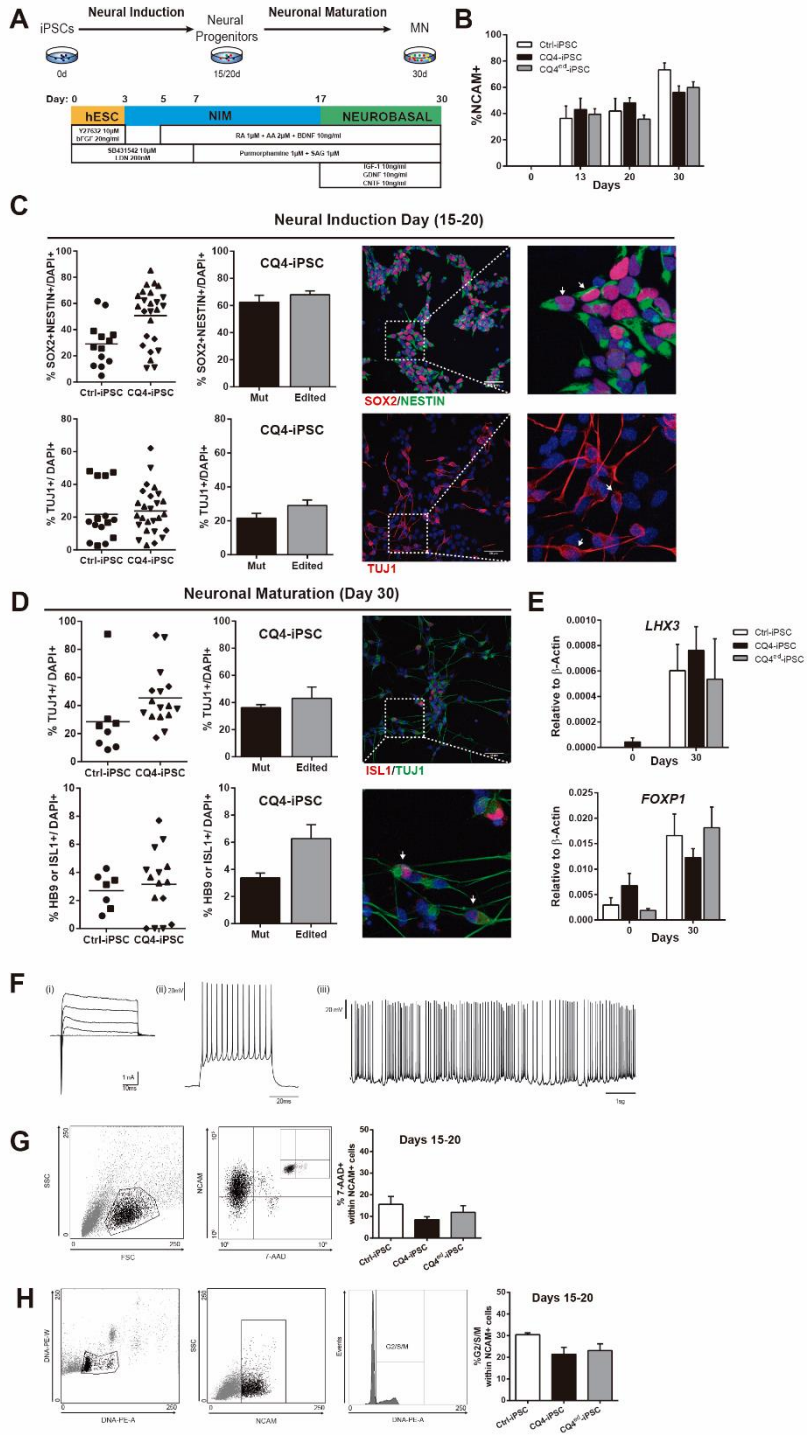
Romero-Moya et al. Fig 3

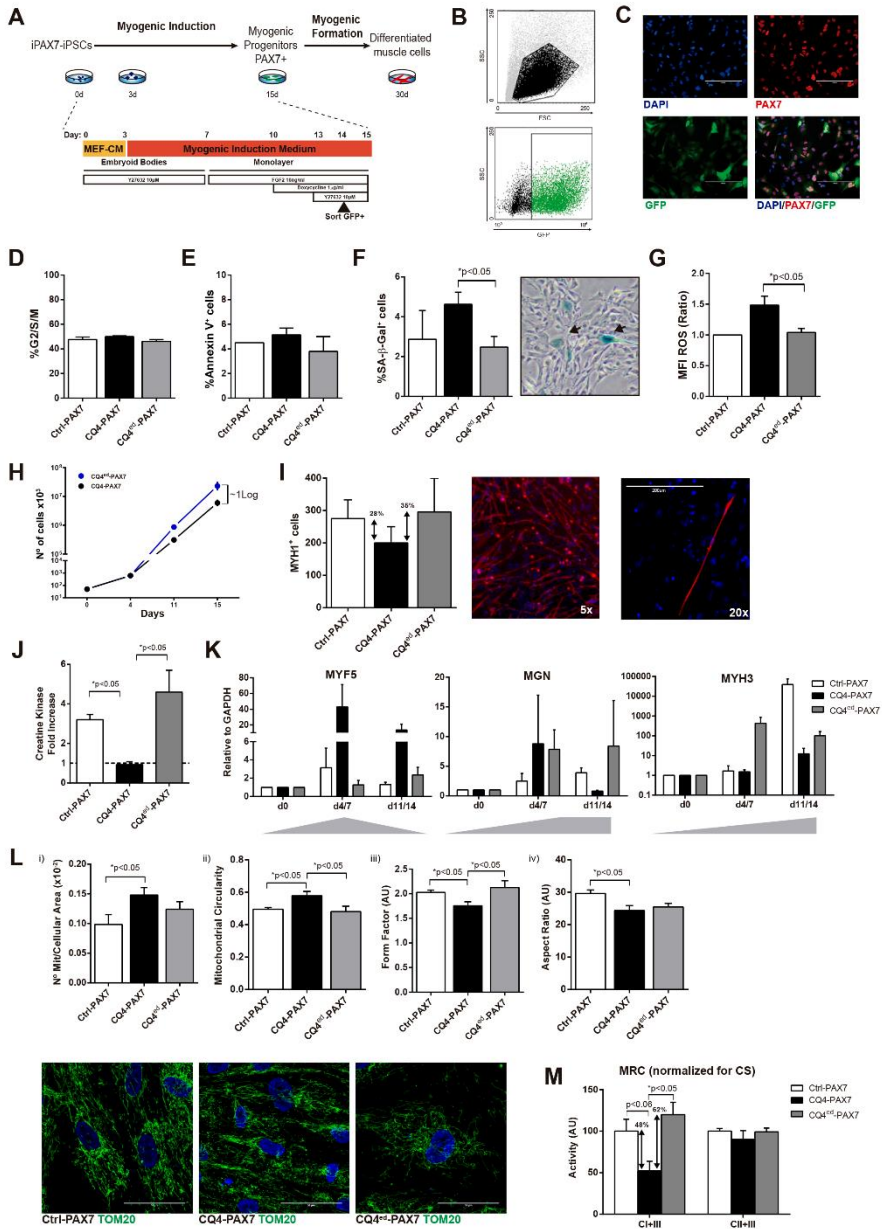




V

Romero-Moya et al. Fig 5





SUPPLEMENTAL FIGURE LEGENDS

Figure S1: Characterization of iPSC. (A) Representative morphology and alkaline phosphatase staining of Ctrl-iPSC and CQ4-iPSC. (B) qRT-PCR for the pluripotency genes *OCT4*, *SOX2*, *REX1*, *NANOG*, *CRIP1* in hESCs, Ctrl-iPSC and CQ4-iPSC. (C) Representative immunostaining for the pluripotency markers OCT4, SSEA-4, NANOG, TRA-1-60 in Ctrl-iPSCs and CQ4-iPSCs. (D) Pyrosequencing revealing demethylation of *NANOG* and *OCT4* promoters in Ctrl-iPSCs and CQ4-iPSCs as compared to original fibroblasts. (E) Diploid karyotype of Ctrl-iPSC and CQ4-iPSC at p20. (F) Teratoma analysis revealing three germ layer differentiation of Ctrl-iPSC and CQ4-iPSC. (G) Flow cytometry for the pluripotency markers SSEA-3, SSEA-4, TRA-1-60, TRA-1-81 in CQ4^{ed}-iPSC. (H) Diploid karyotype of the CQ4^{ed}-iPSC. Values are expressed as mean±SEM; *p<0.001.

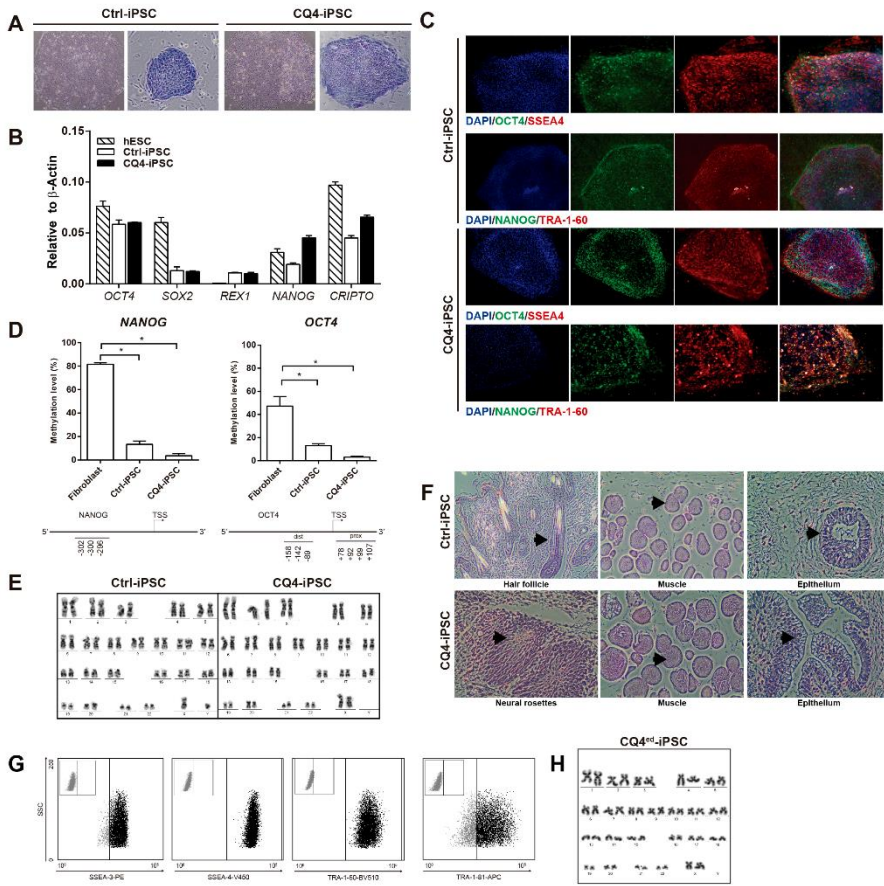


Table S1: Primers used in this study

Pyrosequencing	
NANOG-FW	5'-TATTGGGATTATAGGGGTGGGTTA-3'
NANOG-RV	5'-[Btn]-CCCAACAACAAATACTTCTAAATTCAC-3'
S-NANOG	5'-ATAGGGGTGGGTTAT-3'
OCT4_Prox-FW	5'-GGGGTTAGAGGTTAAGGTTAGTG-3'
OCT4_prox-RV	5'-[Btn]-ACCCCCCTAACCCATCAC-3'
S-OCT4_prox	5'-GGGGTTGAGTAGTTT-3'
OCT4_dist-FW	5'-TTTTTGTGGGGGATTTGTATTGA-3'
OCT4_dist-RV	5'-[Btn]-AACTACTCAACCCCTCTCT-3'
S-OCT4_dist	5'-ATTTGTATTGAGGTTTTGGA-3'
qRT-PCR	
SeV-Fw	GGATCACTAGGTGATATCGAGC
SeV-RV	ACCAGACAAGAGTTTAAGAGATATGTATC
OCT4-FW	GGGTTTTTGGGATTAAGTTCTTCA
OCT4-RV	GCCCCACCCTTTGTGTT
REX1-FW	CCTGCAGGCGGAAATAGAAC
REX1-RV	GCACACATAGCCATCACATAAGG
NANOG-FW	ACAACGGCCGAAGAATAGCA
NANOG-RV	GGTCCCAGTCGGGTTCCAC
SOX2-FW	CAAAAATGGCCATGCAGGTT
SOX2-RV	AGTTGGGATCGAACAAAAGCTATT
CRIPTO-FW	CGGAACTGTGAGCACGATGT
CRIPTO-RV	GGGCAGCCAGGTGTCATG
DNMT3β-FW	GCTCACAGGGCCCGATACTT
DNMT3β-RV	GCAGTCCTGCAGCTCGAGTTTA
β-ACTIN-FW	GATGGCCACGGCTGCTT
β-ACTIN-RV	AGGACTCCATGCCAGGAA
FOXA2-FW	ATTGCTGGTCGTTTGTGTG
FOXA2-RV	TGTACGTGTTTCATGCCGTTT
TH-FW	GAGTACACCGCCGAGGAGATTG
TH-RV	GCGGATATACTGGGTGCACTGG
LHX3-FW	GTTTCAGGAGGGGCAGGAC
LHX3-RV	CCAAGCTCCCGTAGAGG
FOXP1-FW	TGACCTTTTGAGGTGACTATAACTG
FOXP1-RV	TGGCTGAACCGTTACTTTTTG
CDKN2A-FW	GGGTCGGGTAGAGGAGGTG
CDKN2A-RV	ACCGTAACTATTCGGTGCGT

COQ3-FW	TGAACCTCTAGGGCGGCTTG
COQ3-RV	TCCAGGGAACACACTCTGTACTC
COQ4-FW	CTGTCTCCGTCGGCTCTG
COQ4-RV	GCGGTGCCTGTGGTCTCC
COQ6-FW	GTCTGCTGTTGTGGCTACTCTG
COQ6-RV	GGACCAAACCAAGGAAGCAAGG
GAPDH-FW	ACCACAGTCCATGCCATCAC
GAPDH-RV	TCCACCACCCTGTTGCTGT
MYF5-FW	GAGGTGTACCACGACCAACC
MYF5-RV	CCTGCTCTCTCAGCAACTCC
MGN-FW	CCAGGGGATCATCTGCTCACG
MGN-RV	GGTTTCATCTGGGAAGGCCA
MYH3-FW	CTTGTGGGCGGAGGTCTGG
MYH3-RV	AGCAGCTATGCCGAACACTT
Genome editing	
T7-Fw	GTAGAGACAGGGTTTCACCG
T7-Rv	GGACAGCCTCAAACCATTTT
gRNA #1-FW	CACCGCGTATGTGATTCAGCGGTAC
gRNA #1-RV	AAACGTACCGCTGAATCACATACGC
gRNA #2-FW	CACCGTGTGATTCAGCGGTACCGGG
gRNA #2-RV	AAACCCCGGTACCGCTGAATCACAC
gRNA #3-FW	CACCGTCATCATCCACGAAGCGGGT
gRNA #3-RV	AAACACCCGCTTCGTGGATGATGAC
gRNA #7-FW	CACCGCTCATCATCCACGAAGCGGG
gRNA #7-RV	AAACCCCGCTTCGTGGATGATGAC
ssDNA donor	GTTGGTGGGCATCCCAGCAGGGTGTGAAGCATG TCGTGCACCTCTCGATACCGCTGAATCACATACGC TAGCTCCTCATCATCCACGAAGCGGGTGGG
Sequencing	
COQ4-FW	CTGGGAACCATCAGGAAGG
COQ4-RV	CCAAGAGTGAACAGAAGGGAG
COQ4-Mut-FW	ATTCAGCGGTACCGGGAC
SEQ-COQ4-FW	CCAGACACCCGAGCACCC
SEQ-COQ4-RV	AGAAGGGAGTAGGGGATGGA
T7-Fw	GTAGAGACAGGGTTTCACCG
T7-Rv	GGACAGCCTCAAACCATTTT
EXON5 COQ4-Rv	ATGCAGAGGGTGGTGGAGATAG

Table S2: Primary and secondary antibodies used in this study

Antibody	Supplier	Reference	Dilution
OCT-4	ABCAM	AB19857	1:500
SSEA-4	ABCAM	AB16287	1:50
NANOG	ABCAM	AB21624	1:50
TRA-1-60	ABCAM	AB16288	1:50
Alexa Fluor® 488 α-Rabbit	Jackson ImmunoResearch	711-545-152	1:500
Alexa Fluor® 555 α-Mouse	Life Technologies	A31570	1:500
Alexa Fluor® 594 α-Mouse	Life Technologies	A11032	1:500
Alexa Fluor® 647 α-Goat	Life Technologies	A21447	1:500
NESTIN	Neuromics	MO15012	1:300
TUJ1	Covance	mms-435p	1:500
TUJ1	Covance	mrb-435p	1:500
TH	Pel-Freez	p40101	1:1000
SOX2	Neuromics	GT26098	1:500
HB9	DSHB	81.5C10	1:5
ISL1	DSHB	39.4D5	1:5
CD56-V450 (NCAM)	BD Horizon	561984	1:100
PAX7	DSHB	PAX7	1:10
MYH1 (MF20)	DSHB	MF 20	1:10
TOM20 (FL-145)	SantaCruz	sc-11415	1:500

VI.DISCUSSION

VI. DISCUSSION

Mitochondria are multifunctional organelles that play a pivotal role in the cell by providing most of the cellular energy and regulating cell death and proliferation, signaling and differentiation [105, 136, 207-209]. In this study, we first gained insights into the contribution of mitochondrial function/mass for hematopoietic stem *versus* progenitor function. We then used an iPSC model to explore the consequences of CoQ₁₀ deficiency through an analysis of the metabolic and developmental impact of a *COQ4* mutation during differentiation of iPSCs into tissues affected by COQ₁₀.

I. Contribution of mitochondrial function/mass in hematopoietic stem *versus* progenitor function.

Hematopoiesis is a dynamic process that ensures homeostasis of the blood/immune system by maintaining the equilibrium between cell formation and differentiation and cell death. HSPCs are functional reservoirs at the top of the hematopoiesis hierarchy that replenish the hematopoietic system upon physiological demands. The size of a stem cell population depends on the balance between self-renewal and differentiation. Although principally driven by genetic and epigenetic networks, metabolic pathways have recently been linked to this finely tuned regulation. Accordingly, recent work has categorized stem cell populations based on their mitochondrial function [51, 53, 54, 210]. HSCs are classified as being in either quiescent or cycling states, with quiescence viewed as a defense mechanism against the accumulation of damage resulting from physiological/oxidative stress [51, 52]. Generally, quiescent HSCs are enriched in LT-HSCs as shown by their capacity to long-term reconstitute lethally irradiated mice. By contrast, ST-HSCs are mainly cycling cells responsible for the maintenance of

hematopoietic homeostasis during shorter time periods. Human HPCs are the counterparts of mouse ST-HSCs and are enriched in hematopoietic clonogenic capacity when cultured in semisolid media [7, 59, 211]. The metabolic activity of quiescent HSCs is lower than that of cycling HSCs, but increases when they exit from quiescence. This exceptional property is determined by a unique vascular organization of the BM with limited oxygen availability that provides a protective microenvironment for LT-HSCs from oxidative stress and DNA damage [52]. Mechanistically, LT-HSCs reside in a hypoxic niche, which is permissive to maintain cells in a non-dividing state and prevent the detrimental accumulation of ROS. HSCs are glycolytic and are thus adapted to this hypoxic environment, thereby avoiding the excessive production of ATP through a less efficient generation of ATP [50, 52, 55, 212].

We demonstrate that mitochondrial mass correlates with MMP in CB-derived CD34⁺ cells. This observation is supported by comparable results in other studies/cell lines [138, 213, 214]. We sorted cells by flow cytometry based on mitochondrial mass into CD34⁺ Mito^{High} and CD34⁺ Mito^{Low} populations to investigate their *in vitro* clonogenic capacity and *in vivo* repopulating potential. As expected, ATP levels and the expression of mitochondrial-specific genes were higher in CD34⁺ Mito^{High} cells than in CD34⁺ Mito^{Low} cells. Functionally, CD34⁺ Mito^{High} cells exhibited higher *in vitro* clonogenic capacity, whereas the CD34⁺ Mito^{Low} fraction displayed higher *in vivo* hematopoietic reconstitution upon transplantation in mice, thus demonstrating that the CD34⁺ Mito^{Low} fraction is enriched in HSCs and the CD34⁺ Mito^{High} fraction is enriched in progenitors. These data are in agreement with previous reports suggesting that HSCs are quiescent and contain less mitochondria, while proliferating HPCs have higher energetic demands [54, 207]. Importantly, mitochondrial segregation in CB CD34⁺ cells did not skew the

normal stem cell hematopoietic commitment as shown by similar colony forming units (CFU) composition in clonogenic assays and multilineage repopulating assays *in vivo*, revealing a similar cell fate despite differential mitochondrial mass.

Cell surface marker expression allows the purification/isolation of HSCs with high efficiency. Additionally, several reports have defined a metabolic phenotype both in mouse and human HSPCs [51, 53, 54, 56, 215]. It has been demonstrated that LT-HSCs are present in a distinct population of cells characterized by low MMP and ATP, and use mainly glycolysis rather than OXPHOS for energy production. The glycolytic adaptation of HSCs is an evolutionary protective mechanism against oxidative damage originating from OXPHOS [51]. According to the surface markers described for HSCs (CD34⁺CD38⁻) and HPCs (CD34⁺CD38⁺) [7], the proportion of CD34⁺CD38⁻ cells found in the CD34⁺ Mito^{Low} population is higher than that found in the CD34⁺ Mito^{High} population, supporting the concept that CD34⁺ Mito^{Low} cells are enriched in HSC function. Along this line, Simsek *et al.* [54] described that *Meis1* regulates HSC metabolism through transcriptional activation of *Hif-1*. HIF-1 is essential for the cellular and systemic response to reduced oxygen availability [61], and is highly expressed and critical in LT-HSCs [54, 60, 61, 63]. Consistent with these findings, we found that the expression of *HIF-1α* and *MEIS1* was higher in CD34⁺ Mito^{Low} cells than in CD34⁺ Mito^{High} cells.

Studies *in vitro* showed that CD34⁺ Mito^{Low} cells differentiated slower than CD34⁺ Mito^{High} cells, as revealed by a delayed kinetic of CD34 reduction. By day 15, all CD34⁺ cells had differentiated irrespective of mitochondrial mass and the expansion of CD34⁻ derivatives was largely boosted, especially the derivatives of CD34⁺ Mito^{Low} cells.

These results support the higher engraftment exhibited by CD34⁺ Mito^{Low} cells because *in vivo* hematopoietic reconstitution is strictly regulated by a balance between self-renewal and differentiation and a fast progenitor expansion at the moment of CD34 antigen loss. An increase in mitochondrial biogenesis and function during stem cell differentiation has been reported previously [208] and is linked to higher ATP synthesis, which is necessary to maintain tissue/cell homeostasis. In line with this, following 15 days of expansion CD34⁺ Mito^{Low} cells achieved mitochondrial adaptation and increased their ATP levels with subsequent up-regulation of the expression of the mitochondrial genes *ND1* and *COX2*. This mitochondrial adaptation seems to occur through an increase in oxidative stress following the increase in ETC activity [109].

Various studies link ROS levels to preservation of stem cell function, suggesting that high ROS levels are implicated in low HSC function. As expected, ROS levels were lower in the CD34⁺ Mito^{Low} population than in CD34⁺ Mito^{High} cells, indicating that CD34⁺ Mito^{Low} cells are enriched in HSC function while the CD34⁺ Mito^{High} are enriched in progenitor function. This confirms that CD34⁺ Mito^{Low} cells mainly use glycolytic metabolism rather than OXPHOS as a mechanism to reduce the negative impact of the ROS production, which can lead to genomic instability [51]. Cancer cells evolved similarly to stem cells, adopting the Warburg effect, which prevents ROS generation and oxidative damage in aerobic conditions as an evolutionary adaptation advantage of cancer cells to their microenvironment [95, 96].

Mutations in genes involved in cellular metabolism and epigenetic regulation are implicated in the pathogenesis of hematopoietic malignancies *via* metabolic dysregulation [216, 217]. HIF-1 is required for maintenance of HSCs and cancer stem

cells, which share many functional and phenotype characteristics [218]. In cancer cells, HIF-1 seems to be the inductor of the Warburg effect [219] and recent studies have demonstrated that BCR-ABL positive cells and multiple myeloma cells display an up-regulation of HIF-1, together with increased ROS generation and expression of glucose metabolism genes [220-223]. Although leukemic cells are highly glycolytic and release 85% of glucose carbon as lactate, pyruvate and glutamine are important metabolic substrates, which are catabolized by pyruvate dehydrogenase (PDH) and glutamate dehydrogenase, respectively, allowing the utilization of glutamine-derived α -ketoglutarate in mitochondria *via* the α -ketoglutarate dehydrogenase (KDH) complex [223]. Interestingly, cytoplasmic isocitrate dehydrogenase 1 (IDH1) and mitochondrial IDH2 are mutated in 15–20% of patients with acute myeloid leukemia, affecting redox metabolism, methylation and differentiation, among others. These data suggest that several targets involved in glycolytic metabolism, including HIF-1, PDH, KDH, IDH1 and IDH2, could become therapeutic options to treat some hematopoietic malignancies. Indeed, several leukemic cell lines have been treated with mitochondrial/OXPHOS inhibitors [224]. The study of leukemic cell metabolism is an important and promising area of research, but before any potential clinical translation it would be key to determine which specific group of patients would benefit from metabolic targeting therapies [223].

Over the last 20 years, umbilical CB has become an important source of HSCs both for research and clinical transplantation. However, *in vitro* and *ex vivo* expansion protocols for CB-derived HSC have been less than successful [211, 225, 226]. LT-HSCs mainly reside within the BM in specific niches that are physiologically hypoxic or anoxic as a result of low levels of glucose and oxygen [57, 58]. Metabolically controlled HSC

expansion may therefore rely on cell survival signals derived from the niche, such as RET signaling [227]. It has also been reported that BM-derived cells cultured in hypoxia had a superior repopulation activity than those cultured under normoxic conditions [212]. This therefore begs the question of whether we are using the most suitable *in vitro* conditions to expand CD34⁺ cells while also ensuring their genomic stability and function. For example, whereas HSCs reside in a hypoxic niche *in vivo* (<1% of oxygen), they are routinely maintained under normoxic conditions. As mentioned, HIF-1 is a key player in HSC metabolism and is essential for cellular and systemic responses to low oxygen availability and it seems to be crucial for the balance between self-renewal and differentiation of HSCs [51, 61, 228]. Under normoxic conditions, HIF-1 levels are reduced through oxygen-mediated degradation. HSCs increase their ROS generation by OXPHOS under normoxia and are forced to exit hypoxia-dependent quiescence [55, 59, 229]. ROS are also required for recovery after BM injury, increasing the expansion of committed progenitors [230]. These data support the notion that the BM niche, OXPHOS and ROS are linked to control proliferation, self-renewal and differentiation of HSCs.

VI

An interesting and open question currently is why HSCs are routinely maintained in the laboratory (worldwide) using high glucose-containing medium when by default they reside in low-glucose/glucose starvation conditions. In the BM niche, LT-HSCs are deprived of nutrients such as oxygen and glucose, which is the main carbon source of the cell to synthesize ATP and the key substrate for the proliferative PI3K-AKT-mTOR pathway [231]. The constitutive activation of AKT in HSCs causes accelerated proliferation/differentiation and depletion of HSCs [232, 233]. Moreover, genetic deletion of PTEN induces the constitutive activation of PI3K-AKT signaling, resulting

in increased proliferation, ultimately leading to HSC exhaustion [59]. Using nutrient-sensing pathways, stem cells maintain energy production by collectively inhibiting key demanding processes including OXPHOS and promoting glycolysis. This interplay is key for the maintenance of stem cells in various tissues [59, 234, 235]. Taken together, it would be desirable to test for the most appropriate culture conditions to maintain HSCs *in vitro* and *in vivo*.

II. A disease-specific iPSC model for CoQ₁₀ deficiency: metabolic and developmental impact of a *COQ4* mutation during differentiation of iPSCs into tissues affected by the disease.

CoQ₁₀ is a lipid-soluble molecule ubiquitous to cellular membranes that has essential functions in many cellular processes including energy/ATP production, where it shuttles electrons from CI and CII to CIII in the ETC [146, 150]. CoQ₁₀ levels below 50% of standard values are indicative of CoQ₁₀ deficiency, which is a rare and heterogeneous group of metabolic/mitochondrial disorders (OMIM #607426) associated with a broad variety of genetic and clinical manifestation usually detected in the early years of life [157, 179]. CoQ₁₀ deficiencies are commonly classified as either primary or secondary. Primary CoQ₁₀ deficiency is an autosomal recessive syndrome that originates from mutations in genes responsible for CoQ₁₀ biosynthesis (*COQ* genes or regulatory genes). The pathogenesis of secondary CoQ₁₀ deficiency is less well studied but seems linked to assembly defects in OXPHOS complexes/metabolic pathways [157]. Primary CoQ₁₀ deficiency usually affects the ETC due to the central role of CoQ₁₀ as a mobile electron carrier between CI+III and CII+III, causing a mitochondrial phenotype. Given the high energy demand of neurons and muscle and

their dependence on OXPHOS, it is not surprising that mitochondrial diseases are commonly devastating to CNS and SkM as they are unable to synthesize sufficient quantities of ATP for completing physiological processes [154, 173, 174]. The only current treatment for this condition is the oral supplementation of CoQ₁₀; however, there is a variable response to exogenous treatment and almost 50% of patients fail to respond to exogenous oral administration of CoQ₁₀ [173, 236].

CoQ₁₀ biosynthesis involves at least 15 *COQ* and regulator genes in a multienzymatic complex where *COQ4* plays a central structural role [145]. Although several mutations have been identified in numerous genes involved in CoQ₁₀ biosynthesis, there is no clear association between the genotype and the phenotype. That is, mutations in different genes may render the same clinical phenotype while distinct mutations in the same gene may render different phenotypes [153, 177]. It has been suggested that *COQ4* mutations or haploinsufficiency causes CoQ₁₀ deficiency associated with a broad phenotypic spectrum including encephalomyopathy, cerebellar atrophy, hypotonia, respiratory distress and neurological deterioration [175, 178].

We identified a 4-year-old girl with the missense point mutation (c.483G>C; E161D) in *COQ4* who displayed mitochondrial deficits affecting SkM with subsequent fatal rhabdomyolysis. This mutation was associated with low levels of CoQ₁₀ and impaired biosynthesis and also ETC dysfunction. Mutant *COQ4* fibroblasts presented a reduction in proliferative capacity linked to high levels of senescence-associated β-galactosidase activity, reflecting the involvement of CoQ₁₀ in pyrimidine synthesis and ETC dysfunction, which can produce ROS-mediated, oxidative damage/cellular senescence [129-131, 150, 158].

Since their discovery in 1998, hESCs have been the PSCs of choice in stem cell research for applications such as cell therapy and disease modeling due to their potency and long-term proliferation potential. Nevertheless, they have been associated with ethical issues due to their prenatal/embryonic origin [24]. Since 2006, iPSCs represent a unique alternative to model human disease since they share similar properties to hESCs, such as pluripotency and infinite lifespan, while being free from ethical issues since embryonic tissue is not involved. iPSCs are particularly useful to study rare diseases with a known genetic alteration since the low prevalence of the disease challenges the recapitulation of a disease phenotype using primary cells from the patient. Our patient developed CoQ₁₀ deficiency with fatal rhabdomyolysis associated with the E161D mutation in COQ4. Interestingly, a few years later the patient's sibling developed a similar but weaker muscle phenotype (she ultimately died because of vascular cardiac failure) without mutations in genes involved in CoQ₁₀ biosynthesis or CoQ₁₀ deficiency. To harness the full potential of patient-specific iPSCs, it would be crucial to unravel to what extent the specific genomic mutation is the sole pathogenic driver (or genomic modifier) contributing to the genotype-phenotype of the disease. A large number of studies have reported strategies to model disease phenotypes using iPSCs, including monogenic diseases and complex disorders such as Rett syndrome, Parkinson disease, cancer, Fanconi anemia, Huntington disease and Hutchinson-Gilford progeria syndrome, among others [1, 5, 15-17, 24, 89, 92, 186, 188-191, 194, 203]. One example of such an approach was recently reported for ALS [237]. Researchers discovered that iPSC-derived MN from an ALS patient displayed hyperexcitability with reduced survival, and that this phenotype could be corrected by a potassium channel agonist [237]. Another example was reported for Néstor-Guillermo progeria syndrome

(NGPS), where it has been demonstrated that NF- κ B activation blocks iPSC generation. Accordingly, genetic and pharmacological NF- κ B inhibition increases the reprogramming efficiency from premature-aged NGPS cells [193]. To the best of our knowledge, our work is the first to describe an iPSC-based model for CoQ₁₀ deficiency.

The CRISPR/Cas9 adaptive bacterial immunity system is a simple and versatile approach to engineer the eukaryote genome. It has successfully been used to modify/edit genes in monogenic disorders using patient-specific iPSCs [202-204, 206]. Here, we harnessed CRISPR/Cas9 technology to edit/correct a patient-derived iPSC line for the c483 G>C mutation in *COQ4*. The generation of isogenic cell lines allows the drawing of conclusions circumventing genetic and epigenetic variability. While the generation of off-target effects could be a side-effect of the CRISPR/Cas9 system, because it may generate a DSB in the DNA in an undesired region [201, 238], we verified the genome stability and the absence of off-target generation in our edited iPSC line without gross genetic aberrations.

Levels of CoQ₁₀ are usually measured as a diagnostic test in fibroblasts and muscle [171]; however, the levels of CoQ₁₀ and its biosynthesis have not been reported in human PSCs. Here, we measured for the first time the levels of CoQ₁₀ in PSC lines (iPSC/ESC). We characterized a range between ~150 and ~75 pmol of CoQ₁₀/mg protein using a battery of control/healthy PSCs. These reference values allowed us to distinguish iPSCs with low levels of CoQ₁₀, which could explain the key role of CoQ₁₀ in cellular/metabolic homeostasis. We observed that CoQ₁₀ levels and biosynthesis in CQ4-iPSCs were lower than in Ctrl- and CQ4^{ed}-iPSCs, demonstrating the cause-effect of the c.483 G>C mutation in CoQ₁₀ biosynthesis. Interestingly, cell reprogramming

failed to re-establish CoQ₁₀ levels/biosynthesis in CQ4-iPSCs, highlighting the evolutionary conserved role of CoQ₁₀ in cellular homeostasis involving nucleotide synthesis and OXPHOS regulation. Moreover, in order to synthesize an equivalent amount of ATP, CQ4-iPSCs required 2-fold higher levels of OCR and ECAR rates as an indirect measure of OXPHOS and glycolysis, respectively. This increase in energetic metabolism is likely related to the electron leak due to the reduction of CoQ₁₀ in the ETC, which causes a mitochondrial dysfunction. Leaking of protons, which were observed in the OCR, is an indirect measure related to electron leak [239]. Overall, these data suggest an altered metabolism in patient iPSCs, where COQ₁₀ plays a central role stabilizing electrons and its deficiency impairs the proper functioning of the ETC. This dysfunction was reversed after the correction of the c.483 G>C mutation.

Neurological manifestations are very common in CoQ₁₀-deficient patients [157, 172]. We therefore differentiated iPSCs towards the neural lineage using well-established protocols for DANs [27] and MNs [29]. We induced neural differentiation of iPSCs using dual SMAD inhibition, which allows differentiation into early neuroectoderm by blockage of ALKs signaling pathways of BMP (LDN193189) and TGF β (SB431542), reducing the complexity of neural differentiation [82, 240]. We obtained between 15–25% of TUJ⁺ neurons and less than 10% of these showed a DAN or MN phenotype. Although, our data revealed a high percentage of neural differentiation, current neuronal differentiation protocols need to be largely improved to attain a higher proportion of differentiated cells, which would allow functional electrophysiological and metabolic assays on iPSC-neural derivatives. The fact the iPSC-derived neurons failed to reveal a phenotype when compared with control iPSCs is in line with the patient phenotype, which was free from severe neurological symptoms. These data

further validate our iPSC model as a *bona fide* system to reproduce the main features of a given disease.

Fatal rhabdomyolysis was the main clinical alteration in our patient. Because of this, we differentiated iPSCs into SkM following the protocol based on PAX7-mediated differentiation published by the Perlingeiro laboratory [89]. We first generated transgenic iPSC lines by lentiviral transduction with the inducible PAX7-GFP plasmid. Myogenesis was then induced by doxycycline induction of PAX7. After embryoid body differentiation, PAX7⁺ myogenic progenitors were sorted based on the expression of GFP and cultured under myogenic conditions to further promote muscle myogenic maturation. CQ4-PAX7⁺ myogenic precursors had high levels of ROS, possibly underlying the increased senescence and the reduced/impaired proliferation potential of these cells versus their edited counterparts. SkM maturation was assessed by analyzing the percentage of MYH1⁺ cells and measuring creatine kinase activity, which are both specific markers of SkM cells. We found that CQ4-PAX7⁺ progenitors displayed a lower capacity of SkM maturation than their edited counterparts, which was accompanied by a dysregulated expression of myogenic differentiation markers implying a possible blockage of differentiation. We therefore assessed mitochondrial dysfunction in iPSC-derived muscle progenitors by examining mitochondrial dynamics and ETC activity. These studies confirmed a reduction in CI+III activity and also abnormalities in mitochondrial morphology. Collectively, these results establish the utility of an iPSC-based disease model to study genotype-phenotype association, wherein the c.483 G>C mutation faithfully reproduces disease-associated SkM functional and metabolic defects. The combination of altered mitochondrial dynamics and reduced ETC may contribute to the vulnerability of muscle maturation.

In summary, we demonstrate that iPSCs generated from our patient differentiate normally into DAn and MNs using well-established protocols [27, 29], while differentiation to SkM was compromised. Patient-specific iPSCs also reproduced the metabolic defects observed in the *COQ4* mutated cells, and these metabolic and phenotypic defects were reversed when the *COQ4* mutation was genetically corrected. The CoQ₁₀ deficiency model here established represents a unique system for studying CoQ₁₀ pathogenesis, which we believe will facilitate the discovery of novel therapeutic drugs and will provide valuable information about the molecular/genetic basis of responsiveness to CoQ₁₀ treatment.

Human PSCs represent a unique tool for cell therapy strategies and disease modeling because of their ability for self-renewal and differentiation into any tissue of the three embryonic germ layers. The robustness of this system is demonstrated by the use of PSC-derived cells in several clinical applications [33], listed in **Table 1**. For example, in 2014 the first ever clinical trial to test a PSC-based treatment for type 1 diabetes mellitus was initiated. A subcutaneous implantable device containing hESC-derived pancreatic endoderm cells was explored for treatment of diabetes [241-243]. Nevertheless, the most common type of clinical trial (currently standing at nine) testing PSC-based therapies predominantly focuses on a therapeutic window for retinal generation. The eye has many characteristics that make it an attractive organ for clinical trials: it has an immunoprivileged nature, it represents an isolated environment where the transplanted cells are restrained, it is accessible for injection and it can be non-invasively monitored by visualization for the detection of internal tissue. The generation of retinal pigment cells from PSCs may soon be a treatment for the degeneration of light-sensing photoreceptor cells and the retinal pigment epithelium in

the eye, and is being explored in several clinical trials [244-246]. As another example, grafts of PSC-derived cardiac cells may also provide functional restoration of areas of weakened or ischemic heart tissue. Preclinical studies demonstrated that the administration of hESC-derived cardiac progenitors improves overall cardiac function, however, the engrafted cells were undetectable after four months, suggesting that their role in improving cardiac function may have been to enhance the endogenous repair processes [31, 247]. In addition, a clinical trial using hESC-derived oligodendrocytes was initially launched early in 2009 to treat spinal cord injuries, which consisted in the administration of oligodendrocyte progenitor cells to enhance remyelination and improve motor function. The trial was abandoned in 2011, although a new clinical trial was subsequently initiated [248]. Patients with hematopoietic disorders or suffering blood loss require continual transfusions but, unfortunately, blood derivatives obtained from donors are only accessible in limited quantities and have a very short half-life. The generation of a donor-independent system capable of providing constant and sufficiently large numbers of functional cells would therefore be an important step forward in transfusion medicine. Red blood cells and platelets can be generated from hESC/iPSCs, but this is currently an inefficient process [249-255]. Other blood cell types including T cells, HSCs and dendritic cells have yet to be successfully generated [25, 256-258]. Establishing and improving protocols to differentiate these cell types from PSCs may become a future therapeutic option for treating blood disorders. Notwithstanding these challenges, current clinical trials have demonstrated the feasibility of PSC-based cell therapies, although more work on differentiation, molecular and genetic mechanisms are needed to deliver specific and homogeneous cell populations with fully functionality *in vivo*.

Table 1. hESC and iPSC-based products in clinical trials

Cell type	Trial location	Disease	Reference
hESC-derived RPE	USA	Dry AMD	NCT01344993
hESC-derived RPE	USA	Stargard	NCT01345006
hESC-derived RPE	UK	Stargard	NCT01469832
hESC-derived RPE	Korea	Dry AMD	NCT01674829
hESC-derived RPE	Korea	Stargard	NCT01625559
hESC-derived RPE	USA	MMD	NCT02122159
hiPSC-derived RPE	Japan	Wet AMD	[244]
hESC-derived RPE	UK	Wet AMD	NCT01691261
hESC-derived RPE	Israel	Dry AMD	NCT02286089
hESC-derived CD15+ISL-1+ cardiac progenitors	France	Severe heart failure	NCT02057900
hESC-derived pancreatic endoderm	USA	Type I diabetes	NCT02239354
hESC-derived oligodendrocyte progenitors	USA	Spinal cord injury	[248]

AMD: age-related macular degeneration; ISL-1: Islet-1; MMD: myopic macular degeneration; RPE: retinal pigment epithelium.

VII.CONCLUSIONS

Regarding the first part of the PhD thesis, we conclude that:

1. There is a strong correlation between mitochondrial mass and mitochondrial function in cord blood-derived CD34⁺ cells.
2. The CD34⁺ Mito^{High} fraction is enriched in progenitor function, as revealed by higher clonogenic capacity.
3. The CD34⁺ Mito^{Low} fraction is enriched in stem cell function, as revealed by an increased *in vivo* hematopoietic reconstitution.

Regarding the second part of the thesis, we conclude that:

4. Induced pluripotent stem cells from a CoQ₁₀ deficient patient harboring a COQ4 mutation have been generated, characterized and CRISPR/Cas9 edited.
5. The COQ4 mutation directly influences CoQ₁₀ biosynthesis and concentration causing a mitochondrial dysfunction in CQ4-iPSC.
6. The COQ4 mutation does not impair the *in vitro* differentiation of CQ4-iPSCs into either midbrain dopaminergic neurons or spinal motor neurons.
7. The COQ4 mutation negatively alters the differentiation towards skeletal muscle linked to decreased mitochondrial and metabolic function as revealed by a reduced ETC activity and mitochondrial dynamics.

VIII. REFERENCES

1. Avior, Y., I. Sagi, and N. Benvenisty, *Pluripotent stem cells in disease modelling and drug discovery*. Nat Rev Mol Cell Biol, 2016. **17**(3): p. 170-82.
2. Takahashi, K. and S. Yamanaka, *A developmental framework for induced pluripotency*. Development, 2015. **142**(19): p. 3274-85.
3. Thomson, J.A., et al., *Embryonic stem cell lines derived from human blastocysts*. Science, 1998. **282**(5391): p. 1145-7.
4. Tuch, B.E., *Stem cells--a clinical update*. Aust Fam Physician, 2006. **35**(9): p. 719-21.
5. Takahashi, K., et al., *Induction of pluripotent stem cells from adult human fibroblasts by defined factors*. Cell, 2007. **131**(5): p. 861-72.
6. Pardal, R. and J. Lopez Barneo, *Mature neurons modulate neurogenesis through chemical signals acting on neural stem cells*. Dev Growth Differ, 2016. **58**(5): p. 456-62.
7. Seita, J. and I.L. Weissman, *Hematopoietic stem cell: self-renewal versus differentiation*. Wiley Interdiscip Rev Syst Biol Med, 2010. **2**(6): p. 640-53.
8. Rodriguez, R., R. Rubio, and P. Menendez, *Modeling sarcomagenesis using multipotent mesenchymal stem cells*. Cell Res, 2012. **22**(1): p. 62-77.
9. Wu, S.M. and K. Hochedlinger, *Harnessing the potential of induced pluripotent stem cells for regenerative medicine*. Nat Cell Biol, 2011. **13**(5): p. 497-505.
10. Takahashi, K. and S. Yamanaka, *Induction of pluripotent stem cells from mouse embryonic and adult fibroblast cultures by defined factors*. Cell, 2006. **126**(4): p. 663-76.
11. Chin, M.H., et al., *Induced pluripotent stem cells and embryonic stem cells are distinguished by gene expression signatures*. Cell Stem Cell, 2009. **5**(1): p. 111-23.
12. Kim, K., et al., *Donor cell type can influence the epigenome and differentiation potential of human induced pluripotent stem cells*. Nat Biotechnol, 2011. **29**(12): p. 1117-9.
13. Lee, J.H., et al., *Somatic transcriptome priming gates lineage-specific differentiation potential of human-induced pluripotent stem cell states*. Nat Commun, 2014. **5**: p. 5605.

14. Guenther, M.G., et al., *Chromatin structure and gene expression programs of human embryonic and induced pluripotent stem cells*. Cell Stem Cell, 2010. **7**(2): p. 249-57.
15. Bueno, C., et al., *Reprogramming human B cells into induced pluripotent stem cells and its enhancement by C/EBPalpha*. Leukemia, 2016. **30**(3): p. 674-82.
16. Aasen, T., et al., *Efficient and rapid generation of induced pluripotent stem cells from human keratinocytes*. Nat Biotechnol, 2008. **26**(11): p. 1276-84.
17. Giorgetti, A., et al., *Generation of induced pluripotent stem cells from human cord blood using OCT4 and SOX2*. Cell Stem Cell, 2009. **5**(4): p. 353-7.
18. Liu, H., et al., *Generation of endoderm-derived human induced pluripotent stem cells from primary hepatocytes*. Hepatology, 2010. **51**(5): p. 1810-9.
19. Kim, J.B., et al., *Direct reprogramming of human neural stem cells by OCT4*. Nature, 2009. **461**(7264): p. 649-3.
20. Takahashi, K. and S. Yamanaka, *A decade of transcription factor-mediated reprogramming to pluripotency*. Nat Rev Mol Cell Biol, 2016. **17**(3): p. 183-93.
21. Hou, P., et al., *Pluripotent stem cells induced from mouse somatic cells by small-molecule compounds*. Science, 2013. **341**(6146): p. 651-4.
22. Marti, M., et al., *Characterization of pluripotent stem cells*. Nat Protoc, 2013. **8**(2): p. 223-53.
23. Ramos-Mejia, V., et al., *Residual expression of the reprogramming factors prevents differentiation of iPSC generated from human fibroblasts and cord blood CD34+ progenitors*. PLoS One, 2012. **7**(4): p. e35824.
24. Spitalieri, P., et al., *Human induced pluripotent stem cells for monogenic disease modelling and therapy*. World J Stem Cells, 2016. **8**(4): p. 118-35.
25. Ramos-Mejia, V., et al., *HOXA9 promotes hematopoietic commitment of human embryonic stem cells*. Blood, 2014. **124**(20): p. 3065-75.
26. Real, P.J., et al., *SCL/TAL1 regulates hematopoietic specification from human embryonic stem cells*. Mol Ther, 2012. **20**(7): p. 1443-53.
27. Kriks, S., et al., *Dopamine neurons derived from human ES cells efficiently engraft in animal models of Parkinson's disease*. Nature, 2011. **480**(7378): p. 547-51.

28. Grealish, S., et al., *Human ESC-derived dopamine neurons show similar preclinical efficacy and potency to fetal neurons when grafted in a rat model of Parkinson's disease*. *Cell Stem Cell*, 2014. **15**(5): p. 653-65.
29. Amoroso, M.W., et al., *Accelerated high-yield generation of limb-innervating motor neurons from human stem cells*. *J Neurosci*, 2013. **33**(2): p. 574-86.
30. Schwartz, S.D., et al., *Human embryonic stem cell-derived retinal pigment epithelium in patients with age-related macular degeneration and Stargardt's macular dystrophy: follow-up of two open-label phase 1/2 studies*. *Lancet*, 2015. **385**(9967): p. 509-16.
31. Bellamy, V., et al., *Long-term functional benefits of human embryonic stem cell-derived cardiac progenitors embedded into a fibrin scaffold*. *J Heart Lung Transplant*, 2015. **34**(9): p. 1198-207.
32. Kelly, O.G., et al., *Cell-surface markers for the isolation of pancreatic cell types derived from human embryonic stem cells*. *Nat Biotechnol*, 2011. **29**(8): p. 750-6.
33. Kimbrel, E.A. and R. Lanza, *Current status of pluripotent stem cells: moving the first therapies to the clinic*. *Nat Rev Drug Discov*, 2015. **14**(10): p. 681-92.
34. Gafni, O., et al., *Derivation of novel human ground state naive pluripotent stem cells*. *Nature*, 2013. **504**(7479): p. 282-6.
35. Hanna, J., et al., *Human embryonic stem cells with biological and epigenetic characteristics similar to those of mouse ESCs*. *Proc Natl Acad Sci U S A*, 2010. **107**(20): p. 9222-7.
36. Hu, B.Y., et al., *Neural differentiation of human induced pluripotent stem cells follows developmental principles but with variable potency*. *Proc Natl Acad Sci U S A*, 2010. **107**(9): p. 4335-40.
37. Woods, N.B., et al., *Brief report: efficient generation of hematopoietic precursors and progenitors from human pluripotent stem cell lines*. *Stem Cells*, 2011. **29**(7): p. 1158-64.
38. Velasco, I., et al., *Concise review: Generation of neurons from somatic cells of healthy individuals and neurological patients through induced pluripotency or direct conversion*. *Stem Cells*, 2014. **32**(11): p. 2811-7.

39. Gaj, T., C.A. Gersbach, and C.F. Barbas, 3rd, *ZFN, TALEN, and CRISPR/Cas-based methods for genome engineering*. Trends Biotechnol, 2013. **31**(7): p. 397-405.
40. Dzierzak, E. and N.A. Speck, *Of lineage and legacy: the development of mammalian hematopoietic stem cells*. Nat Immunol, 2008. **9**(2): p. 129-36.
41. Ivanovs, A., et al., *Highly potent human hematopoietic stem cells first emerge in the intraembryonic aorta-gonad-mesonephros region*. J Exp Med, 2011. **208**(12): p. 2417-27.
42. Julien, E., R. El Omar, and M. Tavian, *Origin of the hematopoietic system in the human embryo*. FEBS Lett, 2016.
43. Baron, M.H., J. Isern, and S.T. Fraser, *The embryonic origins of erythropoiesis in mammals*. Blood, 2012. **119**(21): p. 4828-37.
44. Menendez, P., et al., *Influence of the different CD34+ and CD34- cell subsets infused on clinical outcome after non-myeloablative allogeneic peripheral blood transplantation from human leucocyte antigen-identical sibling donors*. Br J Haematol, 2002. **119**(1): p. 135-43.
45. Sutherland, D.R. and A. Keating, *The CD34 antigen: structure, biology, and potential clinical applications*. J Hematother, 1992. **1**(2): p. 115-29.
46. Broxmeyer, H.E., *Biology of cord blood cells and future prospects for enhanced clinical benefit*. Cytotherapy, 2005. **7**(3): p. 209-18.
47. Broxmeyer, H.E., et al., *Human umbilical cord blood as a potential source of transplantable hematopoietic stem/progenitor cells*. Proc Natl Acad Sci U S A, 1989. **86**(10): p. 3828-32.
48. Menendez, P., et al., *The composition of leukapheresis products impacts on the hematopoietic recovery after autologous transplantation independently of the mobilization regimen*. Transfusion, 2002. **42**(9): p. 1159-72.
49. Ballen, K.K., E. Gluckman, and H.E. Broxmeyer, *Umbilical cord blood transplantation: the first 25 years and beyond*. Blood, 2013. **122**(4): p. 491-8.
50. Trumpp, A., M. Essers, and A. Wilson, *Awakening dormant haematopoietic stem cells*. Nat Rev Immunol, 2010. **10**(3): p. 201-9.

51. Suda, T., K. Takubo, and G.L. Semenza, *Metabolic regulation of hematopoietic stem cells in the hypoxic niche*. Cell Stem Cell, 2011. **9**(4): p. 298-310.
52. Walter, D., et al., *Exit from dormancy provokes DNA-damage-induced attrition in haematopoietic stem cells*. Nature, 2015. **520**(7548): p. 549-52.
53. Notta, F., et al., *Isolation of single human hematopoietic stem cells capable of long-term multilineage engraftment*. Science, 2011. **333**(6039): p. 218-21.
54. Simsek, T., et al., *The distinct metabolic profile of hematopoietic stem cells reflects their location in a hypoxic niche*. Cell Stem Cell, 2010. **7**(3): p. 380-90.
55. Jang, Y.Y. and S.J. Sharkis, *A low level of reactive oxygen species selects for primitive hematopoietic stem cells that may reside in the low-oxygenic niche*. Blood, 2007. **110**(8): p. 3056-63.
56. Sukumar, M., et al., *Mitochondrial Membrane Potential Identifies Cells with Enhanced Stemness for Cellular Therapy*. Cell Metab, 2016. **23**(1): p. 63-76.
57. Chow, D.C., et al., *Modeling pO₂ distributions in the bone marrow hematopoietic compartment. II. Modified Kroghian models*. Biophys J, 2001. **81**(2): p. 685-96.
58. Harrison, J.S., et al., *Oxygen saturation in the bone marrow of healthy volunteers*. Blood, 2002. **99**(1): p. 394.
59. Ito, K. and T. Suda, *Metabolic requirements for the maintenance of self-renewing stem cells*. Nat Rev Mol Cell Biol, 2014. **15**(4): p. 243-56.
60. Hagg, M. and S. Wennstrom, *Activation of hypoxia-induced transcription in normoxia*. Exp Cell Res, 2005. **306**(1): p. 180-91.
61. Semenza, G.L., *Hypoxia-inducible factor 1 (HIF-1) pathway*. Sci STKE, 2007. **2007**(407): p. cm8.
62. Papandreou, I., et al., *HIF-1 mediates adaptation to hypoxia by actively downregulating mitochondrial oxygen consumption*. Cell Metab, 2006. **3**(3): p. 187-97.
63. Maxwell, P.H., et al., *The tumour suppressor protein VHL targets hypoxia-inducible factors for oxygen-dependent proteolysis*. Nature, 1999. **399**(6733): p. 271-5.

64. Eriksson, P.S., et al., *Neurogenesis in the adult human hippocampus*. Nat Med, 1998. **4**(11): p. 1313-7.
65. Kriegstein, A. and A. Alvarez-Buylla, *The glial nature of embryonic and adult neural stem cells*. Annu Rev Neurosci, 2009. **32**: p. 149-84.
66. Ellis, P., et al., *SOX2, a persistent marker for multipotential neural stem cells derived from embryonic stem cells, the embryo or the adult*. Dev Neurosci, 2004. **26**(2-4): p. 148-65.
67. Poulin, J.F., et al., *Disentangling neural cell diversity using single-cell transcriptomics*. Nat Neurosci, 2016. **19**(9): p. 1131-41.
68. Luo, S.X. and E.J. Huang, *Dopaminergic Neurons and Brain Reward Pathways: From Neurogenesis to Circuit Assembly*. Am J Pathol, 2016. **186**(3): p. 478-88.
69. Hegarty, S.V., A.M. Sullivan, and G.W. O'Keefe, *Midbrain dopaminergic neurons: a review of the molecular circuitry that regulates their development*. Dev Biol, 2013. **379**(2): p. 123-38.
70. Acampora, D. and A. Simeone, *The TINS Lecture. Understanding the roles of Otx1 and Otx2 in the control of brain morphogenesis*. Trends Neurosci, 1999. **22**(3): p. 116-22.
71. Ferri, A.L., et al., *Foxa1 and Foxa2 regulate multiple phases of midbrain dopaminergic neuron development in a dosage-dependent manner*. Development, 2007. **134**(15): p. 2761-9.
72. Nakatani, T., et al., *Lmx1a and Lmx1b cooperate with Foxa2 to coordinate the specification of dopaminergic neurons and control of floor plate cell differentiation in the developing mesencephalon*. Dev Biol, 2010. **339**(1): p. 101-13.
73. Yi, S.H., et al., *Foxa2 acts as a co-activator potentiating expression of the Nurr1-induced DA phenotype via epigenetic regulation*. Development, 2014. **141**(4): p. 761-72.
74. Stifani, N., *Motor neurons and the generation of spinal motor neuron diversity*. Front Cell Neurosci, 2014. **8**: p. 293.
75. Davis-Dusenbery, B.N., et al., *How to make spinal motor neurons*. Development, 2014. **141**(3): p. 491-501.

76. Giorgetti, A., et al., *Cord blood-derived neuronal cells by ectopic expression of Sox2 and c-Myc*. Proc Natl Acad Sci U S A, 2012. **109**(31): p. 12556-61.
77. Chambers, S.M., et al., *Dual-SMAD Inhibition/WNT Activation-Based Methods to Induce Neural Crest and Derivatives from Human Pluripotent Stem Cells*. Methods Mol Biol, 2016. **1307**: p. 329-43.
78. Muratore, C.R., et al., *Comparison and optimization of hiPSC forebrain cortical differentiation protocols*. PLoS One, 2014. **9**(8): p. e105807.
79. Sanchez-Danes, A., et al., *Efficient generation of A9 midbrain dopaminergic neurons by lentiviral delivery of LMX1A in human embryonic stem cells and induced pluripotent stem cells*. Hum Gene Ther, 2012. **23**(1): p. 56-69.
80. Wichterle, H., et al., *Directed differentiation of embryonic stem cells into motor neurons*. Cell, 2002. **110**(3): p. 385-97.
81. Marchetto, M.C., et al., *Non-cell-autonomous effect of human SOD1 G37R astrocytes on motor neurons derived from human embryonic stem cells*. Cell Stem Cell, 2008. **3**(6): p. 649-57.
82. Chambers, S.M., et al., *Highly efficient neural conversion of human ES and iPSC cells by dual inhibition of SMAD signaling*. Nat Biotechnol, 2009. **27**(3): p. 275-80.
83. Yang, N., et al., *Induced neuronal cells: how to make and define a neuron*. Cell Stem Cell, 2011. **9**(6): p. 517-25.
84. Sousa-Victor, P., P. Munoz-Canoves, and E. Perdiguero, *Regulation of skeletal muscle stem cells through epigenetic mechanisms*. Toxicol Mech Methods, 2011. **21**(4): p. 334-42.
85. Olguin, H.C., et al., *Reciprocal inhibition between Pax7 and muscle regulatory factors modulates myogenic cell fate determination*. J Cell Biol, 2007. **177**(5): p. 769-79.
86. Buckingham, M. and P.W. Rigby, *Gene regulatory networks and transcriptional mechanisms that control myogenesis*. Dev Cell, 2014. **28**(3): p. 225-38.
87. Lluís, F., et al., *Regulation of skeletal muscle gene expression by p38 MAP kinases*. Trends Cell Biol, 2006. **16**(1): p. 36-44.

88. F.A., Z., S. M., and E. D., *Skeletal Muscle Regeneration for Clinical Application*. Regenerative Medicine and Tissue Engineering, 2013.
89. Darabi, R., et al., *Human ES- and iPS-derived myogenic progenitors restore DYSTROPHIN and improve contractility upon transplantation in dystrophic mice*. Cell Stem Cell, 2012. **10**(5): p. 610-9.
90. Darabi, R., et al., *Functional skeletal muscle regeneration from differentiating embryonic stem cells*. Nat Med, 2008. **14**(2): p. 134-43.
91. Filareto, A., R. Darabi, and R.C. Perlingeiro, *Engraftment of ES-Derived Myogenic Progenitors in a Severe Mouse Model of Muscular Dystrophy*. J Stem Cell Res Ther, 2012. **10**(1).
92. Chal, J., et al., *Differentiation of pluripotent stem cells to muscle fiber to model Duchenne muscular dystrophy*. Nat Biotechnol, 2015. **33**(9): p. 962-9.
93. Abujarour, R. and B. Valamehr, *Generation of skeletal muscle cells from pluripotent stem cells: advances and challenges*. Front Cell Dev Biol, 2015. **3**: p. 29.
94. Skuk, D., M. Goulet, and J.P. Tremblay, *Intramuscular transplantation of myogenic cells in primates: importance of needle size, cell number, and injection volume*. Cell Transplant, 2014. **23**(1): p. 13-25.
95. Warburg, O., F. Wind, and E. Negelein, *The Metabolism of Tumors in the Body*. J Gen Physiol, 1927. **8**(6): p. 519-30.
96. Alfarouk, K.O., et al., *Glycolysis, tumor metabolism, cancer growth and dissemination. A new pH-based etiopathogenic perspective and therapeutic approach to an old cancer question*. Oncoscience, 2014. **1**(12): p. 777-802.
97. Leese, H.J., *Metabolism of the preimplantation embryo: 40 years on*. Reproduction, 2012. **143**(4): p. 417-27.
98. Brinster, R.L. and D.E. Troike, *Requirements for blastocyst development in vitro*. J Anim Sci, 1979. **49 Suppl 2**: p. 26-34.
99. Zhou, W., et al., *HIF1alpha induced switch from bivalent to exclusively glycolytic metabolism during ESC-to-EpiSC/hESC transition*. EMBO J, 2012. **31**(9): p. 2103-16.
100. Yoshida, Y., et al., *Hypoxia enhances the generation of induced pluripotent stem cells*. Cell Stem Cell, 2009. **5**(3): p. 237-41.

101. Folmes, C.D., et al., *Somatic oxidative bioenergetics transitions into pluripotency-dependent glycolysis to facilitate nuclear reprogramming*. *Cell Metab*, 2011. **14**(2): p. 264-71.
102. Prigione, A., et al., *HIF1alpha modulates cell fate reprogramming through early glycolytic shift and upregulation of PDK1-3 and PKM2*. *Stem Cells*, 2014. **32**(2): p. 364-76.
103. Teslaa, T. and M.A. Teitell, *Pluripotent stem cell energy metabolism: an update*. *EMBO J*, 2015. **34**(2): p. 138-53.
104. Zhang, J., et al., *UCP2 regulates energy metabolism and differentiation potential of human pluripotent stem cells*. *EMBO J*, 2011. **30**(24): p. 4860-73.
105. Wallace, D.C. and W. Fan, *Energetics, epigenetics, mitochondrial genetics*. *Mitochondrion*, 2010. **10**(1): p. 12-31.
106. Efremov, R.G. and L.A. Sazanov, *Respiratory complex I: 'steam engine' of the cell?* *Curr Opin Struct Biol*, 2011. **21**(4): p. 532-40.
107. Dawson, T.M. and V.L. Dawson, *Rare genetic mutations shed light on the pathogenesis of Parkinson disease*. *J Clin Invest*, 2003. **111**(2): p. 145-51.
108. Balaban, R.S., S. Nemoto, and T. Finkel, *Mitochondria, oxidants, and aging*. *Cell*, 2005. **120**(4): p. 483-95.
109. Murphy, M.P., *How mitochondria produce reactive oxygen species*. *Biochem J*, 2009. **417**(1): p. 1-13.
110. Slane, B.G., et al., *Mutation of succinate dehydrogenase subunit C results in increased O₂·, oxidative stress, and genomic instability*. *Cancer Res*, 2006. **66**(15): p. 7615-20.
111. King, A., M.A. Selak, and E. Gottlieb, *Succinate dehydrogenase and fumarate hydratase: linking mitochondrial dysfunction and cancer*. *Oncogene*, 2006. **25**(34): p. 4675-82.
112. Hoekstra, A.S. and J.P. Bayley, *The role of complex II in disease*. *Biochim Biophys Acta*, 2013. **1827**(5): p. 543-51.
113. Qi, X., et al., *Optic neuropathy induced by reductions in mitochondrial superoxide dismutase*. *Invest Ophthalmol Vis Sci*, 2003. **44**(3): p. 1088-96.
114. Benit, P., S. Lebon, and P. Rustin, *Respiratory-chain diseases related to complex III deficiency*. *Biochim Biophys Acta*, 2009. **1793**(1): p. 181-5.

115. Blazquez, A., et al., *Infantile mitochondrial encephalomyopathy with unusual phenotype caused by a novel BCS1L mutation in an isolated complex III-deficient patient*. *Neuromuscul Disord*, 2009. **19**(2): p. 143-6.
116. Shoubridge, E.A., *Cytochrome c oxidase deficiency*. *Am J Med Genet*, 2001. **106**(1): p. 46-52.
117. Hackenbrock, C.R., B. Chazotte, and S.S. Gupte, *The random collision model and a critical assessment of diffusion and collision in mitochondrial electron transport*. *J Bioenerg Biomembr*, 1986. **18**(5): p. 331-68.
118. Lenaz, G. and M.L. Genova, *Kinetics of integrated electron transfer in the mitochondrial respiratory chain: random collisions vs. solid state electron channeling*. *Am J Physiol Cell Physiol*, 2007. **292**(4): p. C1221-39.
119. Lapuente-Brun, E., et al., *Supercomplex assembly determines electron flux in the mitochondrial electron transport chain*. *Science*, 2013. **340**(6140): p. 1567-70.
120. Schagger, H. and K. Pfeiffer, *The ratio of oxidative phosphorylation complexes I-V in bovine heart mitochondria and the composition of respiratory chain supercomplexes*. *J Biol Chem*, 2001. **276**(41): p. 37861-7.
121. Hayyan, M., M.A. Hashim, and I.M. AlNashef, *Superoxide Ion: Generation and Chemical Implications*. *Chem Rev*, 2016. **116**(5): p. 3029-85.
122. Kim, H.J., et al., *Reactive oxygen species induce antiviral innate immune response through IFN-lambda regulation in human nasal epithelial cells*. *Am J Respir Cell Mol Biol*, 2013. **49**(5): p. 855-65.
123. Martindale, J.L. and N.J. Holbrook, *Cellular response to oxidative stress: signaling for suicide and survival*. *J Cell Physiol*, 2002. **192**(1): p. 1-15.
124. Dickinson, B.C. and C.J. Chang, *Chemistry and biology of reactive oxygen species in signaling or stress responses*. *Nat Chem Biol*, 2011. **7**(8): p. 504-11.
125. Harman, D., *The biologic clock: the mitochondria?* *J Am Geriatr Soc*, 1972. **20**(4): p. 145-7.
126. Hansen, J.M., Y.M. Go, and D.P. Jones, *Nuclear and mitochondrial compartmentation of oxidative stress and redox signaling*. *Annu Rev Pharmacol Toxicol*, 2006. **46**: p. 215-34.

127. Ryan, S.D., et al., *Isogenic human iPSC Parkinson's model shows nitrosative stress-induced dysfunction in MEF2-PGC1alpha transcription*. *Cell*, 2013. **155**(6): p. 1351-64.
128. Buhlman, L.M., *Parkin loss-of-function pathology: Premature neuronal senescence induced by high levels of reactive oxygen species?* *Mech Ageing Dev*, 2016.
129. Sitte, N., et al., *Protein oxidation and degradation during cellular senescence of human BJ fibroblasts: part I--effects of proliferative senescence*. *FASEB J*, 2000. **14**(15): p. 2495-502.
130. Passos, J.F. and T. von Zglinicki, *Mitochondria, telomeres and cell senescence*. *Exp Gerontol*, 2005. **40**(6): p. 466-72.
131. Caron, M., et al., *Human lipodystrophies linked to mutations in A-type lamins and to HIV protease inhibitor therapy are both associated with prelamin A accumulation, oxidative stress and premature cellular senescence*. *Cell Death Differ*, 2007. **14**(10): p. 1759-67.
132. Wallace, D.C., *Why do we still have a maternally inherited mitochondrial DNA? Insights from evolutionary medicine*. *Annu Rev Biochem*, 2007. **76**: p. 781-821.
133. Chinnery, P.F., *Mitochondrial disease in adults: what's old and what's new?* *EMBO Mol Med*, 2015. **7**(12): p. 1503-12.
134. Bleazard, W., et al., *The dynamin-related GTPase Dnm1 regulates mitochondrial fission in yeast*. *Nat Cell Biol*, 1999. **1**(5): p. 298-304.
135. Chen, H., A. Chomyn, and D.C. Chan, *Disruption of fusion results in mitochondrial heterogeneity and dysfunction*. *J Biol Chem*, 2005. **280**(28): p. 26185-92.
136. Friedman, J.R. and J. Nunnari, *Mitochondrial form and function*. *Nature*, 2014. **505**(7483): p. 335-43.
137. Xu, X., et al., *Mitochondrial regulation in pluripotent stem cells*. *Cell Metab*, 2013. **18**(3): p. 325-32.
138. Nunnari, J. and A. Suomalainen, *Mitochondria: in sickness and in health*. *Cell*, 2012. **148**(6): p. 1145-59.

139. Bender, A., et al., *High levels of mitochondrial DNA deletions in substantia nigra neurons in aging and Parkinson disease*. Nat Genet, 2006. **38**(5): p. 515-7.
140. Shirendeb, U.P., et al., *Mutant huntingtin's interaction with mitochondrial protein Drp1 impairs mitochondrial biogenesis and causes defective axonal transport and synaptic degeneration in Huntington's disease*. Hum Mol Genet, 2012. **21**(2): p. 406-20.
141. Cho, D.H., T. Nakamura, and S.A. Lipton, *Mitochondrial dynamics in cell death and neurodegeneration*. Cell Mol Life Sci, 2010. **67**(20): p. 3435-47.
142. Costa, V., et al., *Mitochondrial fission and cristae disruption increase the response of cell models of Huntington's disease to apoptotic stimuli*. EMBO Mol Med, 2010. **2**(12): p. 490-503.
143. Festenstein, G.N., et al., *A constituent of the unsaponifiable portion of animal tissue lipids (lambda max. 272 m mu)*. Biochem J, 1955. **59**(4): p. 558-66.
144. Crane, F.L., et al., *Isolation of a quinone from beef heart mitochondria*. Biochim Biophys Acta, 1957. **25**(1): p. 220-1.
145. Desbats, M.A., et al., *Genetic bases and clinical manifestations of coenzyme Q10 (CoQ 10) deficiency*. J Inherit Metab Dis, 2015. **38**(1): p. 145-56.
146. Turunen, M., J. Olsson, and G. Dallner, *Metabolism and function of coenzyme Q*. Biochim Biophys Acta, 2004. **1660**(1-2): p. 171-99.
147. Hines, V., L.D. Keys, 3rd, and M. Johnston, *Purification and properties of the bovine liver mitochondrial dihydroorotate dehydrogenase*. J Biol Chem, 1986. **261**(24): p. 11386-92.
148. Fontaine, E., F. Ichas, and P. Bernardi, *A ubiquinone-binding site regulates the mitochondrial permeability transition pore*. J Biol Chem, 1998. **273**(40): p. 25734-40.
149. Ernster, L. and G. Dallner, *Biochemical, physiological and medical aspects of ubiquinone function*. Biochim Biophys Acta, 1995. **1271**(1): p. 195-204.
150. Lopez-Lluch, G., et al., *Is coenzyme Q a key factor in aging?* Mech Ageing Dev, 2010. **131**(4): p. 225-35.
151. Echtay, K.S., E. Winkler, and M. Klingenberg, *Coenzyme Q is an obligatory cofactor for uncoupling protein function*. Nature, 2000. **408**(6812): p. 609-13.

152. Marbois, B., et al., *The yeast Coq4 polypeptide organizes a mitochondrial protein complex essential for coenzyme Q biosynthesis*. *Biochim Biophys Acta*, 2009. **1791**(1): p. 69-75.
153. Acosta, M.J., et al., *Coenzyme Q biosynthesis in health and disease*. *Biochim Biophys Acta*, 2016.
154. Trevisson, E., et al., *Coenzyme Q deficiency in muscle*. *Curr Opin Neurol*, 2011. **24**(5): p. 449-56.
155. Dhanasekaran, M. and J. Ren, *The emerging role of coenzyme Q-10 in aging, neurodegeneration, cardiovascular disease, cancer and diabetes mellitus*. *Curr Neurovasc Res*, 2005. **2**(5): p. 447-59.
156. Ogasahara, S., et al., *Muscle coenzyme Q deficiency in familial mitochondrial encephalomyopathy*. *Proc Natl Acad Sci U S A*, 1989. **86**(7): p. 2379-82.
157. Quinzii, C.M. and M. Hirano, *Primary and secondary CoQ(10) deficiencies in humans*. *Biofactors*, 2011. **37**(5): p. 361-5.
158. Lopez-Martin, J.M., et al., *Missense mutation of the COQ2 gene causes defects of bioenergetics and de novo pyrimidine synthesis*. *Hum Mol Genet*, 2007. **16**(9): p. 1091-7.
159. Mollet, J., et al., *Prenyldiphosphate synthase, subunit 1 (PDSS1) and OH-benzoate polyprenyltransferase (COQ2) mutations in ubiquinone deficiency and oxidative phosphorylation disorders*. *J Clin Invest*, 2007. **117**(3): p. 765-72.
160. Quinzii, C.M., et al., *Reactive oxygen species, oxidative stress, and cell death correlate with level of CoQ10 deficiency*. *FASEB J*, 2010. **24**(10): p. 3733-43.
161. Salviati, L., et al., *Infantile encephalomyopathy and nephropathy with CoQ10 deficiency: a CoQ10-responsive condition*. *Neurology*, 2005. **65**(4): p. 606-8.
162. Desbats, M.A., et al., *Primary coenzyme Q10 deficiency presenting as fatal neonatal multiorgan failure*. *Eur J Hum Genet*, 2015. **23**(9): p. 1254-8.
163. Heeringa, S.F., et al., *COQ6 mutations in human patients produce nephrotic syndrome with sensorineural deafness*. *J Clin Invest*, 2011. **121**(5): p. 2013-24.

164. Lagier-Tourenne, C., et al., *ADCK3, an ancestral kinase, is mutated in a form of recessive ataxia associated with coenzyme Q10 deficiency*. Am J Hum Genet, 2008. **82**(3): p. 661-72.
165. Mollet, J., et al., *CABC1 gene mutations cause ubiquinone deficiency with cerebellar ataxia and seizures*. Am J Hum Genet, 2008. **82**(3): p. 623-30.
166. Ashraf, S., et al., *ADCK4 mutations promote steroid-resistant nephrotic syndrome through CoQ10 biosynthesis disruption*. J Clin Invest, 2013. **123**(12): p. 5179-89.
167. Duncan, A.J., et al., *A nonsense mutation in COQ9 causes autosomal-recessive neonatal-onset primary coenzyme Q10 deficiency: a potentially treatable form of mitochondrial disease*. Am J Hum Genet, 2009. **84**(5): p. 558-66.
168. Rotig, A., et al., *Quinone-responsive multiple respiratory-chain dysfunction due to widespread coenzyme Q10 deficiency*. Lancet, 2000. **356**(9227): p. 391-5.
169. Lopez, L.C., et al., *Leigh syndrome with nephropathy and CoQ10 deficiency due to decaprenyl diphosphate synthase subunit 2 (PDSS2) mutations*. Am J Hum Genet, 2006. **79**(6): p. 1125-9.
170. Freyer, C., et al., *Rescue of primary ubiquinone deficiency due to a novel COQ7 defect using 2,4-dihydroxybenzoic acid*. J Med Genet, 2015. **52**(11): p. 779-83.
171. Montero, R., et al., *Analysis of coenzyme Q10 in muscle and fibroblasts for the diagnosis of CoQ10 deficiency syndromes*. Clin Biochem, 2008. **41**(9): p. 697-700.
172. Artuch, R., et al., *Cerebellar ataxia with coenzyme Q10 deficiency: diagnosis and follow-up after coenzyme Q10 supplementation*. J Neurol Sci, 2006. **246**(1-2): p. 153-8.
173. Montero, R., et al., *Clinical, biochemical and molecular aspects of cerebellar ataxia and Coenzyme Q10 deficiency*. Cerebellum, 2007. **6**(2): p. 118-22.
174. Artuch, R., et al., *Coenzyme Q10 deficiencies in neuromuscular diseases*. Adv Exp Med Biol, 2009. **652**: p. 117-28.

175. Brea-Calvo, G., et al., *COQ4 mutations cause a broad spectrum of mitochondrial disorders associated with CoQ10 deficiency*. Am J Hum Genet, 2015. **96**(2): p. 309-17.
176. Salviati, L., et al., *Haploinsufficiency of COQ4 causes coenzyme Q10 deficiency*. J Med Genet, 2012. **49**(3): p. 187-91.
177. Emmanuele, V., et al., *Heterogeneity of coenzyme Q10 deficiency: patient study and literature review*. Arch Neurol, 2012. **69**(8): p. 978-83.
178. Chung, W.K., et al., *Mutations in COQ4, an essential component of coenzyme Q biosynthesis, cause lethal neonatal mitochondrial encephalomyopathy*. J Med Genet, 2015. **52**(9): p. 627-35.
179. Quinzii, C.M. and M. Hirano, *Coenzyme Q and mitochondrial disease*. Dev Disabil Res Rev, 2010. **16**(2): p. 183-8.
180. Bujan, N., et al., *Characterization of CoQ(1)(0) biosynthesis in fibroblasts of patients with primary and secondary CoQ(1)(0) deficiency*. J Inherit Metab Dis, 2014. **37**(1): p. 53-62.
181. Boitier, E., et al., *A case of mitochondrial encephalomyopathy associated with a muscle coenzyme Q10 deficiency*. J Neurol Sci, 1998. **156**(1): p. 41-6.
182. Sobreira, C., et al., *Mitochondrial encephalomyopathy with coenzyme Q10 deficiency*. Neurology, 1997. **48**(5): p. 1238-43.
183. Rahman, S., et al., *Neonatal presentation of coenzyme Q10 deficiency*. J Pediatr, 2001. **139**(3): p. 456-8.
184. Casarin, A., et al., *Functional characterization of human COQ4, a gene required for Coenzyme Q10 biosynthesis*. Biochem Biophys Res Commun, 2008. **372**(1): p. 35-9.
185. Bueno, C., et al., *FLT3 activation cooperates with MLL-AF4 fusion protein to abrogate the hematopoietic specification of human ESCs*. Blood, 2013. **121**(19): p. 3867-78, S1-3.
186. Lukovic, D., et al., *Human iPSC derived disease model of MERTK-associated retinitis pigmentosa*. Sci Rep, 2015. **5**: p. 12910.
187. Raitano, S., et al., *Restoration of progranulin expression rescues cortical neuron generation in an induced pluripotent stem cell model of frontotemporal dementia*. Stem Cell Reports, 2015. **4**(1): p. 16-24.

188. Farra, N., et al., *Rett syndrome induced pluripotent stem cell-derived neurons reveal novel neurophysiological alterations*. Mol Psychiatry, 2012. **17**(12): p. 1261-71.
189. Chin, E.W., et al., *Choline Ameliorates Disease Phenotypes in Human iPSC Models of Rett Syndrome*. Neuromolecular Med, 2016.
190. Schondorf, D.C., et al., *iPSC-derived neurons from GBA1-associated Parkinson's disease patients show autophagic defects and impaired calcium homeostasis*. Nat Commun, 2014. **5**: p. 4028.
191. Woodard, C.M., et al., *iPSC-derived dopamine neurons reveal differences between monozygotic twins discordant for Parkinson's disease*. Cell Rep, 2014. **9**(4): p. 1173-82.
192. Liu, G.H., et al., *Modelling Fanconi anemia pathogenesis and therapeutics using integration-free patient-derived iPSCs*. Nat Commun, 2014. **5**: p. 4330.
193. Soria-Valles, C., et al., *NF-kappaB activation impairs somatic cell reprogramming in ageing*. Nat Cell Biol, 2015. **17**(8): p. 1004-13.
194. Liu, G.H., et al., *Recapitulation of premature ageing with iPSCs from Hutchinson-Gilford progeria syndrome*. Nature, 2011. **472**(7342): p. 221-5.
195. Lee, D.F., et al., *Modeling familial cancer with induced pluripotent stem cells*. Cell, 2015. **161**(2): p. 240-54.
196. Horvath, P. and R. Barrangou, *CRISPR/Cas, the immune system of bacteria and archaea*. Science, 2010. **327**(5962): p. 167-70.
197. Nelles, D.A., et al., *Programmable RNA Tracking in Live Cells with CRISPR/Cas9*. Cell, 2016. **165**(2): p. 488-96.
198. Jinek, M., et al., *A programmable dual-RNA-guided DNA endonuclease in adaptive bacterial immunity*. Science, 2012. **337**(6096): p. 816-21.
199. Garneau, J.E., et al., *The CRISPR/Cas bacterial immune system cleaves bacteriophage and plasmid DNA*. Nature, 2010. **468**(7320): p. 67-71.
200. Cong, L., et al., *Multiplex genome engineering using CRISPR/Cas systems*. Science, 2013. **339**(6121): p. 819-23.
201. Ran, F.A., et al., *Double nicking by RNA-guided CRISPR Cas9 for enhanced genome editing specificity*. Cell, 2013. **154**(6): p. 1380-9.

202. Schwank, G., et al., *Functional repair of CFTR by CRISPR/Cas9 in intestinal stem cell organoids of cystic fibrosis patients*. Cell Stem Cell, 2013. **13**(6): p. 653-8.
203. Wu, Y., et al., *Correction of a genetic disease in mouse via use of CRISPR-Cas9*. Cell Stem Cell, 2013. **13**(6): p. 659-62.
204. Flynn, R., et al., *CRISPR-mediated genotypic and phenotypic correction of a chronic granulomatous disease mutation in human iPS cells*. Exp Hematol, 2015. **43**(10): p. 838-848 e3.
205. Jang, Y.Y. and Z. Ye, *Gene correction in patient-specific iPSCs for therapy development and disease modeling*. Hum Genet, 2016. **135**(9): p. 1041-58.
206. Li, H.L., et al., *Precise correction of the dystrophin gene in duchenne muscular dystrophy patient induced pluripotent stem cells by TALEN and CRISPR-Cas9*. Stem Cell Reports, 2015. **4**(1): p. 143-54.
207. Inoue, S., et al., *Mitochondrial respiration defects modulate differentiation but not proliferation of hematopoietic stem and progenitor cells*. FEBS Lett, 2010. **584**(15): p. 3402-9.
208. Parker, G.C., G. Acsadi, and C.A. Brenner, *Mitochondria: determinants of stem cell fate?* Stem Cells Dev, 2009. **18**(6): p. 803-6.
209. Wang, Y. and S. Hekimi, *Understanding Ubiquinone*. Trends Cell Biol, 2016. **26**(5): p. 367-78.
210. Ramos-Mejia, V., et al., *The adaptation of human embryonic stem cells to different feeder-free culture conditions is accompanied by a mitochondrial response*. Stem Cells Dev, 2012. **21**(7): p. 1145-55.
211. Flores-Guzman, P., V. Fernandez-Sanchez, and H. Mayani, *Concise review: ex vivo expansion of cord blood-derived hematopoietic stem and progenitor cells: basic principles, experimental approaches, and impact in regenerative medicine*. Stem Cells Transl Med, 2013. **2**(11): p. 830-8.
212. Eliasson, P. and J.I. Jonsson, *The hematopoietic stem cell niche: low in oxygen but a nice place to be*. J Cell Physiol, 2010. **222**(1): p. 17-22.
213. Jeong, S.H., et al., *Echinochrome a increases mitochondrial mass and function by modulating mitochondrial biogenesis regulatory genes*. Mar Drugs, 2014. **12**(8): p. 4602-15.

214. Jang, K.J., et al., *Mitochondrial function provides instructive signals for activation-induced B-cell fates*. Nat Commun, 2015. **6**: p. 6750.
215. Takubo, K., et al., *Regulation of glycolysis by Pdk functions as a metabolic checkpoint for cell cycle quiescence in hematopoietic stem cells*. Cell Stem Cell, 2013. **12**(1): p. 49-61.
216. Medeiros, B.C., et al., *Isocitrate dehydrogenase mutations in myeloid malignancies*. Leukemia, 2016.
217. Majmundar, A.J., W.J. Wong, and M.C. Simon, *Hypoxia-inducible factors and the response to hypoxic stress*. Mol Cell, 2010. **40**(2): p. 294-309.
218. Lee, K.E. and M.C. Simon, *From stem cells to cancer stem cells: HIF takes the stage*. Curr Opin Cell Biol, 2012. **24**(2): p. 232-5.
219. Mucaj, V., J.E. Shay, and M.C. Simon, *Effects of hypoxia and HIFs on cancer metabolism*. Int J Hematol, 2012. **95**(5): p. 464-70.
220. Sontakke, P., et al., *Hypoxia-Like Signatures Induced by BCR-ABL Potentially Alter the Glutamine Uptake for Maintaining Oxidative Phosphorylation*. PLoS One, 2016. **11**(4): p. e0153226.
221. Ng, K.P., et al., *Physiologic hypoxia promotes maintenance of CML stem cells despite effective BCR-ABL1 inhibition*. Blood, 2014. **123**(21): p. 3316-26.
222. Martin, S.K., et al., *The emerging role of hypoxia, HIF-1 and HIF-2 in multiple myeloma*. Leukemia, 2011. **25**(10): p. 1533-42.
223. Testa, U., et al., *Oxidative stress and hypoxia in normal and leukemic stem cells*. Exp Hematol, 2016. **44**(7): p. 540-60.
224. Skrtic, M., et al., *Inhibition of mitochondrial translation as a therapeutic strategy for human acute myeloid leukemia*. Cancer Cell, 2011. **20**(5): p. 674-88.
225. Shpall, E.J., et al., *Transplantation of ex vivo expanded cord blood*. Biol Blood Marrow Transplant, 2002. **8**(7): p. 368-76.
226. Delaney, C., et al., *Notch-mediated expansion of human cord blood progenitor cells capable of rapid myeloid reconstitution*. Nat Med, 2010. **16**(2): p. 232-6.
227. Fonseca-Pereira, D., et al., *The neurotrophic factor receptor RET drives haematopoietic stem cell survival and function*. Nature, 2014. **514**(7520): p. 98-101.

228. Danet, G.H., et al., *Expansion of human SCID-repopulating cells under hypoxic conditions*. J Clin Invest, 2003. **112**(1): p. 126-35.
229. Tothova, Z. and D.G. Gilliland, *FoxO transcription factors and stem cell homeostasis: insights from the hematopoietic system*. Cell Stem Cell, 2007. **1**(2): p. 140-52.
230. Lewandowski, D., et al., *In vivo cellular imaging pinpoints the role of reactive oxygen species in the early steps of adult hematopoietic reconstitution*. Blood, 2010. **115**(3): p. 443-52.
231. Yuan, T.L. and L.C. Cantley, *PI3K pathway alterations in cancer: variations on a theme*. Oncogene, 2008. **27**(41): p. 5497-510.
232. Kharas, M.G. and K. Gritsman, *Akt: a double-edged sword for hematopoietic stem cells*. Cell Cycle, 2010. **9**(7): p. 1223-4.
233. Kharas, M.G., et al., *Constitutively active AKT depletes hematopoietic stem cells and induces leukemia in mice*. Blood, 2010. **115**(7): p. 1406-15.
234. Zhou, J., et al., *Tsc1 mutant neural stem/progenitor cells exhibit migration deficits and give rise to subependymal lesions in the lateral ventricle*. Genes Dev, 2011. **25**(15): p. 1595-600.
235. Yilmaz, O.H., et al., *mTORC1 in the Paneth cell niche couples intestinal stem-cell function to calorie intake*. Nature, 2012. **486**(7404): p. 490-5.
236. Lopez, L.C., et al., *Treatment of CoQ(10) deficient fibroblasts with ubiquinone, CoQ analogs, and vitamin C: time- and compound-dependent effects*. PLoS One, 2010. **5**(7): p. e11897.
237. McNeish, J., et al., *From Dish to Bedside: Lessons Learned While Translating Findings from a Stem Cell Model of Disease to a Clinical Trial*. Cell Stem Cell, 2015. **17**(1): p. 8-10.
238. Shen, B., et al., *Efficient genome modification by CRISPR-Cas9 nickase with minimal off-target effects*. Nat Methods, 2014. **11**(4): p. 399-402.
239. Cooper, O., et al., *Pharmacological rescue of mitochondrial deficits in iPSC-derived neural cells from patients with familial Parkinson's disease*. Sci Transl Med, 2012. **4**(141): p. 141ra90.

240. Kirkeby, A., et al., *Generation of regionally specified neural progenitors and functional neurons from human embryonic stem cells under defined conditions*. Cell Rep, 2012. **1**(6): p. 703-14.
241. Pagliuca, F.W., et al., *Generation of functional human pancreatic beta cells in vitro*. Cell, 2014. **159**(2): p. 428-39.
242. D'Amour, K.A., et al., *Production of pancreatic hormone-expressing endocrine cells from human embryonic stem cells*. Nat Biotechnol, 2006. **24**(11): p. 1392-401.
243. Schulz, T.C., et al., *A scalable system for production of functional pancreatic progenitors from human embryonic stem cells*. PLoS One, 2012. **7**(5): p. e37004.
244. Reardon, S. and D. Cyranoski, *Japan stem-cell trial stirs envy*. Nature, 2014. **513**(7518): p. 287-8.
245. Schwartz, S.D., et al., *Embryonic stem cell trials for macular degeneration: a preliminary report*. Lancet, 2012. **379**(9817): p. 713-20.
246. Mellough, C.B., et al., *Lab generated retina: realizing the dream*. Vis Neurosci, 2014. **31**(4-5): p. 317-32.
247. Menasche, P., et al., *Human embryonic stem cell-derived cardiac progenitors for severe heart failure treatment: first clinical case report*. Eur Heart J, 2015. **36**(30): p. 2011-7.
248. McCormack, *Treatment for spinal cord injury to start clinical trial funded by California's stem cell agency*. California Institute for Regenerative Medicine, 2014.
249. Ebihara, Y., F. Ma, and K. Tsuji, *Generation of red blood cells from human embryonic/induced pluripotent stem cells for blood transfusion*. Int J Hematol, 2012. **95**(6): p. 610-6.
250. Dias, J., et al., *Generation of red blood cells from human induced pluripotent stem cells*. Stem Cells Dev, 2011. **20**(9): p. 1639-47.
251. Olivier, E.N., et al., *Large-scale production of embryonic red blood cells from human embryonic stem cells*. Exp Hematol, 2006. **34**(12): p. 1635-42.
252. Lu, S.J., et al., *Biologic properties and enucleation of red blood cells from human embryonic stem cells*. Blood, 2008. **112**(12): p. 4475-84.

253. Takayama, N., et al., *Transient activation of c-MYC expression is critical for efficient platelet generation from human induced pluripotent stem cells*. *J Exp Med*, 2010. **207**(13): p. 2817-30.
254. Feng, Q., et al., *Scalable generation of universal platelets from human induced pluripotent stem cells*. *Stem Cell Reports*, 2014. **3**(5): p. 817-31.
255. Toscano, M.G., et al., *SCL/TALI-mediated transcriptional network enhances megakaryocytic specification of human embryonic stem cells*. *Mol Ther*, 2015. **23**(1): p. 158-70.
256. Tseng, S.Y., et al., *Generation of immunogenic dendritic cells from human embryonic stem cells without serum and feeder cells*. *Regen Med*, 2009. **4**(4): p. 513-26.
257. Timmermans, F., et al., *Generation of T cells from human embryonic stem cell-derived hematopoietic zones*. *J Immunol*, 2009. **182**(11): p. 6879-88.
258. Vodyanik, M.A., et al., *Human embryonic stem cell-derived CD34+ cells: efficient production in the coculture with OP9 stromal cells and analysis of lymphohematopoietic potential*. *Blood*, 2005. **105**(2): p. 617-26.

IX.ANNEX

During the progress of this Doctoral Thesis, the scientific articles detailed below have been published by the group and co-authored by the PhD candidate:

- Intrahepatic transplantation of cord blood CD34+ cells into newborn NOD/SCID-IL2R γ (null) mice allows efficient multi-organ and multi-lineage hematopoietic engraftment without accessory cells. Navarro-Montero O*, **Romero-Moya D***, Montes R*, Ramos-Mejía V, Bueno C, Real PJ, Menendez P. **Clin Immunol.** **2012**; 145(2):89-91. *Co-first author. **Pag. 193.**
- FLT3 activation cooperates with MLL-AF4 fusion protein to abrogate the hematopoietic specification of human ESCs. Bueno C, Ayllón V, Montes R, Navarro-Montero O, Ramos-Mejía V, Real PJ, **Romero-Moya D**, Araúzo-Bravo MJ, Menendez P. **Blood.** **2013**; 121(19):3867-78, S1-3. **Pag. 195.**
- Ligand-independent FLT3 activation does not cooperate with MLL-AF4 to immortalize/transform cord blood CD34+ cells. Montes R, Ayllón V, Prieto C, Bursen A, Prella C, **Romero-Moya D**, Real PJ, Navarro-Montero O, Chillón C, Marschalek R, Bueno C, Menendez P. **Leukemia.** **2014**; 28(3):666-74. **Pag. 197.**
- Bone marrow mesenchymal stem cells from patients with aplastic anemia maintain functional and immune properties and do not contribute to the pathogenesis of the disease. Bueno C, Roldan M, Anguita E, **Romero-Moya D**, Martín-Antonio B, Rosu-Myles M, del Cañizo C, Campos F, García R,

Gómez-Casares M, Fuster JL, Jurado M, Delgado M, Menendez P.
Haematologica. 2014 Jul;99(7):1168-75. PMID: 24727813. **Pag. 199.**

- Reprogramming human B cells into induced pluripotent stem cells and its enhancement by C/EBP α . Bueno C, Sardina JL, Di Stefano B, **Romero-Moya D**, Muñoz-López A, Ariza L, Chillón MC, Balanzategui A, Castaño J, Herreros A, Fraga MF, Fernández A, Granada I, Quintana-Bustamante O, Segovia JC, Nishimura K, Ohtaka M, Nakanishi M, Graf T, Menendez P. **Leukemia.** 2016; 30(3):674-82. **Pag. 201.**
- Intra-Bone Marrow Transplantation Confers Superior Multilineage Engraftment of Murine Aorta-Gonad Mesonephros Cells Over Intravenous Transplantation. Sanjuan-Pla A, **Romero-Moya D**, Prieto C, Bueno C, Bigas A, Menendez P. **Stem Cells Dev.** 2016; 25(3):259-65. **Pag. 203.**
- Cellular Ontogeny and Hierarchy Influence the Reprogramming Efficiency of Human B Cells into Induced Pluripotent Stem Cells. Muñoz-López Á, van Roon EH, **Romero-Moya D**, López-Millan B, Stam RW, Colomer D, Nakanishi M, Bueno C, Menendez P. **Stem Cells.** 2016; 34(3):581-7. **Pag. 205.**
- Development Refractoriness of MLL-Rearranged Human B Cell Acute Leukemias to Reprogramming into Pluripotency. Muñoz-López A*, **Romero-Moya D***, Prieto C, Ramos-Mejía V, Agraz-Doblas A,

Varela I, Buschbeck M, Palau A, Carvajal-Vergara X, Giorgetti A, Ford A, Lako M, Granada I, Ruiz-Xivillé N, Rodríguez-Perales S, Torres-Ruíz R, Stam RW, Fuster JL, Fraga MF, Nakanishi M, Cazzaniga G, Bardini M, Cobo I, Bayon GF, Fernandez AF, Bueno C, Menendez P. **Stem Cell Reports. 2016; In press. *Co-first author. Pag. 207.**



LETTER TO THE EDITOR

Intrahepatic transplantation of cord blood CD34+ cells into newborn NOD/SCID-IL2R γ ^{null} mice allows efficient multi-organ and multi-lineage hematopoietic engraftment without accessory cells[☆]

To the Editor:

Advancing the current understanding in experimental and developmental hematopoiesis, hematopoietic transplantation, graft-versus-host-disease (GvHD) and graft-versus-leukemia, immune system, leukemogenic processes as well as testing in pre-clinical models novel cell- and drug-based therapeutic approaches demand the use of xenotransplant systems [1]. Upon discovery of the *scid* mutation, the immune-deficient non-obese diabetic NOD/SCID mouse was developed, and rapidly became the standard model for hematopoietic xenotransplantation. Several NOD/SCID generations have evolved over the last decade [2,3]. Recently, the NOD/SCID-IL2R γ ^{null} strain (NSG) has been developed which allows higher engraftment levels and does not develop thymic lymphoma therefore displaying a longer lifespan [4,5].

Co-transplantation of inactivated accessory cells together with CD34+ hematopoietic stem/progenitor cells (HSPCs) has long been associated with enhanced and more stable hematopoietic reconstitution upon xeno-transplantation [4,5]. In a clinical setting, despite that CD34+ cell-selected HSPCs have been used worldwide in allogeneic transplantation in an attempt to deplete immune cells thus reducing the risk of GvHD [6], it is now considered that accessory-depleted transplants are associated to an increased risk of opportunistic infections, secondary malignancies related to long-term immunosuppression and, more importantly, graft failure [7–9]. In such a context, it has been reported that increasing numbers of T-cells in the graft associates to decreasing graft failure rates [10].

Several experimental scenarios may require HSC or leukemic cell transplantation into newborn mice. For instance,

hematopoietic reconstitution with ontogenically early HSCs such as hematopoietic cells derived from human embryonic stem cells (hESCs), human fetal liver or cord blood (CB) may be more efficient if cells are transplanted into an ontogenically-matched organ such as newborn liver which may provide a more permissive immune-hematopoietic milieu. In addition, successful *de novo* development of functional components of the human adaptive immune system as a pre-clinical model to evaluate *in vivo* immune responses, for example, to vaccines or live infectious pathogens may benefit from cell transplantation into a newborn hematopoietic microenvironment [11].

Here, we analyzed for the first time the ability of CB-derived CD34+ HSCs to reconstitute the hematopoiesis of a newborn NSG mice strain upon intrahepatic transplantation. We compared side-by-side the engraftment efficiency of CB-derived CD34+ cells transplanted alone or in combination with irradiated accessory cells. CB samples from healthy newborns were obtained from local hospitals upon approval by our local ethics and biohazard board committee. CB samples were pooled to reduce variability between individual CB units. Mononuclear cells were isolated using Ficoll-Hypaque density gradient. After red blood lysis, CD34+ cells were purified by magnetic bead separation using a human CD34 MicroBead Kit (Miltenyi Biotec) and an AutoMACS Pro-separator following the manufacturer's instructions. Purity was consistently higher than 95% (data not shown). 3×10^4 CD34+ cells alone or together with 5×10^4 irradiated (15 Gy) CD34-Lineage+ accessory cells were transplanted intrahepatically in 1–2 day old newborn mice (n=20) within 12 h of irradiation (1 Gy). Mice were sacrificed 6 weeks after transplantation and BM was flushed. Peripheral blood, spleen and liver were also collected and analyzed for human chimerism. Human chimerism was determined by flow cytometry using anti-CD45 and anti-HLA-ABC (Fig. 1A). All engrafted mice were assessed for multilineage reconstitution using anti-CD19 (B-cell), anti-CD33 (myeloid) and anti-CD34 (immature cells) (Fig. 1A).

All (100%) mice transplanted with 3×10^4 CD34+ cells without accessory cells showed human engraftment in all organs analyzed (Fig. 1B, left panel). However, 2 out of 10 (20%) mice transplanted with CD34+ cells together with accessory cells failed to engraft (Fig. 1B, left panel). Furthermore, the levels of engraftment were significantly higher in those mice transplanted without accessory cells: BM ($36\% \pm 2.3\%$ vs $24\% \pm 7.3\%$), PB ($6.1\% \pm 1.3\%$ vs $5\% \pm 1.8\%$), liver ($6\% \pm 1\%$ vs $2\% \pm 1\%$) and spleen ($17\% \pm 2\%$ vs $13\% \pm 4.6\%$). We next characterized the engraftment composition and found

[☆] Authorship contributions:

O.N.-M., D.R.-M., R.M.: conception and experimental design, collection and/or assembly data, data analysis, interpretation. P.J.R., C.B.: data analysis and interpretation. P.M.: conception and design, financial support, data analysis and interpretation and manuscript writing.

The manuscript has been seen and approved by all authors.

Regular Article

LYMPHOID NEOPLASIA

FLT3 activation cooperates with MLL-AF4 fusion protein to abrogate the hematopoietic specification of human ESCs

Clara Bueno,¹ Verónica Ayllón,¹ Rosa Montes,¹ Oscar Navarro-Montero,¹ Verónica Ramos-Mejía,¹ Pedro J. Real,¹ Damià Romero-Moya,¹ Marcos J. Araúz-Bravo,² and Pablo Menendez^{1,3,4}

¹Centre for Genomics and Oncological Research, Pfizer-University of Granada-Andalusian Regional Government, Granada, Spain; ²Max Planck Institute for Molecular Biomedicine, Department of Cell and Developmental Biology, Laboratory of Computational Biology and Bioinformatics, Muenster, Germany; ³Josep Carreras Leukemia Research Institute and Cell Therapy Program, Facultat de Medicina, University of Barcelona, Spain; ⁴Institució Catalana de Recerca i Estudis Avançats (ICREA), Barcelona, Spain

Key Points

- *FLT3* activation cooperates with the MLL-AF4 fusion gene to fully abolish blood formation from hESCs.
- *FLT3* activation does not cooperate with the MLL-AF4 fusion oncogene to transform hESCs or hESC-derived hematopoietic progeny.

Mixed-lineage leukemia (MLL)-AF4 fusion arises prenatally in high-risk infant acute pro-B-lymphoblastic leukemia (pro-B-ALL). In human embryonic stem cells (hESCs), MLL-AF4 skewed hemoendothelial specification but was insufficient for transformation, suggesting that additional oncogenic insults seem required for MLL-AF4-mediated transformation. MLL-AF4+ pro-B-ALL expresses enormous levels of *FLT3*, occasionally because of activating mutations, thus representing a candidate cooperating event in MLL-AF4+ pro-B-ALL. Here, we explored the developmental impact of *FLT3* activation alone, or together with MLL-AF4, in the hematopoietic fate of hESCs. *FLT3* activation does not affect specification of hemogenic precursors but significantly enhances the formation of CD45⁺ blood cells, and CD45⁺CD34⁺ blood progenitors with clonogenic potential. However, overexpression of *FLT3* mutations or wild-type *FLT3* (*FLT3*-WT) completely abrogates hematopoietic differentiation from MLL-AF4-expressing hESCs, indicating that *FLT3* activation cooperates with MLL-AF4 to inhibit human embryonic hematopoiesis. Cell cycle/apoptosis analyses suggest that *FLT3* activation directly affects hESC specification rather than proliferation or survival of hESC-emerging hematopoietic derivatives. Transcriptional profiling of hESC-derived CD45⁺ cells supports the *FLT3*-mediated inhibition of hematopoiesis in MLL-AF4-expressing hESCs, which is associated with large transcriptional changes and downregulation of genes involved in hematopoietic system development and function. Importantly, *FLT3* activation does not cooperate with MLL-AF4 to immortalize/transform hESC-derived hematopoietic cells, suggesting the need of alternative (epi)-genetic cooperating hits. (*Blood*. 2013;121(19):3867-3878)

Introduction

Newborn cancer is progressively seen as a developmental biology disease.¹ An intriguing newborn cancer is the infant pro-B/monocyte acute lymphoblastic leukemia (ALL) characterized by the hallmark genetic abnormality t(4;11) encoding the fusion mixed-lineage leukemia (MLL)-AF4, which is associated with a dismal prognosis and very brief latency, raising the question of how this disease evolves so quickly.²⁻⁴ Compelling evidence indicates that MLL-AF4 arises prenatally during embryonic/fetal hematopoiesis.^{2,3,5,6} To understanding the developmental impact of MLL-AF4, we first need to elucidate which is the target cell for transformation and the mechanisms underlying MLL-AF4-mediated transformation.

MLL-AF4-induced leukemogenesis has been difficult to model, and bona fide MLL-AF4 disease models do not exist.⁷⁻¹⁰ Our understanding of MLL fusions comes from murine models, which do not recapitulate the human disease faithfully, suggesting that these mouse models may be missing essential components of leukemogenesis during early human development. It could be

argued that the lack of an MLL-AF4 model may be because (1) a cell in a wrong developmental stage was targeted in the mouse; (2) the impact of other secondary hits has not been properly addressed; (3) MLL-AF4 requires the reciprocal AF4-MLL fusion protein to cause pro-B ALL as shown in the mouse; and (4) MLL-AF4 exerts its transforming function preferentially in human cells, indicating that the MLL-AF4 fusion has to be addressed using ontogenically primitive human stem cells. Among these, neonatal (cord blood [CB]-derived) CD34⁺ hematopoietic stem/progenitor cells (HSPCs) or prenatal (fetal- or embryonic-derived) cells represent ontogenically early candidate target cells. Thus, human embryonic stem cell (hESC)-derived hematopoietic differentiation constitutes a robust human-specific strategy to study the onset of hematopoiesis, representing a promising tool for modeling developmental mechanisms of human disease and lineage specification that cannot be addressed with patient samples or mouse models.^{11,12}

Submitted November 27, 2012; accepted February 27, 2013. Prepublished online as *Blood* First Edition paper, March 11, 2013; DOI 10.1182/blood-2012-11-470146.

The online version of this article contains a data supplement.

The publication costs of this article were defrayed in part by page charge payment. Therefore, and solely to indicate this fact, this article is hereby marked "advertisement" in accordance with 18 USC section 1734.

© 2013 by The American Society of Hematology



ORIGINAL ARTICLE

Ligand-independent FLT3 activation does not cooperate with MLL-AF4 to immortalize/transform cord blood CD34+ cells

R Montes¹, V Ayllón¹, C Prieto^{1,2}, A Bursen³, C Prella³, D Romero-Moya^{1,2}, PJ Real¹, O Navarro-Montero¹, C Chillón⁴, R Marschalek³, C Bueno^{1,2} and P Menendez^{1,2,5}

MLL-AF4 fusion is hallmark in high-risk infant pro-B-acute lymphoblastic leukemia (pro-B-ALL). Our limited understanding of MLL-AF4-mediated transformation reflects the absence of human models reproducing this leukemia. Hematopoietic stem/progenitor cells (HSPCs) constitute likely targets for transformation. We previously reported that MLL-AF4 enhanced hematopoietic engraftment and clonogenic potential in cord blood (CB)-derived CD34+ HSPCs but was not sufficient for leukemogenesis, suggesting that additional oncogenic lesions are required for MLL-AF4-mediated transformation. MLL-AF4+ pro-B-ALL display enormous levels of *FLT3*, and occasionally FLT3-activating mutations, thus representing a candidate cooperating event in MLL-AF4+ pro-B-ALL. We have explored whether FLT3.TKD (tyrosine kinase domain) mutation or increased expression of FLT3.WT (wild type) cooperates with MLL-AF4 to immortalize/transform CB-CD34+ HSPCs. *In vivo*, FLT3.TKD/FLT3.WT alone, or in combination with MLL-AF4, enhances hematopoietic repopulating function of CB-CD34+ HSPCs without impairing migration or hematopoietic differentiation. None of the animals transplanted with MLL-AF4+FLT3.TKD/WT-CD34+ HSPCs showed any sign of disease after 16 weeks. *In vitro*, enforced expression of FLT3.TKD/FLT3.WT conveys a transient overexpansion of MLL-AF4-expressing CD34+ HSPCs associated to higher proportion of cycling cells coupled to lower apoptotic levels, but does not augment clonogenic potential nor confer stable replating. Together, FLT3 activation does not suffice to immortalize/transform MLL-AF4-expressing CB-CD34+ HSPCs, suggesting the need of alternative (epi)-genetic cooperating oncogenic lesions.

Leukemia (2014) 28, 666–674; doi:10.1038/leu.2013.346

Keywords: MLL-AF4; FLT3.TKD; FLT3.WT; CB-CD34+ HSPCs; leukemogenesis

INTRODUCTION

The translocation t(4;11)(q21;q23) encodes the fusion protein MLL-AF4, which is the hallmark genetic abnormality associated to infant pro-B/monocyte acute lymphoblastic leukemia (ALL). This newborn pro-B-ALL is characterized by its dismal prognosis and very brief latency, raising the question of how this disease evolves so quickly.^{1–4} Compelling evidence indicates that MLL-AF4 arises prenatally during embryonic/fetal hematopoiesis.^{5–8} To understand the developmental impact of MLL-AF4, we first need to elucidate which is the target cell for transformation, and the cooperating oncogenic lesions underlying MLL-AF4-mediated transformation.^{5,9,10}

MLL-AF4-induced leukemogenesis has been difficult to model, and *bona fide* MLL-AF4 disease models do not exist.^{11–14} Our understanding of MLL fusions comes from murine models that do not recapitulate the human disease faithfully, suggesting that these mouse models may be missing essential components of leukemogenesis during early human development. It could be argued that the lack of a MLL-AF4 model may be because of (i) a cell in a wrong developmental stage was targeted in the mouse; (ii) the impact of other secondary hits has not been properly addressed; or (iii) MLL-AF4 exerts its transforming function preferentially in human cells, indicating that the MLL-AF4

function has to be addressed using ontogenically primitive human stem cells. Among these, neonatal (cord blood (CB)-derived) CD34+ hematopoietic stem/progenitor cells (HSPCs) or prenatal (fetal- or embryonic-derived) cells represent ontogenically early candidate target cells.

We have recently reported that the expression of MLL-AF4 has a functional impact in CB-CD34+ HSPCs¹⁵ and human embryonic stem cell (hESC)-derived hematopoietic cells.¹⁶ In CB-CD34+ HSPCs, MLL-AF4 enhanced hematopoietic engraftment and clonogenic potential but was not sufficient for leukemogenesis.¹⁵ In hESCs, MLL-AF4 altered the developmental cell fate, skewing the early hemato-endothelial specification of hESCs,¹⁶ but was also unable to transform hESCs or hESC blood derivatives. Considering these data, we hypothesize that the inability to develop a MLL-AF4 model might not be due to the human cell context or cell type targeted, but rather that additional oncogenic lesions are required for leukemogenesis.

Gene expression profiling showed that *FLT3* is highly expressed in MLL-AF4+ pro-B-ALL. Moreover, it was shown that other MLL-rearranged leukemias display FLT3.TKD (tyrosine kinase domain) mutations in up to 20% of the cases, suggesting that they may represent candidate cooperating events.^{17,18} Accordingly, Yamaguchi *et al.*¹⁹ have reported that *FLT3.TKD* cooperates with

¹GENYO, Centre for Genomics and Oncological Research: Pfizer, University of Granada, Andalusian Regional Government, Granada, Spain; ²Faculty of Medicine, Department of Stem Cells, Development and Cancer, Cell Therapy Program of the University of Barcelona, Josep Carreras Leukemia Research Institute, Barcelona, Spain; ³Institute of Pharmaceutical Biology/ZAFES/DCAL, Goethe-University of Frankfurt, Biocenter, Frankfurt, Germany; ⁴Hospital Universitario de Salamanca, Servicio de Hematología, Salamanca, Spain and ⁵Institució Catalana de Recerca i Estudis Avançats (ICREA). Correspondence: Dr C Bueno or Dr P Menendez, Faculty of Medicine, Department of Stem Cells, Development and Cancer, Cell Therapy Program of the University of Barcelona, Josep Carreras Leukemia Research Institute, Carrer de Casanova 143 08036, Barcelona, Spain. E-mail: cbueno@carrerasresearch.org or pmenendez@carrerasresearch.org

Received 22 March 2013; revised 18 October 2013; accepted 8 November 2013; accepted article preview online 18 November 2013; advance online publication, 13 December 2013

Bone marrow mesenchymal stem cells from patients with aplastic anemia maintain functional and immune properties and do not contribute to the pathogenesis of the disease

Clara Bueno,^{1*} Mar Roldán,^{2*} Eduardo Anguita,³ Damia Romero-Moya,⁴ Beatriz Martín-António,⁵ Michael Rosu-Myles,⁴ Consuelo del Cañizo,⁶ Francisco Campos,⁶ Regina García,⁷ Maite Gómez-Casares,⁸ Jose Luis Fuster,⁹ Manuel Jurado,¹⁰ Mario Delgado,¹¹ and Pablo Menendez^{1,12}

¹Josep Carreras Leukemia Research Institute, Cell Therapy Program of the University of Barcelona, Faculty of Medicine, Barcelona, Spain; ²GENYO, Centre for Genomics and Oncological Research: Pfizer/University of Granada/Andalusian Regional Government, Granada, Spain; ³Servicio de Hematología, Hospital Clínico San Carlos, Madrid, Spain; ⁴Biologics and Genetic Therapies Directorate, Health Products and Food Branch, Health Canada, Ottawa, Ontario, Canada; ⁵Department of Hematology, University Hospital of Salamanca and Institute of Biomedical Research of Salamanca (IBSAL), Salamanca, Spain; ⁶Department of Neurology, Neurovascular Area, Clinical Neurosciences Research Laboratory, Hospital Clínico-Health Research Institute of Santiago de Compostela, Spain; ⁷Servicio de Hematología, Hospital Clínico de Málaga, Málaga, Spain; ⁸Servicio de Hematología, Hospital Universitario Insular Materno-Infantil, Las Palmas de Gran Canaria, Spain; ⁹Sección de Oncohematología Pediátrica, Hospital Virgen de Arrixaca, Murcia, Spain; ¹⁰Servicio de Hematología, Hospital Universitario Virgen de las Nieves, Granada, Spain; ¹¹Instituto de Parasitología y Biomedicina López-Neyra, CSIC, Granada, Spain; and ¹²Institució Catalana de Reserca i Estudis Avançats (ICREA), Barcelona, Spain

*CB and MR contributed equally to this work.

ABSTRACT

Aplastic anemia is a life-threatening bone marrow failure disorder characterized by peripheral pancytopenia and marrow hypoplasia. The majority of cases of aplastic anemia remain idiopathic, although hematopoietic stem cell deficiency and impaired immune responses are hallmarks underlying the bone marrow failure in this condition. Mesenchymal stem/stromal cells constitute an essential component of the bone marrow hematopoietic microenvironment because of their immunomodulatory properties and their ability to support hematopoiesis, and they have been involved in the pathogenesis of several hematologic malignancies. We investigated whether bone marrow mesenchymal stem cells contribute, directly or indirectly, to the pathogenesis of aplastic anemia. We found that mesenchymal stem cell cultures can be established from the bone marrow of aplastic anemia patients and display the same phenotype and differentiation potential as their counterparts from normal bone marrow. Mesenchymal stem cells from aplastic anemia patients support the *in vitro* homeostasis and the *in vivo* repopulating function of CD34⁺ cells, and maintain their immunosuppressive and anti-inflammatory properties. These data demonstrate that bone marrow mesenchymal stem cells from patients with aplastic anemia do not have impaired functional and immunological properties, suggesting that they do not contribute to the pathogenesis of the disease.

Introduction

Aplastic anemia (AA) is a rare and life-threatening heterogeneous bone marrow (BM) failure disorder characterized by peripheral pancytopenia and marrow hypoplasia.^{1,2} The majority of AA cases are idiopathic with an unknown primary etiology.^{1,3} In some patients, a drug or infection is implicated in the etiology of AA although it is unclear why only some individuals are susceptible.^{4,7} In ~15% of patients the disease is inherited or congenital, for example Fanconi anemia.^{1,8} The main suggested underlying mechanism in AA is a primary hematopoietic stem cell (HSC) deficiency or a secondary HSC defect due to an abnormal balance between HSC death and differentiation.^{9,8} Importantly, pathological autoimmune responses also seem to be involved in AA BM failure, given the good responses to immunosuppressive treatments.^{1,9}

Mesenchymal stem/stromal cells (MSC) are rare BM multipotent cells that constitute a source of progenitors for meso-

dermal tissues.¹⁰ MSC have emerged as excellent candidates for clinical applications thanks to their immunomodulatory properties and their ability to support hematopoiesis.¹¹⁻¹³ Importantly, MSC are an essential component of the BM hematopoietic microenvironment. The BM hematopoietic microenvironment regulates the homeostasis of hematopoiesis through the production and secretion of cytokines and extracellular matrix molecules.¹⁴ Furthermore, the BM hematopoietic microenvironment plays a role in the pathogenesis of a variety of hematologic malignancies including acute lymphoblastic¹⁵ and myeloblastic leukemias,¹⁶ multiple myeloma,¹⁷ lymphomas,¹⁸ chronic myeloid leukemia¹⁹ and myelodysplastic syndromes.^{16,20}

Because HSC failure and impaired immune responses underlie the pathogenesis of AA, it is plausible that BM-MSC may also contribute, directly or indirectly, to the pathogenesis of AA. However, there is almost no information on whether the functional and immunological properties of BM-MSC are impaired in AA patients or on the potential contribution of

©2014 Ferrata Storti Foundation. This is an open-access paper. doi:10.3324/haematol.2014.103580
The online version of this article has a Supplementary Appendix.
Manuscript received on January 2, 2014. Manuscript accepted on March 27, 2014.
Correspondence: pmenendez@carreirasresearch.org



ORIGINAL ARTICLE

Reprogramming human B cells into induced pluripotent stem cells and its enhancement by C/EBP α

C Bueno^{1,11}, JL Sardina^{2,11}, B Di Stefano², D Romero-Moya¹, A Muñoz-López¹, L Ariza¹, MC Chillón³, A Balanzategui³, J Castaño¹, A Herreros⁴, MF Fraga⁵, A Fernández⁵, I Granada^{1,6}, O Quintana-Bustamante⁷, JC Segovia⁷, K Nishimura⁸, M Ohtaka⁹, M Nakanishi⁹, T Graf² and P Menendez^{1,10}

B cells have been shown to be refractory to reprogramming and B-cell-derived induced pluripotent stem cells (iPSC) have only been generated from murine B cells engineered to carry doxycycline-inducible Oct4, Sox2, Klf4 and Myc (OSKM) cassette in every tissue and from EBV/SV40LT-immortalized lymphoblastoid cell lines. Here, we show for the first time that freshly isolated non-cultured human cord blood (CB)- and peripheral blood (PB)-derived CD19+CD20+ B cells can be reprogrammed to iPSCs carrying complete VDJH immunoglobulin (Ig) gene monoclonal rearrangements using non-integrative tetracistronic, but not monocistronic, OSKM-expressing Sendai Virus. Co-expression of C/EBP α with OSKM facilitates iPSC generation from both CB- and PB-derived B cells. We also demonstrate that myeloid cells are much easier to reprogram than B and T lymphocytes. Differentiation potential back into the cell type of their origin of B-cell-, T-cell-, myeloid- and fibroblast-iPSCs is not skewed, suggesting that their differentiation does not seem influenced by 'epigenetic memory'. Our data reflect the actual cell-autonomous reprogramming capacity of human primary B cells because biased reprogramming was avoided by using freshly isolated primary cells, not exposed to cytokine cocktails favoring proliferation, differentiation or survival. The ability to reprogram CB/PB-derived primary human B cells offers an unprecedented opportunity for studying developmental B lymphopoiesis and modeling B-cell malignancies.

Leukemia (2016) 30, 674–682; doi:10.1038/leu.2015.294

INTRODUCTION

Induced pluripotent stem cells (iPSCs) provide a unique platform to explore donor/patient-specific somatic cells for regenerative medicine, drug screening and disease modeling.¹ Although the most common source for human iPSC derivation is skin dermal fibroblasts, human iPSCs have been generated from a variety of somatic tissues including keratinocytes,² mesenchymal stem cells³ and hematopoietic stem/progenitor cells.^{4–7} Generation of iPSC from human hematopoietic cells is an attractive option because they can be generated from peripheral blood (PB) cells, which are easily accessible through noninvasive methods, and from cord blood (CB) cells, which are young cells carrying minimal somatic mutations stored as large collections in public CB banks.⁸ To date, human iPSCs have been generated from CD34+ hematopoietic stem/progenitor cells^{4,6–8} and also from T cells and myeloid cells.^{8–10} However, whether iPSCs may be induced from human normal or leukemic B cells remains a mystery.^{5,11} Reprogramming CB/PB-derived B cells to pluripotency (iPSCs) will offer a valuable *in vitro* system to study cellular, molecular and epigenetic events underlying the physiology of B-cell lymphopoiesis and the pathogenesis of B-cell malignancies. B cells have been shown to

be refractory to reprogramming,^{9,10,12} and B-cell-derived iPSCs have only been generated from B cells of mice engineered to carry doxycycline-inducible Oct4, Sox2, Klf4 and Myc (OSKM) lentiviruses in every tissue,¹² and from EBV/SV40LT-transformed lymphoblastoid cell lines.^{11,13} Importantly, recent work has revealed that mouse B cells can be reprogrammed into iPSCs with high efficiency when the cells were pulsed with the CCAAT/enhancer binding protein- α (C/EBP α) before of their exposure to the reprogramming factors OSKM.¹⁴ This strongly suggests that biological rather than technical barriers underlie the inability to reprogram B cells to pluripotency. Here, we show for the first time that freshly isolated non-cultured human B cells, derived from both CB and PB, can be reprogrammed into iPSCs carrying complete VDJH immunoglobulin (Ig) gene monoclonal rearrangements, using non-integrative polycistronic Sendai Virus (SeV).^{15,16} We also demonstrate that transient co-expression of C/EBP α with OSKM increases B-cell iPSC generation. Differentiation of B-cell-, T-cell-, myeloid- and fibroblast-iPSCs into B-cell, T-cell and myeloid cell fate revealed that iPSC differentiation potential does not seem influenced by the residual 'epigenetic memory' of the cell type of origin.

¹Josep Carreras Leukemia Research Institute and School of Medicine, University of Barcelona, Barcelona, Spain; ²Gene Regulation, Stem Cells and Cancer Program, Centre for Genomic Regulation (CRG) and University Pompeu Fabra (UPF), Barcelona, Spain; ³Department of Hematology, University Hospital of Salamanca, Instituto Biosanitario de Salamanca (IBSAL), Salamanca, Spain; ⁴Sevei d'Oncologia Radioteràpica, Hospital Clinic, Barcelona, Spain; ⁵Cancer Epigenetics Laboratory, Instituto Universitario de Oncología del Principado de Asturias, Universidad de Oviedo, Asturias, Spain; ⁶Hematology Department, Hospital Germans Trias i Pujol, Institut Català d'Oncologia, Badalona, Spain; ⁷Differentiation and Cytometry Unit, Hematopoietic Innovative Therapy Division, Centro de Investigaciones Energéticas, Medioambientales y Tecnológicas (CIEMAT), Madrid, Spain; ⁸Faculty of Medicine, Laboratory of Gene Regulation, University of Tsukuba, Tsukuba, Ibaraki, Japan; ⁹Research Center for Stem Cell Engineering and National Institute of Advanced Industrial Science and Technology (AIST), Tsukuba, Ibaraki, Japan and ¹⁰Institució Catalana de Recerca i Estudis Avançats (ICREA), Barcelona, Spain. Correspondence: Dr C Bueno or Professor P Menendez, Josep Carreras Leukemia Research Institute School of Medicine, University of Barcelona, Casanova 143, Barcelona 08036, Spain. E-mail: cbueno@carrerasresearch.org or pmenendez@carrerasresearch.org

¹¹These authors contributed equally to this work.

Received 5 January 2015; revised 3 September 2015; accepted 17 September 2015; accepted article preview online 26 October 2015; advance online publication, 27 November 2015

Intra-Bone Marrow Transplantation Confers Superior Multilineage Engraftment of Murine Aorta-Gonad Mesonephros Cells Over Intravenous Transplantation

Alejandra Sanjuan-Pla,¹ Damia Romero-Moya,¹ Cristina Prieto,¹
Clara Bueno,¹ Anna Bigas,² and Pablo Menendez^{1,3}

Hematopoietic stem cell (HSC) engraftment has been achieved using single-cell transplantation of prospectively highly purified adult HSC populations. However, bulk transplants are still performed when assessing the HSC potential of early embryonic hematopoietic tissues such as the aorta-gonad mesonephros (AGM) due to very low HSC activity content early in development. Intra-bone marrow transplantation (IBMT) has emerged as a superior administration route over intravenous (IV) transplantation for assessing the reconstituting ability of human HSCs in the xenotransplant setting since it bypasses the requirement for homing to the BM. In this study, we compared the ability of IBMT and IV administration of embryonic day 11.5 AGM-derived cells to reconstitute the hematopoietic system of myeloablated recipients. IBMT resulted in higher levels of AGM HSC long-term multilineage engraftment in the peripheral blood, BM, spleen, and thymus of primary and secondary recipients, and in limiting dilution experiments. The administration route did not skew the multilineage contribution pattern, but IBMT conferred higher Lineage⁻Sca-1⁺c-kit⁺ long-term engraftment, in line with the superior IBMT reconstitution. Therefore, IBMT represents a superior administration route to detect HSC activity from developmentally early sources with limited HSC activity content, such as the AGM.

Introduction

H^{EMATOPOIESIS} ALLOWS THE FORMATION of blood cells from a hematopoietic stem cell (HSC) through a stepwise process and occurs at different sites through ontogeny in mice and humans [1]. During mouse embryogenesis, definitive HSCs capable of reconstituting adult irradiated recipients are generated at embryonic day (E) 10.5–E11.5 from the ventral wall of the dorsal aorta within the aorta-gonad mesonephros (AGM) [2], from the umbilical vein [3] and from the placenta [4]. Due to the constant migration of HSCs through blood circulation during development, an incomplete picture remains regarding which locations constitute de novo HSC production sites and which are pre-HSC-to-HSC maturation sites. At ~E12.5, HSCs colonize the fetal liver (FL) to further migrate to the bone marrow (BM) where they reside for the life span of the organism [1].

In the murine and human settings, the transplantation assay is the *in vivo* gold standard test to study HSC function. HSC transplantation is widely used in experimental and clinical hematology, and refinement of HSC transplantation assays has

resulted in improved HSC engraftment/readout. For instance, murine HSC transplantation is now optimized to be performed at the single-cell level and has been crucial in revealing the functional heterogeneity of murine and human HSC compartments. In the mouse, HSC transplantation assays are mainly performed by intravenous (IV) administration due to the intrinsic circulatory properties of hematopoietic cells. Successful engraftment then requires blood circulation and migration of HSCs into the BM, which offers a supportive niche. Alternatively, direct injection of cells within the BM has been successfully used to engraft human HSCs [5–8], leukemia cells [9,10], and mesenchymal sarcoma cells [11,12] in immunodeficient mice. Intra-BM transplantation (IBMT) has shed light on the homing and repopulation properties of human HSCs and has been shown to result in higher levels of multilineage long-term reconstitution than IV injection. IBMT also allows detection of HSC potential from nonhematopoietic tissues, such as the liver, muscle, and human pluripotent stem cells. Interestingly, IBMT has also been used with whole murine BM cells [13,14]; however, in one study IBMT did not result in an enhanced engraftment compared with the IV technique [15].

¹Josep Carreras Leukemia Research Institute and School of Medicine, University of Barcelona, Barcelona, Spain.

²Program in Cancer Research, Institut Hospital del Mar d'Investigacions Mèdiques (IMIM), Parc de Recerca Biomèdica de Barcelona, Barcelona, Spain.

³Institució Catalana de Recerca i Estudis Avançats (ICREA), Barcelona, Spain.



EMBRYONIC STEM CELLS/INDUCED
PLURIPOTENT STEM CELLS

Cellular Ontogeny and Hierarchy Influence the Reprogramming Efficiency of Human B Cells into Induced Pluripotent Stem Cells

ALVARO MUÑOZ-LÓPEZ,^a EDDY. H.J. VAN ROON,^b DAMIA ROMERO-MOYA,^a BELÉN LÓPEZ-MILLAN,^a RONALD W. STAM,^b DOLORS COLOMER,^c MAHITO NAKANISHI,^d CLARA BUENO,^a PABLO MENENDEZ^{a,e}

Key Words. Human B cells • Human B-cell progenitors • Fetal liver • Ontogeny • Hierarchy • Induced pluripotent stem cells • Sendai virus • OSKM • Ig gene rearrangements

^aJosep Carreras Leukemia Research Institute (IC) and School of Medicine, Department of Biomedicine, University of Barcelona, Barcelona, Spain and ^bHematopathology Unit, Department of Anatomic Pathology, Hospital Clinic, IDIBAPS, Barcelona, Spain; ^cDepartment of Pediatric Oncology/Hematology, Erasmus MC-Sophia Children's Hospital, Rotterdam, The Netherlands; ^dResearch Center for Stem Cell Engineering and National Institute of Advanced Industrial Science and Technology (AIST), Tsukuba, Ibaraki, Japan; ^eInstitució Catalana de Recerca i Estudis Avançats (ICREA), Barcelona, Spain

Correspondence: Pablo Menendez, Ph.D., Josep Carreras Leukemia Research Institute, School of Medicine, University of Barcelona, Casanova 143, 08036 Barcelona, Spain. Telephone: (+34)935572809; Fax: (+34)933231751; e-mail: pmenendez@carrerasresearch.org; Clara Bueno, Ph.D., Josep Carreras Leukemia Research Institute, School of Medicine, University of Barcelona, Casanova 143, 08036 Barcelona, Spain. Telephone: (+34)935572810; Fax: (+34)933231751; e-mail: cbueno@carrerasresearch.org

Received November 16, 2015; accepted for publication January 8, 2016; first published online in *STEM CELLS EXPRESS* February 6, 2016.

© AlphaMed Press
1066-5099/2016/\$30.00/0

<http://dx.doi.org/10.1002/stem.2303>

ABSTRACT

Although B cells have been shown to be refractory to reprogramming into pluripotency, induced pluripotent stem cells (iPSCs) have been very recently generated, at very low efficiency, from human cord blood (CB)- and peripheral blood (PB)-derived CD19+CD20+ B cells using nonintegrative tetracistronic OSKM-expressing Sendai Virus (SeV). Here, we addressed whether cell ontogeny and hierarchy influence the reprogramming efficiency of the B-cell compartment. We demonstrate that human fetal liver (FL)-derived CD19+ B cells are 110-fold easier to reprogram into iPSCs than those from CB/PB. Similarly, FL-derived CD34+CD19+ B progenitors are reprogrammed much easier than mature B cells (0.46% vs. 0.11%). All FL B-cell iPSCs carry complete VDJH rearrangements while 55% and 45% of the FL B-progenitor iPSCs carry incomplete and complete VDJH rearrangements, respectively, reflecting the reprogramming of developmentally different B progenitors (pro-B vs. pre-B) within a continuous differentiation process. Finally, our data suggest that successful B-cell reprogramming relies on active cell proliferation, and it is MYC-dependent as identical nonintegrative polycistronic SeV lacking MYC (OSKL or OSKLN) fail to reprogram B cells. The ability to efficiently reprogram human fetal primary B cells and B precursors offers an unprecedented opportunity for studying developmental B-lymphopoiesis and modeling B-cell malignancies. *STEM CELLS* 2016;34:581–587

SIGNIFICANCE STATEMENT

Using tetracistronic OSKM-expressing nonintegrative Sendai vectors, we show that the developmental ontogeny and cellular hierarchy largely influence the reprogramming efficiency of human B cells into iPSCs. We also show that Ig/VDJH rearrangements do not constitute a reprogramming barrier and that B-cell reprogramming seems to rely on cell proliferation and it is cMYC-dependent. The ability to efficiently reprogram human fetal primary B cells and B precursors offers an unprecedented opportunity for studying developmental B-lymphopoiesis and modeling B-cell malignancies.

INTRODUCTION

Induced pluripotent stem cells (iPSCs) hold tremendous potential to explore donor/patient-specific somatic cells for regenerative medicine, compound screening, tissue development, and disease modeling [1]. Human iPSCs have been generated from many tissues including fibroblasts, keratinocytes [2], mesenchymal stem cells [3], nasal epithelial cells [4], and several blood cell populations such as hematopoietic stem/progenitor cells (HSPCs) [5–8], T cells [8–10], and myeloid cells [8–10]. Very recently, iPSCs were generated at very low efficiency from cord blood (CB) and peripheral blood (PB) B cells representing a

breakthrough advance since human B cells had been shown previously to be refractory to reprogramming into pluripotency [11]. Reprogramming B cells will offer a valuable in vitro system to study the mechanisms underlying the physiology and development of B lymphopoiesis and the pathogenesis of B-cell malignancies.

Several lines of evidence indicate that reprogramming of tissue stem cells is more efficient than reprogramming their differentiated progeny [12, 13]. First, studies on nuclear transfer have revealed that stem/progenitor cells are more amenable to reprogramming [14]. Second, reprogramming neural stem cells proved to be very efficient and achievable

Please cite this article in press as: Muñoz-López et al., Development Refractoriness of MLL-Rearranged Human B Cell Acute Leukemias to Reprogramming into Pluripotency, *Stem Cell Reports* (2016), <http://dx.doi.org/10.1016/j.stemcr.2016.08.013>

Stem Cell Reports



Article

OPEN ACCESS

Development Refractoriness of MLL-Rearranged Human B Cell Acute Leukemias to Reprogramming into Pluripotency

Alvaro Muñoz-López,^{1,2,16} Damià Romero-Moya,^{1,2,16} Cristina Prieto,^{1,2} Verónica Ramos-Mejía,³ Antonio Agraz-Doblas,^{1,2,4} Ignacio Varela,⁴ Marcus Buschbeck,¹ Anna Palau,¹ Xonia Carvajal-Vergara,⁵ Alessandra Giorgetti,¹ Anthony Ford,⁶ Majlinda Lako,⁷ Isabel Granada,^{1,8} Neus Ruiz-Xivillé,^{1,8} Sandra Rodríguez-Perales,⁹ Raul Torres-Ruiz,^{1,9} Ronald W. Stam,¹⁰ Jose Luis Fuster,¹¹ Mario F. Fraga,¹² Mahito Nakanishi,¹³ Gianni Cazzaniga,¹⁴ Michela Bardini,¹⁴ Isabel Cobo,^{1,12} Gustavo F. Bayon,¹² Agustín F. Fernández,¹² Clara Bueno,^{1,2,*} and Pablo Menendez^{1,2,15,*}

¹Josep Carreras Leukemia Research Institute, School of Medicine, University of Barcelona, Casanova 143, 08036 Barcelona, Spain

²Department of Biomedicine, School of Medicine, University of Barcelona, 08036 Barcelona, Spain

³Genomic Oncology Department, Centre for Genomics and Oncology GENyO, 18016 Granada, Spain

⁴IBBTFC, CSIC-University of Cantabria, 39011 Santander, Spain

⁵Cell Therapy Department, Centro de Investigación Médica Aplicada (CIMA), 31008 Pamplona, Spain

⁶Centre for Evolution and Cancer, Institute of Cancer Research, London SW7 3RP, UK

⁷Institute of Genetic Medicine, Newcastle University, Newcastle NE1 7RU, UK

⁸Hematology Department, Hospital Germans Trias i Pujol, Institut Català d'Oncologia, 08916 Badalona, Spain

⁹Cytogenetics Group, Centro Nacional de Investigaciones Oncológicas (CNIO), 28029 Madrid, Spain

¹⁰Department of Pediatric Oncology/Hematology, Erasmus Medical Center, Erasmus University, 3015 CN Rotterdam, the Netherlands

¹¹Department of Pediatric Oncohematology, Clinical University Hospital Virgen de la Arrixaca, 30120 Murcia, Spain

¹²Cancer Epigenetics Laboratory, Instituto Universitario de Oncología del Principado de Asturias (IUOPA-HUCA), Universidad de Oviedo, 33003 Oviedo, Spain

¹³Research Center for Stem Cell Engineering, National Institute of Advanced Industrial Science and Technology (AIST), Tsukuba, Ibaraka 305-0046, Japan

¹⁴University di Milano-Bicocca, Ospedale San Gerardo/Fondazione MBBM, 20052 Monza MB, Italy

¹⁵Institució Catalana de Recerca i Estudis Avançats (ICREA), 08036 Barcelona, Spain

¹⁶Co-first author

*Correspondence: cbueno@carrerasresearch.org (C.B.), pmendez@carrerasresearch.org (P.M.)

<http://dx.doi.org/10.1016/j.stemcr.2016.08.013>

SUMMARY

Induced pluripotent stem cells (iPSCs) are a powerful tool for disease modeling. They are routinely generated from healthy donors and patients from multiple cell types at different developmental stages. However, reprogramming leukemias is an extremely inefficient process. Few studies generated iPSCs from primary chronic myeloid leukemias, but iPSC generation from acute myeloid or lymphoid leukemias (ALL) has not been achieved. We attempted to generate iPSCs from different subtypes of B-ALL to address the developmental impact of leukemic fusion genes. OKSM(L)-expressing mono/polycistronic-, retroviral/lentiviral/episomal-, and Sendai virus vector-based reprogramming strategies failed to render iPSCs in vitro and in vivo. Addition of transcriptomic-epigenetic reprogramming “boosters” also failed to generate iPSCs from B cell blasts and B-ALL lines, and when iPSCs emerged they lacked leukemic fusion genes, demonstrating non-leukemic myeloid origin. Conversely, MLL-AF4-overexpressing hematopoietic stem cells/B progenitors were successfully reprogrammed, indicating that B cell origin and leukemic fusion gene were not reprogramming barriers. Global transcriptome/DNA methylation profiling suggested a developmental/differentiation refractoriness of MLL-rearranged B-ALL to reprogramming into pluripotency.

INTRODUCTION

Leukemia is generally studied once the full transformation events have already occurred and, therefore, the mechanisms by which leukemia-specific mutations transform to a pre-leukemic state followed by rapid transition to overt leukemia are not amenable to analysis with patient samples (Ramos-Mejía et al., 2012c). Therefore, it is imperative to develop effective disease models to study the developmental impact of leukemia-specific genetic aberrations on human stem cell fate. Induced pluripotent stem cells (iPSCs) are a powerful tool for modeling different aspects of human disease that cannot otherwise be addressed by patient sample analyses or animal models (Menendez et al., 2006; Wu and Hochedlinger, 2011). Because leuke-

mia manifests as a developmental cell blockage, the generation and differentiation of leukemia-specific iPSCs offers a promising strategy to study the earliest events leading to the specification of both normal and abnormal hematopoietic tissue, thus illuminating molecular mechanisms underlying the pathogenesis of human leukemia.

iPSCs are routinely generated from tissues obtained from healthy donors and patients and cell types at different developmental stages. Reprogramming human primary cancer cells, however, remains challenging. Despite significant interest in generating iPSCs from leukemia cells (Curry et al., 2015; Ramos-Mejía et al., 2012c; Yilmazer et al., 2015), only a few reports have demonstrated successful reprogramming and, unfortunately, only seven of these studies reprogrammed human primary leukemias (the

X.NOTES

